

Dissertation zur Erlangung des Doktorgrades
der Fakultät für Chemie und Pharmazie
der Ludwig-Maximilians-Universität München

**Expression, functions, and new target genes of the
transcription factor SOX10 in human melanoma**

Saskia Anna Graf

aus

Neumarkt in der Oberpfalz

2016



Erklärung

Diese Dissertation wurde im Sinne von § 7 der Promotionsordnung vom 28. November 2011 von Frau Prof. Dr. Carola Berking betreut und von Herrn Prof. Dr. Karl-Peter Hopfner von der Fakultät für Chemie und Pharmazie vertreten.

Eidesstattliche Versicherung

Diese Dissertation wurde eigenständig und ohne unerlaubte Hilfe erarbeitet.

München, den 01.03.2016

.....
Saskia Graf

Dissertation eingereicht am 04.03.2016

1. Gutachter: Prof. Dr. Karl-Peter Hopfner
2. Gutachterin: Prof. Dr. Carola Berking

Mündliche Prüfung am 20.05.2016

*“The storms come and go,
the waves crash overhead,
the big fish eat the little fish,
and I keep on paddling.” (Lord Varys)*
- George R. R. Martin, A Clash of Kings

Diese Arbeit widme ich meinen Eltern
und meinem Mann Simon

This thesis has been prepared in the laboratory of Prof. Dr. Carola Berking at the Department of Dermatology of the Ludwig Maximilian University of Munich.

Parts of this thesis were published in the Journal of Investigative Dermatology in 2014:

Graf SA, Busch C, Bosserhoff AK, Besch R, Berking C. SOX10 promotes melanoma cell invasion by regulating melanoma inhibitory activity. *Journal of Investigative Dermatology* 134: 2212-20 (2014)

A manuscript containing other parts of this thesis is currently in preparation for submission to the Journal of Investigative Dermatology:

Graf SA, Krebs S, Hornig E, Heppt MV, Kammerbauer C, Hamel A, Besch R, Blum H, Berking C. The myelin protein PMP2 is regulated by SOX10 and drives melanoma cell invasion.

Table of contents

1	Summary.....	1
	Zusammenfassung.....	3
2	Introduction.....	5
2.1	Melanocyte Development.....	5
2.2	From melanocytes to melanoma.....	8
2.3	Malignant melanoma.....	11
2.4	Melanoma therapy and resistance.....	12
2.5	Linking melanomagenesis to the embryonic development of melanocytes.....	15
2.6	SOX transcription factors in development and disease.....	17
2.7	Aims of this study.....	21
3	Materials and Methods.....	22
3.1	Materials.....	22
3.1.1	Media.....	22
3.1.2	Buffers and solutions.....	23
3.1.2.1	Buffers and solutions for immunoblotting.....	24
3.1.2.2	Buffers and solutions for fluorescence-activated cell sorting.....	25
3.1.2.3	Buffers and solutions for luciferase reporter assay.....	26
3.1.2.4	Buffers and solutions for electrophoretic mobility shift assay.....	26
3.1.2.5	Buffer for immunohistochemistry.....	26
3.1.2.6	Buffers for chromatin immunoprecipitation.....	27
3.1.2.7	Further buffers and solutions.....	28
3.1.3	Commercial kits.....	28
3.1.4	Transfection reagents.....	30
3.1.5	Oligonucleotides.....	30
3.1.5.1	Primers for quantitative real-time PCR.....	30
3.1.5.2	Primers for polymerase chain reaction.....	32
3.1.5.3	Oligonucleotides for electrophoretic mobility shift assay.....	34
3.1.5.4	Small interfering ribonucleic acids.....	35
3.1.6	Plasmids and vectors.....	35
3.1.7	Enzymes and polypeptides.....	37
3.1.8	Antibodies.....	38
3.1.8.1	Primary antibodies.....	38

3.1.8.2	Secondary antibodies.....	39
3.1.9	Cell lines	39
3.1.10	Appliances	40
3.1.11	Consumables	41
3.1.12	Software.....	42
3.2	Methods	44
3.2.1	Cell culture	44
3.2.1.1	Cultivation of human melanoma cell lines.....	44
3.2.1.2	Isolation of melanoma cells from patient samples	44
3.2.1.3	Cultivation of primary skin cells	45
3.2.2	Molecular biological methods	45
3.2.2.1	Gene silencing using RNA interference.....	45
3.2.2.1.1	Design of small interfering RNAs.....	45
3.2.2.1.2	Transfection of siRNAs.....	45
3.2.2.2	Transient and stable transfection of plasmid DNA.....	46
3.2.2.3	Cell invasion assays.....	46
3.2.2.3.1	Matrigel invasion assay	46
3.2.2.3.2	Spheroid assay	47
3.2.2.3.3	Chick embryo invasion assay	48
3.2.2.4	Cell viability assay	49
3.2.2.5	Flow cytometry	50
3.2.2.5.1	Cell cycle analysis	50
3.2.2.5.2	Cell death analysis	50
3.2.2.6	Luciferase reporter assay.....	50
3.2.2.7	Cloning of expression vectors	51
3.2.2.8	Transformation and conservation of chemical competent Escherichia coli ...	52
3.2.3	Biochemical methods	53
3.2.3.1	Isolation of nucleic acids	53
3.2.3.1.1	Plasmid isolation	53
3.2.3.1.2	RNA isolation	53
3.2.3.2	Quantification of gene expression	54
3.2.3.2.1	Copy DNA synthesis	54
3.2.3.2.2	Quantitative real-time PCR.....	54

3.2.3.3	Copy DNA sequencing	56
3.2.3.4	RNA sequencing	56
3.2.3.5	Protein isolation.....	58
3.2.3.5.1	Whole cell extracts	58
3.2.3.5.2	Nucleic extracts.....	58
3.2.3.5.3	Proteins from cell supernatants	59
3.2.3.6	Immunoblot according to Laemmli.....	59
3.2.3.6.1	Polyacrylamide gel electrophoresis	59
3.2.3.6.2	Immunoblotting.....	60
3.2.3.6.3	Protein detection	60
3.2.3.7	Electrophoretic mobility shift assay.....	61
3.2.3.8	Immunohistochemistry	61
3.2.3.9	Chromatin immunoprecipitation.....	63
3.2.4	Statistical analyses.....	64
4	Results.....	65
4.1	Expression of SOX9 and SOX10 in human skin and melanoma cells.....	65
4.1.1	Expression in human fibroblasts, melanocytes, and melanoma cell lines	65
4.1.2	Expression in short term-cultured melanoma cells	69
4.2	Inhibition of SOX9 and SOX10 via RNA interference.....	70
4.3	Phenotypic effects of SOX10 inhibition in melanoma cells.....	72
4.3.1	Effects of SOX10 inhibition on melanoma cell proliferation.....	72
4.3.2	Effects of SOX10 inhibition on melanoma cell death	79
4.3.3	Effects of SOX10 inhibition on melanoma cell invasion	84
4.4	Identification of MIA as a target gene of SOX10	90
4.4.1	Expression of MIA and regulation by different transcription factors.....	90
4.4.2	Analysis of SOX10 binding to the <i>MIA</i> promoter.....	93
4.4.3	Investigation of potential coregulators of SOX10	100
4.4.4	Analysis of MIA-mediated invasion after SOX10 inhibition	103
4.5	Analysis of known target genes of SOX10.....	105
4.6	Effects of SOX10 overexpression on melanoma cell invasion	108
4.7	Identification of further SOX10 target genes by RNA sequencing.....	110
4.8	Identification of PMP2 as a target gene of SOX10.....	115
4.8.1	Analysis of the regulation of PMP2 by SOX10.....	115
4.8.2	Analysis of SOX10 binding to the <i>PMP2</i> promoter	117
4.8.3	Investigating EGR2 as a transcriptional coregulator of SOX10.....	121

4.9	Expression and functional characterization of PMP2 in melanoma	122
4.9.1	PMP2 expression in human skin cells and melanoma cell lines	122
4.9.2	Phenotypic effects of PMP2 inhibition and overexpression in melanoma cells ..	125
4.9.2.1	Inhibition of PMP2 via RNA interference	125
4.9.2.2	Effects of PMP2 inhibition on melanoma cell proliferation	126
4.9.2.3	Analysis of PMP2-mediated invasion after SOX10 inhibition	129
4.9.2.4	Effects of PMP2 overexpression on melanoma cell invasion	130
4.10	Analysis of further SOX10 target genes.....	133
5	Discussion.....	135
5.1	Expression of SOX9 and SOX10 in human cell lines, tissues, and cancer	135
5.2	SOX9 and SOX10 inhibition in melanoma cells and mutual regulation	137
5.3	Influence of SOX10 on melanoma cell survival and cell death.....	138
5.4	Influence of SOX10 on melanoma cell invasion.....	139
5.5	Target genes of SOX10.....	141
5.5.1	Previously identified SOX10 target genes	141
5.5.2	Melanoma inhibitory activity (MIA).....	143
5.5.3	Peripheral myelin protein 2 (PMP2).....	146
5.6	SOX10 regulated genes – parallels between Schwann cell, Schwannian tumor, and melanoma development.....	151
5.7	Conclusion and outlook	153
6	References.....	156
7	Supplementary figures	176
8	Abbreviations	179
9	Acknowledgements	184
10	Curriculum vitae	185

1 Summary

Melanoma is the deadliest form of skin cancer with over 20,000 deaths alone in Europe each year. Novel therapeutic strategies targeting mutated kinases in the mitogen-activated protein kinase (MAPK) signaling pathway as well as the blockade of immune checkpoints lead to significantly improved response and survival rates compared to standard chemotherapies. However, not all patients profit from these new therapeutics and acquired resistance remains an unsolved problem. Therefore, discovering new potential targets for therapy is still in focus of basic melanoma research.

Melanoma develops from malignant transformation of melanocytes. During embryonic development melanocytes derive from multipotent neural crest cells (NCCs). Typical features of NCCs are a high proliferation rate, an enormous plasticity, and a strong migratory ability along defined routes.

A key factor for proliferation and survival of NCCs and subsequent differentiation to melanocytes is the transcription factor sex determining region-Y (SRY)-box 10 (SOX10). SOX10 is not only expressed during embryonic development of melanocytes but also serves as a specific marker of the melanocytic lineage. Characteristic features during embryonic development of melanocytes resemble key features in tumor initiation and progression. It stands to reason that SOX10 may regulate similar capacities during melanoma progression. Therefore, this study focused on investigating the role of SOX10 in melanoma.

Expression of SOX10 and the closely related transcription factor SOX9 were examined in human skin and melanoma cells. SOX10 expression was found abundantly in melanocytes and most melanoma cell lines but not in fibroblasts, whereas SOX9 expression was weak in melanocytes and fibroblasts and highly variable in melanoma cell lines. In a subset of melanoma cell lines, SOX10 and SOX9 expression correlated inversely.

Inhibition of SOX10 expression in melanoma cells by RNA interference induced cell cycle arrest, reduced cell viability and led to onset of (intrinsic) apoptosis. Moreover, SOX10 inhibition significantly reduced melanoma cell invasion in two- and three-dimensional invasion models, independent of onset of cell death. It was discovered that the reduced invasion capacity was mediated by melanoma inhibitory activity (MIA). MIA is a well-described secreted protein in melanoma cells that promotes migration and invasion and negatively correlates with patient's prognosis. Direct transactivation of MIA by SOX10 was found in this study.

Moreover, another novel target gene of SOX10 was detected by RNA sequencing studies and verified by promoter binding studies: peripheral myelin protein 2 (PMP2).

PMP2 is a small, lipid-binding, and membrane-associated β -barrel protein that is one of the most important proteins in the composition of the myelin sheath of Schwann cells. In this study, PMP2 expression was found in a subset of melanoma cell lines, along with other myelin proteins. Strikingly, PMP2 overexpression was able to enhance melanoma cell invasion.

In summary, this study shows that SOX10 is a key regulator of the invasion capacity of melanoma cells and activates invasion-promoting proteins such as MIA and PMP2. Therefore, SOX10 seems to be not only essential for the development of melanocytes but also critical for their neoplastic transformation and melanoma progression.

Zusammenfassung

Das Melanom ist die tödlichste Form des Hautkrebses mit jährlich über 20.000 Todesfällen allein in Europa.

Neue Therapiemöglichkeiten, insbesondere die Blockade von mutierten Kinasen des mitogenassoziierte Proteinkinase-Signalwegs und von Immun-Kontrollstellen, haben zu signifikant verbesserten Ansprech- und Überlebensraten verglichen mit Standard-Chemotherapien geführt. Jedoch profitieren nicht alle Patienten von den neuen Therapien und das häufige Auftreten erworbener Resistenzen bleibt weiterhin ein ungelöstes Problem. Daher stellt die Identifizierung neuer potenziell therapierbarer Faktoren im Melanom weiterhin einen wesentlichen Forschungsschwerpunkt dar.

Melanomzellen stammen von entarteten Melanozyten ab. Während der Embryonalentwicklung entstehen Melanozyten aus multipotenten Neuralleistenzellen. Charakteristische Eigenschaften der Neuralleistenzellen sind eine hohe Proliferationsrate, eine ausgeprägte Plastizität und eine Migrationsfähigkeit entlang definierter Wege.

Ein wesentlicher Faktor, der die Proliferation und das Überleben der Neuralleistenzellen sowie ihre Differenzierung zu Melanozyten sicherstellt, ist der Transkriptionsfaktor sex determining region-Y (SRY)-box 10 (SOX10). SOX10 wird nicht nur während der Embryonalentwicklung von Neuralleistenzellen exprimiert, sondern stellt auch einen spezifischen Marker für melanozytäre Zellen dar.

Charakteristische Schritte bei der Embryonalentwicklung von Melanozyten ähneln denen der Tumorentstehung und Progression. Es liegt nahe, dass SOX10 ähnliche Funktionen bei der Melanomentstehung regulieren könnte. Deshalb konzentrierte sich diese Arbeit auf die Erforschung der Rolle von SOX10 im Melanom.

Die Expression von SOX10 und dem nah verwandten Transkriptionsfaktor SOX9 wurde in humanen Haut- und Melanomzellen untersucht. Während SOX10 ausgeprägt in Melanozyten und in den meisten Melanom-Zelllinien, aber nicht in Fibroblasten nachgewiesen werden konnte, war die Expression von SOX9 in Fibroblasten und Melanozyten schwach und sehr variabel in Melanom-Zelllinien. In einigen Melanom-Zelllinien wurde eine inverse Expression von SOX10 und SOX9 festgestellt.

Eine Hemmung der SOX10-Expression in Melanomzellen mittels RNA-Interferenz führte zu Zellzyklus-Arrest, reduzierter Zellvitalität und (intrinsischer) Apoptose. Darüber hinaus wurde die Invasivität von Melanomzellen nach SOX10-Hemmung signifikant herabgesetzt und zwar unabhängig vom Einsetzen des Zelltods. Dies wurde in zwei-

und drei-dimensionalen Invasionsmodellen gezeigt. Als Vermittler dieser reduzierten Migrationsfähigkeit wurde melanoma inhibitory activity (MIA) entdeckt. MIA ist ein bereits gut beschriebenes sezerniertes Protein im Melanom, welches Migration und Invasivität fördert und einen negativen prognostischen Faktor für Melanompatienten darstellt. Die direkte Transaktivierung von MIA durch SOX10 konnte in dieser Studie gezeigt werden.

Darüber hinaus wurde peripheral myelin protein 2 (PMP2) als weiteres neues Zielgen von SOX10 mittels RNA-Sequenzierung entdeckt und durch Promotor-Bindestudien verifiziert.

PMP2 ist ein kleines, Lipid-bindendes und Membran-assoziiertes β -Fass-Protein, welches eines der wichtigsten Proteine beim Aufbau der Myelinscheide von Schwann-Zellen darstellt. In dieser Studie konnten PMP2 und andere Myelin-Proteine in wenigen Melanom-Zelllinien nachgewiesen werden. Eine Überexpression von PMP2 erhöhte die Melanomzell-Invasivität.

Zusammenfassend konnte gezeigt werden, dass SOX10 maßgeblich die Invasions-Kapazität von Melanomzellen reguliert und Invasions-fördernde Proteine wie MIA und PMP2 direkt reguliert. Somit scheint SOX10 nicht nur essenziell für die Entwicklung von Melanozyten zu sein, sondern auch eine entscheidende Rolle bei ihrer neoplastischen Transformation und der Melanomprogression zu spielen.

2 Introduction

Cancer is a leading cause of death worldwide, accounting for 8.2 million deaths and 14.1 million new cases in 2012 [269]. A substantive increase in cancer-related deaths is estimated due to growth and ageing of the global population. In Germany, 25% of death cases are related to cancer, which makes it the second common cause of death behind cardiovascular diseases (www.destatis.de).

Over 25 years of research have focused on the issue of how a normal human body cell can transform into a malignant one. The basis of this research has been set by the discovery of specific mutations: oncogenes with gain-of-function or suppressors with loss-of-function, which cause cancer phenotypes in experimental models. Hence, it seems that most types of human cancer share a small number of molecular, biochemical, and cellular changes that drive the progressive malignant conversion [95]. Cancer cells are characterized by their potential to proliferate indefinitely. They grow independent from growth signals and are resistant to growth inhibitors. Furthermore they show a high resistance against controlled cell death (apoptosis). They provide their own nutrition and oxygen by sustaining angiogenesis and are capable to overcome natural borders by invading in the surrounding tissue. Thereby they can spread to other organs, a process that is called metastasis.

Melanoma, the black skin cancer, is one of the deadliest types of cancer due to its rapid potential to progress, metastasize, and its high resistance against standard radio- and chemotherapies. Melanoma originates from neoplastically transformed melanocytes, the pigment cells of the skin.

2.1 Melanocyte Development

Pigment-producing melanocytes populate in the integument, inner ear, and eyes of vertebrate organisms. They originate as melanoblasts from the neural crest, which is formed at the edge of the neural plate on the border between the neural and non-neural ectoderm [131], [223]. Neural crest cells (NCCs) constitute a multipotent, highly migratory cell population that has the ability of self-renewal and is unique to vertebrate embryos. During or after neural tube closure, NCCs undergo epithelial-to-mesenchymal transition (EMT), start to migrate on distinct ways throughout the body and give rise to many cell derivatives (Figure 1). The fate of NCCs mostly depends on where they locally originate along the neuraxis, migrate and settle.

Cranial NCCs migrate dorsolaterally to produce the craniofacial mesenchyme that differentiates into cartilage, bone, cranial neurons, glia, and connective tissue of the face [233]. Cells from the vagal and sacral neural crest generate the parasympathetic (enteric) ganglia of the gut. The cardiac neural crest lies between the cranial and trunk neural crest and gives rise to smooth muscle cells from the heart outflow tract.

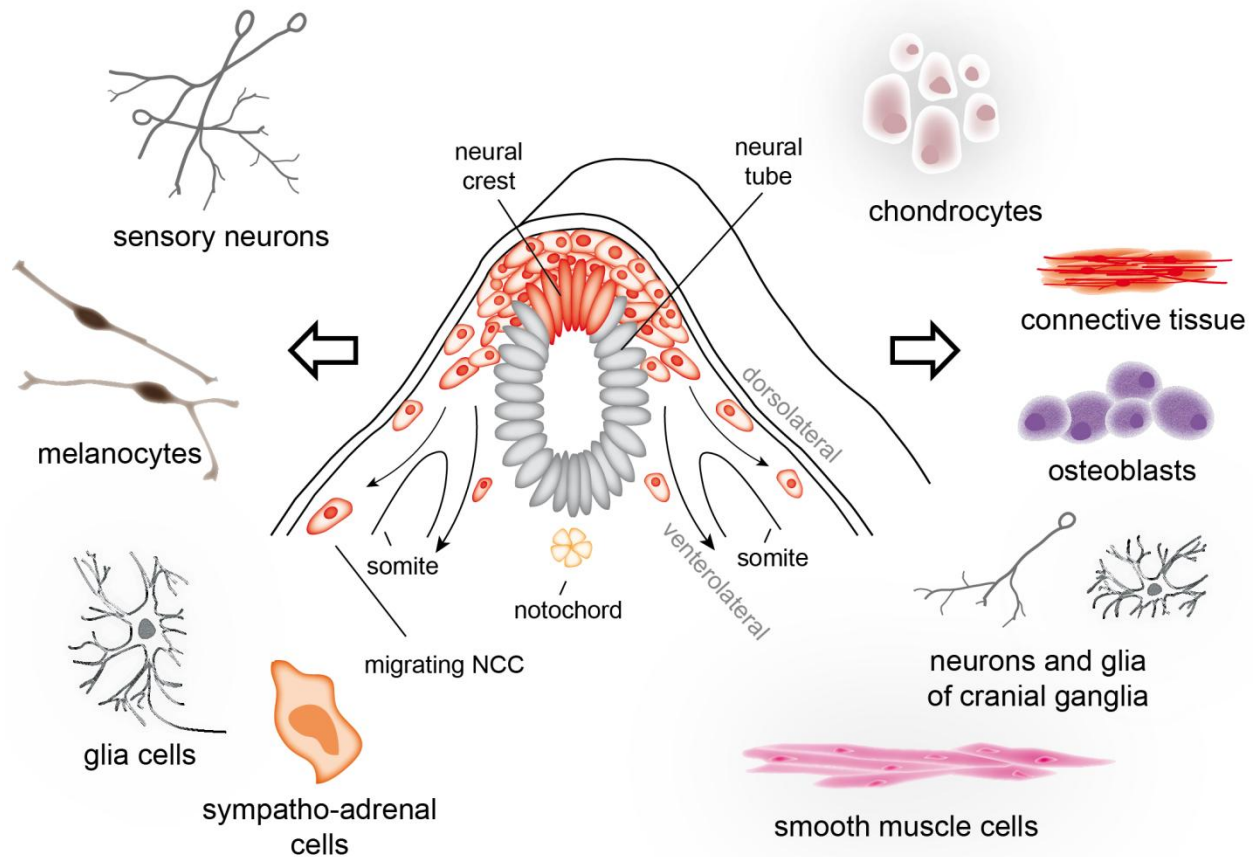


Figure 1: Embryonic development of neural crest cells.

After neurulation NCCs migrate out and differentiate into multiple cell types. While ventrolaterally migrating trunk NCCs differentiate to neurons and glial cells, dorsolaterally migrating cells become melanocytes.

Cells originating from the trunk neural crest after closure of the neural tube take two different pathways: ventrally and ventrolaterally migrating NCCs, between the somites and neural tube, form the sensory (dorsal root) and sympathetic neurons, adrenomedullary cells, and glial cells. On the other hand, cells migrating dorsolaterally into the ectoderm and continue toward the ventral midline of the belly become melanoblasts. While some studies demonstrate that melanocyte specification occurs in multipotent neural crest stem cells, others propose that lineage segregation already occurs in a premigratory stage [34], [138]. Non-melanoblast cells migrating along the dorsolateral pathway are eliminated by apoptosis [280]. However, it was shown that a

fraction of melanoblasts arises from NCCs migrating ventrally along the nerves that innervate the skin to acquire the melanocytic fate after detaching from these nerves at around embryonic stage 11 in mice [2].

The induction and specification of the neural crest depends on a strictly regulated network of signaling molecules and transcription factors. Neural crest formation, initiated during gastrulation by formation of a neural plate border, is dependent on fibroblast growth factor (FGF), bone morphogenic protein (BMP), Notch, and wingless (Wnt) signaling [66], [79], [142]. These signaling pathways activate transcription factors that define the neural plate border, e.g., zinc finger protein 1 (ZIC1), msh homeobox 1 (MSX1), MSX2, distal-less homeobox 3 (DLX3), DLX5, paired box protein 3 (PAX3), PAX7, and activator protein 2 (AP-2) [224]. To acquire the capability to emigrate from the neuroepithelium during EMT, NCCs undergo changes in their cytoskeleton, morphology, and cell contact molecules. Thereby they interact differently with other cells and their environment in comparison to non-migratory cells. These events are orchestrated by another class of transcription factors termed neural crest specifiers such as Snail, Slug, sex determining region Y (SRY)-box E (SoxE), forkhead box D3 (FOXD3), AP-2, Twist, avian myelocytomatosis viral oncogene homolog c (c-Myc), and inhibitor of DNA-binding protein (ID) family members. They furthermore regulate NCC proliferation, cell cycle control, and differentiation into several derivatives as mentioned before.

NCCs, designated to become melanoblasts, express specific markers like the receptor tyrosine kinase c-KIT. KIT signaling is required for melanoblast proliferation, survival, and migration [290]. A further marker is microphthalmia-associated transcription factor (MITF). Its expression is a key event in melanocyte specification [154], [190]. MITF regulates melanoblast proliferation through its target gene T-box 2 (TBX2) and survival through the anti-apoptotic protein B-cell lymphoma 2 (Bcl-2) [273]. Furthermore, it drives differentiation by activating enzymes for melanogenesis, i.e., tyrosinase, tyrosinase-related protein 1 (TYRP1), and dopachrome tautomerase (DCT), melanocytic surface proteins, i.e., silver, melanocortin 1 receptor (MC1R) and melanoma antigen (MLANA) as well as the tumor suppressor absent in melanoma 1 (AIM1). It has also been suggested that MITF transcriptionally activates Slug [221], a transcription factors that promotes EMT as mentioned before. MITF expression itself is regulated by PAX3, lymphoid enhancer-binding factor-1 (LEF1) through canonical Wnt signaling, cyclic

adenosine monophosphate (cAMP) response element-binding protein (CREB) via MC1R signaling, and sex determining region Y (SRY)-box 10 (SOX10) [273].

Melanoblast specification and proliferation is further regulated by transcription factors as FOXD3, SOX9, SOX10, PAX3, Slug, AP-2, and transcription factor AP-2 alpha (TCFAP2 α) [88], [179], [249].

At their target sites, the fully specified melanocytes produce melanin and transfer the pigment in melanosomes to adjacent keratinocytes. This pigment transfer leads to hair and skin coloring and protects the skin cells from damage by ultraviolet (UV) radiation [120]. Defects in NCC migration, proliferation and/or differentiation can cause genetic disorders, like Hirschsprung disease with reduced enteric ganglia, Waardenburg Syndrome (reduced melanocytes and hypopigmentation), and a number of cancers including melanoma.

2.2 From melanocytes to melanoma

One hallmark of cancer is the ability to reproduce indefinitely. Normal cells require mitogenic growth signals to change from a quiescent state into an active proliferative state. For cancer cells, three common molecular strategies are evident for achieving autonomy: altering extracellular growth signals, transcellular transducers of these signals, or intracellular circuits that translate those signals into action [95].

Malignant transformation of melanocytes to melanoma cells requires several simultaneous or sequential steps. Some melanomas develop de novo in the dermis or in association with congenital nevi [93], [287]. Others arise within the epidermis and invade across the basement membrane.

Wallace H. Clark described a classical histopathological pathway for the progression of melanocytes to melanoma [50] (Figure 2). The initiating step is the deregulated proliferation of melanocytes forming benign nevi followed by the formation of dysplastic nevi (clinical atypical nevus) occurring in pre-existing nevi or at new locations. Following transformation, melanocytes require the ability to proliferate intraepidermally and therefore this state is termed radial growth phase (RGP). The critical step in melanomagenesis is the progression of radial to vertical growth phase (VGP), where melanoma cells gain the ability to invade the dermis. This deep invasion enhances the potential of melanoma cells to disseminate via lymphatic or hematogenous routes, spread to distant organs and form distant tumors (metastases).

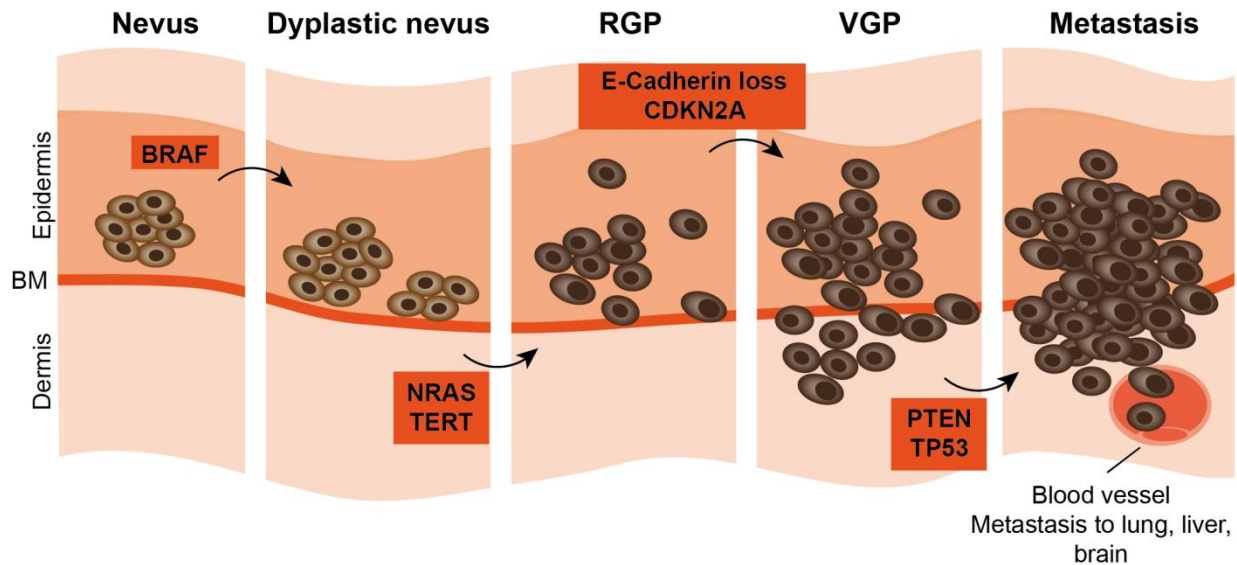


Figure 2: Clark model describing the development of malignant melanoma.

Typical genetic changes leading to progression of the stages nevus to metastasis are depicted within the figure and described in the text. BM = basement membrane, RGP = radial growth phase, VGP = vertical growth phase.

Under normal conditions, melanocyte proliferation in the epidermis is strictly regulated by their symbiotic relationship with keratinocytes. Melanocytes and keratinocytes are physically attached to each other with E-cadherin as the major adhesion molecule being expressed on both cell types [113], [264]. During melanoma progression, changes in expression of adhesion molecules contribute to deregulated proliferation and transformation. E-cadherin, P-cadherin, and desmoglein are downregulated through autocrine secretion of growth factors (GFs) or altered secretion of GFs by keratinocytes and fibroblasts upon ultraviolet (UV) irradiation [13], [14], [117], [156]. E-cadherin loss is a crucial event in the progression from RGP to VGP and is likely mediated by Snail, which is expressed in melanoma cells but not in melanocytes [202]. Furthermore, upregulation of receptors and signaling molecules such as N-cadherin and melanoma cell adhesion molecule (Mel-CAM) as well as altered expression of cell-matrix adhesion molecules and metalloproteases enhances self-assembly and decoupling from the basement membrane in transformed melanocytes [98], [113]. Thus, the microenvironment influences melanoma progression distinctively and its alteration is mediated by UV irradiation.

An important signaling pathway in melanocyte transformation and melanoma progression is the mitogen-activated protein kinase (MAPK) pathway. This pathway is activated by GFs that are recognized by cell surface receptors. Upon binding of these GFs, an intracellular signaling chain of kinases is turned on, that eventually activates

factors, which promote cell growth and proliferation. Mutations of mediators in this pathway lead to constitutive activation and thereby deregulated cell cycle progression.

The first oncogene identified in melanoma was neuroblastoma rat sarcoma viral oncogene homolog (NRAS) [61], [192]. It is a membrane-associated guanosine triphosphate (GTP)-binding protein, which can trigger a number of intracellular signaling pathways including the MAPK and phosphoinositide 3-kinase (PI3K) / protein kinase B (PKB also known as AKT) / mammalian target of rapamycin (mTOR) pathways. The PI3K pathway is an intracellular signaling pathway that regulates quiescence and proliferation.

V-Raf murine sarcoma viral oncogene homolog B (BRAF), a serine/threonine kinase in the MAPK pathway, is mutated in around 50-60% of melanomas [110]. *BRAF* mutations occur also in benign nevi suggesting that they represent an early event in the progression of neoplastically transformed melanocytes to melanoma [57], [201], [236].

Notwithstanding, additional genetic changes are required for malignant transformation of nevus cells. Another early event in the neoplastic progression are mutations within the *telomerase reverse transcriptase (TERT)* promoter that causes lengthening of telomeres in DNA strands [236]. Thereby, cells of early neoplastic lesions are dividing rather than being senescent presumably with reduced proliferation due to counteracting events e.g. replicative stress.

Mutations in the *cyclin-dependent kinase N2A (CDKN2A)* gene locus, encoding for inhibitor of cyclin-dependent kinase 4a (p16^{INK4A}) and alternative reading frame (p14^{ARF}), eliminate tumor suppressive pathways. *CDKN2A* mutation carriers have a higher risk of developing melanoma [16]. In a well established melanoma mouse model, overexpression of NRAS together with loss of p16^{INK4A} has resulted in melanoma formation, whereas loss of p16^{INK4A} alone was not sufficient for malignant transformation [1].

It was suggested that BRAF and phosphatase and tensin homolog (PTEN) cooperate in melanoma progression [270]. PTEN is an inhibitor of the PI3K. Loss of PTEN activates the PI3K/AKT/mTOR pathway, promoting cell growth and survival.

Inactivation of the tumor suppressor p53 is a general event in cancer development. Although mutations in the *tumor protein 53 (TP53)* gene are rare in melanoma, functional inactivation of p53 has been shown through several alternative mechanisms such as amplification of mouse double minute 2 homolog (MDM2), which abrogates p53 functions [181].

Another signaling pathway that is highly susceptible for mutations in melanocytes is the pathway of melanogenesis. Upon UV radiation, keratinocytes produce and secrete α -melanocyte stimulating hormone (α -MSH) binding to MC1R on melanocytes and thereby upregulating MITF via cAMP and CREB [177]. Genetic variants of *MC1R* and *MITF* are associated with pigmented phenotypes and an increased melanoma risk. *MITF* gene amplification and mutations have been found in metastatic melanoma and overexpression of MITF together with BRAF V600E contributes to melanocyte transformation [54], [80].

In summary, multiple events act together in the progression from melanocytes to melanoma, including genetic aberrations and influences from the microenvironment, which both can be induced by UV irradiation.

2.3 Malignant melanoma

Over 90% of melanoma cases evolve from a primary tumor that develops from melanocytes in the skin as the most common site of origination (cutaneous melanoma). Less common sites are the choroidal and retina layer of the eye (uveal melanoma) as well as respiratory, gastrointestinal, and genitourinary mucosal surfaces. In 1969, Clark and colleagues described criteria for clinical and histological subtypes of malignant melanoma with the main types superficial spreading, nodular, lentigo maligna, and acral lentiginous melanoma (ALM) [51]. These types allow a clinical diagnosis according to the ABCDE rule (A=asymmetry, B=border, C=color, D=diameter > 6mm, E=evolving) in 80% of cases [74].

So far, early detection and surgical excision remain the best gold standard of tumor therapy. Once the primary tumor has metastasized, the prognosis worsens dramatically. For evaluation of prognosis, appropriate therapy and follow-up, melanoma is classified in stages and subcategories according to the American Joint Committee on Cancer (AJCC). These implicate thickness, ulceration, and mitotic rate (mitoses per mm²) of the primary tumor, affection of lymph nodes, and distant metastases [9]. While the 10-year survival rate of patients with a small primary tumor (< 1mm) is about 90%, the 5-year survival rate of patients with distant metastasis is only about 17%.

Risk factors for the development of melanoma include a history of sunburns and intermittent exposure to strong sunlight, i.e., UV radiation. UVB (290-320 nm) can directly induce DNA damage, resulting in the formation of highly genotoxic cyclobutane pyrimidine dimers and pyrimidine(6-4)pyrimidone photoproducts. UVA (320-400 nm)

can generate free radicals, in particular reactive oxygen species, which also can cause DNA damage. Besides of these direct effects on DNA, indirect effects of UV radiation such as immunosuppression and stimulation of GFs, as mentioned before, contribute to melanoma development [12].

A family history of melanoma occurs in about 10% of melanoma patients and confers an approximately two-fold increase in melanoma risk [78]. Also phenotypical aspects like fair skin, red hair, freckles, numerous nevi, and atypical nevi are associated with increased melanoma risk.

Melanoma is an immunogenic tumor, i.e., a healthy immune system generates a strong immune response to melanoma cells. As a consequence the risk for melanoma is higher in immunocompromised patients like organ transplant recipients and acquired immune deficiency syndrome (AIDS) patients [175].

Considering the risk factors for melanoma and the ability of early detection of primary lesions, preventive measures such as sun protection and regular skin examinations have been propagated for many years. This may be the reason why in spite of increasing incidences the melanoma mortality rate remains rather constant.

2.4 Melanoma therapy and resistance

The first-line therapies of melanoma are surgical excision of the primary tumor and biopsy of the sentinel lymph node, the first draining lymph node of the site of the primary tumor. Advanced metastatic melanoma is characterized by high resistance against radiation and chemotherapy with a median survival of only 6-9 months and a 3-year survival rate of only 10-15% of patients [9]. Therefore, the development of novel therapeutical strategies against malignant melanoma is of utmost importance.

Although melanoma is an immunogenic tumor, cytokine-based immunotherapy with interferon (IFN) and interleukin-2 (IL-2) has only shown limited benefit.

Nevertheless, novel immunotherapeutic strategies targeting the blockade of T-cell activation with anti-cytotoxic T-lymphocyte-associated protein 4 (CTLA-4), anti-programmed cell death ligand 1 (PD-L1), and anti-programmed cell death 1 receptor (PD1) antibodies showed promising efficacy [109], [217], [298]. CTLA-4 is a transmembrane inhibitory receptor expressed on activated T-lymphocytes that downregulates T-cell activation upon binding to antigen presenting cells (APCs) [114]. PD-1 is expressed on T-cells and its ligand PD-L1 on melanoma cells and both act as negative regulators of T-cells. CTLA-4 antibody ipilimumab and PD-1 antibodies

nivolumab and pembrolizumab have been approved for treatment of metastatic melanoma by the Food and Drug Administration (FDA) and the European medicines agency (EMA) in 2011 and 2014/2015, respectively.

A milestone of melanoma treatment was set by the discovery of activating somatic point mutations in the *BRAF* gene driving melanoma cell proliferation and transformation via the MAPK-pathway (Figure 3) [57]. About 50% of all cutaneous melanomas carry a BRAF mutation, with V600E as the most common in about 80% and V600K in about 12-20% of cases [162], [163]. The frequency of *BRAF* mutations is higher in melanoma than in other human cancers. It has become an ideal target for therapy. Indeed, the treatment of patients with a BRAF V600-mutated melanoma with the BRAF-specific inhibitor vemurafenib (PLX4032) showed unprecedented objective response rates and a significant increase in overall survival in comparison to standard chemotherapy [42], [174]. Vemurafenib has been approved for melanoma therapy in 2011 in the USA and 2012 in Europe. Despite of the great success of this targeted monotherapy, about 50% of patients relapsed after about 7-8 months due to acquired resistance to therapy. Investigations of the underlying resistance mechanisms demonstrated that the MAPK signaling pathway is reactivated in 70-80% of cases most commonly by *RAS* mutations, *BRAF* amplifications, *BRAF* alternative splicing, or by mutations in *mitogen-activated protein kinase kinases (MEK)* or *MITF* [216], [272]. Other resistance mechanisms include the activation of the PI3K/AKT pathway, an upregulation of receptor tyrosine kinase (RTK) signaling (e.g. fibroblast growth factor receptor 3 [FGFR3], platelet-derived growth factor receptor β [PDGFR β], insulin-like growth factor 1 receptor [IGF1R]), and a downregulation of Bcl-2 homology (BH3)-only proteins [184], [240], [242], [277], [300].

Recent studies have demonstrated that the combination of BRAF-specific inhibitors (vemurafenib or dabrafenib) with MEK inhibitors (cobimetinib or trametinib) could further increase response rates, progression-free survival and overall survival in comparison to BRAF inhibitor monotherapy in advanced *BRAF*-mutated melanoma patients [147], [161]. The dabrafenib/trametinib combination has been approved by the FDA 2014 and by the EMA 2015, while the vemurafenib/cobimetinib combination has been approved 2015. However, also these combined therapies show relapses after around 11-12 months due to acquired resistance, especially by reactivation of the MAPK pathway [160]. Thus, new therapeutic strategies are based on a combination of inhibitors that abrogate resistance [106].

Although the majority of therapeutic strategies have been focused on mutations in BRAF, NRAS was the first identified oncogene in melanoma [192]. NRAS mutations are present in about 20% of melanoma cases with the most common mutations in codon 61 [150]. NRAS and BRAF mutations are mutually exclusive and 75% of melanomas have either mutation [85]. However, mutated NRAS is not targetable with drugs competing for the catalytic site, because NRAS activating mutations impair GTPase activity and an inhibitor would have to restore the GTPase activity, which has not been found yet. Thus, an alternative therapeutic strategy for NRAS mutant melanoma patients is targeting the downstream signaling of RAS including MEK, extracellular signal-related kinase (ERK), PI3K, and cyclin-dependent kinase 4 and 6 (CDK4/6) [7], [209].

In uveal melanoma BRAF and NRAS mutations are very rare, while 46% of cases show a mutation in the heterotrimeric guanine nucleotide binding protein Q (GNAQ) gene at position Q209, leading to an active G α protein that activates the MAPK pathway via BRAF [189]. Another mutation in this family of receptor molecules is the mutation of guanine nucleotide binding protein 11 (GNA11), which is mutually exclusive to the GNAQ mutation and occurs in 32% of uveal melanoma cases [274].

Further common mutations in malignant melanoma include activating mutations in the receptor tyrosine kinase c-KIT (20-30 % of ALM, mucosal melanomas and melanomas on chronically sun-damaged skin), inactivation of PTEN (30-50% of melanomas), mutations in the PI3K/AKT pathway (PI3K subunit phosphatidylinositol-4,5-bisphosphate 3-kinase catalytic subunit alpha [PIK3CA] and AKT3), and loss-of-function mutations in neurofibromin 1 (NF1) - a negative regulator of RAS-signaling - in approximately 25% of BRAF/NRAS-wild type melanomas [48], [56], [85], [110], [232], [270].

In summary, a lot of achievements have been made in terms of melanoma therapy especially regarding immune checkpoint blockade and targeted mutation-based therapy. However the complex network of oncogenes and signal transduction requires interventions at multiple sites and therefore the identification of novel therapeutical targets is still a requisite for the successful treatment of melanoma.

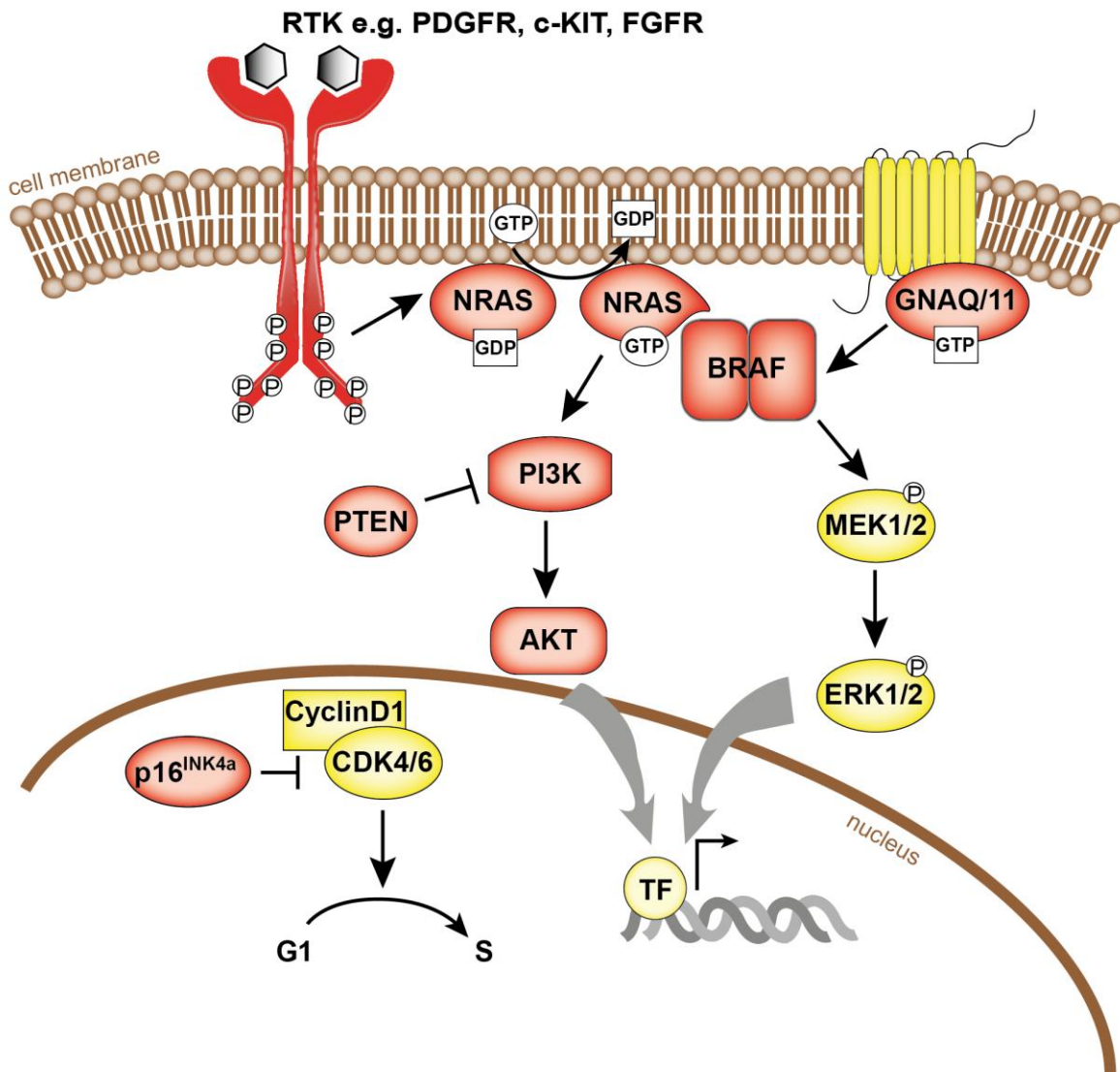


Figure 3: Mutation-prone signaling pathways in melanoma.

Illustrated is the MAPK pathway, activated via RTKs and mediated by GTP-coupled NRAS or GNAQ/11, leading to activation of BRAF that in turn activates MEK and ERK by phosphorylation. NRAS also activates the PI3K/AKT pathway. CDK4/6, which can be blocked by p16^{INK4A}, drives cell cycle progression from G1- to S-phase. Several mediators of these pathways are commonly mutated in melanoma as described in the text (section 2.4). TF = transcription factor.

2.5 Linking melanomagenesis to the embryonic development of melanocytes

Fundamental processes of embryonic melanocyte development and regeneration share a great deal of cellular and genetic events with their malignant transformation [294]. During early embryonic development, NCCs represent a highly proliferative and multipotent cell population before specification into certain cell types. Melanoblasts migrate along the dorsolateral axis of the embryo while they continue to expand and promote their own survival. They possess an almost unlimited capacity of self-renewal,

which can be also found in regenerative processes of adult melanocytes, e.g., during hair and skin coloration.

In contrast to malignant progression, embryogenesis and regenerative processes are strictly regulated. Regenerative melanocytic stem cells can be found in the bulge of hair follicles. During the hair follicle cycle, differentiated melanocytes are generated in the bulge region and migrate from the bulge to the bulb where they transfer melanin to hair-producing keratinocytes and thereby induce hair coloring [244]. The process of hair graying can be linked to a gradual failure to maintain the melanocyte stem cell self-renewal in the hair follicle bulge and can be analyzed in mouse models with defects in hair pigmentation [186], [187].

Characteristics of embryonic and adult stem cells, which are the potential of self-renewal, differentiation, and almost unlimited proliferation [213] have also been described in a subpopulation of cancer cells that are extremely aggressive, resistant to radiation and chemotherapy, and have a specific capacity for tumor initiation: the cancer stem cells. This subpopulation has also been characterized in melanoma and can be detected by the expression of stem cell markers like CD133 (also known as prominin-1), ATP binding cassette sub-family B member 5 (ABCB5), CD271 (also known as p75 neurotrophin receptor or nerve growth factor receptor), and the enzyme aldehyde dehydrogenase [19], [23], [73], [225].

Another feature that melanoma cells share with developing melanoblasts is the ability to migrate extensively, since NCCs migrate out, and „metastasize“ to numerous sites of the body. Strikingly, melanoma cells express a number of lineage-specific markers that are typical for embryonic and regenerating melanocytes like endothelins and their corresponding receptor endothelin receptor type B (EDNRB), and c-KIT [143], [183].

Interestingly, transcription factors commonly expressed in melanoma cells are also required specifically during melanocyte development, especially in migratory NCCs. The transcription factor Slug, which plays an important role in EMT in NCCs, promotes metastasis of transformed melanocytes [91]. Another example is MITF, which is the key factor for melanocyte differentiation during embryogenesis, and which has been shown to be involved in melanoma initiation and progression [154]. Therefore, studies of lineage specific transcription factors, which regulate developmental programs that are recapitulated during melanomagenesis, can provide insight into the genetic causes of melanoma and its progression.

2.6 SOX transcription factors in development and disease

The SOX transcription factor family comprises approximately 30 vertebrate and over a dozen invertebrate gene or gene fragment members, with 20 orthologous pairs of SOX genes in human and mice, which are named after the original member SRY (sex-determining region-Y) [29], [227]. All Sox members share a similar DNA-binding high-mobility group (HMG) domain that recognizes the consensus sequence 5'-(A/T)(A/T)CAA(A/T)G-3'. The HMG domain contains two nuclear localization signals and a nuclear export signal for shuttling the protein between nucleus and cytoplasm. With this domain, SOX transcription factors bind to the minor groove of the DNA and induce a strong structural bend, indicating that they exert structural roles on regulatory DNA regions [289]. SOX factors can bind the DNA as monomers or hetero- and homodimers [164], [197], [255]. They often function in cooperation with other transcription factors that influence their activity. SOX proteins are involved in a diverse range of developmental processes, reflecting their evolutionary history in metazoans. They can be divided into nine subgroups: A, B1, B2, C, D, E, F, G, and H (Table 1).

SOX group	Genes and major known or deduced functions
A	<i>SRY</i> (testis determination)
B1	<i>SOX1</i> (lens development, neural determination), <i>SOX2</i> (neural induction, lens induction, pluripotency), <i>SOX3</i> (neural determination, lens induction)
B2	<i>SOX14</i> (interneuron specification, limb development), <i>SOX21</i> (central nervous system patterning)
C	<i>SOX4</i> (heart, lymphocyte, thymocyte development), <i>SOX11</i> (neuronal, glial maturation), <i>SOX12</i> (ortholog <i>SOX22</i> ; development of many tissues)
D	<i>SOX5</i> (chondrogenesis), <i>SOX6</i> (chondrogenesis, cardiac myogenesis), <i>SOX13</i> (development of arterial wall, pancreatic islets)
E	<i>SOX8</i> (development of many tissues), <i>SOX9</i> (chondrogenesis, sex determination), <i>SOX10</i> (neural crest specification)
F	<i>SOX7</i> (development of vascular and many other tissues), <i>SOX17</i> (endoderm specification), <i>SOX18</i> (vascular and hair follicle development)

G	SOX15 (ortholog SOX20; myogenesis)
H	SOX30 (male germ cell maturation)

Table 1: SOX groups with according genes and their major known or deduced functions.

Modified from Bowles et al. and Schepers et al. [29], [227].

In general, SOX-transcription factors play a key role in embryonic development of NCCs and are also major determinants of stem cell behavior [222]. SoxE transcription factors, comprising SOX8, SOX9, and SOX10, are major players in the neural crest development [223]. As mentioned before (section 2.1), they are neural crest specifiers, i.e., they regulate effector genes that mediate terminal differentiation of the derivative cell. Structurally they share highly conserved domains, which are a DNA-dependent dimerization domain, the DNA-binding HMG domain, a K2 domain, and a C-terminal transactivation domain [288]. The K2 domain provides an additional transactivation capacity in selected cell types and under specific developmental conditions. It still needs to be clarified how SoxE factors are modulated to allow such functional diversity and nuclear/cytoplasmatic translocation [92]. Many mechanisms might be involved, including post-translational modifications as phosphorylation, acetylation, and small ubiquitine like modifier (SUMO)ylation, as well as context-dependent interactions with other factors. The interaction with other transcription factors is mediated by the HMG domain [297]. In several organ systems each of the SoxE member's function is likely to be redundant and possibly compensated by other family members.

SOX8 is expressed in various tissues during embryonic development but is often turned off in the mature stage of the cell, while its expression continues in the brain, spinal cord, and testis [199], [226], [245]. During embryogenesis and in tissue development, it rather plays an auxiliary role, e.g., by reinforcing SOX9 in testis differentiation [40] and SOX10 during adrenal gland and enteric nervous system development [169], [212].

Another SoxE family member, SOX9, has specific functions in the development of chondrocytes and in testis formation by regulating extracellular matrix proteins like collagen type II $\alpha 1$ [153] and the anti-Müllerian hormone [59]. Heterozygous loss-of-function mutations in the SOX9 gene causes campomelic dysplasia, a human disorder characterized by defective chondrogenesis, male-to-female sex reversal, and other variable organ defects [279]. SOX9 is also expressed in various adult tissues where it maintains stem cell homeostasis and regeneration [77]. However, dysregulation of these qualities promotes neoplasia and SOX9 has been implicated in the formation and

growth of tumors in the prostate, central nervous system, skin, pancreas, ovary, and esophagus [121].

Furthermore, SOX9 plays a crucial role during the embryonic development in the neural crest together with the structurally related factor SOX10. During melanocyte development, SOX9 and SOX10 come up in different developmental stages with SOX9 particularly expressed in pre-migratory NCCs and shut off soon after EMT, and SOX10 expressed in early delaminating and migrating NCCs [101]. Both factors control multipotency, survival, and proliferation of NCCs and promote their differentiation into glial cells and melanocytes but not into the neuronal lineage at later stages [46]. While SOX9 expression continues in glial cells [46], [257], SOX10 expression persists in glial cells of the peripheral nervous system (including Schwann cells), in oligodendrocytes of the central nervous system, and in melanocytes [47], [101], [126].

SOX10-deficient mice lose most or all of their melanocytes [31], [107], [125], [248], emphasizing the crucial role of SOX10 for melanocyte differentiation. As mentioned in section 2.1, SOX10 transactivates MITF expression with which it controls DCT, an enzyme that is essential for the synthesis of melanin, and other melanogenic enzymes like TYRP1 and tyrosinase [119], [164], [180], [207].

Furthermore, *in vivo* analyses of transgenic mice showed that SOX10 is also expressed in melanocyte stem cells (McSCs) in hair follicles [102]. SOX10 knockout led to loss of McSCs and melanocytes while SOX10 overexpression led to premature differentiation and loss of McSCs causing hair graying. Thus, SOX10 levels seem to be critical for McSC function and maintenance.

SOX10 also plays a role in fate determination of other neural crest derivatives such as sympathetic neurons by regulating the achaete-scute homologue *ash1* (MASH1) and paired like homeobox 2b (PHOX2B) [128], the sensory neurons via neurogenin-1 [126], and Schwann cells by activating Schwann-cell specific genes like myelin protein zero (MPZ), myelin basic protein (MBP), and proteolipid protein 1 (PLP1) [196], [256]. Furthermore, it regulates differentiation of the enteric nervous system by activating the RTK c-RET together with PAX3 [145], [146], and EDNRB in collaboration with endothelin-3 [253], [306].

Since SOX10 regulates the development of several cell lineages, loss of SOX10 causes different phenotypic manifestation in disorders. Homozygous deletion of *SOX10* in mice leads to embryonic lethality, while *SOX10* haploinsufficiency causes pigmentary defects, and a dominant megacolon [31], [248]. In zebrafish, all pigment cells are absent

when SOX10 expression is abrogated [64]. In humans, heterozygous mutations of *SOX10* cause Waardenburg syndrome Type 2, which is characterized by partial depigmentation of the hair, skin or iris, and sensory deafness due to melanocyte loss from the stria vascularis of the inner ear, as well as Waardenburg-Hirschsprung disease or Waardenburg-Shah syndrome (a combination of Waardenburg syndrome and Hirschsprung disease) causing aganglionosis of the colon [20], [200]. Additionally, truncating mutations of SOX10 can cause Peripheral demyelinating neuropathy, central dysmyelination, Waardenburg syndrome, and Hirschsprung disease (PCWH), in which Waardenburg-Hirschsprung disease is combined with peripheral demyelinating neuropathy and central dysmyelinating leukodystrophy [20], [115].

In context of melanomagenesis, the distinct roles of SOX9 and SOX10 remain widely unclear so far. SOX10 is expressed in melanocytes, congenital nevi, primary and metastatic melanoma, while SOX9 expression has been found present and absent in melanocytes, nevi, and melanoma [4], [8], [52], [195], [238], [239]. Other data demonstrate that upregulation of SOX9 reduces melanoma cell growth but increases invasion [44], [195]. A recent study suggests that SOX9 and SOX10 are functional antagonists in postnatal melanocyte and melanoma development [238]. Besides this potential antagonistic role, SOX9 and SOX10 both regulate factors like MITF and DCT in melanocytes or the intermediate filament nestin in melanoma cells [72], [194].

Several recent studies indicate that SOX10 appears to be oncogenic and is responsible for melanoma initiation as well as survival and proliferation [53], [239]. Furthermore, low frequencies of intragenic mutations in the *SOX10* gene suggest that SOX10 wild type function is required for melanoma formation and maintenance [53], [54]. SOX10 also appears to play a role in reversible and adaptive resistance to BRAF inhibition in melanoma [261]. Therefore, a crucial relation of SOX10 to melanomagenesis is suggested.

However, targeting SOX10 or other transcription factors that are dysregulated in melanoma is difficult as these proteins lack an enzymatic domain, which would allow the development of allosteric or competitive small molecule inhibitors. Agents that block association to coregulators or the binding region of these transcription factors in target genes would be necessary. On the other hand, pleiotropic effects on the expression of a multitude of genes resulting in unacceptable toxicity by the inhibition of a specific transcription factor are most likely. Therefore understanding the biological contribution

of its target genes is of utmost importance and might lead to the discovery of alternative targets that are amenable to pharmacologic therapy.

2.7 Aims of this study

SOX10 seems to play an important role in melanoma initiation, progression and survival. However, the distinct functions of this transcription factor in melanoma remain unclear. To elucidate the function of SOX10 in comparison to SOX9, following issues have been addressed:

1. Analysis of the expression of SOX10 and SOX9 in melanoma cell lines at different progression stages and in in-house generated short term cultures on messenger ribonucleic acid (mRNA) and protein levels as well as in human skin cells (primary fibroblasts and melanocytes).
2. Phenotypic effects of SOX10 inhibition via RNA interference and SOX10 ectopic overexpression on cell morphology, invasion capacity, proliferation, and cell death.
3. Identification of SOX10 target genes that could mediate the observed phenotypic effects based on literature and on RNA sequencing analysis.
4. Evaluating direct transcriptional activation/repression of these identified targets and analyzing their functions in melanoma cells.

3 Materials and Methods

3.1 Materials

3.1.1 Media

Melanocyte growth medium

Medium 254CF (Gibco® by Life Technologies; Carlsbad, California, USA)	500 ml
CaCl ₂ (0.2 M; Gibco® by Life Technologies)	0.5 ml
HMGS-2 (Gibco® by Life Technologies)	5 ml

Fibroblast growth medium

DMEM (Gibco® by Life Technologies)	500 ml
Fetal bovine serum (FBS superior; Millipore/Merck, Darmstadt, Germany)	50 ml
L-glutamine (200 mM, Gibco® by Life Technologies)	5 ml

Fibroblast-conditioned medium

Fibroblast-conditioned medium as required for Matrigel invasion assays was generated by incubating a confluent T75 flask of primary human fibroblasts with 10 ml DMEM/1% L-glutamine at 37°C and 5% CO₂ for 24 hours. The supernatant containing the conditioned medium was centrifuged at 1000 rpm and room temperature for 3 minutes. This supernatant was aliquoted in 1.5 ml tubes and stored at -20°C.

Tumor 2% (TU2%)

MCDB153 (Sigma, Taufkirchen, Germany, in H ₂ O bidistilled); pH 7.4 adjusted with NaHCO ₃ (Gibco® by Life Technologies)	500 ml
Leibovitz L-15 (Gibco® by Life Technologies)	50 ml
FBS	10 ml
Insulin (10 µg/ml, Sigma)	0.25 ml
CaCl ₂ (2 M, Sigma)	0.42 ml

Luria-Bertani Broth (LB) Medium

12.5 g LB powder (Sigma) in 500 ml H₂O bidestilled, autoclaved

Agar plates

7.5 g Select-Agar (Life Technologies) in 500 ml LB medium, autoclaved

Antibiotics for selection

Ampicillin (100 mg/ml, Sigma)	100x
Kanamycin (10 mg/ml, Gibco® by Life Technologies)	100x
Puromycin (10 mg/ml, Life Technologies)	cell line dependent

Further solutions for cell culture usage

0.05% Trypsin-EDTA in HBSS (Gibco® by Life Technologies)	for cell detachment
0.2% EDTA in PBS (phosphate-buffered saline; Pharmacy of the University Hospital of Munich)	for gentle detachment of cells
ABAM (100x, Gibco® by Life Technologies)	antibiotics, antimycotics
Deep-freezing solution (FBS + 10% DMSO, Sigma)	for cell storage in liquid nitrogen
HBSS (Hank's balanced salt solution; Gibco® by Life Technologies)	for cell washing

10x Digestion solution for preparation of primary melanoma cells

Collagenase (Sigma)	0.5%
Dispase (Sigma)	0.73%
Hyaluronidase (Sigma) in HBSS	1%

3.1.2 Buffers and solutions

If not otherwise stated, buffers and solutions were prepared with bidestilled H₂O from the Pharmacy of the University Hospital of Munich or with aqua ad injectabilia (Braun, Melsungen, Germany).

3.1.2.1 Buffers and solutions for immunoblotting

Cold Spring Harbor (CSH) buffer for whole cell lysate preparation

Tris-HCl pH 7.4 (Sigma)	50 mM
NaCl (Sigma)	250 mM
EDTA (Sigma)	1 mM
TritonX-100 (Sigma)	0.1 %
Protease inhibitors complete mini (Roche, Penzberg, Germany)	1x
PhosStop phosphatase inhibitors (Roche)	1x

RIPA buffer for whole cell lysate preparation

Tris-HCl pH 7.4 (Sigma)	50 mM
NaCl	150 mM
SDS (Sigma)	0.1%
Deoxycholic acid sodium salt (Merck)	1%
Triton X-100	1%
Protease inhibitors complete mini (Roche)	1x
PhosStop phosphatase inhibitors (Roche)	1x

Running buffer

NuPAGE® MES SDS Running Buffer (Life Technologies)	1x
NuPAGE® Antioxidant (Life Technologies)	0.25%

Transfer buffer

NuPAGE® Transfer buffer (Life Technologies)	1x
NuPAGE® Antioxidant (Life Technologies)	0.1%
Methanol pro analysi (p.a.) ≥ 99.8% (Merck)	10% (20% for blotting two gels at one time)

Ponceau S staining solution

Ponceau S (Sigma)	0.1%
Acetic acid (Merck)	5%

Blocking buffer

Western blocking reagent, solution (Roche)	10%
Sodium fluoride (Sigma)	50 mM
in PBS	

Washing buffer

0.1% Tween20 (Calbiochem/Merck) in PBS

*3.1.2.2 Buffers and solutions for fluorescence-activated cell sorting***ANPI staining buffer**

HEPES pH 7.4 (Sigma)	10 mM
NaCl	140 mM
CaCl ₂ (Sigma)	5 mM

Annexin V-staining solution for one sample

Annexin V-Fluos (Roche)	1 µl
ANPI staining buffer	49 µl

Propidium iodide staining solution for one sample

Propidium iodide (Sigma, 0.5 mg/ml in PBS)	10 µl
ANPI staining buffer	50 µl

Fixing solution for cell cycle analysis

75% Ethanol p.a. (VWR, Fontenay-sous-Bois cedex, France) in H₂O bidistilled

Washing buffer for cell cycle analysis

1% BSA (w/v, Sigma) in PBS

Cell cycle staining solution for one sample

Propidium iodide (Sigma, 5 mg/ml)	0.8 µl
RNAse A (Sigma, 10 mg/ml in PBS)	0.8 µl
Washing buffer	300 µl

3.1.2.3 Buffers and solutions for luciferase reporter assay

Lysis buffer

5x passive lysis buffer (Promega, Madison, Wisconsin, USA) diluted to 1x with PBS

TE buffer

Tris-HCl pH 8	1%
EDTA pH 8	0.2%

Luciferase reporter solution

50% ATP substrate (in TE buffer; Biothema, Handen, Switzerland)

50% Luciferin substrate (in TE buffer; Biothema)

Renilla Substrate

1 μ l Coelenterazine (Promega; 1 μ g in 1 ml Methanol p.a.) in 800 ml H₂O bidistilled

3.1.2.4 Buffers and solutions for electrophoretic mobility shift assay

10x Binding buffer

HEPES (pH 7.4)	100 mM
NaCl	500 mM
EDTA pH 8	1 mM
Glycerol (Merck)	50%
MgCl ₂ (Merck)	50 mM

1x TBE

Trizma® base (Sigma)	89 mM
Boric acid (Sigma)	89 mM
EDTA	2 mM

3.1.2.5 Buffer for immunohistochemistry

Tris buffer

0.5 M Tris-HCl buffer pH 7.6	10%
1.5 M NaCl	10%

3.1.2.6 Buffers for chromatin immunoprecipitation

Cell lysis buffer

PIPES pH 8 (Sigma)	5 mM
KCl (Fluka/Sigma)	85 mM
NP-40 (Sigma)	0.5%
Protease inhibitors complete mini	1x

Nuclear lysis buffer

Tris-HCl pH 8	50 mM
EDTA pH 8	10 mM
SDS	1%
Protease inhibitors complete mini	1x

IP dilution buffer

Tris-HCl pH 8	16.7 mM
NaCl	167 mM
EDTA pH 8	1.2 mM
Triton X-100	1%
SDS	0.01%
Protease inhibitors complete mini	1x

Low salt wash buffer

Tris-HCl pH 8	20 mM
NaCl	150 mM
EDTA pH 8	2 mM
Triton X-100	1%
SDS	0.1%

High salt wash buffer

Tris-HCl pH 8	20 mM
NaCl	500 mM
EDTA pH 8	2 mM
Triton X-100	1%
SDS	0.1%

LiCl wash buffer

Tris-HCl pH 8	10 mM
EDTA pH 8	1 mM
LiCl (Sigma)	0.25 mM
NP-40	1%
Deoxycholic acid sodium salt (Merck)	1%

Elution buffer

SDS	1%
NaHCO ₃ (Merck)	0.1 M

3.1.2.7 Further buffers and solutions**RNase free water (H₂O/DEPC)**

0.1% (w/v) Diethylpyrocarbonat (Sigma) in H₂O bidestilled, autoclaved

Collagen mix (for spheroid assay)

10x EMEM (Lonza, Basel, Switzerland)	420 µl
L-glutamine (100x)	38 µl
FBS	462 µl
NaHCO ₃ (Gibco® by Life Technologies, 7.5%)	78 µl
Collagen (Type I, rat tail; BD Biosciences, Bedford, Massachusetts, USA; adjusted to 1.3 mg/ml with 0.05% acetic acid)	3.5 ml

The collagen mix was prepared on ice and adjusted to an orange/red color by adding further NaHCO₃.

3.1.3 Commercial kits

Buffers and solutions from commercial kits are not listed separately.

Name	Supplier	Application
Amersham™ ECL™ Prime Western Blot Detection Reagent	GE Healthcare (Buckinghamshire, Great Britain)	immunoblot detection
Bio-Rad Protein Assay	Bio-Rad (Munich, Germany)	measuring protein concentration according to Bradford [30]

Pierce™ BCA Protein Assay Kit	ThermoFisher Scientific (Bonn, Germany)	measuring protein concentration
CellTiter-Blue® Cell Viability Assay	Promega	determination of cell viability
Dako REAL™ Detection System	Dako (Glostrup, Denmark)	detection of immunohistochemistry (IHC)
DIG luminescent detection kit	Roche	Electrophoretic mobility shift assay (EMSA), detection of digoxigenin (DIG)-labeled oligonucleotides
Gateway® LR Clonase® II enzyme mix	Life Technologies	<i>in vitro</i> recombination
LightCycler® TaqMan® Master	Roche	quantitative real-time polymerase chain reaction (qRT-PCR)
LIVE/DEAD® viability/cytotoxicity kit	Life Technologies	staining of viable cells with calcein AM and dead cells with ethidium homodimer-1 (EthD-1)
Venor® GeM	Minerva Biolabs (Berlin, Germany)	detection of mycoplasma contamination in cell culture
Nuclear extract kit	Active Motif (La Hulpe, Belgium)	purification of nuclear proteins
NucleoSpin® Plasmid Kit	Macherey-Nagel (Düren, Germany)	plasmid extraction
NucleoSpin® Gel and PCR Clean-up (with NTB buffer)	Macherey-Nagel	purification of DNA from PCR, agarose gels, and chromatin immunoprecipitation (ChIP)
QuikChange Lightning Site-Directed Mutagenesis Kit	Agilent Technologies (Santa Clara, California, USA)	introducing point mutations in plasmids
Rapid DNA Ligation Kit	Roche	DNA ligation for cloning
Reverse transcriptase	Roche	reverse transcription to generate copy DNA (cDNA) from mRNA

RNeasy™ Mini Kit	Qiagen (Hilden, Germany)	RNA extraction
SIGMA FAST™ Fast Red TR/Naphthol AS-MX	Sigma	Alkaline Phosphatase Substrate Tablets Set for IHC detection

Table 2: Commercial kits.

3.1.4 Transfection reagents

Lipofectamin™ RNAiMAX (Life Technologies) for small interfering RNA (siRNA) transfection.

FuGENE® 6 Transfection Reagent (Promega) for plasmid transfection.

3.1.5 Oligonucleotides

Productions of oligonucleotides as well as sequencing analyses were performed by Eurofins Genomics, Ebersberg, Germany.

3.1.5.1 Primers for quantitative real-time PCR

Primers for mRNA quantification from cDNA after reverse transcription			
Gene	Forward (5'→3')	Reverse (5'→3')	Probe
<i>CtBP1</i>	CGAGTCGGAACCCTTCAG	CAGATGAGGTTGGGTGCA	#81
<i>GJB1</i>	TGCAGACATTCTCTGGGAAA	ATCCTGCCTCATTACACACCT	#71
<i>GJC2</i>	AGGGCTCTGAGGGAGACTG	CAGCTCATGTTGGTCATAGG G	#80
<i>ERBB3</i>	CACAATGCCGACCTCTCCC	CACGAGGACATAGCCTGTCA	#86
<i>FTL</i>	GCTGAACCAGGCCCTTTT	TCCAGGAAGTCACAGAGATG G	#37
<i>GH1</i>	TCACCTAGCTGCAATGGCTA	AGGCACTGCCCTCTTGAA	#13
<i>H1FX-AS1</i>	TTTTTGTGAAGCCGTTGC	CCTCAACGTTGTCCTGTGC	#60
<i>HMG1</i>	CATTGAGCTCCATAGAGACA GC	GGATCTCCTTTGCCCATGT	#73
<i>HPRT</i>	TGACCTTGAATTTATTTTGC ATACC	CGAGCAAGACGTTTCAGTCCT	#73

<i>ITGA3</i>	GAGGACATGTGGCTTGGAG T	GTAGCGGTGGGCACAGAC	#13
<i>ITGA4</i>	GATGAAAATGAGCCTGAAA CG	GCCATACTATTGCCAGTGTTG A	#22
<i>ITGAV</i>	ACTTGACTGTGGTGAAGAC AATG	GGGTTGTCATCCCCAATATA GA	#11
<i>ITGB1</i>	CGATGCCATCATGCAAGT	ACACCAGCAGCCGTGTAAC	#65
<i>ITGB3</i>	CGCTAAATTTGAGGAAGAAC G	GAAGGTAGACGTGGCCTCTT T	#76
<i>KLF10</i>	TCTGAAGGCCACACGAG	ACCTCCTTTCACAACCTTTCC	#2
<i>MIA</i>	GGCCAAGTGGTGTATGTC T	CAGATCTCCATAGTAATCTCC CTGA	#16
<i>M-MITF</i>	CATTGTTATGCTGGAAATGC TAGA	TGCTAAAGTGGTAGAAAGGT ACTGC	#62
<i>MPZ</i>	TATCCTGGCTGTGCTGCTC	TGTCGGTGTAACCACGATG	#56
<i>NR1D1</i>	AACTCCCTGGCGCTTACC	GAAGCGGAATTCTCCATGC	#17
<i>PLP1</i>	CTGCCAGTCTATTGCCTTCC	AGCATTCCATGGGAGAACAC	#53
<i>PMP2</i>	TTGACGATTACATGAAAGCT CTG	GCTGATGATCACAGTGGGTT T	#48
<i>PPP1R15 A</i>	GCTTCTGGCAGACCGAAC	GTAGCCTGATGGGGTGCTT	#24
<i>RPL27a</i>	CGATACCTCGCGAGACTTG	CCTAAGTTTCCGGGTCTTCC	#26
<i>SOX9</i>	GTACCCGCACTTGCACAAC	TCGCTCTCGTTCAGAAGTCTC	#61
<i>SOX10</i>	GACCAGTACCCGCACCTG	CGCTTGTCACCTTTCGTTTCAG	#61
<i>TIPARP</i>	GGAAATTCTTCTGTAGGGAC CA	AATCAATCGAATGACAGACTC G	#58
Primers for DNA quantification after ChIP			
Name	Forward (5'→3')	Reverse (5'→3')	Probe
MIChIP _Set3	TGGGCTGTTTCTGGTAATC A	CACCTTGGAATTTCTGTGC	#43
PMP2_	TGCTCTGCTGCAATCGACT	GAAGGCTTGGCATAGTTCACA	#13

ChIP1	GAC		
PMP2_ ChIP2	GCAGGGTAAGATCATGGT TCA	AAATTGCTCCCAAAGTTGAAT	#55
hActin intron 2	CGCCCTTTCTCACTGGTTC	TCCAAAGGAGACTCAGGTCAG	#29

Table 3: Primers for mRNA and ChIP-DNA quantification.

Primers for qRT-PCR were designed with the open software “Assay Design Center” from Roche (www.universalprobelibrary.com) including an intron spanning assay. For design of primers for DNA quantification after ChIP, the intron spanning was excluded. Probes derived from the “Universal Probe Library, Human” from Roche.

3.1.5.2 Primers for polymerase chain reaction

Name	Sequence (5'→3')	Purpose
KpnI_SOX9_fwd	AGGAGGTACCAAATGAATCTC CTGGACC	Cloning of SOX9 into pENTRY4-flag.
XhoI_SOX9_rev	AGGACTCGAGTCAAGGTCGAG TGAG	Cloning of SOX9 into pENTRY4-flag.
KpnI_SOX10_fwd	ATTAGGTACCAAATGGCGGAG GAGCAG	Cloning of SOX10 into pENTRY4-flag.
XhoI_SOX10_rev	ATTACTCGAGTTAGGGCCGGG ACAGT	Cloning of SOX10 into pENTRY4-flag.
KpnI_PMP2_fwd	ATTAGGTACCGCAAATAGCA ACAAATTC	Cloning of PMP2 into pENTRY4-flag.
XhoI_PMP2_rev	ATTACTCGAGCTGGACCTTCT CATAGA	Cloning of PMP2 into pENTRY4-flag.
pMIA_ATtoCG_fwd	CTTTGGACCTTATCTGGGACG TTCCTTGGGCTTACAGCC	Mutation of SOX binding site G1/G2 (AT to CG) in the <i>MIA</i> promoter.
pMIA_ATtoCG_rev	AGGCTGTAAGCCCAAGGAACG TCCCAGATAAGGTCCAAAG	
MIAmutV2_fwd	CTGCTTTGGACCTTATCTGCG TCGACCCTTGGGCTTACAGCC TTT	Mutation of SOX binding site G1/G2 based on the previous mutation AT to CG in the <i>MIA</i> promoter.
MIAmutV2_rev	AAAGGCTGTAAGCCCAAGGGT CGACGCAGATAAGGTCCAAAG	

	CAG	
MIAmutV3fwd	CCTTATCTAGGCCTCTGTCAG GGTTGAGGAGGGGGCTGGTC	Mutation of SOX binding site G3/J6 in the <i>MIA</i> promoter.
MIAmutV3rev	GACAGCCCCCTCCTCAACCCT GACAGAGGCCTAGATAAGG	
MIAmutV4fwd	GGCTGGGCTGTTTCTGGTAAT CGGAGGGCTGCCTTGTT	Mutation of SOX binding site J9 in the <i>MIA</i> promoter.
MIAmutV4rev	AACAAGGCAGCCCTCCGATTA CCAGAAACAGCCCAGCC	
MIAmutV5fwd	CTGGTAATCAAAGGGCTGCCG GTGTCTCCTGCCCCACAGCAC AG	Mutation of SOX binding site G4/J8 in the <i>MIA</i> promoter.
MIAmutV5 rev	CTGTGCTGTGGGGCAGGAGA CACCGGCAGCCCTTTGATTAC CAG	
MIAmutV6_fwd	TCACTGGGAAAGTTGTGAGCT GCGGGTGACCTTATCTGGGAA TTTCCTTG	Mutation of SOX binding site J5 in the <i>MIA</i> promoter.
MIAmutV6_res	CAAGGAAATTCCCAGATAAGG TCACCCGCAGCTCACAACCTTT CCCAGTGA	
MIAcDNA_fwd	GGACAAGACCAAGAACAACAAG	Amplification of <i>MIA</i> cDNA and subsequent sequencing.
MIAcDNA_rev	AAAGCCAAGGAGGGGAAAC	
PMP2_R106E_fwd	GGATGGCAAAGAGACAACCAT AAAGGAAAAGCTAGTGAATGG GAAAATG	Introducing a point mutation (R106E) in pLenti-PMP2-R126E-Y128F.
PMP2_R106E_rev	CATTTTCCCATTCACTACCTTT TCCTTTATGGTTGTCTCTTTGC CATCC	Introducing a point mutation (R106E) in pLenti-PMP2-R126E-Y128F.
PMP2_R126E_Y128F_fwd	AGGGCGTGGTGTGCACCGAA ATCTTTGAGAAGGTCTAGGAC C	Introducing two point mutations (R126E and Y128F) in pLenti-PMP2.

PMP2_R126E_Y128F_rev	GGTCCTAGACCTTCTCAAAGA TTTCGGTGCACACCACGCCCT	Introducing two point mutations (R126E and Y128F) in pLenti-PMP2.
PMP2_L27D_fwd	AAGCTCTGGGTGTGGGGGAT GCCACCAGAAAAGTGGG	Introducing a point mutation (L27D) in pLenti-PMP2.
PMP2_L27D_rev	CCCAGTTTTCTGGTGGCATCC CCCACACCCAGAGCTT	Introducing a point mutation (L27D) in pLenti-PMP2.
SOX10cDNA_fwd1	ATGGCGGAGGAGCAGGAC	Amplification of SOX10 cDNA and subsequent sequencing performed with two overlapping fragments.
SOX10cDNA_rev1	GGTACTGGTCCAAGTCAAGCC	
SOX10cDNA_fwd2	CCATGTCAGATGGGAACCCC	
SOX10cDNA_rev2	AGTGTGGGTGCAACAGTCAA	

Table 4: Primers for PCR.

Primers for introducing point mutations were designed with the QuikChange primer design software from Agilent Technologies (<http://www.genomics.agilent.com/primerDesignProgram.jsp>). Other PCR primers were designed with the primer3web suite (<http://primer3.ut.ee/>).

3.1.5.3 Oligonucleotides for electrophoretic mobility shift assay

Name	Sense (5'→3')	Antisense (5'→3')
DIG_SOX10pMIA	TGGTAATCAAAGGGCTGCC TTGTTCTCCTGC	GCAGGAGAACAAGGCAGCCC TTTGATTACCA
PMP2_EMSA_P1	TTGGAGACAAAGGGAAGTA TTATGTG	CACATAATACTTCCCTTTGTCT CCAA
PMP2_EMSA_P2	CAATAGACTGACTTCTTTGT CTGCCT	AGGCAGACAAAGAAGTCAGTC TATTG
PMP2_EMSA_P3	TTCTAGCTGAAAATCTTTGT TGTGCT	AGCACAACAAGATTTTCAGC TAGAA
SOX consensus (according to Cook et al. [52])	AGACTGAGAACAAGCGCT CTCACAC	GTGTGAGAGCGCTTTGTTCTC AGTCT

Table 5: Oligonucleotides for EMSA.

Oligonucleotides were labeled with DIG at the 5' end.

3.1.5.4 Small interfering ribonucleic acids

Name	Gene	Sequence (5' → 3')
siEGR2	<i>EGR2</i>	GAUCCACCUGAGACAGAAA(dT)(dT)
siMIA	<i>MIA</i>	GCCAAGUGGUGUAUGUCUU(dT)(dT)
siRELA	<i>RELA</i>	GCCCUAUCCCUUUACGUCA(dT)(dT)
siPMP2a	<i>PMP2</i>	CCACAGCUGACAAUAGAAA(dT)(dT)
siPMP2b	<i>PMP2</i>	GUGAGAACUUUGACGAUUA(dT)(dT)
siSOX9a	<i>SOX9</i>	GGAGGAAGUCGGUGAAGAA(dT)(dT)
siSOX9b	<i>SOX9</i>	CAGCGAACGCACAUCAAGA(dT)(dT)
siSOX10a	<i>SOX10</i>	CCGUAUGCAGCACAAGAAA(dT)(dT)
siSOX10b	<i>SOX10</i>	GUAUGCAGCACAAGAAAGA(dT)(dT)
siControl	-	GCGCAUUC CAGCUUACGUA(dT)(dT)

Table 6: Small interfering RNAs (siRNAs) for gene silencing.

Small interfering RNAs were designed according to 3.2.2.1.1.

3.1.6 Plasmids and vectors

Name	Backbone	Description
pCDNA4/to	(Life Technologies)	Control vector (pControl)
pCMV6	pCMV6-XL5	Generated from pCMV6- SOX10 by Not1 digestion and re-ligation of the vector backbone. Control vector for RNA sequencing.
pCMV6-SOX9	pCMV6-AC (Origene Technologies, Rockville, USA)	Vector for constitutive ectopic SOX9 overexpression.
pCMV6-SOX10	pCMV6-XL5 (Origene Technologies)	Vector for constitutive ectopic SOX10 overexpression.
pCMV-PAX6	pCMV-Sport6	Vector for constitutive ectopic PAX6 overexpression.
pCMX-MIA	pCMX-PL1	Vector for constitutive ectopic MIA overexpression.
pDONR221-PMP2	pDONR221 (Harvard plasmid)	Donor vector including the coding sequence of PMP2.

	HsCD00043524)	
pDONR221-PMP2-L27D	pDONR221-PMP2	Donor vector including the coding sequence of PMP2 with the mutation L27D.
pDONR221-PMP2-Mut3	pDONR221-PMP2	Donor vector including the coding sequence of PMP2 with the mutations R106E, R126E, and Y128F.
pENTRY4-flag	(Addgene)	Entry vector for <i>in vitro</i> recombination.
pENTRY4-flag-SOX9	pENTRY4-flag	Ligation of PCR fragment containing the SOX9 coding sequence via restriction enzyme digestion (KpnI/XhoI) into pENTRY4-flag.
pENTRY4-flag-SOX10	pENTRY4-flag	Ligation of PCR fragment containing the SOX10 coding sequence via restriction enzyme digestion (KpnI/XhoI) into pENTRY4-flag.
pENTRY4-flag-PMP2	pENTRY4-flag	Ligation of PCR fragment containing the PMP coding sequence via restriction enzyme digestion (KpnI/XhoI) into pENTRY4-flag.
pGL2-MIA-493	pGL2-basic (Promega)	Encodes the firefly luciferase coding sequence under control of a part of the <i>MIA</i> promoter (-493bp).
pGL2-MIA-275	pGL2-basic	Encodes the firefly luciferase coding sequence under control of a part of the <i>MIA</i> promoter (-275bp).
pGL2-MIA-212	pGL2-basic	Encodes the firefly luciferase coding sequence under control of a part of the <i>MIA</i> promoter (-212bp).
pGL2-MIA-200	pGL2-basic	Encodes the firefly luciferase coding sequence under control of a part of the <i>MIA</i> promoter (-200bp).
pGL2-MIA-160	pGL2-basic	Encodes the firefly luciferase coding

		sequence under control of a part of the <i>MIA</i> promoter (-160bp).
pGL3-MIA	pGL3-basic (Promega)	Encodes the firefly luciferase coding sequence under control of the full-length <i>MIA</i> promoter (-1376bp).
pLenti CMV Puro dest	(Addgene)	Lentiviral expression vector with <i>CMV</i> promoter and puromycin selection, destination vector for pENTRY. Also for control vector pLenti-Control.
pLenti-flag-SOX9	pLenti CMV Puro dest	<i>In vitro</i> recombination of pENTRY4-flag-SOX9 into pLenti CMV Puro dest.
pLenti-flag-SOX10	pLenti CMV Puro dest	<i>In vitro</i> recombination of pENTRY4-flag-SOX10 into pLenti CMV Puro dest.
pLenti-PMP2	pLenti CMV Puro dest	<i>In vitro</i> recombination of pDONR221-PMP2 into pLenti CMV Puro dest.
pLenti-flag-PMP2	pLenti CMV Puro dest	<i>In vitro</i> recombination of pENTRY4-flag-PMP2 into pLenti CMV Puro dest.
pLenti-PMP2 L27D	pLenti CMV Puro dest	<i>In vitro</i> recombination of pDONR221-PMP2 L27D into pLenti CMV Puro dest.
pLenti-PMP2 Mut3	pLenti CMV Puro dest	<i>In vitro</i> recombination of pDONR221-PMP2 Mut3 into pLenti CMV Puro dest.

Table 7: Plasmids and vectors used or established in this study.

Vectors containing *MIA* promoter and promoter fragments for reporter assays as well as for *MIA* overexpression were kind gifts from Professor Anja-Katrin Bosserhoff.

3.1.7 Enzymes and polypeptides

Herculase II Fusion DNA Polymerase (Agilent Technologies, Waldbronn, Germany)

IgG goat (1.7 mg/ml in 150 nM NaCl, Sigma)

IgG rabbit (0.5 mg/ml in 150 nM NaCl, Sigma)

poly(dG:dC) (2 mg/ml in sterile H₂O bidistilled; InvivoGen, San Diego, USA)

MB Taq DNA polymerase (Minerva Biolabs)

3.1.8 Antibodies

3.1.8.1 Primary antibodies

Name	Source	Supplier	Dilution
Anti- β -Actin	mouse	Sigma	1:5000
Anti-Bak	rabbit	Cell Signaling (Denvers, Massachusetts, USA)	1:1000
Anti-Bax	mouse	Santa Cruz	1:200
Anti-Bid	rabbit	Cell Signaling	1:1000
Anti-Bcl-2	mouse	Calbiochem (Merck/Millipore)	1:1000
Anti-caspase 3	rabbit	Cell Signaling	1:1000
Anti-caspase 8	Mouse (1C12)	Cell Signaling	1:1000
Anti-caspase 9	rabbit	Cell Signaling	1:1000
Anti-ERBB3	rabbit	Cell Signaling	1:1000
Anti-HMG1	rabbit	Cell Signaling	1:1000
Anti-p21	mouse	Santa Cruz (Santa Cruz, California, USA)	1:200
Anti-p65	rabbit	Cell Signaling	1:1000
Anti-phospho-p65	rabbit	Cell Signaling	1:1000
Anti-PMP2	mouse	Santa Cruz	1:200
Anti-PMP2	rabbit	Bioss Antibodies (Woburn, Massachusetts, USA)	1:200
Anti-MITF	mouse	Thermo Scientific (Waltham, Massachusetts, USA)	1:100

Anti-SOX9 pSer181	rabbit	Anaspec Inc. (San Jose, USA)	1:200
Anti-SOX9	rabbit	Millipore/Merck	1:2000
Anti-SOX9	rabbit	Zytomed Systems (Berlin, Germany)	1:1000
Anti-SOX9	rabbit	Chemicon (Temecula, CA, Germany)	1:1000
Anti-SOX10 sc-17342x	Goat	Santa Cruz	1:2000
Anti-SOX10	rabbit	Medac Diagnostika, Wedel, Germany	1:25 (for IHC)

Table 8: List of primary antibodies used in this study.

The MIA antibody (source: rabbit, dilution 1:2000) was a kind gift from Professor Anja-Katrin Bosserhoff.

3.1.8.2 Secondary antibodies

Name	Source	Supplier	Dilution
Anti-mouse IgG HRP-linked	Horse	Cell Signaling	1:5000
Anti-rabbit IgG HRP-linked	Goat	Cell Signaling	1:2000
Anti-goat IgG HRP-linked	Donkey	Santa Cruz	1:30000

Table 9: List of secondary antibodies used in this study.

3.1.9 Cell lines

Human melanoma cell lines were a kind gift from Meenhard Herlyn (Wistar Institute, Philadelphia, USA). Cells were isolated from primary tumors or metastases and classified according to their growth state as RGP, VGP, or metastasis [108]. Tissue origins of metastatic melanoma cell lines were lymph nodes (WM239A, WM9, WM1158, and WM1232) and lungs (451Lu and 1205Lu). Melanoma cells were cultivated as described under 3.2.1.1. Short term-cultured melanoma cells from patient's tissue were prepared as described in section 3.2.1.2. Primary melanocytes and fibroblasts had been in-house isolated from human foreskins and cultivated in melanocyte or fibroblast medium, respectively.

3.1.10 Appliances

Name	Supplier
Biological safety cabinet Class II Type A/B3	NuAire (Plymouth, Massachusetts, USA)
Centrifuge RC-5B	Sorvall (Bad Homburg, Germany)
Centrifuge Rotixa 50 RS	Hettich AG (Baech, Switzerland)
CO ₂ incubator HeraCell	Heraeus (Hanau, Germany)
EpiShear™ Probe Sonicator	Active Motif
KODAK RP X-OMAT Developer and Replenisher	Kodak (Stuttgart, Germany)
Flow cytometer FACScan	Becton Dickinson (Franklin Lakes, New Jersey, USA)
Fluorescence microscope Axioskop with cameras Mrc and Mrc 5	Zeiss (Munich, Germany)
Fluorimeter Cytofluor 2350	Millipore/Merck
Gel Doc 2000	Bio-Rad
HERAsafe biological safety cabinet	Heraeus
Horizontal Gel Electrophoresis System	Life Technologies
LightCycler® Instrument	Roche (Penzberg, Germany)
Luminometer GloMax® 96	Promega
Microcentrifuge 5415 R	Eppendorf (Hamburg, Germany)
Microcentrifuge 5415 C	Eppendorf
Microscope Olympus BX51 with camera DP21	Olympus, Hamburg, Germany
Photometer SmartSpec 3000	Bio-Rad
PS500XT DC Power Supply	Hoefer Scientific Instruments (San Francisco, California, USA)
Power supply model 200/2.0 and Pac300	Bio-Rad
RoboCycler® Thermal Cycler	Stratagene/Agilent Technologies (Santa Clara, California, USA)
Stratalinker® UV Crosslinker	Stratagene
TissueFAXS	TissueGnostics (Vienna, Austria)
Ultraviolet Crosslinker	Amersham Life Science/GE

	Healthcare
XCell II™ Blot Module	Invitrogen/Life Technologies
XCell SureLock™ mini-cell electrophoresis system	Invitrogen/Life Technologies

Table 10: List of appliances.

3.1.11 Consumables

Name	Supplier
6-, 24-, and 96-well plates	Greiner bio-one (Frickenhausen, Germany)
10 cm ² dish	TPP (Trasadingen, Switzerland)
25 and 75 cm ² filter cap cell culture flasks	Greiner bio-one
Amicon® Ultra 0.5 ml centrifugal filters 3K	Millipore/Merck
Biocat® 25 cm ² collagen vented flasks	Becton Dickinson
Carbon steel safety scalpel	Braun
Cell scrapers 24 cm	TPP
Cell strainer 100µm Nylon	BD Falcon™ (Franklin Lakes, New Jersey, USA)
Cryo tubes 2 ml	Greiner bio-one
Disposable cuvettes 1.5 ml semi-micro PMMA	Brand (Wertheim, Germany)
Disposable safety scalpels	Braun (Tuttlingen, Germany)
Disposable serological pipettes, 10 ml	Corning (New York, USA)
Disposable syringe discardit	Becton Dickinson
DNA retardation gel (6%), 1 mm, 10 well	Life Technologies
EpiShear™ Probe Sonicator	Active Motif
FACS-PE tubes 5 ml	Falcon/Becton Dickinson
Filtered pipette tips	Kisker (Steinfurt, Germany)
Filtropur BT50 500 ml bottle filter 0.2 µm pore size	Sarstedt (Nuembrecht, Germany)
High performance chemiluminescence film	GE Healthcare (Solingen, Germany)
LightCycler capillaries	Roche
Microscope slides and cover glasses	Menzel-Glaeser (Braunschweig, Germany)

NuPAGE® Novex® 4-12% Bis Tris Gel, 1.0 mm, 10 well	Invitrogen/Life Technologies
Nylon membrane, positively charged	Roche
Parafilm	Bemis (Soignies, Belgium)
Pasteur pipettes	Hirschmann (Eberstadt, Germany)
PCR tubes 0.6 ml thin well	Agilent Technologies
Petri dishes 94x16 mm	Greiner bio-one
Pipette tips	Sarstedt
Rotilabo®-syringe filters 0.22 µm pore size	Roth (Karlsruhe, Germany)
Round bottom tubes 12 ml	Greiner bio-one
Safe-lock tubes 2 ml	Eppendorf
Safe Seal Micro Tubes 1.5 ml	Sarstedt
ThinCerts™ cell culture inserts, 8 µm pore size	Greiner bio-one
Tubes 15 ml	Greiner bio-one
Tubes 50 ml	Sarstedt

Table 11: List of consumables.

3.1.12 Software

Name	Supplier
AxioVision rel. 4.7.2 microscope software	Zeiss
Assay Design Center	Roche; www.universalprobelibrary.com
CellQuest software	Becton Dickinson, Heidelberg, Germany
CpG Island searcher	http://www.cpgislands.usc.edu
EMBOSS Cpgplot	http://www.ebi.ac.uk/Tools/seqstats/emboss_cpgplot/
Fiji ImageJ	http://Fiji.sc immunoblot quantification was performed as described in http://www.yorku.ca/yisheng/Internal/Protocols/ImageJ.pdf
HeatMapper Version 13	GenePattern http://genepattern.broadinstitute.org/gp/)
Human Gene Atlas	www.proteinatlas.org/ <u>MIA expression data:</u> http://www.proteinatlas.org/ENSG00000261857-MIA/cancer

	<p><u>SOX9 expression data:</u> http://www.proteinatlas.org/ENSG00000125398-SOX9/tissue http://www.proteinatlas.org/ENSG00000125398-SOX9/cancer</p> <p><u>SOX10 expression data:</u> http://www.proteinatlas.org/ENSG00000100146-SOX10/tissue http://www.proteinatlas.org/ENSG00000100146-SOX10/cancer</p> <p><u>PMP2 expression data:</u> http://www.proteinatlas.org/ENSG00000147588-PMP2/tissue</p>
Illustrator CS5	http://www.adobe.com
JASPAR version 5.0_alpha	http://jaspar.genereg.net/
MatInspector, ModellInspector	Genomatix Software GmbH, Munich https://www.genomatix.de/
Microsoft Office 2010	Department for medical technique and IT, LMU Munich
ModFit LT software	Verity Software, Topsham, USA
PhotoShop CS2	Adobe / Department for medical technique and IT, LMU Munich
Primer3 web suite	http://primer3.ut.ee/
Prism 5 v 5.04	GraphPad Software, San Diego, CA www.graphpad.com
QuikChange primer design software	Agilent Technologies http://www.genomics.agilent.com/primerDesignProgram.jsp

Table 12: List of software used in this study.

3.2 Methods

3.2.1 Cell culture

3.2.1.1 Cultivation of human melanoma cell lines

Human melanoma cell lines were isolated from primary tumors or melanoma metastases at the Wistar Institute, Philadelphia, USA. Cells were cultivated in TU2% in T75 flasks at 37°C and 5% CO₂. At about 90% confluence, adherent cells were washed with HBSS and dissolved with 2 ml trypsin/EDTA for about 3 minutes. The trypsin digestion was stopped with 3 ml TU2% medium and the cell suspension was transferred into a 50 ml tube. Cells were spun down at 1000 rpm and room temperature for 3 minutes. According to their density, cells were diluted into a new T75 flask with fresh TU2% medium, generating a new cell passage, termed splitting. Cells were splitted twice a week. Antibiotics and antimycotics were not used for standard cell cultivation. Cell lines were analyzed for mycoplasma contamination using Venor® GeM (Minerva Biolabs) PCR control frequently. For further experiments, the cell number was calculated with a Neubauer counting chamber (Marienfeld, Lauda-Königshofen, Germany) and cells were seeded to a confluence of 60-70% in 6-, 24-, or 96-well plates. For cell storage, 1/3 of cells from a confluent T75 flask were spun down as described above, resuspended in 1 ml deep-freezing medium, and transferred into Cryo tubes. These tubes were instantly stored in a freezing box at -80°C. For long-term storage, cells were stored in a tank with liquid nitrogen. For cell thawing, deep-frozen Cryo tubes were thawed at 37°C and the cell suspension was mixed with 4 ml TU2%. Cells were spun down at 1000 rpm and room temperature for 3 minutes, resuspended in fresh TU2% medium with ABAM and transferred into a T75 flask. Twenty-four hours later, the medium was exchanged with fresh TU2% medium. Cells were splitted at least one time before starting experiments.

3.2.1.2 Isolation of melanoma cells from patient samples

Fresh tumor samples from primary or metastatic melanoma were washed with HBSS. In a 10 cm² dish, excessive skin, connective, and adipose tissue were removed with a scalpel and the tumor was transferred in a fresh 10 cm² dish and covered with 5 ml 1x digestion solution, a mixture of collagenase, dispase, and hyaluronidase. The tumor was cut into small pieces of about 1 mm³ size and incubated for 1 hour at 37°C to allow the decomposition of extracellular matrix and thereby discharge the melanoma cells.

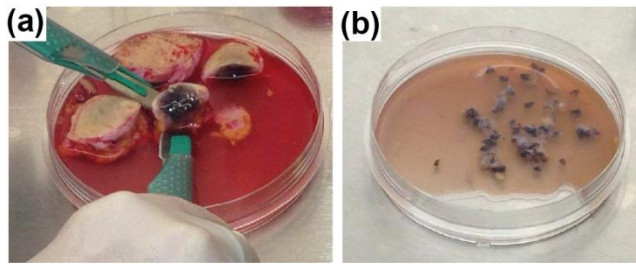


Figure 4: Isolation of tumor cells from patient samples.

(a) Removal of skin, adipose, and connective tissue from cutaneous melanoma samples washed with HBSS. (b) Dissected melanoma tissue in digestion solution.

The proteolytic digestion was stopped with 5 ml DMSO/10% FBS and the cell suspension was pressed through a cell strainer to separate the cells. The cells were spun down with 2000 rpm at room temperature for 5 minutes and the cell pellet was resuspended in 5 ml TU2% with ABAM. Fresh isolated melanoma cells were cultivated in Biocat® 25 cm² collagen vented flasks to facilitate the cell attachment and the medium was changed 24 hours after the isolation. When freshly isolated cells reached about 80-90% confluence, they were transferred and further cultivated in flasks without collagen surface.

3.2.1.3 Cultivation of primary skin cells

Primary fibroblasts and melanocytes were in-house isolated from human foreskins according to [15]. Fibroblasts were cultivated in fibroblast growth medium containing DMEM, FBS, and L-glutamine. Melanocytes were cultivated in melanocyte growth medium containing 254CF, CaCl₂, and human melanocyte growth supplements (HMGS-2). Primary fibroblasts were cultivated to a maximum of 20 passages, melanocytes up to 10 passages in T75 flasks at 37°C and 5% CO₂. Cell splitting, freezing, and thawing has been performed as described in section 3.2.1.1.

3.2.2 Molecular biological methods

3.2.2.1 Gene silencing using RNA interference

3.2.2.1.1 Design of small interfering RNAs

All siRNAs used in this study were designed according to published algorithms from Reynolds [214] and Ui-Tei [271]. The control siRNA was designed in terms of not to interfere with the human transcriptome.

3.2.2.1.2 Transfection of siRNAs

Cells were transfected at a confluence of about 70% 24 hours after seeding. For cells in a 6-well plate, 1.5 µl siRNA (concentration 20 µM) were mixed with 125 µl Opti-MEM®

reduced serum medium (Life Technologies). One μl Lipofectamine® RNAiMAX were mixed in the same volume Opti-MEM. After a short incubation of 2 minutes, both solutions were combined and mixed by inversion. An incubation for 15-20 minutes at room temperature allowed complex formation between siRNA and Lipofectamine. Meanwhile, the medium covering the cells was exchanged with 1.25 ml fresh medium. After the incubation, the mixture containing Lipofectamine-complexed siRNAs was added dropwise to the cells. The final siRNA concentration was 20 nM per well. Gene silencing after siRNA transfection was assessed by qRT-PCR and immunoblotting. If cell death was blocked by caspase and necroptosis inhibitors, 100 μM Z-VAD (N-Benzyloxycarbonyl-Val-Ala-Asp[O-ME]-fluoromethyl ketone, stock 100 mM in methanol, Sigma Aldrich) or 50 μM Nec-1 (necrostatin-1, stock 50 mM in DMSO, Sigma Aldrich) were added prior to siRNA transfection.

3.2.2.2 *Transient and stable transfection of plasmid DNA*

FuGENE® 6 transfection reagent was used to insert plasmid DNA into cells. For transfection of a 6-well plate well, 3 μl FuGENE reagent were mixed with 50 μl Opti-MEM and incubated at room temperature for 5 minutes. One μg plasmid DNA was added, mixed by inversion, and incubated for 30 minutes at room temperature. The cell medium was exchanged with 1 ml fresh medium and the mixture containing DNA/reagent complexes was added dropwise. For a T25 flask, 2.6 μg plasmid DNA were transfected using 7.8 μl FuGENE reagent in 122.2 μl Opti-MEM and 3 ml medium on top of the cells, for a T75 flask using 7.8 μg plasmid DNA with 23.4 μl FuGENE reagent in 366 μl Opti-MEM and 7.8 ml medium on top of the cells.

If the DNA transfection followed a siRNA transfection, the DNA transfection was performed 24 hours later and cells were washed with HBSS before adding the DNA/reagent mixture into the new medium.

For stable plasmid DNA transfection, the medium was exchanged to medium containing antibiotics for selection (e.g. 0.5 $\mu\text{g}/\text{ml}$ puromycin for pLenti-PMP2 and WM3211 cells, 0.25 $\mu\text{g}/\text{ml}$ puromycin for WM278) 48 hours after plasmid transfection.

3.2.2.3 *Cell invasion assays*

3.2.2.3.1 Matrigel invasion assay

For the Matrigel invasion assay, ThinCert™ cell culture inserts for 24-well plates (Greiner bio-one) were coated with 50 μl cold PBS-diluted Matrigel matrix (Matrigel™

Basement Membrane Matrix, BD Biosciences; 39 mg per well), incubated at 37°C and 5% CO₂ for 3 hours, and dried under the clean bench overnight. Twenty-four hours after siRNA or plasmid transfection, melanoma cells were harvested by trypsinization, washed with TU medium without FBS, and counted. 150,000 cells in case of inhibition and 120,000 cells in case of overexpression studies were resuspended in 200 µl TU medium without FBS and seeded on top of the Matrigel-coated ThinCert™ inserts. The well below the inserts was filled with 600 µl fibroblast-conditioned medium (for preparation see section 3.1.1). The assay was performed for 5 hours at 37°C and 5% CO₂. Afterwards, non-invasive cells and the remaining Matrigel matrix were removed with cotton swabs and the invaded cells on the lower side of the ThinCert™ insert were fixed and stained with a Diff-Quik® staining set (Medion Diagnostics, Duedingen, Switzerland). Invaded cells were counted from whole inserts with microscopical magnification. Macroscopical pictures of stained inserts were taken with a Canon G11 camera (Canon, Krefeld, Germany).

3.2.2.3.2 Spheroid assay

To form spheroids, 5,000 melanoma cells per well in 100 µl TU2% medium were seeded on an agar-coated 96-well plate. Coating was performed directly before seeding the cells, by pipetting 50 µl sterilized liquid agar solution (1.5% agar noble from Beckton Dickinson Difco™, New Jersey, USA, in PBS) per well and letting the agar solidify by cooling down to room temperature for 45 min. After seeding, cells were incubated at 37°C with 5% CO₂ for 48 to 96 hours (depending on cell line), to allow aggregation and spheroid formation. Spheroids were harvested with a 1,000 µl pipette and transferred into a 1.5 ml reaction tube. After 5 to 10 minutes, spheroids settled down at the bottom of the reaction tube. Meanwhile, wells of a 24-well plate were covered with 300 µl collagen mix and incubated at 37°C, 5% CO₂, for 15-30 min to solidify. The medium on top of the spheroids was removed. Spheroids were resuspended in 300 µl collagen mix per well and added on top of the previous layer, followed by further incubation at 37°C and 5% CO₂. The cell invasion was monitored by light microscopy. In case of investigating cell viability, spheroids were stained with calcein AM and EthD-1 from the LIVE/DEAD® viability/cytotoxicity kit according to the manufacturer's protocol and fluorescence microscopy had been performed 45 minutes later. The cell invasion was quantified using FIJI ImageJ software by determination of the complete area covered with cells and subtracting the non-invasive spheroid core.

3.2.2.3.3 Chick embryo invasion assay

Chick embryo invasion assay was performed in collaboration with Dr. Christian Busch at the Section Dermato-Oncology, University of Tübingen, Tübingen. Fertilized eggs of chicken from a local farmer were incubated in a water-filled incubator at 38°C for 60 hours. The upper side of each egg was marked. When the chick embryos had reached embryonic stage 12-13 according to Hamburger and Hamilton [94] (Figure 5 d), the egg was prepared for melanoma cell injection with the marked side facing up. Two ml of egg white were removed with a syringe after tapping the egg on one side to lower the embryo. A window was carefully cut in the egg shell with a small hacksaw (Figure 5 a and b) and 2 ml PBS were injected to lift the embryo up again. For a better contrast, a bit of writing ink was injected with a mouth pipette behind the embryo (Figure 5 c). 1205Lu melanoma cells of a T75 flask were harvested by trypsinization and washed twice with PBS. The supernatant was removed and 10 µl of the cell suspension were injected in the rhomboid fossa, in the hindbrain of the chick embryo, using a mouth pipette. The window in the egg was closed with a tape and the embryo was incubated for further 96 hours at 38°C before fixation, paraffin embedding, and serial sectioning. For quantification of melanoma cell invasion, the three middle sections with the largest tumor diameters were analyzed in each embryo by counting the invading mindbomb E3 ubiquitin protein ligase 1 (MIB1)-positive melanoma cells. The mean value represented the number of invading melanoma cells per embryo. The maximum diameter of each tumor on the same section was measured in two dimensions using an Olympus BX51 microscope with a DP21 camera (Olympus, Hamburg, Germany).

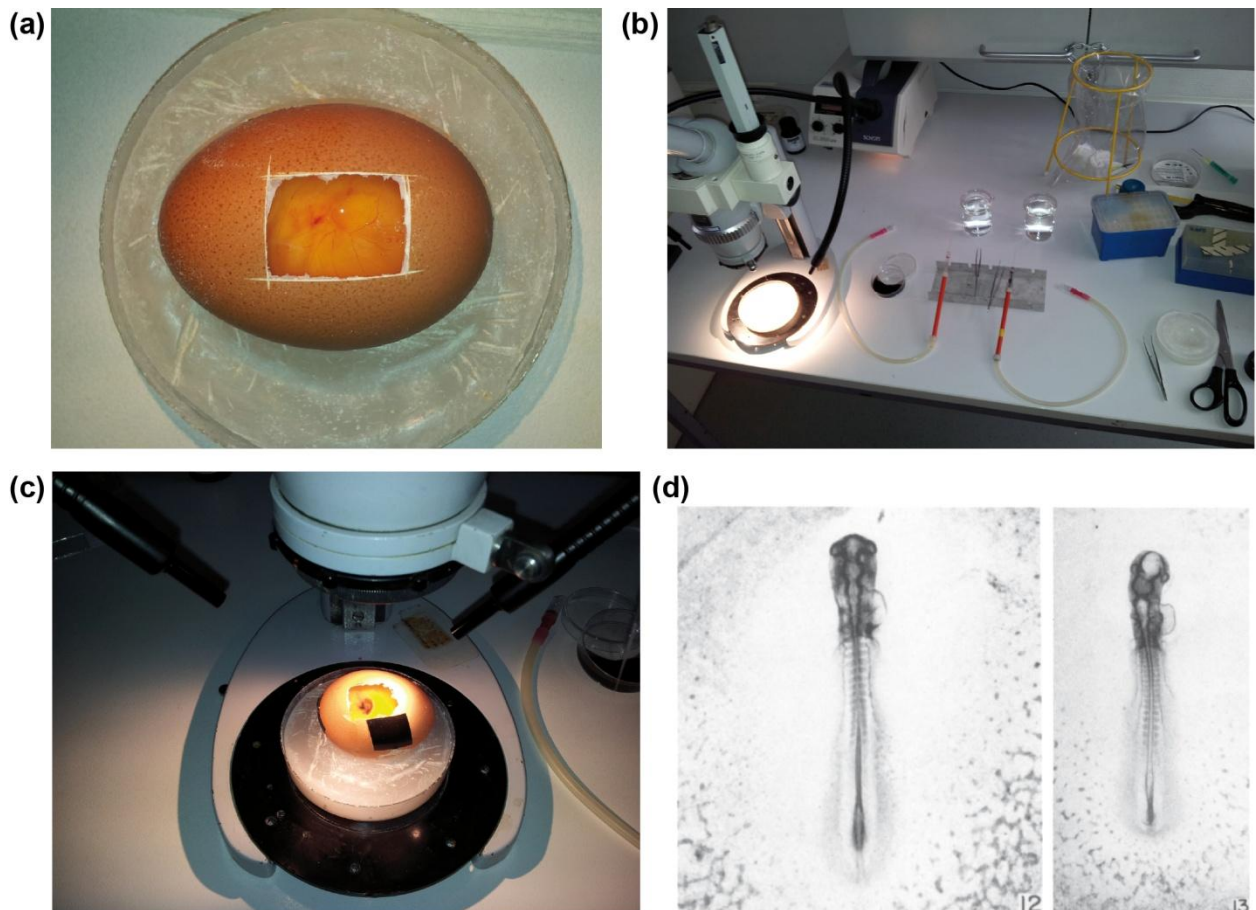


Figure 5: Chick embryo invasion assay.

(a) Windowed chick egg with embryo in the middle surrounded by blood vessels. (b) Tools for the assay. (c) Ink injected behind the chick embryo for better visualization of the injection side. (d) Chick embryos in the developmental stages 12 and 13 according to Hamburger and Hamilton (modified from [94]).

3.2.2.4 Cell viability assay

The viability of cells in multiwell plates was determined with the CellTiter-Blue® Cell Viability Assay (Promega). In case of a 6-well format, the cell medium was exchanged with 750 μ l medium and 150 μ l of the dark blue CellTiter-Blue® reagent were added and mixed, followed by incubation at 37°C, 5% CO₂, for one hour. A control containing medium without cells plus the reagent was included as reference for the fluorescence signal. After the incubation, 100 μ l of the cell supernatant (1 to 3 technical replicates) as well as from the control were transferred into a 96-well plate and measured at a Cytofluor 2350 Fluorimeter (Millipore) with an excitation of 560 nm and emission at 590 nm.

3.2.2.5 *Flow cytometry*

3.2.2.5.1 Cell cycle analysis

For cell cycle analysis, the supernatant of a 6-well plate well was transferred into a 2 ml tube and the adherent cells were washed twice with PBS before detachment by trypsinization. The detached cells were added to the supernatant and washed twice with PBS with centrifugation at 2000 rpm, 4°C, for 5 minutes in between. PBS was reduced to a volume of 100 µl and 1.4 ml ice-cold 75% ethanol (end concentration 70%) was added dropwise while gentle mixing to permeabilize the cell membrane and fix the DNA. The fixed cells were incubated at 4°C overnight and then washed again twice with 500 µl washing buffer (PBS/0.5% BSA). Cell pellets were resuspended in 300 µl cell cycle staining solution followed by RNase A (Sigma) digestion with incubation at 37°C for 15 minutes. The samples were transferred into fluorescence-activated cell sorting (FACS) tubes and the amount of DNA was detected with a FACScan flow cytometer (Becton Dickinson) and evaluated with the ModFit LT software.

3.2.2.5.2 Cell death analysis

The supernatant of one 6-well plate well was transferred into a 1.5 ml tube and adherent cells were washed twice with PBS and detached with 0.2% EDTA in PBS at 37°C for 10 minutes. Cells were transferred to the supernatant-containing tube and washed again twice with PBS and centrifugation at 2,600 rpm, 4°C, 3 minutes in between. Cells were resuspended in 50 µl Annexin staining solution and incubated in dark at room temperature for 15 minutes. During this incubation time, 60 µl PI staining solution were pipetted into a FACS tube and Annexin V-Fluos-stained cells were added and mixed. Samples were immediately analyzed with a FACScan flow cytometer and evaluated with the CellQuest software (Becton Dickinson, Heidelberg, Germany).

3.2.2.6 *Luciferase reporter assay*

Cells in a 6-well plate were transfected with 800 ng luciferase reporter vector and 200 ng renilla vector per well as described in 3.2.2.2. Twenty-four hours later, cells were washed twice with PBS and lysed by adding 250 µl 1x lysis buffer (Promega) and incubating at 4°C for 10 minutes. The cell lysate was transferred into a 1.5 ml tube. Twenty-five µl of the cell lysate were transferred into a white 96-well plate. Twenty-five µl of a 1:1 mixture of luciferin and ATP substrate (Biothema) for the firefly luciferase

reaction or 25 µl coelenterazine substrate (1:800 in H₂O bidistilled, Promega) for the renilla luciferase reaction were added and mixed by shaking. The bioluminescence was immediately measured in a GloMax® luminometer (Promega). Firefly and renilla luciferase reactions were measured in triplicates.

MIA promoter activity was tested with the full length promoter in pGL3 (-1376bp, in relation to the protein start ATG) or promoter fragments (-493bp, -275bp, -212bp, -200bp, and -160bp) in a pGL2 reporter vector backbone (kindly provided by Prof. Anja-Katrin Bosserhoff [25], [203], [204]). SOX-binding sites were predicted using Genomatix software (Genomatix Software GmbH, Munich, Germany) and JASPAR version 5.0_alpha (<http://jaspar.genereg.net/>) with the MIA promoter sequence according to >gi|224589810|ref|NC_000019.9|:41279500-41280875 Homo sapiens chromosome 19, GRCh37.p5. Mutations in predicted SOX-binding sites in the MIA promoter were introduced using the QuikChange Lightning Site-Directed mutagenesis kit (Agilent Technologies) by exchanging A to C or T to G and vice versa. In case of measuring MIA reporter activity after SOX10 inhibition, siRNA transfection was carried out as described in section 3.2.2.1.2 twenty-four hours prior to reporter plasmid transfection.

3.2.2.7 Cloning of expression vectors

PCR with a proofreading Herculase II Fusion DNA polymerase (Agilent Technologies) was carried out with the following composition and PCR program in a RoboCycler® Thermo cycler (Stratagene):

Template DNA	10-30 ng plasmid DNA or 2 µl cDNA
DMSO (Agilent Technologies)	0-8%
MgCl ₂ (Agilent Technologies)	2-4 mM
Primers	0.25 µM each
Deoxyribonucleotide triphosphates (dNTPs; Agilent Technologies)	250 µM each dNTP
Herculase II Fusion DNA polymerase	1 µl
	total volume 50 µl

Concentration of DMSO and MgCl₂ were varied to optimize the PCR.

PCR program:

Initial denaturation	95°C, 5 minutes	1 cycle
Denaturation	95°C, 1 minute	30 cycles

Primer annealing	Primer melting temperature minus 5°C, 1 minute	1 cycle
Extension	72°C, 30 seconds per kb	
Final extension	72°C, 5 minutes	

PCR products were controlled on a 1% agarose gel (1 g w/v peqGold Universal Agarose, Peqlab, Erlangen, Germany, in 100 ml TBE, microwaved for dissolving) and detected on a Gel Doc 2000 apparatus (Bio-Rad). If fragments had to be cut out of the agarose gel, these fragments were purified with a NucleoSpin® Gel and PCR Clean-up Kit (Macherey-Nagel) according to the manufacturer's protocol.

Restriction enzyme digestion was carried out with corresponding restriction enzymes from NEB (Ipswich, Massachusetts, USA) according to the manufacturer's protocol.

For assemble vector insert and backbone, the Rapid DNA Ligation Kit (Roche) was used. Therefore, vector and insert DNA were mixed in a molecular ratio of 3:1 or 5:1 with DNA dilution buffer in a final volume of 10 µl. Ten µl T4 DNA ligase buffer as well as 1 µl T4 DNA ligase were added and mixed. The reaction mixture was incubated at room temperature for 10 minutes. Five µl of the ligation was transformed in chemical competent DH5α bacteria cells according to section 3.2.2.8.

Entry or donor vectors were recombined in a pLenti Puro CMV Dest vector with a Gateway® LR Clonase® II enzyme mix (Life Technologies) by mixing 75 ng of each vector in a final volume of 6 µl in TE buffer (pH 8). One µl of the LR Clonase® II enzyme was added and incubated at room temperature for 3 hours. Three µl were transformed in chemical competent StBI3 bacteria cells as described in section 3.2.2.8. Successful cloning was monitored by restriction enzyme digestion and sequencing (1.7 µg plasmid DNA and 10 µM sequencing primer in 20 µl H₂O, performed by Eurofins genomics).

3.2.2.8 Transformation and conservation of chemical competent *Escherichia coli*

For transformation of plasmid DNA in chemical competent *Escherichia coli* bacteria, 200 µl One Shot StBI3 (Life Technologies) or DH5α were thawed in a 12 ml round bottom tube on ice. Ten ng plasmid DNA were added, mixed, and further incubated for 30 minutes on ice. At the heat shock step, the tube was dipped in a water bath at 42°C for 90 seconds followed by a further incubation on ice for 2 minutes. Eight-hundred µl SOC medium (Life Technologies) were added and the bacteria suspension was incubated at 37°C, 300 rpm, for one hour. One-hundred µl of the suspension were streaked on an

agar plate with the appropriate selection antibiotic and incubated at 37°C overnight. For long-term storage, one colony was inoculated in 5 ml LB medium containing antibiotics for selection at 37°C, 300 rpm overnight. Eight-hundred µl of the bacteria suspension were mixed with 200 µl glycerol and stored at -80°C.

3.2.3 Biochemical methods

3.2.3.1 Isolation of nucleic acids

3.2.3.1.1 Plasmid isolation

To isolate plasmid DNA from bacteria, 5 ml of an overnight culture were spun down at 13,000 rpm, room temperature, for 30 seconds. The pellet was either stored at -20°C or directly used for plasmid DNA isolation with the NucleoSpin® Plasmid Kit (Macherey-Nagel) according to the manufacturer's protocol. Plasmid DNA was eluted with 50 µl AE buffer (5 mM Tris-HCl, pH 8.5) and a 1:40 dilution of the DNA was prepared. The absorbance of this dilution was measured in a quartz cuvette in a SmartSpec 3000 photometer (Bio-Rad) at 260 and 280 nm with AE buffer as reference. The quotient A_{260}/A_{280} determines the purity of isolated DNA and should range between 1.6 and 2 (with a value of 1.8 for pure DNA and 2 for pure RNA). Lower values indicate protein contamination with absorption of aromatic amino acids at 280 nm. The DNA concentration was then calculated using the following formula: $DNA \left(\frac{\mu g}{\mu l} \right) = A_{260} \times 40 \text{ (dilution factor)} \times 50 \frac{\mu g}{\mu l} \text{ (conversion factor)}$.

Plasmid DNA was stored at -20°C.

3.2.3.1.2 RNA isolation

For RNA isolation, cells cultivated in a 6-well plate were washed twice with PBS. One ml phenol-containing QIAzol (Qiagen) was added and incubated at room temperature for 5 minutes. The lysed cells were scratched with a cell scraper and transferred into a 1.5 ml tube. Two-hundred µl chloroform (Sigma) were added and mixed by strong shaking for 15 seconds. The mixture was incubated for 2 minutes. To separate the two phases, the mixture was centrifuged at 4°C and 13,200 rpm for 15 minutes. The upper liquid phase was transferred into a new 1.5 ml tube containing 700 µl 70% ethanol in RNase-free water and mixed. Further RNA purification was performed with an RNeasy Mini Kit (Qiagen) according to the manufacturer's protocol and eluted with 35 µl RNase-free water. The concentration of RNA was measured in a 1:20 dilution with a SmartSpec

3000 photometer and RNase-free water as reference as described in section 3.2.3.1.1.

The concentration was calculated using the following formula: $RNA \left(\frac{g}{l} \right) = A \times (dilution\ factor) \times \frac{\mu g}{\mu l} (conversion\ factor)$.

The isolated RNA was stored at -80°C.

3.2.3.2 Quantification of gene expression

3.2.3.2.1 Copy DNA synthesis

Gene expression can be measured by the relative amount of copies of an mRNA transcript of a gene in a sample. To quantify gene expression, isolated single-stranded mRNA was first transcribed into cDNA with a RNA-dependent DNA polymerase called reverse transcriptase. Oligo-deoxythymidine (dT) was used as primer for the transcription because it specifically hybridizes with the poly-adenosine-tailed mRNA, allowing only mRNA but no other RNA species to be transcribed. Therefore, 300–1,000 ng isolated RNA was incubated with 500 ng poly-dT (15 dTs, Eurofins Genomics) in a final volume of 10.5 μ l with RNase-free water for 10 minutes at 65°C in a RoboCycler® Thermo Cycler (Stratagene) for denaturing the RNA and cooled down immediately afterwards for total hybridization of the primers. First strand DNA synthesis was carried out in following composition:

Preparation 1 (RNA with poly-dT)	10.5 μ l
5x First Strand Buffer (Roche)	4 μ l
Dithiothreitol (DTT, 0.1 M; Roche)	2 μ l
dNTPs (10 mM, Roche)	2 μ l
RNAsin (Promega)	0.5 μ l
Reverse Transcriptase (Roche)	1 μ l
	total volume 20 μ l

The reverse transcription was carried out in a water bath at 42°C for one hour. Afterwards, 40 μ l RNase-free water were added to each reaction and 3 μ l were used for qRT-PCR. The cDNA was stored at -80°C.

3.2.3.2.2 Quantitative real-time PCR

The quantification of a specific sequence from the cDNA transcripts was performed with the Lightcycler® Taqman® Master Kit (Roche), including a thermostable Taq DNA

polymerase. A qRT-PCR follows the general principle of a PCR reaction, while the amplified DNA produced during the reaction is detected in real-time by using a fluorescence dye. This fluorescence dye can either be a DNA intercalating molecule or – as used in this study – a fluorescence-labeled probe. The detected fluorescence signal increases proportionally to the amount of amplified DNA. Quantification is carried out during the exponential phase under following conditions: the ratio of template DNA, primer, and polymerase is optimal, the other reactants (e.g. dNTPs) are sufficient, and the amount of side products is marginal. The end phase of the reaction is indicated with a plateau, creating a sigmoid curve during the measurement as typical for an enzymatic reaction. The starting point of the exponential phase is named threshold cycle (CT-value) or crossing point. At this point, the measured fluorescence exceeds significantly the background fluorescence. The fluorescence-labeled probes from the Universal Probe Library (Roche) are short locked nucleic acids, which are chemically modified nucleic acids that bind with a higher affinity as natural nucleic acids. Thereby, these short locked nucleic acids hybridize at the same temperature as longer, specific primers with a length of 20-25 nucleotides. The probes are coupled with a quencher dye at the 3' end. When the Taq polymerase approaches and degrades the hybridized probe due to its 5'-3' exonuclease activity, the reporter fluorophore is released from the quencher dye and the fluorescence signal can be detected.

The Universal Probe Library allows detection of more than 98% of the 37,000 human gene transcripts included in the National Center for Biotechnology Information (NCBI) Reference Sequence Database with only 90 different probes due to the combination with gene-specific primers, which were designed with the Assay Design Center (section 3.1.12). Primer pairs and respective probes for each gene measured in this study are listed in section 3.1.5.1.

In each quantification reaction a control sample (non-treated 1205Lu) with dilutions served as standard curve. With the CT-values in the standard curve the relative value of a specific gene expression was determined. To normalize the relative amount of the measured target gene, a ubiquitously expressed gene was quantified in the same sample. In this study all quantified genes were normalized to the expression of hypoxanthin-guanine phosphoribosyltransferase (HPRT), an enzyme that plays a central role in the generation of purine nucleotides through the purine salvage pathway. Each reaction was carried out in LightCycler capillaries (Roche) in the composition:

H ₂ O, PCR grade	4.5 µl
Probe	0.1 µl
Forward primer (10 µM)	0.2 µl
Reverse primer (10 µM)	0.2 µl
Reaction master mix (including enzyme)	2 µl
cDNA	3 µl

Capillaries were spun down at 1,000 rpm, 4°C, for 30 seconds.

The program for qRT-PCR reaction was:

Initial denaturation (1 cycle)	94°C	10 minutes
Amplification/quantification (50 cycles)	94°C	10 seconds
	60°C	30 seconds
	72°C	1 second
Cooling down to 40°C	0.1°C per second	

3.2.3.3 Copy DNA sequencing

To identify the mutation status of *SOX10* and *MIA* in cell lines WM278, WM1232, and 1205Lu, cDNA of these cell lines was generated as described in section 3.2.3.2.1. A PCR reaction with a proof reading DNA polymerase (Herculase II) was performed as described in section 3.2.2.7. Primers for amplification of *SOX10* or *MIA* cDNA are listed in section 3.1.5.2. The PCR product was controlled on a 1% agarose gel and purified with a NucleoSpin® Gel and PCR Clean-up Kit (Macherey-Nagel). Four-hundred ng of the DNA was sequenced with primers according to section 3.1.5.2 by Eurofins Genomics.

3.2.3.4 RNA sequencing

For RNA sequencing analysis, 1×10^6 1205Lu melanoma cells were seeded in a T75 flask. Twenty-four hours later, the cells were transfected with 7.8 µg pCMV-SOX10 or pCMV6 according to section 3.2.2.2. Twenty-four hours later, cells were lysed in 1.2 ml QIAzol and 0.2 ml was used in order to control *SOX10* overexpression by RNA isolation and qRT-PCR. The other part was delivered to the group of Dr. Helmut Blum at the Gene Center Munich, where the RNA sequencing analysis was performed with a GenomeAnalyzer IIX (Illumina, San Diego, USA).

RNA was isolated with the trizol method (according to https://tools.thermofisher.com/content/sfs/manuals/trizol_reagent.pdf). Copy DNA was generated with the NuGEN (Leek, Netherlands) RNAseq complete library preparation kit by using 100 ng of the total RNA for mixed random-/poly adenosine-primer first-strand cDNA synthesis. The cDNA was bead-purified (AmpureXP, Beckman-Coulter) and fragmented by sonication (Bioruptor, Diagenode, 25 cycles 30s on/30s off). The fragmented cDNA was used for preparation of Illumina-compatible sequencing libraries using the NuGEN RNAseq complete library preparation kit according to the manufacturer's protocol. In brief, the cDNA fragments are ligated to adapters with known sequences and sample-specific barcodes, which allows pooling of the samples and assignment of the SOX10-overexpressing and control samples at the mapping step. Adapter ligation was done with sample-specific barcodes and the resulting library was amplified (KAPA high fidelity polymerase, eight cycles, 95°C 80 sec, 55°C 30 sec, 72°C 60 sec) and quantified on a Bioanalyzer 2100 (Agilent) for quality control. Barcoded libraries were pooled at 10 nM concentration for multiplexed sequencing. Libraries were hybridized to a flow cell, amplified for generation of clusters and sequenced with an Illumina Genome Analyzer IIx. Hereby, blocked, fluorescence-labeled nucleotides are incorporated stepwise by a DNA-polymerase. After each step, the fluorescence is measured on the clusters enabling the determination of incorporated nucleotide by its fluorescence. After deblocking and read extension the sequence of the library can be determined. Sequencing was performed to a mean coverage of 20×10^6 reads each. Sequencing runs were done in single-read mode with an 80-base read length.

For each sample replicate, raw reads were filtered for adapter sequences. After removing the first five bases due to random priming effects, the raw reads were filtered from the 3' and 5' end with a quality cutoff of 20. Reads below a length of 30 were discarded. Filtered reads were mapped with Tophat2 (v.2.0.3) to the human reference genome (HG19) supplied by annotated gene models in the GTF format from the online available iGenomes project of Illumina. Only uniquely mapped reads were used to calculate the number of reads falling into each gene with the HTSeq-count script (v.0.5.3) in the union mode and using no strand information from the HTSeq package. Differentially expressed genes were calculated with the DESeq package. Genes were regarded as differentially expressed when the adjusted *P* value was < 0.05 . The mapped reads from each replicate were merged, and the numbers of reads falling into

the exonic regions of the annotated genes were counted. A gene was determined as expressed if more than 15 reads could be properly aligned to that gene.

In the first sequencing experiment, a high rate of reads mapped to the sequence of the transfected plasmid and had to be excluded from the analysis. Another sequencing experiment was performed with the same isolated mRNA but with DNA digestion (Thermo Scientific ds DNase #EN0771) prior to cDNA synthesis and library generation. Description of RNA sequencing is based on the material and method section from [90].

3.2.3.5 *Protein isolation*

3.2.3.5.1 Whole cell extracts

To isolate whole cell proteins, adherent cells were washed twice with PBS and detached with 0.2% EDTA in PBS at 37°C, 5% CO₂, for 10 minutes. The pellet was centrifuged at 2,600 rpm, 4°C, for 3 min, washed twice with PBS, and resolved in 50 µl CSH or RIPA (in case of detection of PMP2) buffer. After incubation for 30 minutes on ice, the soluble protein fraction was separated from the cell debris by centrifugation at 13,200 rpm, 4°C, and 20 minutes. The supernatant was transferred into a new tube. The protein concentration in cell extracts was determined with the Pierce™ BCA Protein Assay Kit (ThermoFisher Scientific). This assay combines chelation of Cu²⁺ by the peptide backbone and subsequent reduction to Cu¹⁺ in an alkaline environment (biuret reaction) with the reaction of bicinchoninic acid (BCA) and the reduced cuprous cation, generating an intense purple-colored complex. Reagents A was diluted 1:50 in reagent B and 1 ml of the solution were added in a plastic cuvette. Ten µl of the protein lysate were added and mixed. A standard curve generated by a dilution row of bovine serum albumin (BSA, New England Biolabs, 10 mg/ml) in the lysis buffer with final concentrations of 80, 40, 20, 10, and 5 mg/ml in the cuvette was included in each measurement. After an incubation step at room temperature for 20 minutes, the optical density at 562 nm was determined with a SmartSpec 3000 photometer with reagent A plus B and lysis buffer as reference. The protein extract was stored at -80°C.

3.2.3.5.2 Nucleic extracts

Fractional cell lysis to isolate nucleic proteins was performed with the Nuclear Extract Kit from Active Motif. Cells from a confluent T75 flask were washed with 5 ml ice cold PBS/phosphatase inhibitor provided in the kit and cells were detached in 3 ml of this solution with a cell scraper followed by centrifugation at 500 rpm, 4°C, for 5 minutes.

The pellet was resuspended in 500 µl hypotonic buffer and incubated on ice for 15 minutes. To release nuclei, cells were lysed with 25 µl detergent and mixed for 15 seconds. To separate nuclei from the cytoplasmic fraction, the suspension was centrifuged at 13,200 rpm, 4°C, for 30 seconds. The supernatant (cytoplasmic fraction) was stored at -80°C. The nuclei were resuspended in 50 µl complete lysis buffer, mixed for 10 seconds, and centrifuged at 13,200 rpm, 4°C, for 10 minutes. The supernatant, containing soluble nucleic proteins, was transferred into a new tube. To determine the concentration of a nuclei extract, 5 µl of the lysate were added to 800 µl H₂O bidistilled in a plastic cuvette followed by addition of 200 µl Bio-Rad Protein Assay reagent (based on the Bradford dye-binding method) and mixing. A standard curve as described in section 3.2.3.5.1 was included. The optical density of a sample, generated by the complex formation of Coomassie brilliant blue G-250 with amino acids, was determined in a SmartSpec 3000 photometer at 595 nm without further incubation. The complete lysis buffer included in the kit served as reference. The nucleic extract was stored at -80°C.

3.2.3.5.3 Proteins from cell supernatants

To analyze proteins in the supernatant of a 6-well plate, two times 0.5 ml medium from on top of the cells were concentrated in an Amicon® Ultra 0.5 ml Centrifugal Unit 3K (nominal molecular weight limit 3 kDa, Millipore/Merck) with two times centrifugation at 13,200 rpm, 4°C, for 20 minutes in a provided 2 ml tube. The insert was positioned head first in a new 1.5 ml tube and centrifuged at 2,000 rpm, 4°C, for 2 minutes. In the end, the supernatant was concentrated 200 times and stored at -80°C. Protein concentration was determined as described in section 3.2.3.5.1.

3.2.3.6 *Immunoblot according to Laemmli*

3.2.3.6.1 Polyacrylamide gel electrophoresis

Protein separation by polyacrylamide gel electrophoresis was carried out with protein extracts prepared according to section 3.2.3.5.1. For protein denaturation, 10 µg protein extract were incubated together with 6 µl NuPAGE® LDS Sample Buffer and 2.4 µl NuPAGE® Reducing Agent in a total volume of 24 µl at 70°C for 10 minutes. The polyacrylamide gel electrophoresis was carried out in a XCell SureLock™ mini-cell electrophoresis system (Life Technologies). Denaturated proteins were loaded on a NuPAGE® Novex® 4-12% Bis Tris Gel, and 10 µl SeeBlue® Plus2 pre-stained standard

served as size marker. The inner chamber was filled with 200 ml running buffer including 500 µl NuPAGE® Antioxidant, the outer chamber with running buffer without oxidant. The running time was about 45 minutes at 150 Volt. All reagents and gels were purchased from Life Technologies.

3.2.3.6.2 Immunoblotting

Proteins separated by polyacrylamide gel electrophoresis were transferred on a PVDF membrane using the XCell II module. Blotting pads, filter paper and membrane (all from Life Technologies) were soaked in transfer buffer with 0.1% antioxidant and 10% methanol p.a. (20% for blotting 2 gels). Arrangement in the module was: cathode – 3 pads – filter paper – membrane – filter paper – 3 pads – anode for one gel and cathode – 2 pads – filter paper – membrane – filter paper – 1 pad – filter paper – membrane – filter paper – 2 pads – anode for two gels blotting. The module was filled with transfer buffer and the outer chamber with water for cooling. Blotting was performed with 30 Volt for 70 minutes. Afterwards the membrane was incubated in blocking solution while shaking at room temperature for one hour to reduce nonspecific antibody binding. For reversible Ponceau S staining, the blot was incubated in 10 ml Ponceau S staining solution for 5 minutes while shaking before the blocking step. Ponceau S-stained proteins on the membrane were visualized by subsequent washing with H₂O bidistilled.

3.2.3.6.3 Protein detection

Detection of specific proteins in the whole cell lysates was accomplished by incubating the immunoblot membrane in a solution of the primary antibody as listed in section 3.1.8.1 in blocking solution or 5% BSA/0.1% Tween20 (in case of Cell Signaling antibodies) with 0.02% sodium azide at 4°C and shaking overnight. To remove non-bound antibodies the membrane was washed with PBS/0.1% Tween20 three times. The correlating secondary antibody, coupled with horse radish peroxidase (HRP), was diluted as described in section 3.1.8.2 in blocking buffer and incubated with shaking at room temperature for one hour. The membrane was washed again three times to remove excessive secondary antibody. Proteins were analyzed via chemiluminescence generated by the reaction of HRP with the Amersham Enhanced Chemiluminescence (ECL) Prime Western Blotting Detection Reagent (GE Healthcare; 1.5 ml per membrane) for 5 minutes in darkness. The luminescence signal was detected with high

performance chemiluminescence films (GE Healthcare) and automatically developed in a KODAK RP X-OMAT Developer and Replenisher.

3.2.3.7 *Electrophoretic mobility shift assay*

To hybridize DIG-labeled oligonucleotides, 22.5 μl of the sense (100 μM) and 22.5 μl of the antisense strand (100 μM ; for sequences see section 3.1.5.3) were mixed with 1 μl MgCl_2 (0.5 M) and 1.3 μl Tris-HCl pH 8 (1 M) and incubated at 95°C in a heating block for 10 minutes. Afterwards, the heating block was turned off and allowed to cool down to room temperature for about 3 hours. One-hundred picomol of double-stranded, DIG-labeled oligonucleotide were incubated with 2 μg protein extract (prepared from 1205Lu according to section 3.2.3.5.2) at 37°C for 30 minutes in a 20 μl reaction mixture containing 1x EMSA binding buffer (10 mM Hepes pH 8, 50 mM NaCl, 0.1 mM EDTA, 5 mM MgCl_2 , 5% glycerol), 2 μg poly(dG:dC) (InvivoGen) to compete non-specific DNA binding, 2 mM DTT, and 4 μg BSA. For supershift, 1 μl anti-SOX10 antibody (sc-17342x, Santa Cruz) or IgG control (Sigma) was added to the nuclear extract and incubated for 30 minutes on ice prior to oligonucleotide addition. DNA-protein complexes were separated at 4°C on a 6% DNA retardation gel (Invitrogen/Life Technologies) with TBE as running buffer for about 45 minutes at 150 Volt. Afterwards DNA-protein complexes were transferred to a positively-charged nylon membrane (Roche) by electro blotting with 0.5x TBE as transfer buffer at 30 Volt and cooling on ice for 70 minutes. After the transfer, the DNA was UV cross-linked to the membrane with an ultraviolet crosslinker (Amersham Life Science/GE healthcare) and energy 900,000 to 700,000 $\mu\text{J}/\text{cm}^2$. DIG-labeled oligonucleotides were visualized using DIG luminescent detection kit (Roche) according to the manufacturer's protocol and SOX10 was detected by immunoblotting on the same membrane.

3.2.3.8 *Immunohistochemistry*

Immunohistochemistry (IHC) allows the detection of antigens in cells of a tissue and is widely used in the identification of abnormal cells as found in cancers, staining of biomarkers, and analysis of differentially protein expression in different parts of a biological tissue. There are several options of visualizing the antigen-antibody binding on a tissue e.g., with a coupled enzyme that catalyzes a color-producing reaction or a fluorophore tag as fluorescein or rhodamine.

In this study, SOX10 expression in the tumor cells of the chick embryo invasion assay (section 3.2.2.3.3) was detected with the alkaline phosphatase-anti-alkaline-phosphatase (APAAP) method. Therefore, paraffin-embedded slices were deparaffinized by incubation twice in xylene (Merck) at room temperature for 10 minutes followed by incubation in 100%, 96%, 80%, 70% 2-propanol p.a. (AppliChem, Darmstadt, Germany) and H₂O bidistilled for 4 minutes each. Afterwards, the slides were boiled twice for 10 minutes in IHC Select® Citrate Buffer pH 6 (Millipore/Merck) in a microwave. After cooling down for 20 minutes, the citrate buffer was exchanged with tap water followed by washing twice for 5 minutes with Tris buffer. For localizing the antibody solution, each slice was circled with a Dako Delimiting Pen (Dako, Glostrup, Denmark). Non-specific binding sites were blocked by covering the slides with 20% BSA/Tris buffer. After blocking, the primary antibody (anti-SOX10 rabbit polyclonal antibody, Medac Diagnostika, dilution 1:25 in Tris buffer) was added and incubated at 4°C in a wet chamber overnight. The excessive antibody was removed by washing twice with Tris buffer for 4 minutes. Antibody detection was carried out with the Dako REAL™ Detection System (Dako). First, a mouse-anti-rabbit antibody was added in a 1:100 dilution in 12.5% BSA/Tris buffer at room temperature for one hour followed by washing twice with Tris buffer for 4 minutes. Then a rabbit-anti-mouse antibody was added in a 1:20 dilution in 12.5% BSA/Tris buffer at room temperature for 30 minutes followed by washing as described before. The APAAP antibody was added in a 1:50 dilution in 12.5% BSA/Tris buffer for 30 minutes followed by washing. The alkaline phosphatase was detected with a SIGMA FAST™ Fast Red TR/Naphthol AS-MX Alkaline Phosphatase Substrate Tablets Set (Sigma) by resolving the tablets in 1 ml H₂O bidistilled. The substrate was added and incubated for 6 to 20 minutes in darkness with monitoring the color change. After color change, the substrate was removed by washing twice for 4 minutes with Tris buffer. A counterstaining with Mayer's hemalum solution (hemalum solution acid according to Mayer, Roth) followed by a short wash in H₂O bidistilled, 1 minute incubation in hemalum solution, two times short wash in tap water, 5 minutes incubation in tap water and short wash in H₂O bidistilled. For conservation, a cover glass was fixed on top of the tissue slices with about 150 µl Kaiser's glycerol gelatin (Merck, preheated to 50°C in a water bath) per microscope slide. H&E staining and MIB1 IHC were performed as previously described by Busch et al. [38]. Pictures were taken with a TissueFAXS (TissueGnostics).

3.2.3.9 Chromatin immunoprecipitation

For analyzing protein-DNA binding *in vivo* by chromatin immunoprecipitation (ChIP) 7.5×10^6 1205Lu cells in 10 ml TU2% medium were fixed with 1% formaldehyde (Merck) at room temperature and shaking for 10 minutes. The reaction was stopped by adding 125 mM glycine (1.25 M stock solution, Fluka/Sigma) and incubating at room temperature while shaking for 5 minutes. Cells were washed twice with ice-cold PBS and centrifugation (1,000 rpm, 4°C, and 3 minutes) in between. Pellets were resuspended in 1 ml cell lysis buffer and incubated on ice for 10 minutes followed by a centrifugation at 5,000 rpm at 4°C for 5 minutes. The supernatant was aspirated and the pellet deep frozen at -80°C. The next step was to expose the genomic DNA and shatter it into fragments of 100 to 1,000 bp size. This was accomplished by resuspending the cell pellet in 250 µl nuclear lysis buffer followed by incubation for 10 minutes on ice. Nuclei were sonicated twice with the settings 30 seconds on, 30 seconds off for 10 minutes, and 25% amplitude with an EpiShear™ Probe Sonicator (Active Motif). To control DNA shearing, 25 µl of the sheared chromatin were added to 5 µl of a 10% chelex (Sigma) suspension in TE buffer and 20 µg Proteinase K (Qiagen). The chromatin was digested at 56°C for 15 minutes, heated to 95°C for 15 minutes, and controlled on a 1% agarose gel. If shearing was successful, the chromatin was diluted 1:10 in IP dilution buffer and pre-cleared with salmon sperm DNA/Protein G agarose beads (Millipore, washed 3 times with IP dilution buffer prior to usage) at 4 °C for 30 minutes to get rid of non-specific DNA binding. Beads were removed by spinning down at 1000 rpm, 4°C, for 2 minutes and the supernatant (pre-cleared, sheared chromatin) was used for further steps. One-tenth of this chromatin was kept as input control. In the next step, DNA fragments that were bound by SOX10 were precipitated by adding 2.4 µg anti-SOX10 antibody to one half of the sheared chromatin and an 2.4 µg control IgG (Sigma) to the other half followed by incubation on a wheel at 4°C overnight. For immunoprecipitation, 30 µl salmon sperm DNA/Protein G agarose beads were added and incubated on the wheel at 4°C for further 2 hours. To remove non-specific bound protein-DNA complexes, following washing steps were performed while shaking on ice with 600 µl of each buffer and centrifugation at 1,000 rpm, 4°C, for 1 minute in between:

IP dilution buffer	1 minute
Low salt wash buffer	1 minute
High salt wash buffer	5 minutes

LiCl wash buffer	5 minutes
TE buffer	1 minute

The cross-link between protein-DNA complexes was removed by incubating the beads in 120 μ l elution buffer with 6 μ l 5 M NaCl at 65°C overnight. The input control was included in this step analogously. RNA and proteins were removed by adding 30 μ g RNase and incubating at 37°C for 1-2 hours followed by adding Proteinase K to a final concentration of 0.4 mg/ml and further incubation at 56°C for 2 hours. NTB buffer (Macherey-Nagel) was added in the range 5:1 followed by a column purification of the DNA fragments with the Nucleospin PCR Clean-up Kit (Macherey-Nagel) according to manufacturer's protocol and elution with 50 μ l NE buffer. Three μ l were subjected to qRT-PCR with primers according to section 3.1.5.2. Co-purified DNA in anti-SOX10 and control IgG samples was determined relative to the input control.

3.2.4 Statistical analyses

Unless otherwise stated, all experiments were performed in at least three independent experiments. Data show mean values \pm standard deviation (SD). Statistics were calculated in Prism v 5.04 (GraphPad Software, San Diego, CA, USA). Two groups were compared using an unpaired two-tailed *t*-test. For multiple comparisons, one-way analysis of variance (one-way ANOVA) with Dunnett's post hoc test was used. The (linear) correlation of expression between two genes in human skin and melanoma cell lines was evaluated by Pearson's correlation. Differences were considered significant at a *P*-value of 0.05 or less.

4 Results

4.1 Expression of SOX9 and SOX10 in human skin and melanoma cells

To characterize the role of selected proteins in a specific tissue type, the expression of these proteins has to be analyzed. Concerning the analysis of proteins in tumor cells, it is important to determine the relative expression compared to non-transformed cells in the first step. The expression of SOX9 and SOX10 in melanocytes, melanocytic naevi, primary and metastatic melanoma cell lines and tissues have already been investigated [4], [8], [44], [52], [238], [239]. However, expression values varied substantially between the different studies.

In this study expression of SOX9 and SOX10 was analyzed in a panel of human skin cells, melanoma cell lines, and short term-cultured melanoma cells.

4.1.1 Expression in human fibroblasts, melanocytes, and melanoma cell lines

SOX10 and SOX9 mRNA levels were measured by qRT-PCR in cultivated primary human fibroblasts from two different donors (Figure 6 a and Figure 7 a, white bars), primary human melanocytes from three different donors (Figure 6 a and Figure 7 a; black bars), and 12 melanoma cell lines derived from tumors of different progression stages (Figure 6 a and Figure 7 a, grey bars; RGP = radial growth phase, VGP = vertical growth phase). The expression on protein level was determined in the same samples by immunoblotting (Figure 6 b and Figure 7 b, c).

SOX10 mRNA levels in fibroblasts were low and no protein was detected by immunoblotting (Figure 6 a and b). Although higher amounts of SOX10 mRNA were detected in melanocytes compared to melanoma cells on mRNA level, this observation was less pronounced on protein level. Among the different melanoma cell lines SOX10 mRNA levels varied and SOX10 protein was detected in 8 of 12 melanoma cell lines. Two of the four negative ones derived from tumors of radial growth phase (SbCl2, WM3211) suggesting that SOX10 protein expression is associated with a more invasive or metastatic phenotype. Measured protein and mRNA amounts of SOX10 correlated in all analyzed melanoma cell lines except for cell line SbCl2.

Mean levels of SOX10 mRNA and protein in fibroblasts, melanocytes, and melanoma cell lines were compared. SOX10 was significantly decreased in fibroblasts and melanoma cells compared to melanocytes on mRNA (Figure 6 c) as well as on protein level (Figure 6 d).

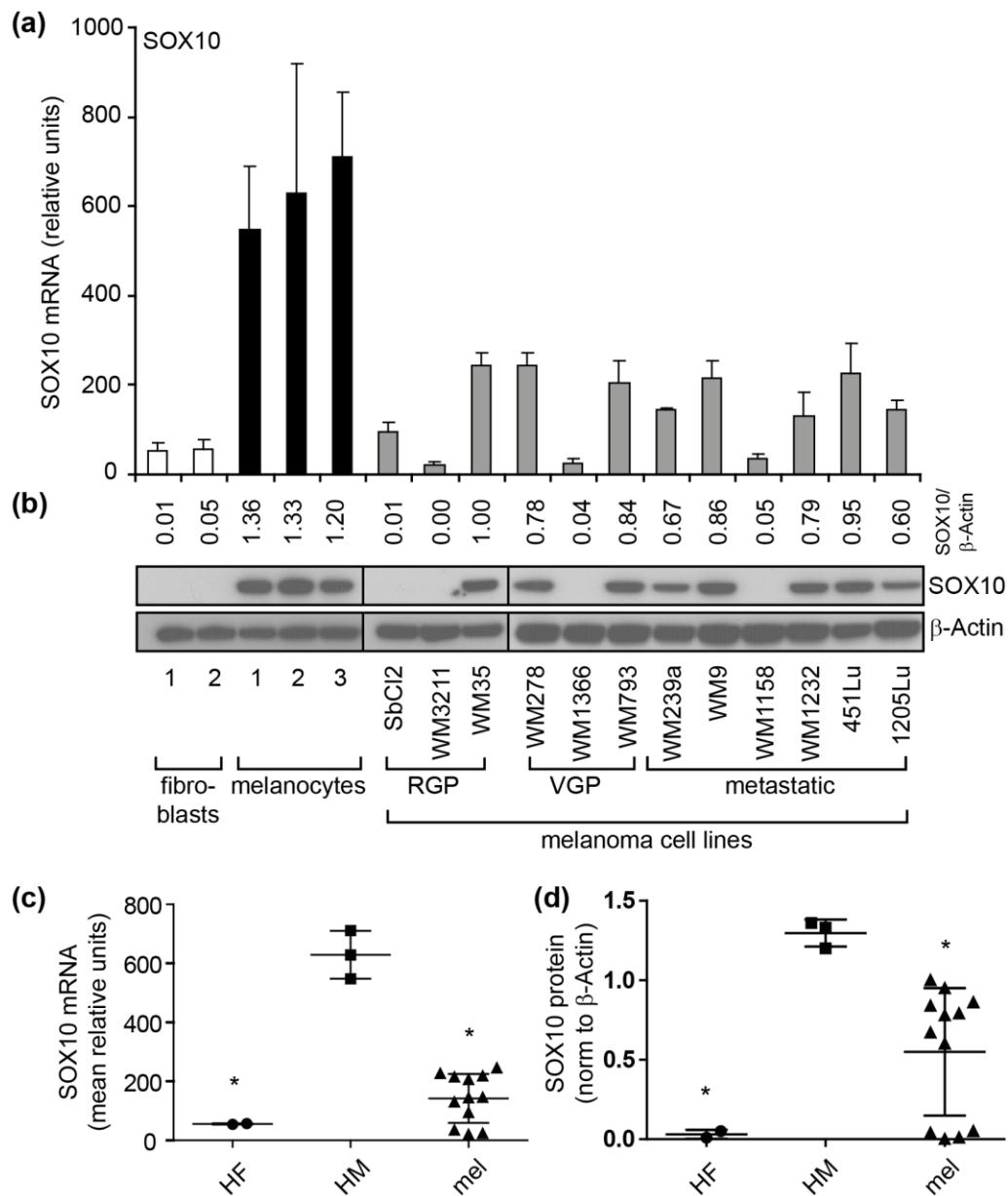


Figure 6: Expression of SOX10 in human skin cells and melanoma cell lines.

(a) SOX10 mRNA (mean \pm SD of three independent experiments) was assessed by qRT-PCR in fibroblasts (two donors, white bars), melanocytes (three donors, black bars), and melanoma cell lines of different progression stages (RGP = radial growth phase, VGP = vertical growth phase, and metastatic; grey bars). **(b)** SOX10 protein levels were assessed in the same cells as described in (a) using a SOX10-specific antibody. Detection of β -Actin served as loading control. Numbers above the blots display quantification of the SOX10 bands with Fiji ImageJ, normalized to β -Actin. Mean mRNA **(c)** and protein **(d)** amounts of SOX10 in human fibroblasts (HF), melanocytes (HM), and melanoma cell lines (mel) were compared with a scatter blot. Significant decrease of SOX10 in HF and mel compared to HM were found on mRNA and protein level (one-way ANOVA versus HM, $*P < 0.0001$ for mRNA and $*P < 0.01$ for protein). No significant change between HF mRNA and protein was found compared to mel (*t*-test).

In case of SOX9, moderate mRNA levels were measured in fibroblasts and melanocytes, while varying amounts were detected in the different melanoma cell lines (Figure 7 a).

Antibodies against SOX9 from the companies Chemicon, Zytomed Systems, and Millipore were used in this study. In addition to SOX9 (predicted molecular weight 56 kDa, detected about 65 kDa), a protein in the molecular weight range of SOX10 (predicted molecular weight 50 kDa, detected 58 kDa) was detected with these antibodies. As example, the Millipore antibody was used in Figure 7 b. Thus, the tested SOX9 antibodies fail to discriminate between SOX9 and SOX10 epitopes and so deteriorate the discrimination, a problem that was also described by Shakhova et al. [238]. An antibody against SOX9 phosphorylated at serine 181 (Anaspec Inc.) was included in the studies, which specifically detected the SOX9 epitope without non-specific SOX10 binding (Figure 7 c). Serine 181 (S181) in the SOX9 amino acid sequence represents a consensus phosphorylation site for the protein kinase A (PKA). Phosphorylation at this site leads to nuclear localization of SOX9 by enhancing its binding to the nucleocytoplasmic transport protein importin β [172]. Therefore, SOX9 phosphorylated at S181 represents transcriptionally active, nuclear SOX9. Using SOX9- and phospho-SOX9 specific antibodies for detection, SOX9 protein levels were found to be weak in fibroblasts and melanocytes, while melanoma cells displayed varying expression levels (Figure 7 b and c).

Phospho-SOX9 (pSOX9) protein correlated with mRNA levels in the analyzed melanoma cell lines except for WM1366, WM239A, and WM9.

Mean levels of SOX9 mRNA and protein in fibroblasts, melanocytes, and melanoma cell lines were compared. No significant change was found on mRNA for the three cell types (Figure 7 d). Also on protein level no significant change was found, although a tendency of higher expression in melanoma cell lines compared to fibroblasts and melanocytes was observed (Figure 7 e).

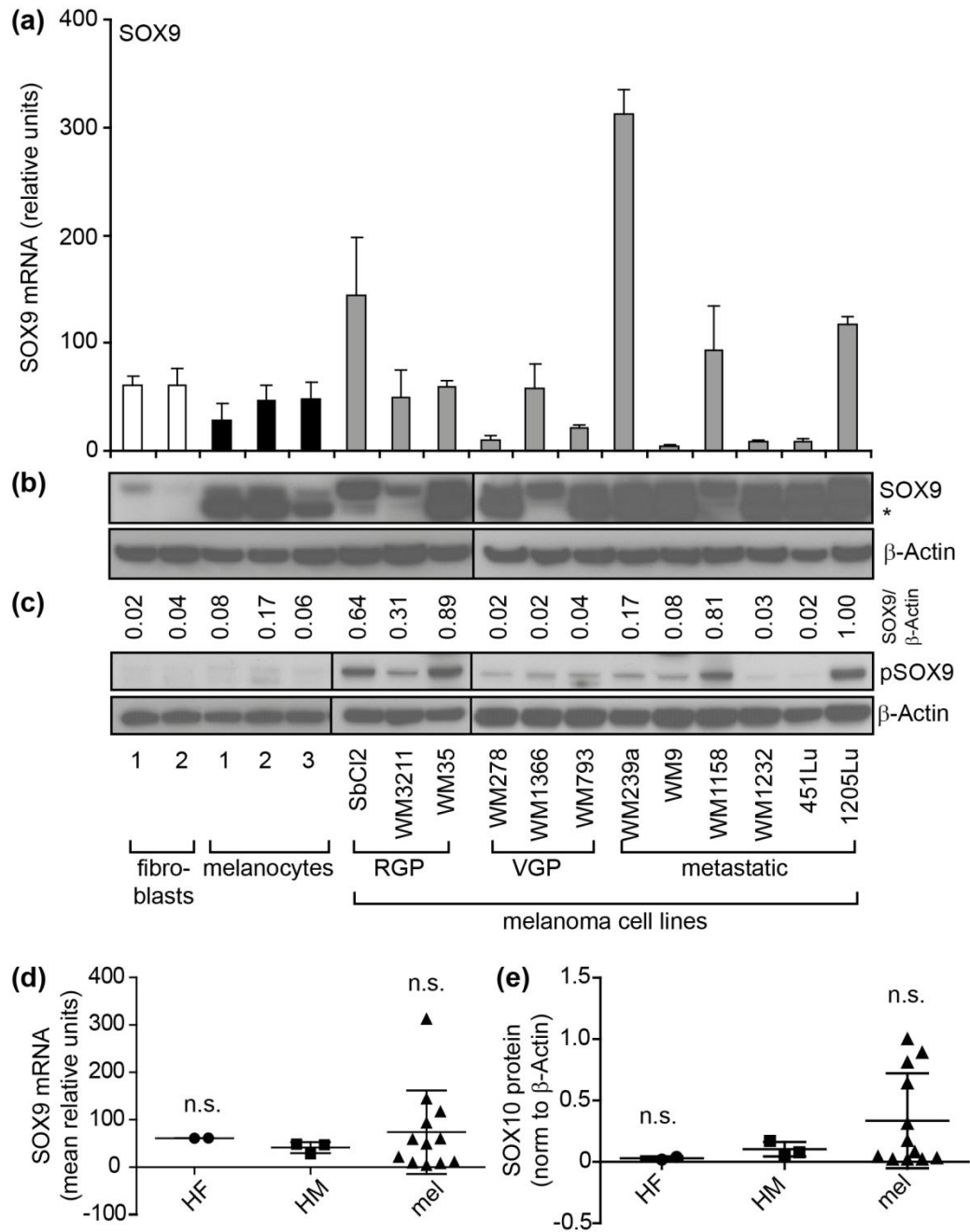


Figure 7: Expression of SOX9 in human skin cells and melanoma cell lines.

SOX9 expression was assessed in the same cell lines as described in Figure 6 on mRNA (a) and on protein (b, c) level. SOX9 expression on protein level was detected with a SOX9-specific antibody (Millipore, b) or a phospho-SOX9 specific antibody (c). An asterisk marks the non-specific SOX10 signal detected with the SOX9 antibody (Millipore). Detection of β -Actin served as loading control. Numbers above the blots display quantification of the bands with Fiji ImageJ, normalized to β -Actin. Mean mRNA (d) and protein (e) amounts of SOX9 in human fibroblasts (HF), melanocytes (HM), and melanoma cell lines (mel) were compared with a scatter blot. No significant change of SOX9 in HF and mel compared to HM were found on mRNA and protein level (one-way ANOVA versus HM, n.s. = not significant). No significant change between HF mRNA and protein was found compared to mel (*t*-test).

Inverse mRNA expression of SOX9 and SOX10 was observed in 8 of 12 analyzed melanoma cell lines (WM3211, WM278, WM1366, WM793, WM9, WM1158, WM1232, 451Lu). A significant negative linear correlation was found in these cell lines (Figure 8, Pearson coefficient $\rho = -0.8343$, $*P = 0.01$).

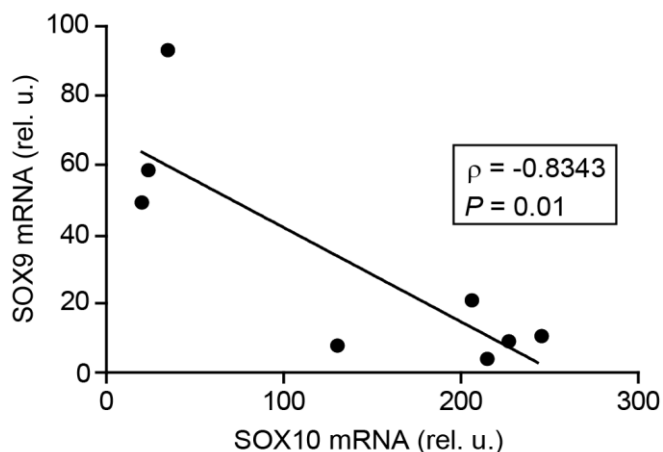


Figure 8: Inverse correlation of SOX9 and SOX10 mRNA expression.

Negative linear correlation between SOX10 and SOX9 mean mRNA values (according to Figures 6 and 7) was found in melanoma cell lines WM3211, WM278, WM1366, WM793, WM9, WM1158, WM1232, and 451Lu (Pearson correlation, $\rho = -0.8343$, $*P = 0.01$). rel. u. = relative units.

4.1.2 Expression in short term-cultured melanoma cells

Cancer cell lines proliferate indefinitely in cell culture. However, long term cultivation of cells can cause genotypic and phenotypic alterations. Therefore, melanoma cells were freshly isolated from patient tumor samples (ρm = primary melanoma, km = cutaneous metastasis, gm = brain metastasis). MITF and human melanoma black 45 (HMB45) detected by immunoblotting were used as markers for melanoma cells (Figure 9) [89], [129]. SOX10, pSOX9, and SOX9 protein levels were detected by immunoblotting in these cells (Figure 9). Compared to primary melanoma and most cutaneous melanoma samples SOX10 was little expressed in cell line LMU-KM04 and highly expressed in brain metastasis cell line LMU-GM01. SOX9 and pSOX9 protein was detected in variable amounts in all analyzed short term-cultured melanoma cell lines.

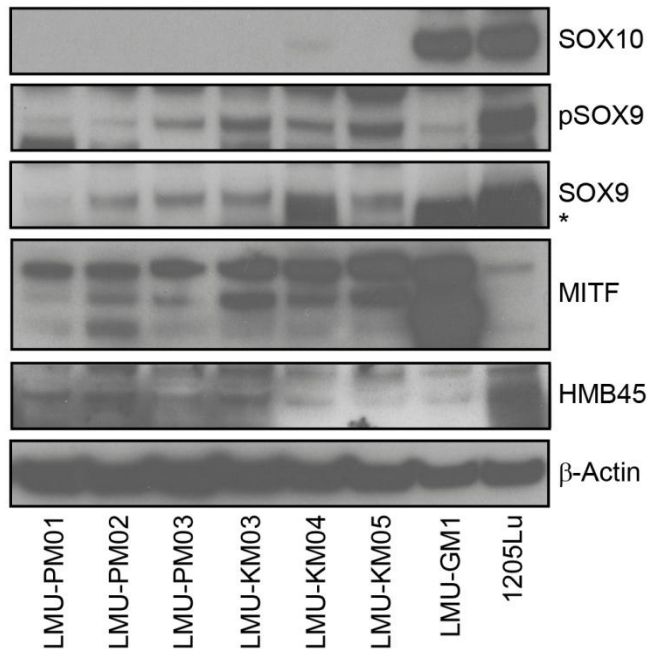


Figure 9: Expression of SOX9 and SOX10 in short term-cultured human melanoma cells.

SOX10, pSOX9, and SOX9 protein expression was assessed by immunoblotting in short term-cultured human melanoma cells from primary tumors (LMU-PM01, LMU-PM02, and LMU-PM03), cutaneous metastases (LMU-KM03, LMU-KM04, and LMU-KM05), a brain metastasis (LMU-GM1), and 1205Lu as reference. Detection of MITF and HMB45 served as markers for melanoma cells, β -Actin served as loading control. An asterisk marks the non-specific SOX10 signal detected with the SOX9 antibody.

Analyses of SOX9 and SOX10 expression in melanoma cell lines as well as in short term-cultured melanoma cells indicate an inverse expression pattern of SOX9 and SOX10 and an association of SOX10 with tumor metastasis.

4.2 Inhibition of SOX9 and SOX10 via RNA interference

RNA interference is a frequently used method to manipulate gene expression and thereby gaining insight into its cellular functions. Generally, RNA interference prevents the cell from virus infections via small interfering RNAs (siRNAs), regulates gene expression via microRNAs (miRNAs), or controls transposons via P-element induced wimpy testis (PIWI) interacting RNAs (piRNAs). The potential of double-stranded RNA (dsRNA) to effectively silence selected genes was first described 1998 in the nematode worm *Caenorhabditis elegans* by Andrew Fire and Craig Mello [71], who shared the Nobel Prize in Physiology and Medicine 2006. The dsRNA is recognized by the Dicer enzyme that processes it into 21-23 nucleotide siRNAs. These siRNAs are incorporated into a multicomponent nuclease complex, the RNA-induced silencing complex (RISC), and is unwound into single strands [97]. After degradation of the sense strand, the antisense strand serves as a matrix for sequence-specific RNA degradation.

Small interfering RNAs for silencing SOX9 (siSOX9b) and SOX10 (siSOX10a) have been described previously [72]. All siRNAs have been designed according to the algorithms of Reynolds [214] and Ui-Tei [271]. To minimize the risk of non-specific effects of the RNA interference, two different siRNAs were included in the analyses.

The effectiveness of the gene knockdown was tested in metastatic melanoma cell line 1205Lu by transfection of the two different siRNAs and a control siRNA, which was designed not to interfere with the human transcriptome.

Inhibition of SOX9 by both SOX9-targeting siRNAs led to a decrease of SOX9 mRNA down to 40% (Figure 10 a), while siSOX10a reduced SOX10 mRNA expression down to approximately 50%, and siSOX10b down to approximately 60% (Figure 10 b).

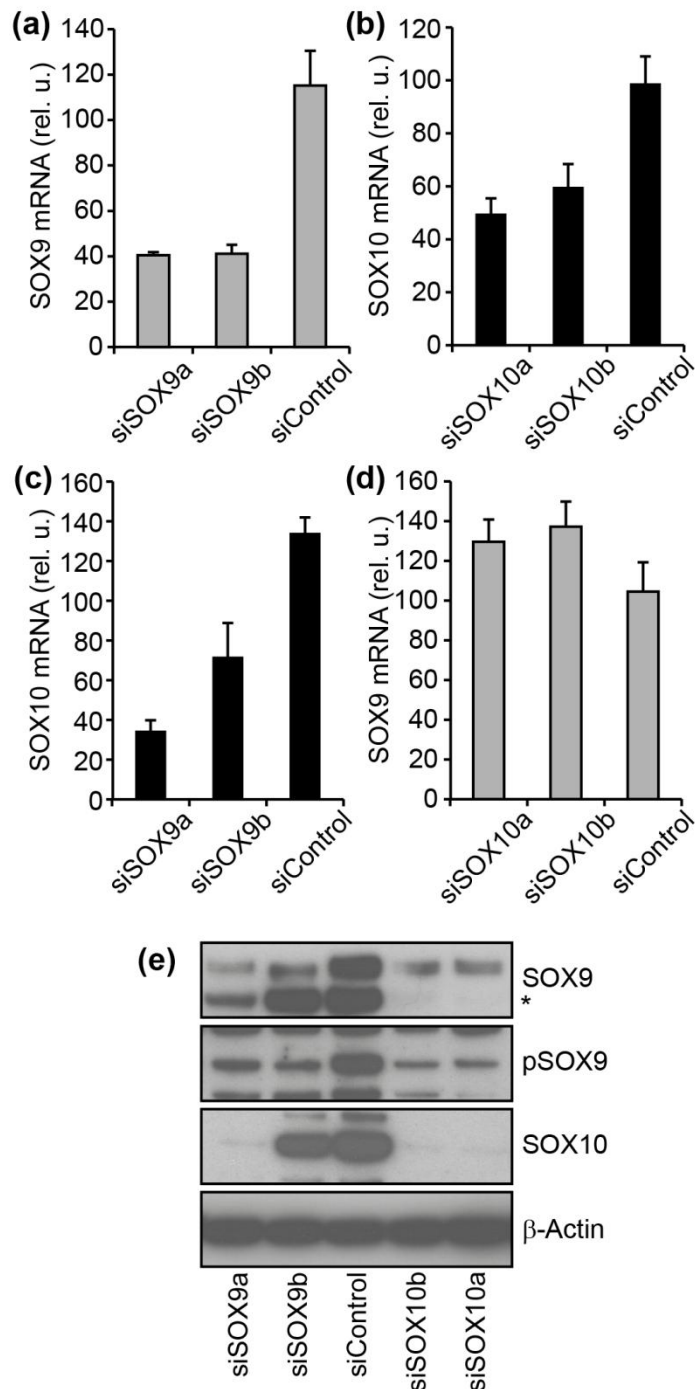


Figure 10: Inhibition of SOX9 and SOX10 via RNA interference.

(a) SOX9 mRNA (mean \pm SD of three independent experiments) was measured in 1205Lu cells 48 hours after transfection of SOX9-targeting siRNAs (siSOX9a and siSOX9b) in comparison to a control siRNA (siControl). **(b)** SOX10 mRNA expression was analyzed according to (a) after transfection of SOX10-targeting siRNAs (siSOX10a and siSOX10b) in comparison to siControl. **(c)** SOX10 mRNA expression was analyzed in the SOX9-inhibited 1205Lu cells described in (a). **(d)** SOX9 expression was analyzed in the SOX10-inhibited cells described in (b). **(e)** SOX9, pSOX9, and SOX10 were detected 72 hours after transfection of both SOX9- and SOX10-targeting and control siRNAs. An asterisk marks the non-specific SOX10 signal detected with the SOX9 antibody (Millipore). Detection of β -Actin served as loading control.

To analyze a potential cross-regulation, SOX10 mRNA was assessed after SOX9 inhibition and vice versa. Transfection of siSOX9a and siSOX9b reduced SOX10 mRNA

expression down to approximately 30% and 70%, respectively (Figure 10 c), while both SOX10-targeting siRNAs did not decrease but slightly increase SOX9 mRNA expression (Figure 10 d).

On protein level, SOX9 and SOX10 were effectively reduced using both specific siRNAs (Figure 10 e). The reduction on protein level was more pronounced for SOX10 than for SOX9. Similar to the observation on mRNA level, transfection of SOX9-targeting siRNAs also reduced SOX10 protein levels, especially when using siSOX9a. In contrast to the findings on mRNA level, SOX10 inhibition reduced SOX9 protein expression. These data indicate that the effect of SOX9 on SOX10 is on a transcriptional level, while the effect of SOX10 on SOX9 is on a post-transcriptional level.

Further analyses focused on the functional characterization of SOX10 in melanoma. Three different cell lines (VGP cell line WM278 and metastatic cell lines WM1232 and 1205Lu) were examined in this study to find out whether effects were cell line dependent. Effective inhibition of SOX10 on protein level is shown in Figure 11. Transfection of SOX10-targeting siRNA led to strong decrease (in WM1232) up to complete abolishment (in WM278 and 1205Lu) of detectable SOX10 protein already after 24 hours.

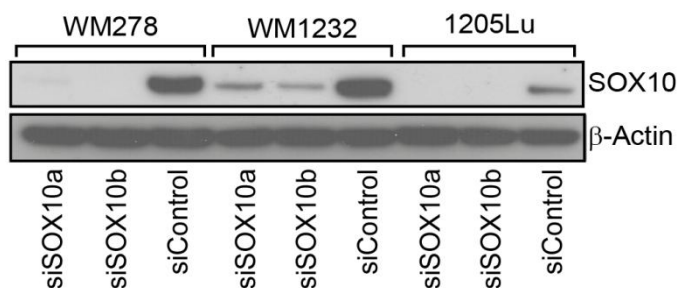


Figure 11: SOX10 inhibition in cell lines WM278, WM1232, and 1205Lu.

SOX10 protein expression was detected by immunoblotting in cell lines WM278, WM1232, and 1205Lu 24 hours after transfection of two SOX10-targeting siRNAs (siSOX10a and siSOX10b) and a control siRNA (siControl). Detection of β -Actin served as loading control.

4.3 Phenotypic effects of SOX10 inhibition in melanoma cells

4.3.1 Effects of SOX10 inhibition on melanoma cell proliferation

Effects of SOX10 inhibition were analyzed in time course experiments with melanoma cell lines WM278, WM1232, and 1205Lu every 24 hours up to 120 hours post transfection. Microscopically imaging revealed changes in cell number and morphology starting from 72 hours post transfection of both SOX10-targeting siRNAs compared to control cells.

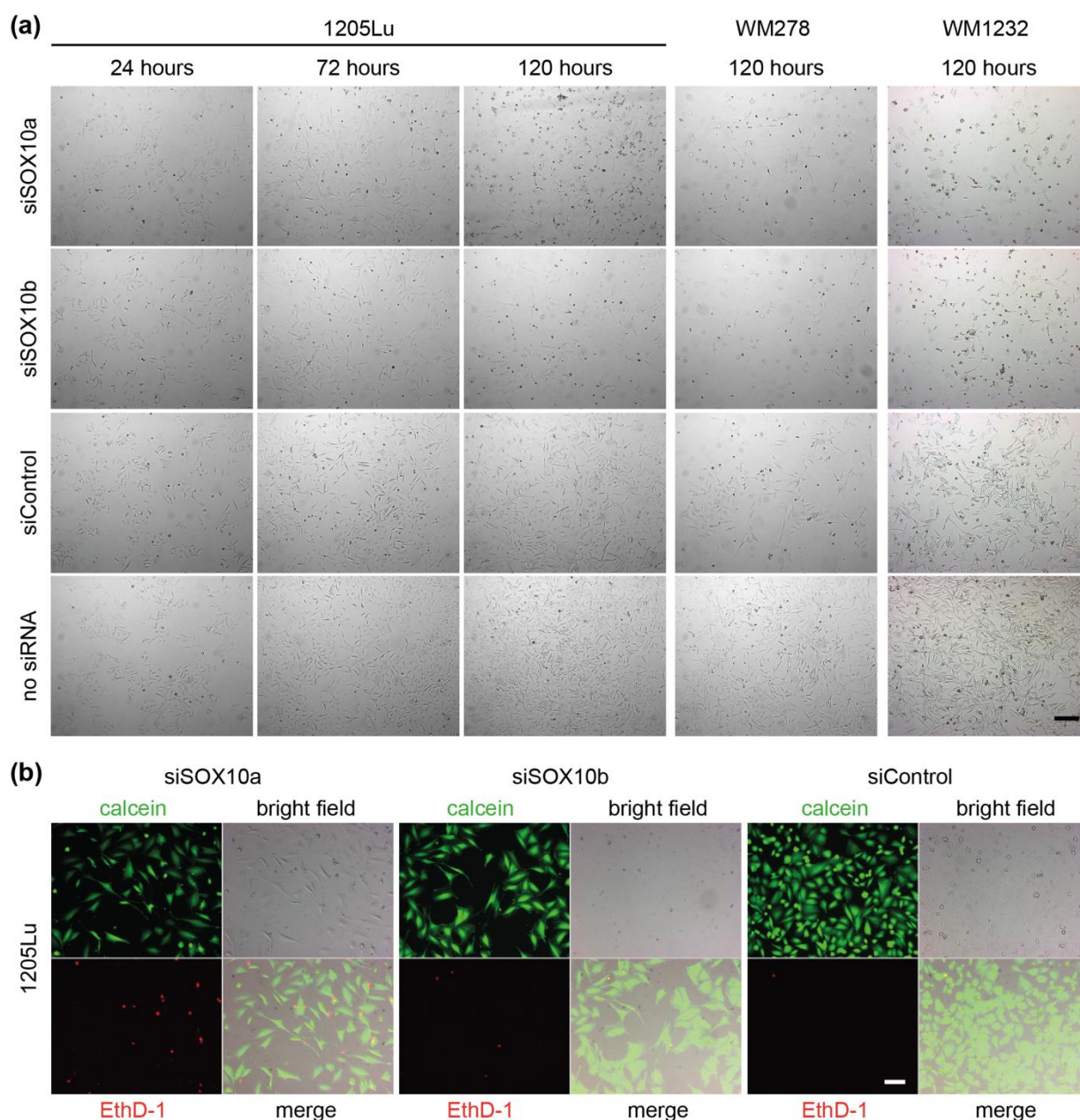


Figure 12: Alteration of cell morphology and reduction of number after SOX10 inhibition.

Cell morphology after SOX10 inhibition was monitored by bright field and fluorescence imaging every 24 hours up to 120 hours post transfection of siSOX10a, siSOX10b, siControl or without siRNA in cell lines 1205Lu, WM278, and WM1232. **(a)** Representative pictures after 24, 72, and 120 hours are shown for 1205Lu and after 120 hours for WM278 and WM1232. Scale bar = 200 μm . **(b)** 1205Lu cells were stained with a calcein AM and EthD-1 120 hours post transfection with siSOX10a, siSOX10b or siControl and fluorescence pictures were taken about 45 minutes after adding the dye. Scale bar = 50 μm .

Some cells started to round up and die, while others had increased protrusions and showed a change towards a more dendritic phenotype, which was most prominent after 120 hours and observed in all analyzed cell lines (Figure 12 a).

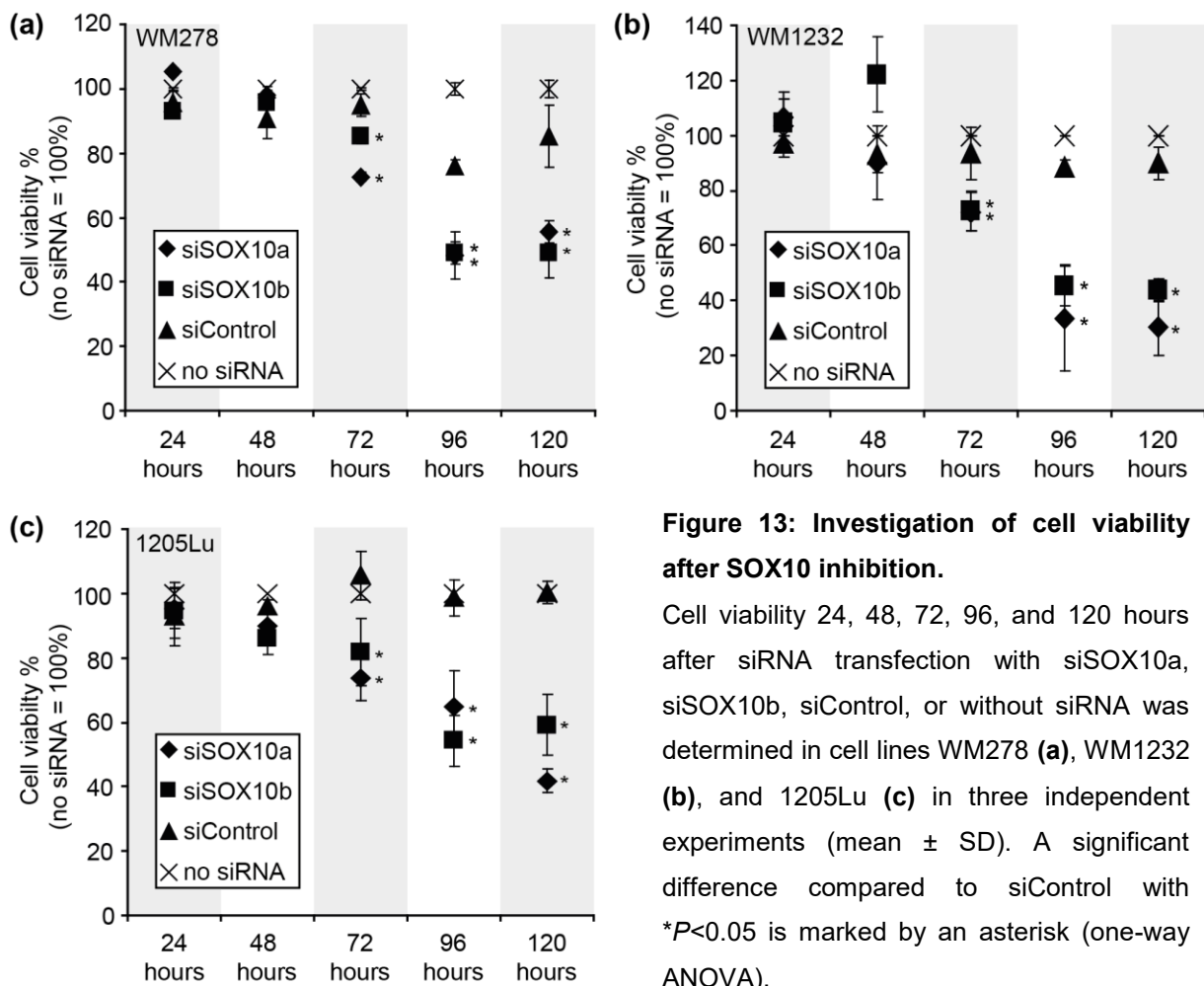
To discriminate between living and dead cells, 1205Lu melanoma cell were stained with a LIVE/DEAD® viability/cytotoxicity kit (Life Technologies) according to the

manufacturer's protocol. Living cells possess ubiquitous intracellular esterase activity that converts the non-fluorescent membrane-permeant calcein AM to a strong fluorescent polyanionic calcein. This non-membrane-permeant calcein has an extinction maximum of 495 nm and an emission maximum of 515 nm. The other dye in this assay, ethidium homodimer (EthD-1), cannot permeate the intact cellular membrane. However, it enters damaged membranes and binds nucleic acids. Thereby, its fluorescence is enhanced around 40-fold, with an extinction maximum of 495 nm and an emission maximum of 635 nm. In conclusion, living cells appear green under a fluorescence microscope while dead cells appear with red colored nuclei.

Compared to the cells transfected with control siRNA, the confluence of SOX10-inhibited cells was reduced to around 50% (Figure 12 b). They showed altered cell morphology although their cell membrane stayed intact. Red staining from EthD-1 incorporation increased upon SOX10 inhibition with both siRNAs, with siSOX10a more than with siSOX10b.

Because SOX10 inhibition reduced the number of adherent cells it possibly affects melanoma cell proliferation. To test this hypothesis the viability of SOX10-inhibited melanoma cells compared to cells transfected with control siRNA or without siRNA was determined with a CellTiter-Blue® Cell Viability Assay (Promega). This method is based on the metabolic capacity of cells, as viable cells reduce the provided indicator dye resazurin into the highly fluorescent resorufin. As nonviable cells lose their metabolic capacity, they cannot generate the pink resorufin leading to a lack of signal in the corresponding probing channel.

Cell viability analysis demonstrated that both SOX10-targeting siRNAs significantly reduced cell viability after 72 hours in all three cell lines (Figure 13 a-c). After 120 hours, cell viability was reduced down to around 50% in cell line WM278 for both siRNAs (Figure 13 a), down to 30.2% in cell line WM1232 for siSOX10a and 43.7% for siSOX10b (Figure 13 b), and down to 41.8% in cell line 1205Lu for siSOX10a and 59.2% for siSOX10b, respectively (Figure 13 c). Thus, the effect on cell viability was in a similar range for both SOX10-targeting siRNAs in all three analyzed melanoma cell lines.



SOX10 might also affect cell proliferation by influencing cell cycle progression. Cell cycle progression can be directly measured by flow cytometry. Generally, the cell cycle can be divided into three stages: the interphase, the mitotic phase, and cytokinesis. Interphase is the prerequisite for every cell division and requires about 90% of the total time of a cell cycle. It is subdivided into Gap1- (G1-), synthesis- (S-), and Gap2- (G2-) phases. Every passage between these phases is strictly controlled by checkpoints. They ensure that the cell is ready for the next step in the cycle and that damaged or incomplete DNA is not passed on to daughter cells. During G1-phase the cell harbors a single chromosome set (2N) and it increases its supply of proteins, the number of organelles, as well as its size. The G1 checkpoint control makes sure that all preparations for DNA replication have been completed. From this phase, cells can enter a non-dividing quiescent G0-phase, which is common for fully differentiated cells as e.g. neurons and which can last permanently. When cell cycle continues, the DNA replication commences during S-phase where all chromosomes gain two sister chromatids.

In G₂-phase the cell harbors a double chromosome set (4N) and continues to grow. The G₂ checkpoint control makes sure that the cell is ready to enter mitosis and thereby cell division. The change in the amount of DNA during cell cycle progression can be quantified after staining of proliferating cells with the DNA intercalating agent propidium iodide (PI). One molecule PI incorporates every 4 to 5 DNA bases while the excitation maximum shifts about 30-40 nm to the red, the emission maximum about 15 nm to the blue, and the fluorescence is about 10-fold enhanced [6]. The proportional binding of PI to DNA allows direct conclusion to the amount of DNA present in a cell as the cell doubles its DNA amount in S phase. Thus, a cell in G₂- and early M-phase will have twice the DNA amount of a cell in G₁-phase and thereby intercalates twice the amount of PI. The change in fluorescence can be directly detected by flow cytometry. PI is impermeable for the membrane of a living cell and therefore cell membranes have to be permeabilized with 70% ethanol. Removal of RNA is also required for this assay as PI can also bind RNA. Figure 14 shows a typical histogram of actively proliferating 1205Lu melanoma cells.

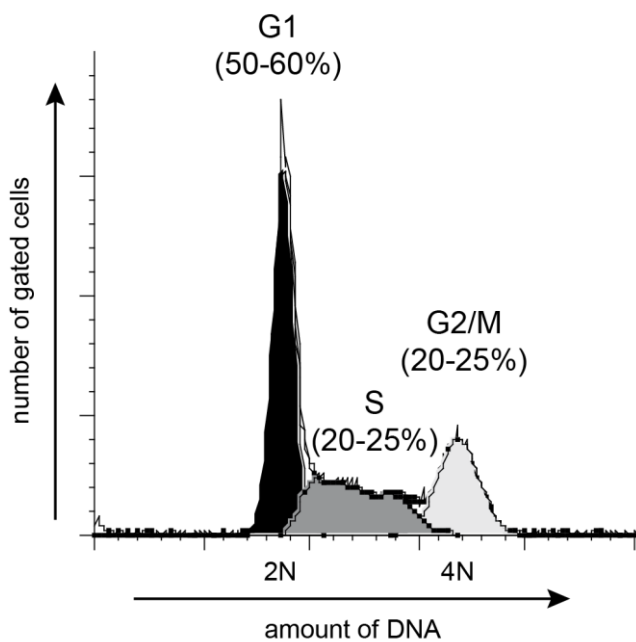


Figure 14: Schematic profile of cell cycle progression in 1205Lu cells.

The scheme represents a typical histogram of non-treated 1205Lu cells after staining with PI and analysis by FACS. This method allows the differentiation of cell cycle phases due to their different amounts of DNA. As displayed in the histogram, a strong signal is detected for cells in G₀- and G₁-phase (left peak, black), that carry a single chromosome set (2N) and a weaker signal for cells in G₂- or mitosis (M)-phase (right peak, light grey), that possess a double chromosome set (4N). The signal for cells in S-phase, which are replicating their DNA, is located in between (medium grey).

For non-treated 1205Lu cell a distribution of 50-60% in G₁-, 20-25% in S-, and 20-25% in G₂/M-phase was measured.

The distribution of cells in G₁-, S-, and G₂/M-phase differed between SOX10-inhibited and control 1205Lu cells from 24 to 48 hours after siRNA transfection (Figure 15 a).

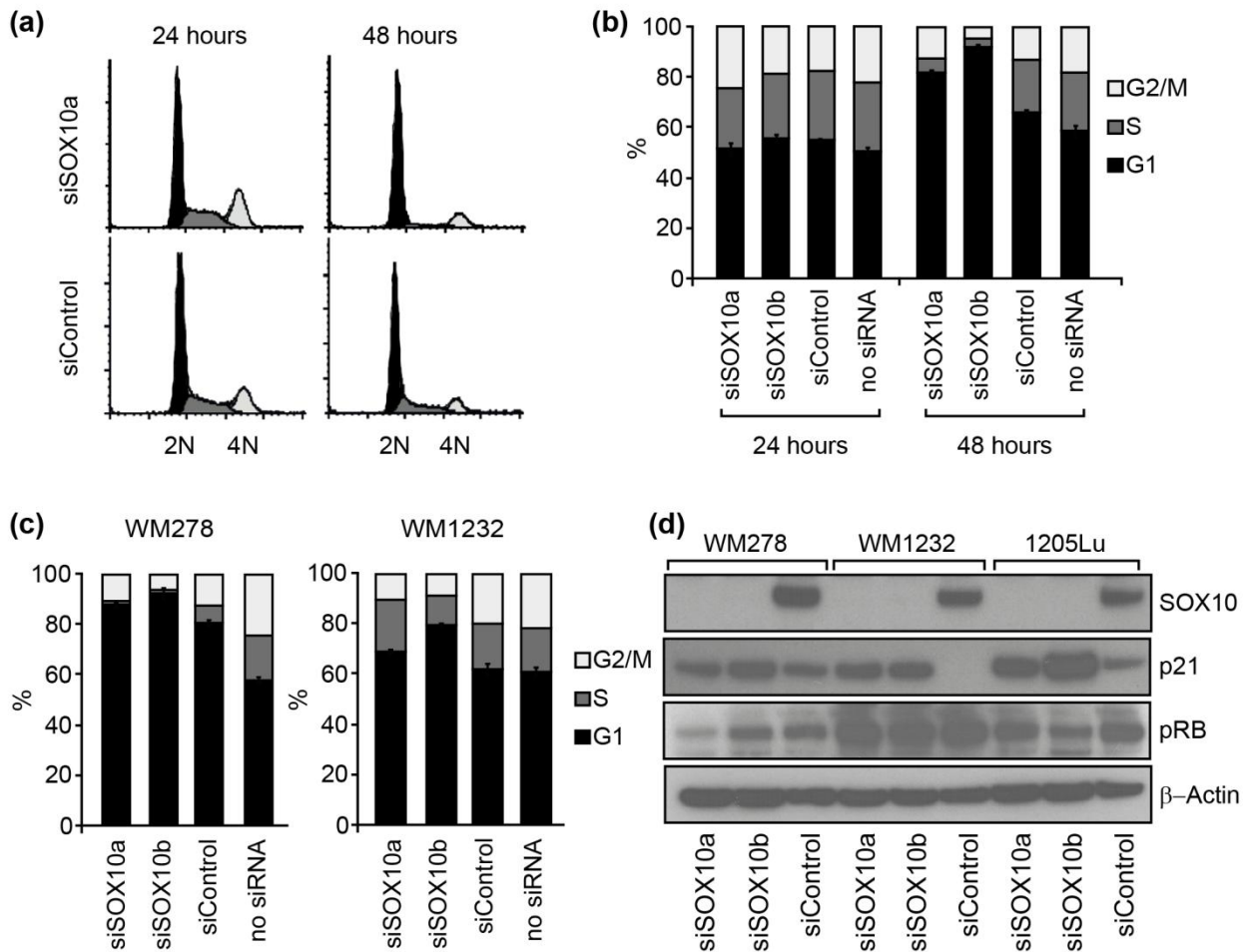


Figure 15: Influence of SOX10 inhibition on cell cycle progression.

(a) Representative histograms after staining with PI and flow cytometry of 1205Lu melanoma cells 24 and 48 hours after transfection with siSOX10a or siControl are depicted. **(b)** Bar charts represent the percentage distribution of 1205Lu cells in G1- (black), S- (medium grey), and G2/M- (light gray) phases 24 and 48 hours after transfection with siSOX10a, siSOX10b, siControl, or without siRNA and cell cycle analysis. Error bars represent mean \pm SD of cells in G1-phase from three independent experiments. **(c)** Bar charts of WM278 and WM1232 cells treated as described in (b) 48 hours after siRNA transfection. **(d)** SOX10, p21, and pRB were detected by immunoblotting 48 hours after transfection of siSOX10a, siSOX10b, and siControl in cell lines WM278, WM1232, and 1205Lu. Detection of β -Actin served as loading control.

The amount of SOX10-inhibited 1205Lu cells in S- and G2/M-phase were reduced compared to control cells and the number in G1-phase was increased 48 hours after siRNA transfection. Quantification revealed an increase of cells in G1-phase for SOX10 inhibition with both SOX10-targeting siRNAs compared to control cells after 48 hours (Figure 15 b). This effect was more pronounced for siSOX10b compared to siSOX10a. Similar effects were found in the cell lines WM278 and WM1232 after 48 hours (Figure 15 c).

As mentioned before, cell cycle progression is regulated at so-called checkpoints. These checkpoints are controlled by cyclins and cyclin-dependent kinases (CDKs) [185]. CDKs are constitutively expressed in cells but they are inactive without cyclins. Cyclins themselves have no catalytic subunit and they are synthesized at specific stages of the cell cycle in response to growth signals. Together they form active complexes. These complexes themselves can be blocked by several inhibitors that stop cell cycle progression e.g. upon DNA damage. P21 belongs to the *CDK interacting protein/kinase inhibitory protein* gene family and it can arrest cell cycle in G1 by direct binding to cyclin/CDK-complexes [100]. It can be activated by p53 as response to DNA damage [281]. P21 was found upregulated upon SOX10 inhibition in all three investigated cell lines 48 hours after siRNA transfection (Figure 15 d). Another protein that regulates G1- to S-phase transition is retinoblastoma protein (RB). RB physically associates with E2F transcription factors and blocks their transactivation domain in G0- and early G1-phase [83]. In late G1, phosphorylated RB (pRB) releases E2F transcription 1 to transcribe genes, which are necessary for S-phase progression. A decrease in pRB was found in all cell lines upon SOX10 inhibition with a higher effect for siSOX10a in cell line WM278 and for siSOX10b in cell lines WM1232 and 1205Lu (Figure 15 d). Increased p21 levels and decreased RB phosphorylation are a sign of cell cycle arrest in G1.

Furthermore, the DNA damage marker γ H2A.X was upregulated upon SOX10 inhibition as detected by immunoblotting (Figure 16 upper panel).

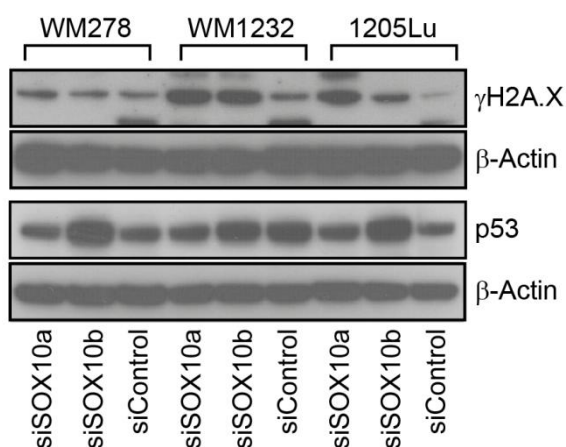


Figure 16: Increase in DNA damage markers after SOX10 inhibition.

The DNA-damage marker γ H2A.X and the transcription factor p53 were detected by immunoblotting in cell lines WM278, WM1232, and 1205Lu 72 hours after transfection of siSOX10a, siSOX10b, and siControl. Detection of β -Actin served as loading control.

H2A.X is phosphorylated at Ser139 (named γ H2A.X) by PI3K-like kinases, which attracts DNA damage response proteins [305]. Thus, it is required for checkpoint-mediated cell cycle arrest and DNA repair following DNA double-strand breaks.

Furthermore, p53 was found accumulated especially after transfection of siSOX10b (Figure 16 lower panel). P53 is a transcription factor that acts as “guardian of the genome” [144]. Usually it is inactive and continuously degraded upon ubiquitinylation. As a response to DNA damage, p53 is stabilized through phosphorylation, accumulates, and triggers responses such as cell cycle arrest, DNA repair, apoptosis, and senescence.

In conclusion, these data suggest that SOX10 inhibition reduces melanoma cell proliferation, leads to cell cycle arrest in G1, and causes DNA damage.

4.3.2 Effects of SOX10 inhibition on melanoma cell death

To further investigate the influence of SOX10 inhibition on melanoma cell survival, SOX10-inhibited compared to control cells were analyzed by flow cytometry quantifying cell death.

Phosphatidylserine (PS) is a phospholipid membrane component, which is actively being held towards the cytosolic side of the membrane by the enzyme flippase. When a cell undergoes apoptosis, PS is no longer restricted by flippase and flips to the extracellular surface. It is a well known mechanism to signal macrophages to engulf a dying cell [276]. This mechanism serves as marker to analyze apoptosis. The protein Annexin V (AN) specifically binds to PS and therefore enables its detection. In this study, AN labeled with the fluorescent dye fluorescein (Annexin V-Fluos) was used for detection with excitation at 488 nm and emission at 518 nm by flow cytometry. During cell death the membrane integrity is lost and allows AN to bind the intracellular facing PS. This status is discriminated from apoptosis by simultaneously staining with PI, which is only permeable for disordered membranes.

FACS analyses demonstrated an increase in cell death, i.e., AN- and PI-positive cells, about 72 hours after siSOX10 transfection (Figure 17 a-c). Cell death increased significantly with both SOX10-targeting siRNAs in all three cell lines after 96 hours. After 120 hours, the population of AN- and PI-positive cells was raised up to 41.6% (siSOX10a) and 28.2% (siSOX10b) in cell line WM278 (Figure 17 a), to around 60% with both SOX10-targeting siRNAs in cell line WM1232 (Figure 17 b), and to 55.9% (siSOX10a) and 33% (siSOX10b) in cell line 1205Lu (Figure 17 c). Thus, the effect of siSOX10a on cell death is stronger than siSOX10b in cell lines WM278 and 1205Lu. Minor differences in onset of cell death were found for both SOX10-targeting siRNAs in cell line WM1232.

No increase in AN- and PI-positive cells could be detected 96 hours after transfection of SOX10-targeting siRNAs compared to controls in the SOX10-negative cell line WM3211 (Figure S1). Therefore, SOX10 inhibition leads to an increase in cell death in SOX10-positive but not in SOX10-negative melanoma cells.

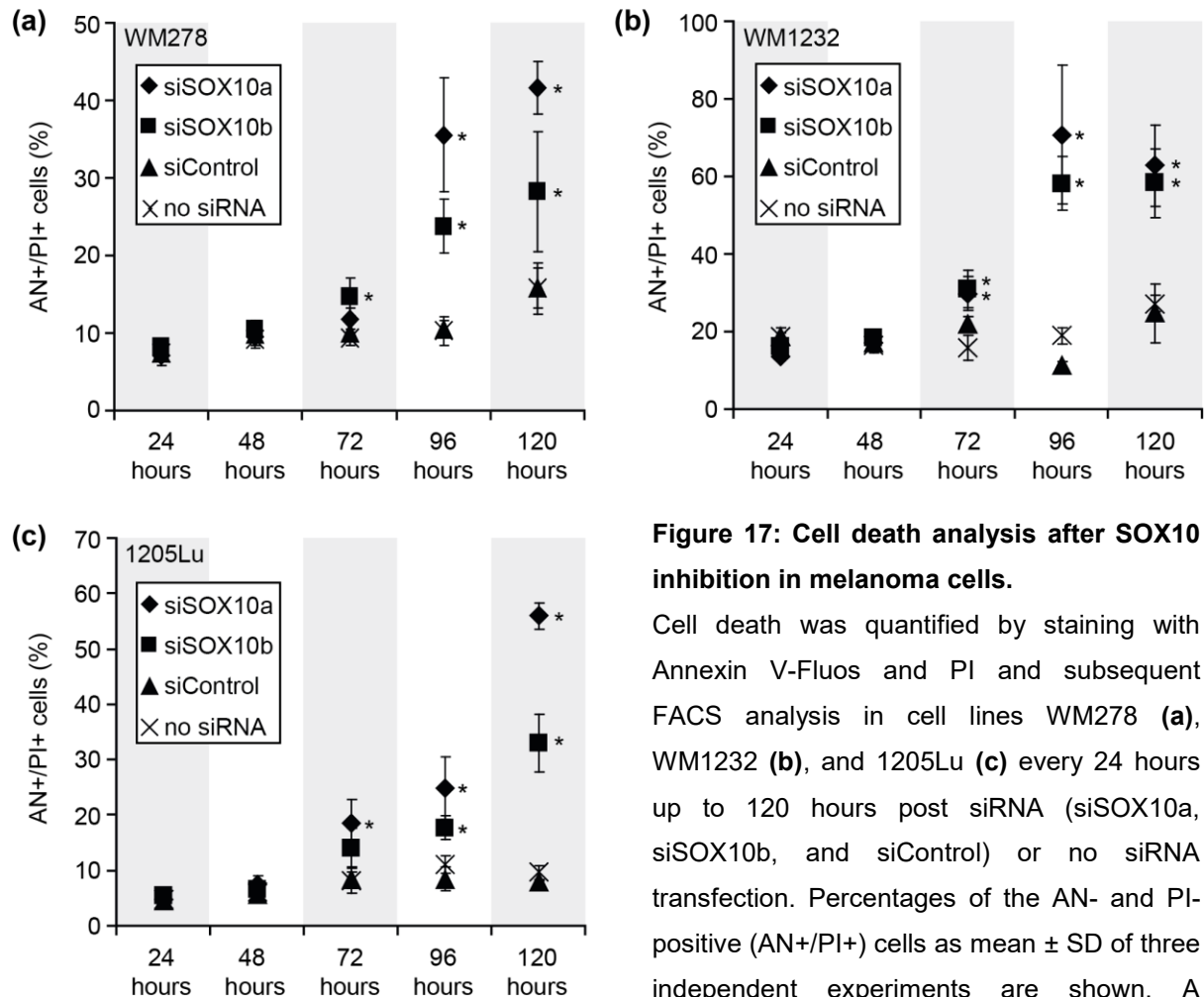


Figure 17: Cell death analysis after SOX10 inhibition in melanoma cells.

Cell death was quantified by staining with Annexin V-Fluos and PI and subsequent FACS analysis in cell lines WM278 (a), WM1232 (b), and 1205Lu (c) every 24 hours up to 120 hours post siRNA (siSOX10a, siSOX10b, and siControl) or no siRNA transfection. Percentages of the AN- and PI-positive (AN+/PI+) cells as mean \pm SD of three independent experiments are shown. A significant difference to siControl with $*P < 0.05$ is marked by an asterisk (one-way ANOVA).

FACS analysis of Annexin V-Fluos- and PI-stained SOX10-inhibited or control 1205Lu cells demonstrated an increase in the AN- and PI-positive but also in the AN-positive and PI-negative cell fraction (apoptotic cell fraction) in SOX10-inhibited cells after 72 hours (Figure 18 a). This observation was also made during time course analysis: SOX10 inhibition increased the amount of AN-positive and PI-negative cells, which was significant for siSOX10 after 72 hours and for siSOX10b after 120 hours (Figure 18 b). These data indicate that SOX10 inhibition induces apoptosis in melanoma cells.

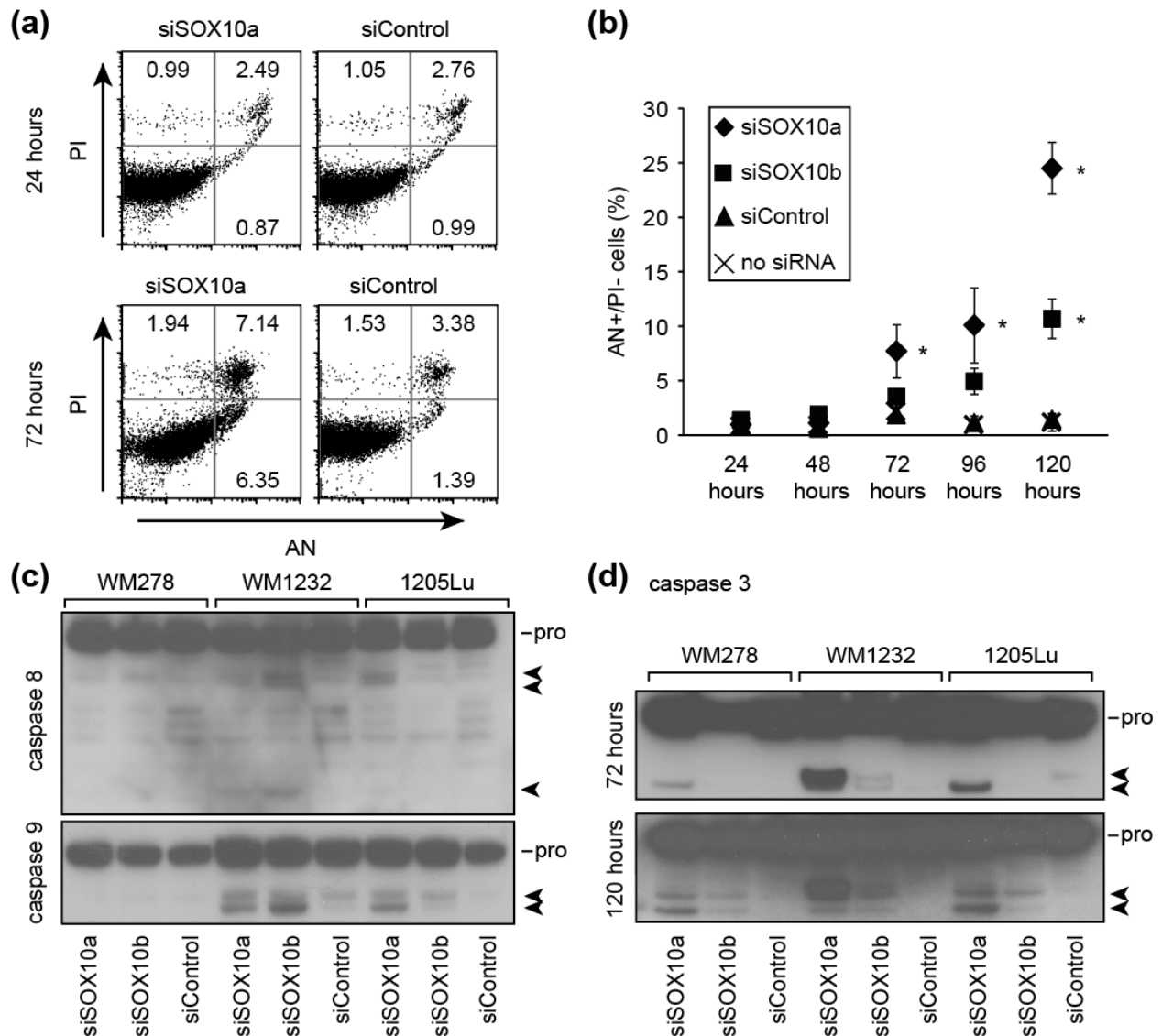


Figure 18: Increase in the apoptotic cell fraction and activation of caspase 8, caspase 9, and caspase 3 after SOX10 inhibition.

(a) Representative dot blots of 1205Lu cells after staining with Annexin V-Fluos and PI are shown 24 and 72 hours after transfection of siSOX10a and siControl. An increase of the AN-positive and the AN+/PI+ cell fractions were detected in the SOX10-inhibited cells after 72h. **(b)** Time course analysis of AN-positive and PI-negative cells showed a significant increase in apoptotic cells 72 and 96 hours after transfection with siSOX10a ($*P = 0.0028$ after 72 hours and $*P = 0.001$ after 96 hours, one-way ANOVA versus siControl), while it was significantly increased in siSOX10a and siSOX10b-transfected cells after 120 hours ($*P < 0.0001$, one-way ANOVA versus siControl). **(c)** Pro- and cleaved (arrows) isoforms of caspase 8 and caspase 9 were analyzed 72 hours after transfection of siSOX10a, siSOX10b, and siControl in cell lines WM278, WM1232, and 1205Lu. **(d)** Caspase 3 activation (arrows) was detected in siSOX10a-transfected WM278 and 1205Lu cells and in both SOX10-targeting siRNAs-transfected WM1232 cells 72 hours after siRNA transfection. After 120 hours, caspase 3 activation in SOX10-inhibited cells was found in all analyzed melanoma cell lines with a stronger effect for siSOX10a than siSOX10b.

Apoptosis is one of three forms of programmed cell death (PCD) together with autophagy and necroptosis. The term PCD defines the death of a cell, mediated by intracellular signaling that is executed via a programmed mechanisms [191]. It is an essential process, e.g., during the development of fingers and toes in the human embryo, to preserve tissue homeostasis, and to remove damaged cells.

However, it is also a common feature in the development of cancer. In contrast, necrosis is initiated by external factors as injury or infection. While autophagy can lead either to survival or to death, apoptosis and necroptosis only end up in cell death. PCD by necroptosis is mediated by receptor interacting protein (RIP) kinases, poly (adenosine phosphate ribose) polymerase-1 (PARP1), nicotinamide adenine dinucleotide phosphate (NADPH) oxidases, and calpains. During necroptosis, the integrity of the cell membrane is disrupted and intracellular material is released into the extracellular milieu leading to inflammatory responses.

Apoptosis, which is activated through irreparable DNA damage, has been described for the first time by Kerr et al. [127]. It is characterized by morphological changes like cell shrinkage, nuclear condensation and fragmentation, constriction of cell content in membrane-sealed vesicles, and loss of adhesion to either adjacent cells or the extracellular matrix (ECM). On cellular level, apoptosis is characterized by chromosomal DNA cleavage, PS externalization due to loss of flippase activity, and a number of specific proteolytical processes. Apoptosis can be induced by two different pathways: the extrinsic death receptor pathway and the intrinsic mitochondrial pathway. The extrinsic pathway is triggered by binding of death ligands (e.g. Fas ligand, tumor necrosis factor [TNF], and TNF-related apoptosis-inducing ligand [TRAIL]) to death receptors (e.g. FAS, TNF-receptor 1, TRAIL-receptor 1, and TRAIL-receptor 2) upon death stimuli. These complexes recruit Fas-associated protein with death domain (FADD) and initiator pro-caspases 8 and 10 to become the death-inducing signaling complex (DISC). Through proteolytical cleavage, caspase 8 becomes activated and further activates the effector caspase 3, which promotes the apoptotic phenotype by destroying structural proteins, e.g., microfilament actin and intermediate filament lamin and by activating nucleases. The intrinsic pathway controls cell death through mitochondrial pro-enzymes. Upon initiation, the mitochondrial membrane becomes permeable and releases cytochrome c into the cytosol. Cytochrome c recruits apoptotic protease activating factor 1 (APAF-1) and pro-caspase 9 forming the apoptosome that activates the caspase 9/3 signaling cascade eventually leading to apoptosis.

The mitochondrial membrane integrity is regulated by Bcl-2 proteins. The Bcl-2 family is composed of key regulators of apoptosis and they play a central role in regulating the survival of tumor cells. This family includes a number of pro- and anti-apoptotic members, which are subdivided into three different classes according to their Bcl-2 homology domains (BH-domains) and functions. Bcl-2, Bcl-XL, Bcl-w, Mcl-1, and A1 are anti-apoptotic Bcl-2 proteins, Bak, Bax, and Bok are pro-apoptotic Bcl-2 effector proteins, and Bid, Bim, Bad, Bmf, Hrk, Bik, Noxa, and Puma are pro-apoptotic BH3-only proteins [304]. Melanoma cells require the presence of specific anti-apoptotic Bcl-2 proteins [234]. Bax and Bak are essential for induction of intrinsic apoptosis [291]. It is suggested that they form pores at the outer mitochondrial membrane to release pro-apoptotic factors to the intermembrane.

Caspase 8 and 9 activation was analyzed by immunoblotting 72 hours after siRNA transfection in cell lines WM278, WM1232, and 1205Lu. Cleaved caspase 8 fragments were detected for both SOX10-targeting siRNAs in case of WM1232 and for siSOX10a in case of 1205Lu cells (Figure 18 c upper panel). Caspase 9 activation was detected for both SOX10-targeting siRNAs in cell lines WM1232 and 1205Lu (Figure 18 c lower panel). Neither caspase 8 nor caspase 9 activation was found for WM278 cells.

Activation of effector caspase 3 was found in all cell lines for siSOX10a and in cell line WM1232 for siSOX10b after 72 hours (Figure 18 d upper panel). After 120 hours, activation of effector caspase 3 was detectable in all three cell lines with both SOX10-targeting siRNAs (Figure 18 d lower panel). Time point and extent of detectable caspase 3 activation is comparable with the onset of cell death as determined by FACS (Figure 17).

To further analyze the mechanism of induced cell death through SOX10 inhibition the expression of Bcl-2 family member Bax and Bak, which are essential for induction of intrinsic apoptosis as mentioned before, and the anti-apoptotic Bcl-2 were investigated. Immunoblot detection 72 hours after siRNA transfection revealed an increase of Bax in all three cell lines transfected with siSOX10a and siSOX10b compared to siControl (Figure 19 a). Bak was only increased in SOX10-inhibited 1205Lu.

Intrinsic apoptosis can also be induced by caspase 8 activation through procession of the 22 kDa protein Bid to the 15 kDa fragment t-Bid [157], [165]. Since not only activation of caspase 9 but also of caspase 8 was found upon SOX10-inhibition, Bid expression was examined (Figure 19 a). However, no procession of Bid to t-Bid was

found. Bcl-2 was found downregulated in SOX10-inhibited cells from all three cell lines (Figure 19 b). These data indicate that SOX10 inhibition can trigger intrinsic apoptosis.

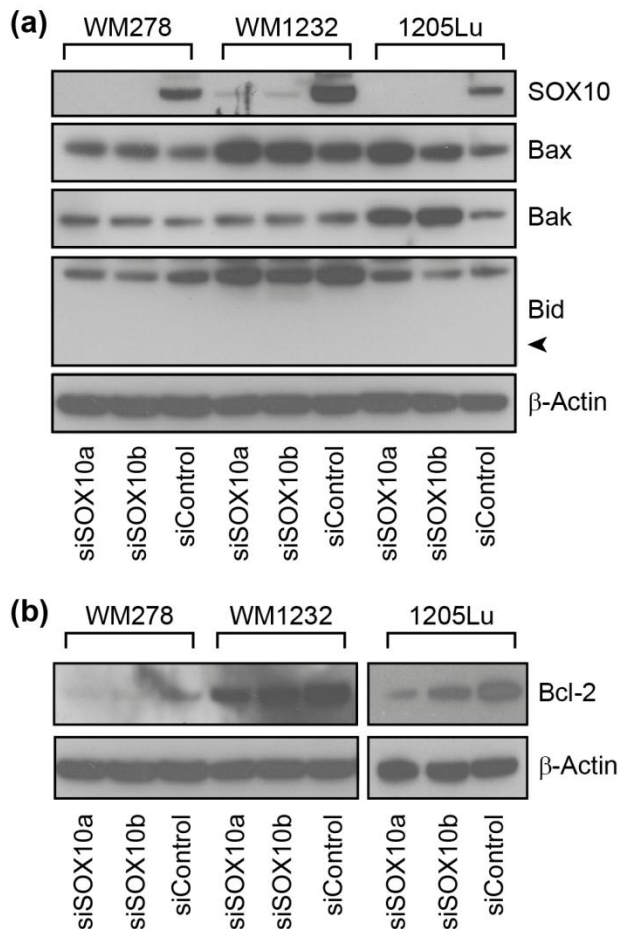


Figure 19: Increase of the pro-apoptotic factors Bax and Bak and decrease of the anti-apoptotic Bcl-2 after SOX10 inhibition.

Expression of the Bcl-2 family members Bax, Bak, and Bid (arrow points to estimated size of tBid) as well as SOX10 (a) and Bcl-2 (b) was detected in cell lines WM278, WM1232, and 1205Lu 72 hours after transfection of siSOX10a, siSOX10b, and siControl. Detection of β -Actin served as loading control.

4.3.3 Effects of SOX10 inhibition on melanoma cell invasion

During embryogenesis, SOX10 expression can be found in early migrating NCCs and melanoblasts [126], [179]. Migration and invasion are also important attributes of the malignant potential of melanoma cells. Therefore, it was investigated if SOX10 also contributes to the migratory capacity of melanoma cells.

As SOX10 inhibition also affected melanoma cell proliferation and survival (sections 4.3.1 and 4.3.2), an *in vitro* Matrigel invasion assay was selected to analyze the migratory capacity of SOX10-inhibited melanoma cells. This assay allows examination of cell invasion within 5 hours. The Matrigel matrix is a soluble basement membrane preparation extracted from an Engelbreth-Holm-Swarm mouse sarcoma and contains extracellular matrix proteins like laminin, collagen IV, heparin sulfate proteoglycans, and entactin/nidogen. It also contains several growth factors that naturally occur in tumors and thereby mimicking the *in vivo* environment of tumor cells. To pass the Matrigel layer cells need to migrate, actively degrade, and proteolyse the ECM-related Matrigel.

To conduct this assay, melanoma cells were seeded in nutrition-free medium on top of a pored Matrigel-coated membrane. To stimulate melanoma cells to pass the Matrigel layer, the well below was filled with fibroblast-conditioned medium. This medium contains secreted factors that attract melanoma cells. Invaded melanoma cells at the bottom of the pored membrane can be stained and quantified. A schematic overview over this assay is presented in Figure 20.

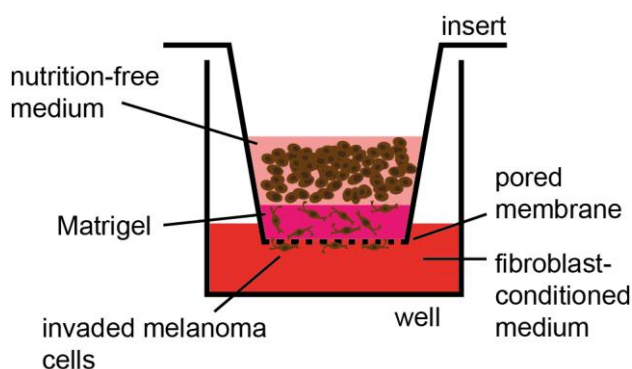


Figure 20: Schematic overview of the Matrigel invasion assay.

To test invasion through an extracellular matrix-mimicking Matrigel layer, melanoma cells are seeded in nutrition-free medium on top of a Matrigel-coated transwell insert. The Matrigel layer is covering a pored membrane. Below the insert, the well contains fibroblast-conditioned medium, which attracts melanoma cells. Through migration

and proteolysis, melanoma cells can reach the lower part of the insert. To quantify the invaded cells, the remaining cells and the Matrigel on the upper part of the insert are removed with cotton swabs and cells on the lower part are fixed and stained with a Diff-Quik staining set (Medion Diagnostics). Invaded cells can be counted by microscopic magnification.

As transfection of SOX10-targeting siRNAs reduced SOX10 expression already 24 hours after siRNA transfection (section 4.2, Figure 11), it was possible to determine the effect of SOX10 on invasion at a time point when cell death has not been induced yet. Matrigel invasion assays with SOX10-inhibited and control WM278, WM1232, and 1205Lu cells revealed a significant reduction of melanoma cell invasion at an early time point after SOX10 inhibition (Figure 21 a-c). As expected due to their tumor's origin, control cells of metastatic melanoma cell line 1205Lu showed the highest invasion capacity in this assay (Figure 21 c), while cells from the VGP cell line WM278 migrated slower, leading to a reduced cell yield under the membrane (Figure 21 a). Against expectations, control WM1232 invaded less than WM278 and 1205Lu (Figure 21 b). Figure 21 d shows representative pictures of membranes with fixed and stained invaded melanoma cells.

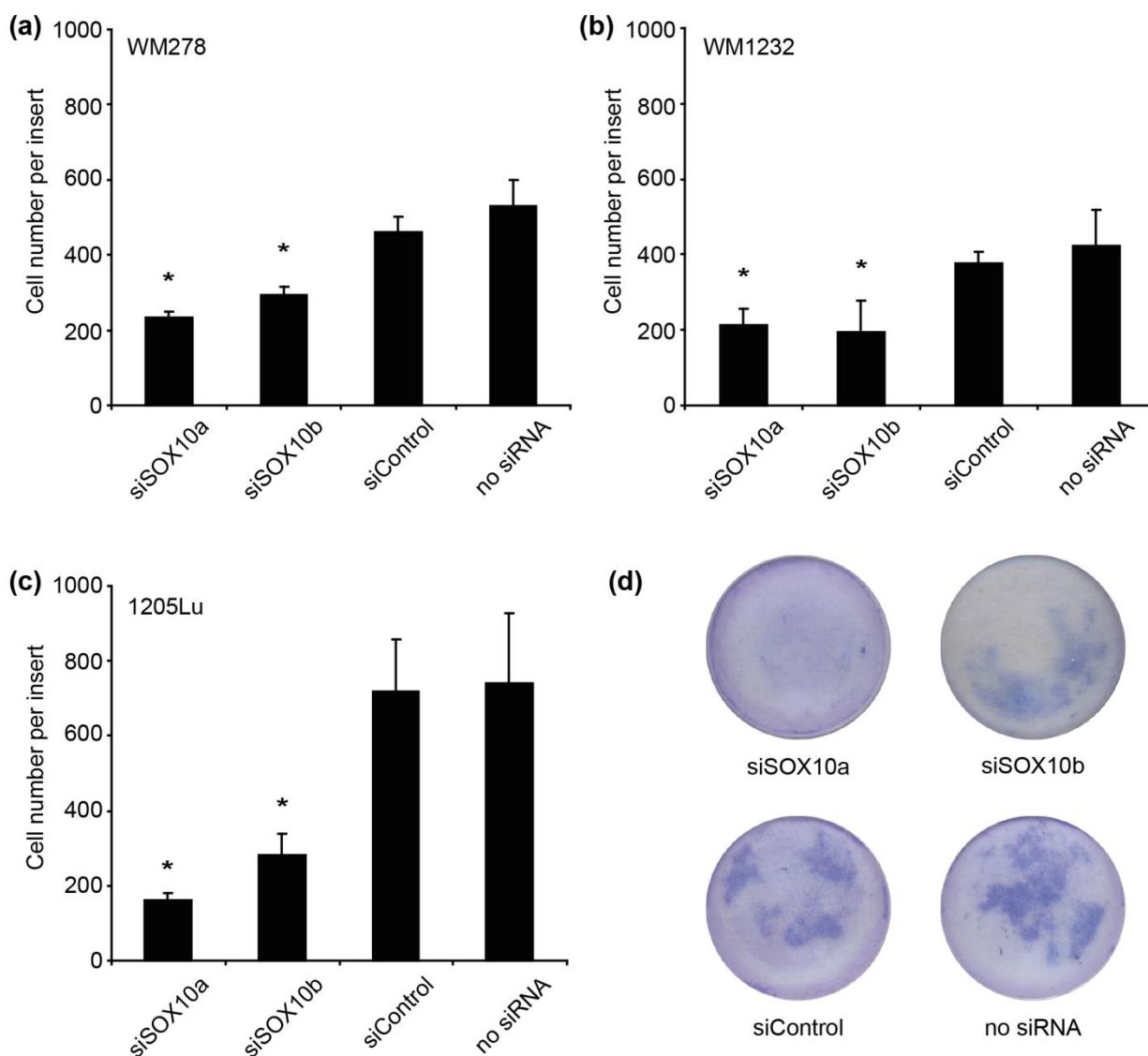


Figure 21: Matrigel invasion assay with SOX10-inhibited melanoma cells.

Invasion through a Matrigel layer was assessed with cell lines WM278 (a), WM1232 (b), and 1205Lu (c) 24 hours after transfection of siSOX10a, siSOX10b, siControl, or without siRNA in three independent experiments. Compared to the control siRNA-transfected cells, SOX10 inhibition significantly reduced the number of invaded cells in three independent experiments. A significant difference compared to siControl with $*P < 0.05$ is marked by an asterisk (one-way ANOVA). (d) Representative pictures of membranes after Matrigel invasion assay and cell staining with 1205Lu melanoma cells are shown.

Another *in vitro* model system for investigating melanoma cell invasion is the three-dimensional spheroid assay. In the first step, tumor cell aggregates are formed by cultivating melanoma cells on top of an agar-coated well. The agar prevents cell adhesion to the well's bottom. These so-called spheroids are more representative for tumors *in vivo* in terms of morphology, cell-cell contacts, decreased proliferation rates, and a hypoxic core. It is a well accepted tumor model, which is broadly used for, e.g., screening of small molecule inhibitors [140].

As a second part of this assay, spheroids can be embedded in an ECM-mimicking collagen matrix that requires active migration and invasion for tumor cell spreading. Nutrition for the cells is provided in the collagen matrix.

To perform this assay with SOX10-inhibited cells, siRNAs were transfected 24 hours before seeding the melanoma cells on top of the agar-coated wells. However, in contrast to control treatment, SOX10 inhibition impaired the formation of compact cell aggregates as tested in cell lines 1205Lu (Figure 22 a) and WM278 (Figure 22 b) at early time points (24 and 48 hours after seeding on the agar-coated wells).

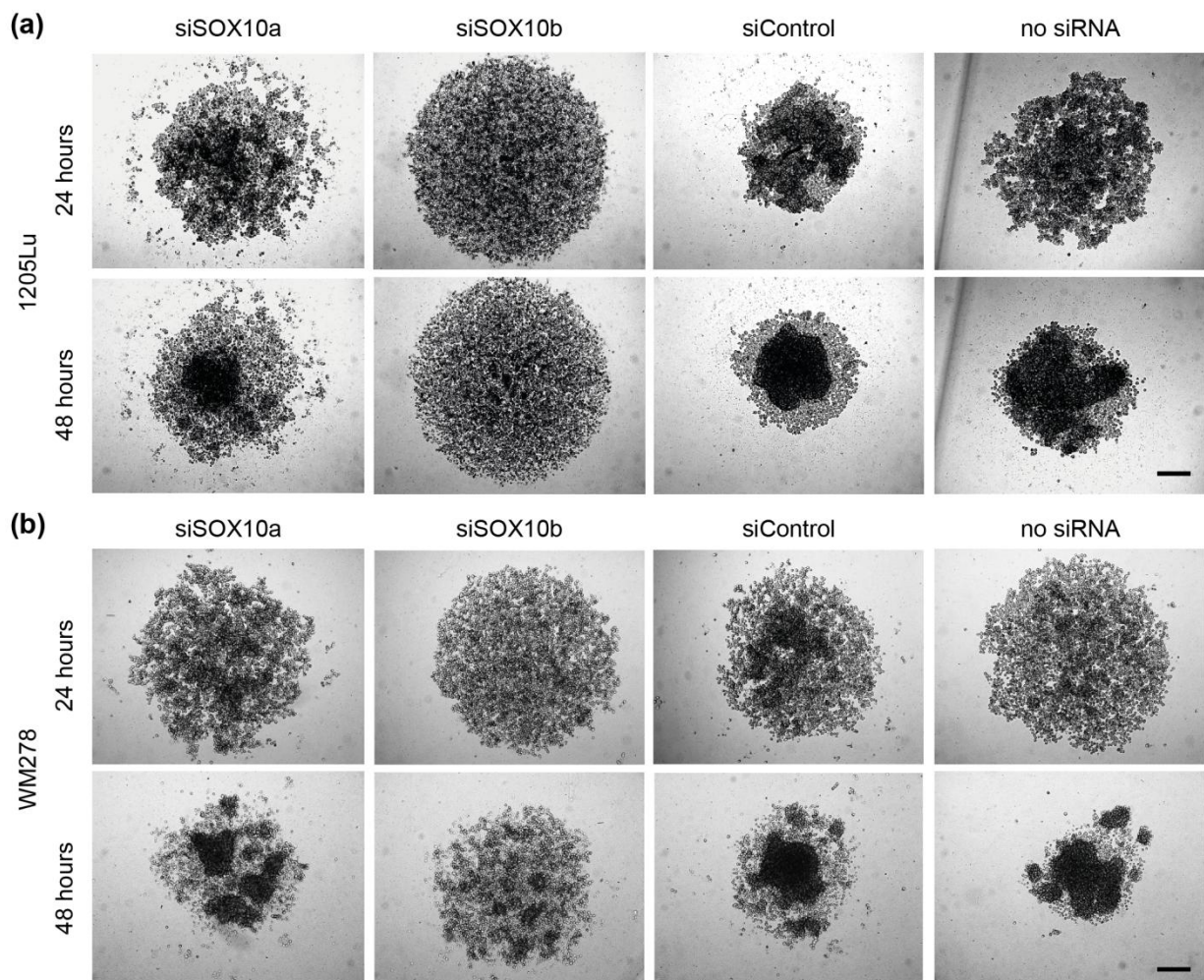


Figure 22: Analysis of spheroid formation after SOX10 inhibition.

1205Lu (a) and WM278 (b) melanoma cells were subjected to spheroid formation by cultivation on agar-coated wells 24 hours post transfection with siSOX10a, siSOX10b, siControl, or no siRNA.

Representative pictures were taken 24 and 48 hours after seeding. Compared to the control cells, SOX10-inhibited cells did not form compact spheroids. Scale bar = 200 μm .

To analyze the molecular background of impaired spheroid formation, integrin expression was examined after SOX10 inhibition. Integrins mediate cell-matrix- as well as cell-cell-contacts. Downregulation of ITGA(integrin α)4 and ITGB(integrin β)3 was

found in the cell line WM278 upon SOX10 inhibition while ITGA3 and ITGB1 were upregulated in all three analyzed cell lines (WM278, WM1232, 1205Lu) upon SOX10 inhibition (chapter 7, Figure S2). No tendency was found for ITGAV. Thus, impaired spheroid formation might be related to a change in cell adhesion proteins.

Furthermore, LIVE/DEAD staining of the forming spheroids demonstrated that no change in the amount of EthD-1-positive cells could be found in SOX10-inhibited compared to control cells (chapter 7, Figure S3 a). Even calcein-positive SOX10-inhibited cells did not form compact spheroids. Thus, impaired spheroid formation in SOX10-inhibited melanoma cells seems not to be related to increased cell death.

To further investigate the role of cell death in SOX10-mediated cell invasion cell death after SOX10-inhibition was blocked by treatment with Z-VAD and Nec-1 (chapter 7, Figure S3 b). Z-VAD is a caspase inhibitor and Nec-1 blocks necroptosis, which could be also activated by SOX10 inhibition due to an early increase of the AN- and PI-positive cell fraction (section 4.3.2, Figure 18 a). Due to this treatment, SOX10 inhibition did not induce cell death after 96 hours anymore but the invasion capacity of SOX10-inhibited melanoma cells remained significantly reduced (chapter 7, Figure S3 b). These data also indicate that reduced invasion after SOX10 inhibition is not only related to onset of cell death.

In the end, another assay was selected to further examine the effect of SOX10 on melanoma cell invasion. With the chick embryo invasion assay invasion capacity can be analyzed and quantified *in vivo*, located in an embryonic microenvironment [38]. This assay was performed in collaboration with Dr. Christian Busch at the Section Dermato-Oncology, University of Tübingen, Tübingen, Germany. In short, 1205Lu cells transfected with siSOX10a, siControl, or no siRNA were injected into brain vesicles at the hindbrain (rhombencephalon) of chick embryos at an early stage of their development (stages 12-13 according to Hamburger and Hamilton [94]). Melanoma cells form tumors in the dorsal neuroepithelium with single cells invading in the surrounding brain tissue. Histological analysis 96 hours after injection revealed the formation melanoma nodules in all embryos, also when SOX10-inhibited melanoma cells had been injected (Figure 23 a). Sections were stained for the proliferation marker MIB (Figure 23 b). More than 90% of tumor cells stained positive for MIB1, also tumor cells in nodules of SOX10-inhibited tumors, except for the central necrotic area. Strikingly, the invasion of tumor cells in the surrounding host tissue was impaired upon SOX10 inhibition (Figure 23 a and b).

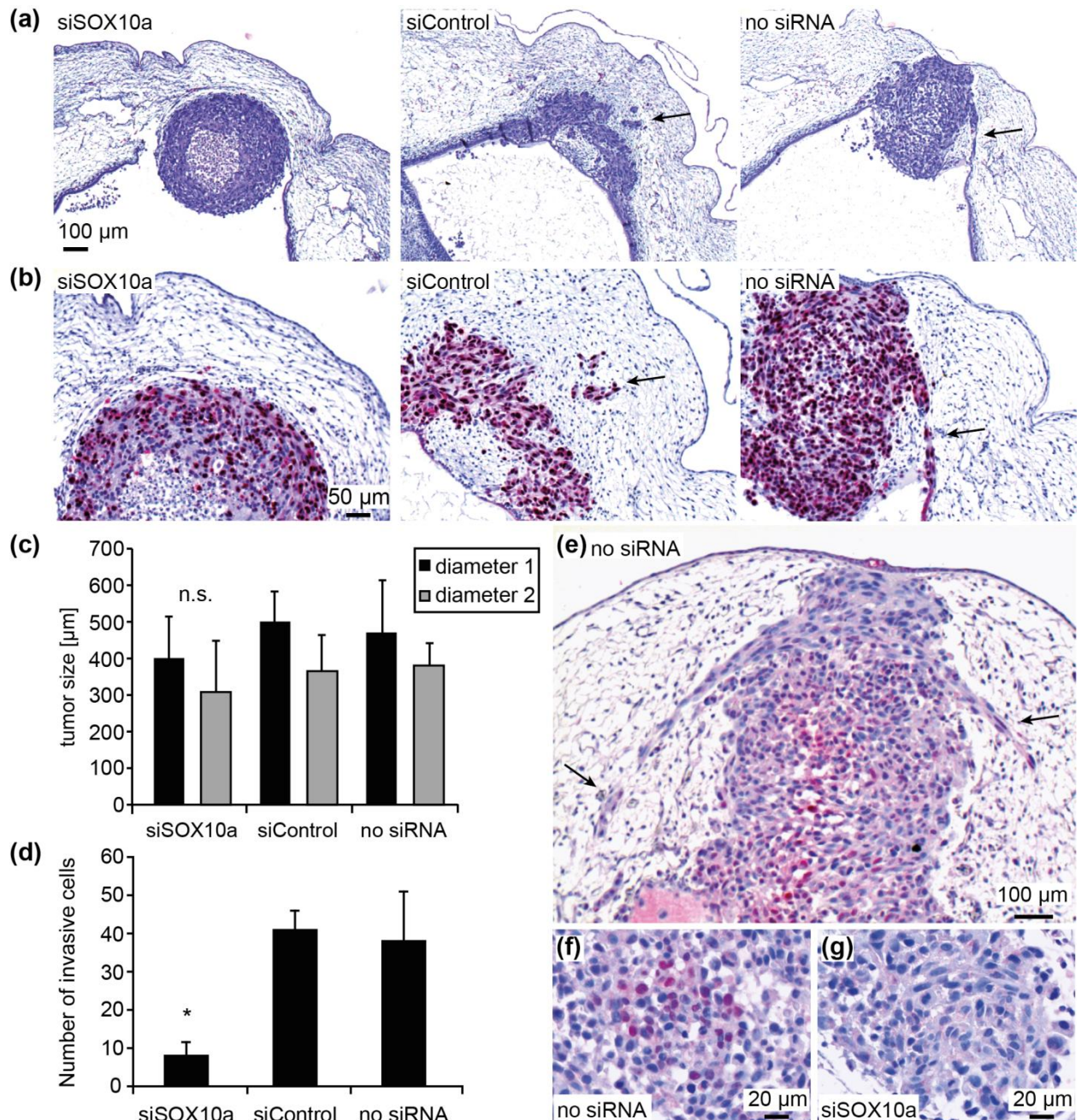


Figure 23: Chick embryo invasion assay with SOX10-inhibited and control 1205Lu cells.

1205Lu melanoma cells were injected into the rhombencephalic brain vesicle of chick embryos 24 hours after transfection with siSOX10a, siControl, or without siRNA. Tumor formation and invasion were analyzed 96 hours later. Representative chick embryo sections were stained with H&E (a), MIB1 (b), or anti-SOX10 antibodies (e), (f), (g). Scale bar sizes are depicted in the pictures. Arrows point to invading melanoma cells. (c) The maximum diameter of each tumor was measured microscopically in two directions. Tumor sizes did not change significantly when comparing siSOX10a- and siControl-tumors ($P = 0.1702$ for diameter 1 and $P = 0.5034$ for diameter 2; t -test). (d) Quantification of invading cells was performed by counting three sections of the largest tumor diameter of each embryo (siSOX10a $n = 6$, siControl $n = 4$, no siRNA $n = 7$; one-way ANOVA versus siControl, $*P < 0.001$).

Regarding the control cells, invasion in single cells and clusters was evident (Figure 23 a and b, arrows). Nodules of the three experimental groups were measured in two directions and no significant difference was found indicating that the tumor formation and size was not affected by SOX10 inhibition (Figure 23 c). Quantification of invaded tumor cells in all embryos demonstrated a significant decrease of tumor cell invasion by SOX10 inhibition (Figure 23 d). SOX10 staining revealed strong nuclear signals in the tumor nodules and invading tumor cells in the control group (Figure 23 e and f) whereas SOX10 staining was reduced or absent in the tumors formed by SOX10-inhibited melanoma cells (Figure 23 g) demonstrating that the siRNA had still been preventing SOX10 expression. Thus, SOX10 inhibition seems to directly influence the invasion capacity of melanomas but not their proliferative potential at least in this model system. Taken together, these data suggest that SOX10 has a critical influence on melanoma cell invasion independent of cell proliferation or survival.

4.4 Identification of MIA as a target gene of SOX10

4.4.1 Expression of MIA and regulation by different transcription factors

As a transcription factor, SOX10 can influence a large variety of cellular processes either by directly or indirectly controlling the transcription of specific genes that mediate these processes. As the reduction of melanoma cell invasion upon SOX10 inhibition *in vitro* was observed at an early time point, even before onset of cell death, SOX10 might directly affect the transcription of a factor that is actively promoting cell migration.

Literature research revealed that not SOX10 but the closely related SOX9 regulates melanoma inhibitory activity (MIA) in chondrocytes [299]. MIA was first identified during the search for autocrine growth factors in melanoma as part of a fraction of the supernatant of a melanoma cell line derived from a central nervous system metastasis [18]. It was shown that the fraction containing MIA could effectively inhibit tumor cell proliferation and colony formation. MIA was found to be specifically expressed in melanoma while it was absent in melanocytes and normal skin biopsies [27], [198]. But rather than functioning as a tumor inhibitor, it was shown that MIA is actively promoting melanoma cell migration [205]. Secreted at the rear part of a migrating melanoma cell it binds to and thereby inhibits the attachment of integrins to fibronectins causing cell detachment from the ECM [10], [28], [254]. Further studies revealed that MIA contributes to melanoma cellular invasion and formation of metastases [24], [28]. MIA was also described as a serum marker for melanoma progression [27], [252]. Figure 24

a shows an immunoblot analysis of MIA expression after SOX9 and SOX10 inhibition in 1205Lu cells.

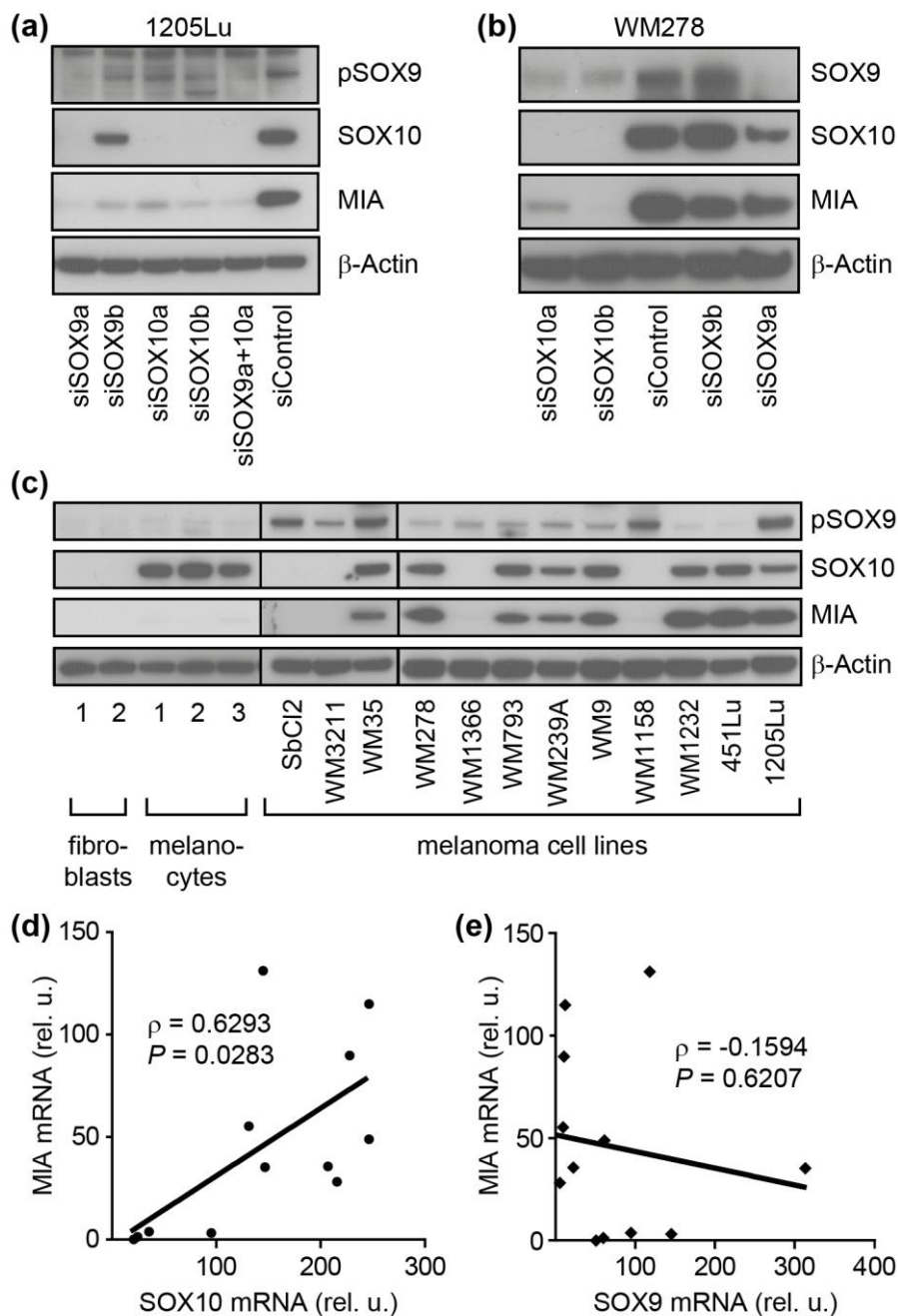


Figure 24: MIA expression after SOX9 and SOX10 inhibition and correlation of MIA with SOX10 expression in melanoma cells.

MIA, SOX9, pSOX9, and SOX10 expression was assessed by immunoblotting 72 hours after SOX9 and SOX10 inhibition in cell lines 1205Lu **(a)** and WM278 **(b)**. Detection of β -Actin served as loading control. **(c)** MIA expression was assessed by immunoblotting in fibroblasts (two donors), melanocytes (three donors), and 12 melanoma cell lines. Phospho-SOX9 and SOX10 immunoblots from Figures 6 and 7 are shown for better comparison. **(d)** Positive linear correlation between SOX10 and MIA mean mRNA values of

three independent experiments was found in melanoma cell lines SbCl2, WM3211, WM35, WM278, WM1366, WM793, WM239A, WM9, WM1158, WM1232, 451Lu, and 1205Lu (Pearson correlation, $\rho = 0.6293$, $*P = 0.0283$). **(e)** No significant correlation between SOX9 and MIA mRNA was found in these cell lines (Pearson correlation, $\rho = -0.1594$, $P = 0.6207$).

MIA expression was strongly downregulated by SOX9 but also by SOX10 inhibition. A combination of siRNAs targeting both transcription factors did not completely abolish MIA expression. However, in cell line WM278, where merely siSOX9a effectively downregulated SOX9 expression, MIA protein levels were only slightly decreased

(Figure 24 b). On the other hand, SOX10 inhibition in this cell line strongly reduced MIA expression. MIA expression was then investigated in the same cells as described in section 4.1.1. Confirming previously published data [25], [198], MIA was expressed in the majority (8 of 12) of melanoma cell lines while it was absent in fibroblasts and melanocytes (Figure 24 c). In contrast to SOX9, a striking correlation was observed for SOX10 and MIA protein expression in all melanoma cell lines. This correlation was significant on mRNA level for SOX10 (Figure 24 d) but not for SOX9 (Figure 24 e). These data suggest that SOX10 rather than SOX9 is relevant for MIA expression in melanoma cells.

Previously, it has been shown that the transcription factors HMG1 and the p65 subunit of nuclear factor kappa B (NFκB) bind to a highly conserved region within the MIA promoter and thereby function as regulators of MIA [203]. Expression of HMG1 and p65 as well as p65 phosphorylation (p-p65) was investigated in fibroblasts, melanocytes and melanoma cell lines (Figure 25 a).

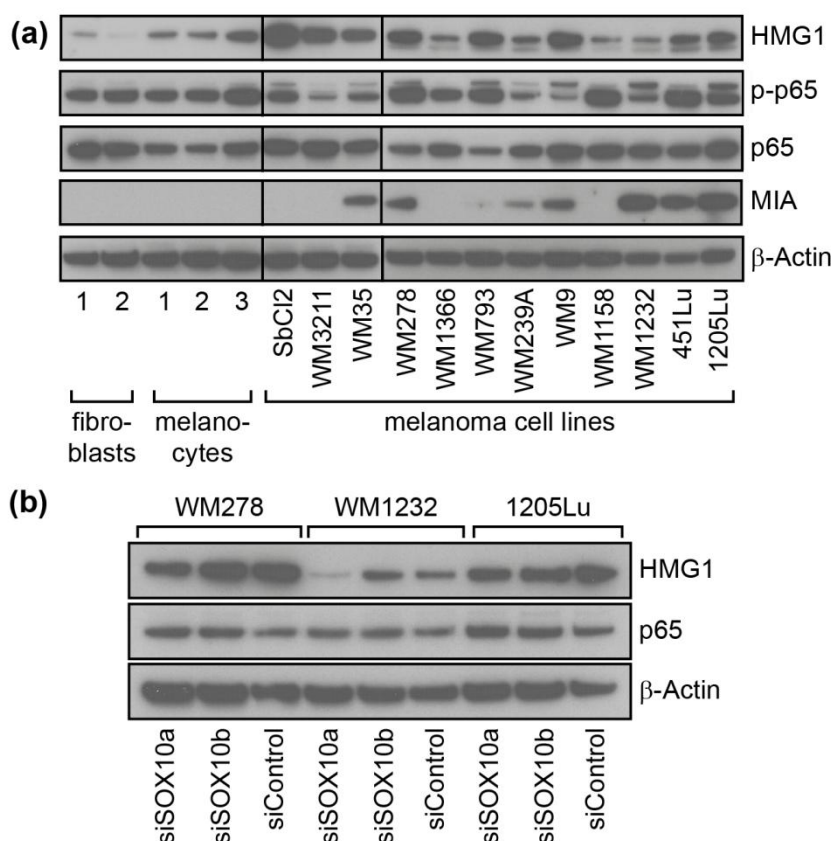


Figure 25 : Expression of HMG1 and p65 in human skin cells and melanoma cell lines and their expression after SOX10 inhibition.

(a) HMG1, p65, and MIA protein expression as well as p65 phosphorylation (p-p65) was assessed by immunoblotting in fibroblasts (two donors), melanocytes (three donors), and 12 melanoma cell lines. No correlation could be observed. β-Actin served as a loading control. **(b)** HMG1 and p65 expression levels were detected by immunoblotting in cell lines WM278, WM1232,

and 1205Lu 48 hours after transfection with siSOX10a and siSOX10b or control siRNA. No reduction in protein expression was found for p65, while HMG1 was reduced only by siSOX10a in WM1232 cells. β-Actin served as a loading control.

However, expression of HMG1 and p65 or p65 phosphorylation did not correlate with MIA expression in skin cells or melanoma cell lines. Furthermore, SOX10 inhibition did only reduce the expression of HMG1 using siSOX10a in one cell line (WM1232) but not using siSOX10b and not in other cell lines (Figure 25 b). Moreover, p65 expression was not affected by SOX10 inhibition.

These data strengthen the important regulatory role of SOX10 in MIA expression.

4.4.2 Analysis of SOX10 binding to the *MIA* promoter

Immunoblot analysis of MIA expression in cell lines WM278, WM1232, and 1205Lu early after SOX10 inhibition demonstrated that MIA protein levels were decreased already 24 hours after transfection of SOX10-targeting siRNAs and almost abolished after 72 hours (Figure 26 a).

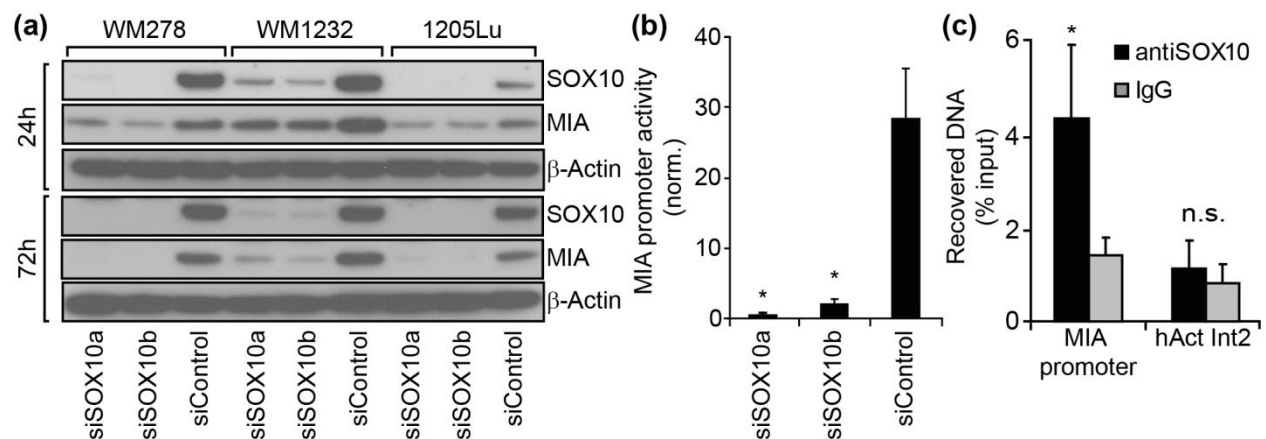


Figure 26: Regulation of MIA expression and promoter activity by SOX10 as well as *MIA* promoter binding studies.

(a) SOX10 and MIA expression was assessed by immunoblotting 24 and 72 hours after transfection with siSOX10a, siSOX10b, or siControl in melanoma cell lines WM278, WM1232, and 1205Lu. Detection of β -Actin served as a loading control. **(b)** *MIA* full-length promoter activity in a pGL3-reporter construct was determined by luciferase assay 48 hours after transfection of 1205Lu cells with siSOX10a, siSOX10b, or siControl and 24 hours after transfection of pGL3-MIA and a renilla vector. Mean \pm SD of three independent replicates are shown. A significant reduction of *MIA* reporter activity compared to siControl is marked by an asterisk (* $P = 0.0003$, one-way ANOVA). Norm. = normalized to renilla activity. **(c)** Percentages of precipitated DNA in relation to the input DNA after CHIP assay with anti-SOX10 antibody (black bars) or IgG control (grey bars) are shown. Recovered DNA (mean \pm SD) with primers hybridizing in the *MIA* promoter region or a control locus (hAct Int 2) was determined by qRT-PCR in four independent experiments. Significant increase of recovered *MIA* promoter DNA was found using the SOX10-specific antibody compared to IgG control and the recovered DNA of hAct Int 2 (t -test, * $P < 0.05$). No significant change was found comparing recovered DNA of hAct Int 2 using the SOX10-specific antibody compared to IgG control.

Of note, the intensity of MIA reduction correlated with that of siRNA-mediated downregulation of SOX10 since SOX10 inhibition has been less effective in WM1232 and so was MIA reduction.

A luciferase reporter assay was used to analyze *MIA* promoter activation. This assay is based on a firefly luciferase vector that contains the promoter sequence or promoter fragments of the gene of interest in front of the expression sequence for the enzyme firefly luciferase. An activation of the promoter leads to transcription and translation of luciferase while the amount of produced enzyme is proportional to the strength of promoter activation. The enzyme in turn is detected by adding its substrate luciferin, which is converted to oxyluciferin in the presence of O₂ and ATP. This reaction forms oxyluciferin in an electronically excited state and thereby generating bioluminescence when the excited oxyluciferin returns to the ground state by releasing a photon. The light emission was directly measured with a luminometer (Luminometer GloMax 96, Promega). To emend difference in cell number or transfection efficiency, a control vector leading to constitutive expression of a renilla luciferase was co-transfected. The renilla luciferase converts its substrate coelenterazine to coelenteramid, which can be detected independently from the oxyluciferin production and is therefore used for normalization of the reaction.

MIA promoter activity was assessed after SOX10 inhibition. Figure 26 b shows that both SOX10-targeting siRNAs significantly reduced the *MIA* promoter activity compared to control treatment (Figure 26 b).

A ChIP assay was performed in order to investigate direct binding of SOX10 to the *MIA* promoter. This assay allows the analysis of protein-DNA interactions in living cells. At the beginning of this assay, the specific binding of a protein - in this study the transcription factor SOX10 - to a promoter site was fixed with formaldehyde, which cross-links proteins to the genomic DNA. The genomic DNA was then fragmented and DNA fragments bound by SOX10 were purified by precipitation with a SOX10-specific antibody. A control antibody (IgG) was included to examine non-specific binding. After several washing steps and de-crosslinking, the precipitated DNA was purified and further analyzed by qRT-PCR.

Thereby, the *MIA* promoter region but not a control DNA region - human actin intron 2 (hAct Int2) - was found to be significantly enriched around 4-fold using a SOX10-specific antibody (Figure 26 c). Thus, direct binding of SOX10 to the *MIA* promoter was verified.

To further determine SOX10-responsive elements within the *MIA* promoter region, deletion constructs of the *MIA* promoter were analyzed after SOX10 inhibition or control transfection (Figure 27 a). The residues between -493 and -1, with respect to the translation start site, have been described to be necessary and sufficient to mediate high levels of cell type-specific *MIA* gene expression [25]. Truncated promoter fragments -200- and -212 bp displayed reduced activation upon SOX10 inhibition while this effect was increased in longer constructs (-275 and -493 bp) and lost in the -160 bp fragment. Therefore, SOX10 seems to affect the activity of proximal *MIA* promoter regions.

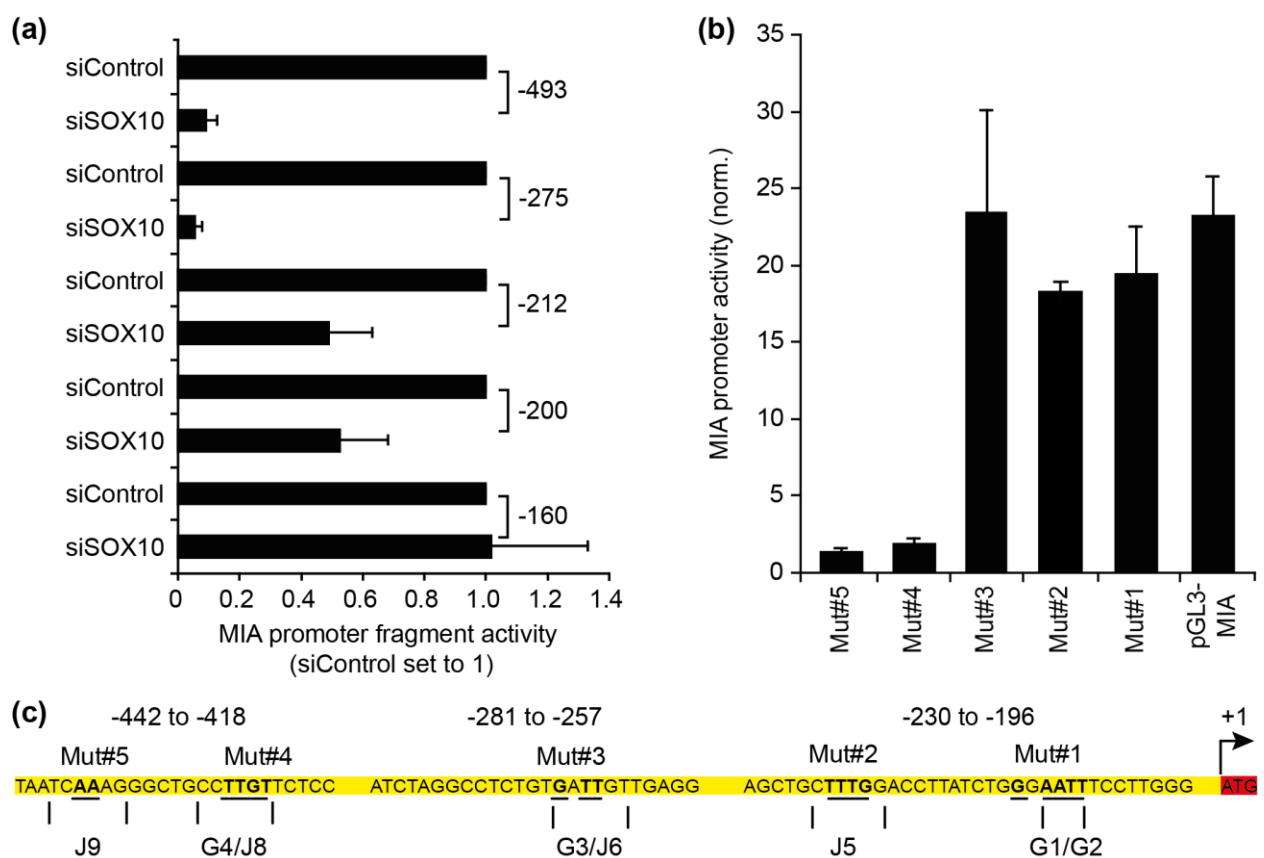


Figure 27: *MIA* promoter constructs and mutation studies.

(a) Reporter constructs containing truncated *MIA* promoter fragments were subjected to luciferase reporter assays in 1205Lu cells after transfection with siSOX10b or siControl. Promoter activity as mean \pm SD of three independent experiments is displayed. Baseline expression levels of constructs were similar (data not shown) and siControl activities were set to 1. **(b)** Luciferase assays with the full-length *MIA* promoter including mutations in five predicted SOX binding sites in 1205Lu cells are shown as mean \pm SD from three independent experiments. **(c)** The proximal element of the *MIA* promoter is depicted. Sequences including the predicted binding sites as mentioned in the text are shown. Underlined nucleotides were mutated (A to C, T to G, and vice versa) in the full-length *MIA* reporter construct.

To identify the specific binding site of SOX10 within the *MIA* proximal promoter region, *in silico* analysis were performed with the MatInspector from Genomatix Software GmbH and JASPAR version 5.0_alpha and the *MIA* promoter sequence according to >gi|224589810|ref|NC_000019.9|:41279500-41280875 Homo sapiens chromosome19, GRCh37.p5 from the NCBI data base.

The MatInspector uses general SOX binding site alignment matrices (V\$SORY based on SOX/SRY-sex/testis determining and related HMG box factors) for binding site prediction as no specific SOX10 alignment matrix is available for this software. Predicted binding sites are listed in Table 13. Nine potential SOX binding sites were found within the *MIA* promoter region with five binding sites within the first 493 bp. Binding sites G1 and G2 comprise the same core binding position.

Binding site	Matrix	Matrix sequence according to IUPAC	Start position	End position	Anchor position	Strand	Sequence
G1	V\$HM GIY.01	RNRAATTTNC SNN	-213	-189	-201	+	tctgggAATTtctt gggcttacag
G2	V\$HM GIY.01	RNRAATTTNC SNN	-222	-198	-210	-	caaggaAATTccc agataaggcca
G3	V\$SO X5.01	NNAACAATN N	-281	-257	-269	-	cctcaaCAATcac agaggcctagat
G4	V\$SO X9.03	NNACAADGG MRSBCTTTB MDMV	-442	-418	-430	-	ggagaACAAGgc agcccttgatta
G5	V\$SO X5.01	NNAACAATN N	-487	-463	-475	+	agcataCAATattc agtcagtactc
G6	V\$SO X5.02	NNGAACAAT WNN	-633	-609	-621	-	tgggaACAAtaaa aaagccaatagt
G7	V\$SO X9.03	NNACAADGG MRSBCTTTB MDMV	-730	-706	-718	+	gaaaaAAAAGgg aggggttataatc
G8	V\$HM GA.01	NDKCSNNRT NAATKANK	-897	-873	-885	-	tatgcccaattAAT Ctatttttta
G9	V\$HM GA.01	NDKCSNNRT NAATKANK	-1070	-1046	-1058	-	tatgccagttAAT Ttttgattt

Table 13: General SOX binding sites as evaluated with the MatInspector from Genomatix.

Matrices that define the binding site prediction are presented according to the International Union of pure and Applied Chemistry (IUPAC): R = G or A; Y = T or C; K = G or T; M = A or C; S = G or C; W = A or T; B = G or T or C; D = G or A or T; H = A or C or T; V = G or C or A; N = any. Positions of binding sites are given in relation to the protein start ATG. Binding site prediction is related to the sense, anti-coding (+) strand or the antisense, coding (-) strand of the DNA. Capital letters in the predicted sequence mark the core binding nucleotides.

With the JASPAR database, binding site prediction with a specific SOX10 alignment matrix was possible (Model-ID MA0442.1; Figure 28).

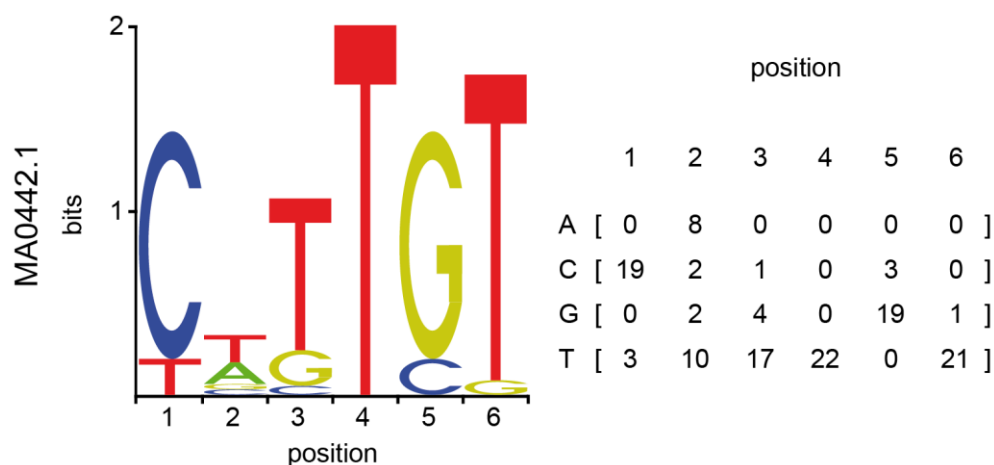


Figure 28: Model-ID MA0442.1 for SOX10 binding site prediction.

The model-ID for SOX10 binding site prediction MA0442.1 from the JASPAR database is shown as graphical

design and mathematical matrix. The illustration was obtained from http://jaspar.binf.ku.dk/cgi-bin/jaspar_db.pl?ID=MA0442.1&rm=present&collection=CORE.

Thirty-one potential binding sites were found with this software and are listed in Table 14. J1 to J10 lie within the first 493 bp.

Binding site	Score	Relative score	Start	End	Strand	Predicted site sequence
J1	7.094	0.919	-81	-76	+	CCTTGT
J2	4.824	0.819	-90	-85	-	TTGTGT
J3	4.605	0.809	-98	-93	-	CTTGG
J4	4.820	0.818	-102	-97	-	TCTTGT
J5	5.559	0.851	-225	-220	+	CTTTGG
J6	4.521	0.805	-267	-262	+	GATTGT
J7	5.846	0.864	-273	-268	+	CTCTGT
J8	7.094	0.919	-428	-423	+	CCTTGT
J9	4.669	0.812	-439	-434	-	CTTTGA
J10	6.352	0.886	-482	-477	-	TATTGT
J11	4.669	0.812	-507	-502	+	CTTTGC
J12	8.910	1.000	-585	-580	+	CTTTGT
J13	4.521	0.805	-610	-605	+	CATTTT
J14	6.352	0.886	-619	-614	+	TATTGT
J15	4.805	0.818	-625	-620	+	CTTTT
J16	5.846	0.864	-640	-636	+	CTCTGT
J17	4.605	0.809	-651	-646	+	CTTGGT
J18	5.846	0.864	-688	-683	-	CTCTGT
J19	4.805	0.818	-726	-721	-	CTTTT
J20	4.805	0.818	-735	-730	-	CTTTT
J21	4.824	0.819	-743	-738	+	CTGTCT
J22	4.521	0.805	-893	-888	-	CATTTT
J23	5.846	0.864	-929	-924	-	CTCTGT

J24	5.561	0.851	-970	-965	-	CACTGT
J25	4.521	0.805	-1048	-1043	-	CATTAT
J26	6.636	0.899	-1066	-1061	-	TTTTGT
J27	5.559	0.851	-1157	-1152	+	CTTTGG
J28	4.605	0.809	-1186	-1181	+	CTTGGT
J29	4.824	0.819	-1214	-1209	+	CTGTCT
J30	5.561	0.851	-1246	-1241	+	CACTGT
J31	6.352	0.886	-1341	-1336	-	CATTCT

Table 14: SOX10 binding sites as evaluated with the JASPAR database and model-ID MA0442.1.

Score and relative score evaluate the sequence alignment of input profile and model-ID using a modified Needleman-Wunsch algorithm. Positions of binding sites are given in relation to the protein start ATG. Binding site prediction is related to the sense, anti-coding (+) strand or the antisense, coding (-) strand of the DNA. Bold letters mark the binding sequences, which were also predicted with the MatInspector from Genomatix. Identical core binding sites are underlined.

Ten binding sites within the *MIA* promoter as predicted with JASPAR (J6 – J10, J14, J15, J19, J22, and J26) were also predicted with the MatInspector. Five of these ten sites even included the same core nucleotides (J6, J8, J10, J14, and J19). Thus, binding site G3 equals J6 and J7, G4 equals J8 and J9, G5 equals J10, G6 equals J14 and J15, G7 equals J19, G8 equals J22, and G6 equals J26.

Predicted binding sites between -493 and -160 bp of the full-length *MIA* reporter construct were mutated consecutively with a QuikChange Lightning Site-Directed mutagenesis kit (Agilent Technologies) by exchanging A to C or T to G and vice versa (Figure 27 c) followed by luciferase assay analyses. Although promoter activity of the truncated fragments -200 and -212 were reduced by SOX10 inhibition (Figure 27 a), mutations in G1/G2 (Mut#1) had almost no effect on the whole *MIA* promoter activity (Figure 27 b). Also mutation of J5 (-220 to -225 bp; Mut#2) did not affect the *MIA* promoter activity and same is true for mutation of G3 (J6; Mut#3). Strikingly, with the reporter constructs Mut#4 (G4/J8) and Mut#5 (J9), the *MIA* promoter activity was almost abrogated.

Binding sites G4/J8 and J9 lie in close proximity. Monomeric as well as dimeric binding of SOX10 to DNA was demonstrated before [228]. Thus, J8 and J9 display potential SOX10 homodimeric binding sites. Further predicted binding sites were not analyzed but binding to these sites cannot be excluded.

Direct binding of SOX10 to the binding sites G4/J8 and J9 was assessed by EMSA. This assay was performed with a nuclear extract from 1205Lu cells and DIG-labeled oligonucleotides. The nuclear extract was incubated with the oligonucleotides at 37°C before separation on a 6% DNA retardation gel. In case of supershift experiments using

a SOX10-specific or a control IgG antibody, nuclear extract and antibodies were incubated on ice prior to oligonucleotide addition. After electrophoretic separation, protein-bound oligonucleotides were transferred on a positively charged nylon membrane before fixation by UV crosslink. This method allows the detection of the oligonucleotides through their DIG-label and specific protein detection via immunoblotting.

The oligonucleotide cons (DIG-AGACTGAG**AACA**AAGCGCTCTCACAC) contains a published SOX binding consensus sequence (bold letters), which was shown to be bound by SOX10 [52] and was defined as a consensus SOX binding sequence (5'-A/TATCAAT/A-3' and complementary sequence 5'-T/ATTGT/AT/A-3') according to Mollaaghababa and Pavan [179]. The oligonucleotide MIA_B (DIG-5'-TGGTAAT**CAAAGGGCTGCCTT**GTTCTCCTGC)-3' contains the binding sites G4/J8 and J9 (bold letters).

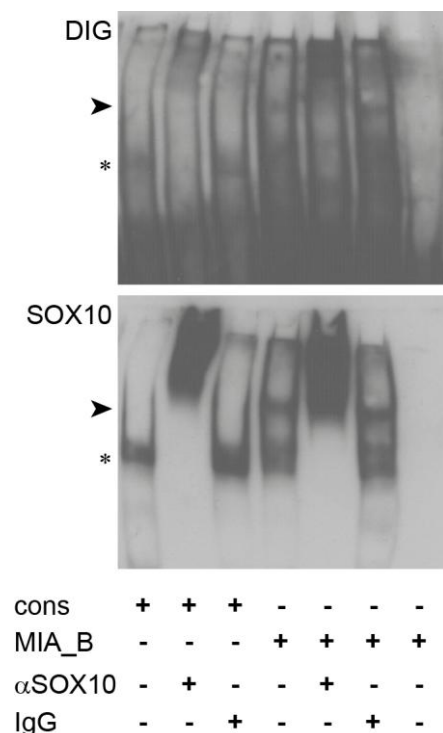


Figure 29: EMSA with DIG-labeled oligonucleotides containing a SOX consensus binding sequence and the predicted SOX10 binding sites in the *MIA* promoter.

EMSA was performed with a DIG-labeled SOX consensus binding sequence (cons) or a DIG-labeled *MIA* promoter oligonucleotide (MIA_B) containing both predicted SOX10 binding sites (G4/J8 and J9). Supershifts were performed with an anti-SOX10 antibody or IgG control. DIG (upper) and SOX10 (lower) signals were detected on the EMSA membrane.

An asterisk marks SOX10 monomeric, an arrow SOX10 dimeric binding.

Results of EMSA analyses are shown in Figure 29. Both oligonucleotides were bound by SOX10 as shown by supershift of the DNA fragments when pre-incubated with the SOX10 antibody but not with a control IgG. However, different shift patterns were observed when using either the cons or the MIA_B oligonucleotide by detecting DIG or SOX10 on the EMSA membrane. Restricted protein-DNA complexes that resemble monomeric SOX10 to the control oligonucleotide were observed. With the MIA_B oligonucleotide, protein-DNA complexes were detected that had a different restriction

pattern than the monomer-bound oligonucleotide. These differences in shift patterns point to dimeric binding of SOX10 to the MIA_B oligonucleotide and thus to the G4/J8 and J9 binding sites.

In conclusion, the secreted protein MIA, which was described to be directly involved in melanoma cell migration, was identified as a direct target gene of SOX10.

4.4.3 Investigation of potential coregulators of SOX10

In contrast to SOX10, MIA is not expressed in melanocytes. Previously, it was suggested that COOH-terminal binding protein 1 (CtBP1) affects cell type-specific *MIA* promoter activation. It has been shown that CtBP1 binds to the *MIA* promoter and functions as transcriptional repressor of *MIA* [204]. Furthermore, CtBP1 has been shown to be expressed in human melanocytes and normal skin biopsies. Analysis of CtBP1 expression in the cell lines investigated in this study revealed higher expression levels of CtBP1 in fibroblasts and melanocytes compared to melanoma cell lines (Figure 30 a). The expression of CtBP1 was significantly decreased in melanoma cell lines compared to melanocytes (Figure 30 b). Therefore, it is possible that the presence of repressors in melanocytes override the activity of transcription factors such as SOX10.

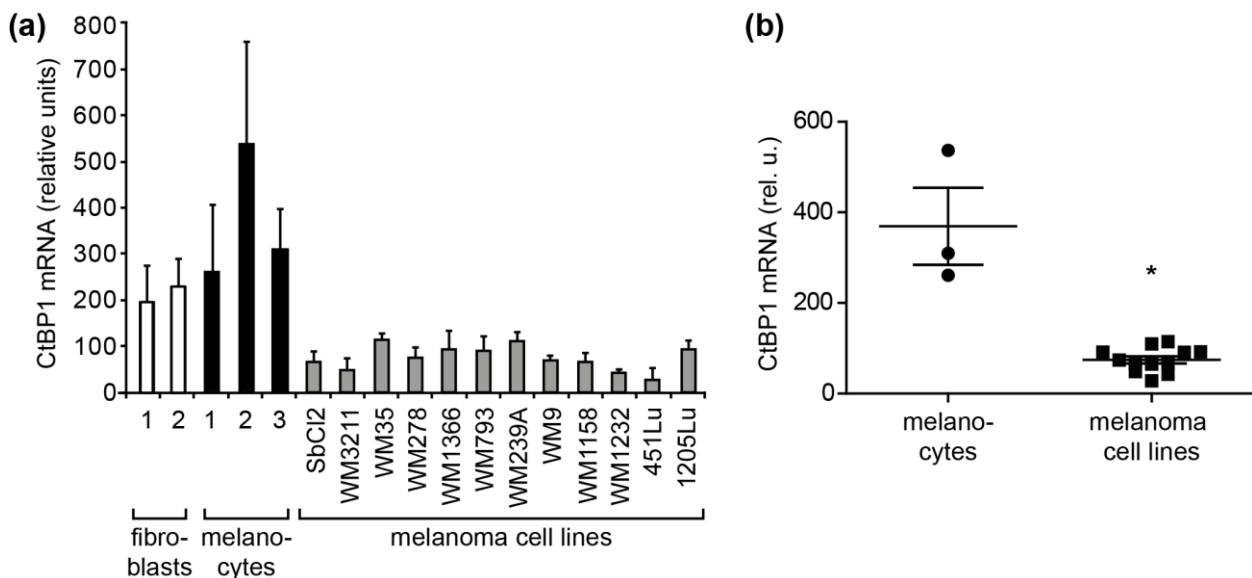


Figure 30: Expression of the transcriptional repressor CtBP1 in fibroblasts, melanocytes, and melanoma cell lines.

(a) CtBP1 expression on mRNA level (mean \pm SD) was assessed by qRT-PCR in fibroblasts (two donors, white bars), melanocytes (three donors, black bars), and 12 different melanoma cell lines (grey bars) in three independent experiments. (b) Analysis of median CtBP1 expression levels with a scatter blot demonstrates a significant decrease in expression of melanoma cells (mel) compared to human melanocytes (HM; *t*-test, $*P < 0.0001$).

Furthermore, it is possible that coregulators of SOX10 are present in melanoma cell lines but not in melanocytes. Potential coregulators of SOX transcription factors were analyzed *in silico* with the ModelInspector from the Genomatix software by determination of published interaction motifs. Three such motifs were identified within, upstream, and downstream of the *MIA* promoter region (Figure 31 a).

The motif identified downstream of the promoter region (+358 to +448; V\$SORY, V\$SORY, V\$EGFR) includes binding of early growth response 2 (EGR2) and SOX10. EGR2 and SOX10 have been shown to activate the MPZ first intron element individually as well as synergistically and that EGR2 facilitates binding of SOX10 [148], [149]. EGR2 was inhibited via siRNA (Figure 31 b). Despite effective downregulation of EGR2 with the siRNA, EGR2 inhibition did not affect *MIA* expression and was therefore excluded as part of a coregulatory model.

The motif within the promoter region (-225 to -191; V\$NFkB, V\$SORY) includes binding of NFkB and HMG1. This cooperative binding was described by Poser et al. [203] and others [155], [266], [295], [302]. However, no effective reduction of *MIA* expression could be achieved by p65 inhibition (Figure 31 c) and p65 and *MIA* expression did not correlate in melanocytes or melanoma cells as demonstrated before (section 4.4.1, Figure 25).

The third motif lies upstream of the *MIA* promoter region and includes SOX and paired box 6 (PAX6) alignment matrices (-2148 to -2102; V\$SORY, V\$PAX6). A cooperative binding of PAX6 and SOX2 was demonstrated in the chicken delta-crystallin enhancer region [124], [134]. Inhibition of PAX6 by siRNA reduced *MIA* expression on mRNA and protein level but did not affect SOX10 expression (Figure 31 d and e). SOX10 inhibition also had no effect on PAX6 expression (data not shown). As a control, *MIA* promoter activation was analyzed after PAX6 inhibition (Figure 31 f). Interestingly, PAX6 inhibition decreased *MIA* promoter activity indicating further PAX6 binding sites within the *MIA* promoter region. The effect of PAX6 and SOX10 overexpression on the *MIA* promoter region is shown in Figure 31 g. *MIA* promoter activity was increased by SOX10 but not by PAX6 overexpression. Also overexpression of both factors did not further enhance the promoter activity. Therefore, it is not suggested that PAX6 and SOX10 function as coregulators of *MIA* at least not within the *MIA* promoter region.

Considering these experiments, the absence of *MIA* expression in melanocytes might be rather due to the presence of transcriptional repressors than absence of coregulators of SOX10.

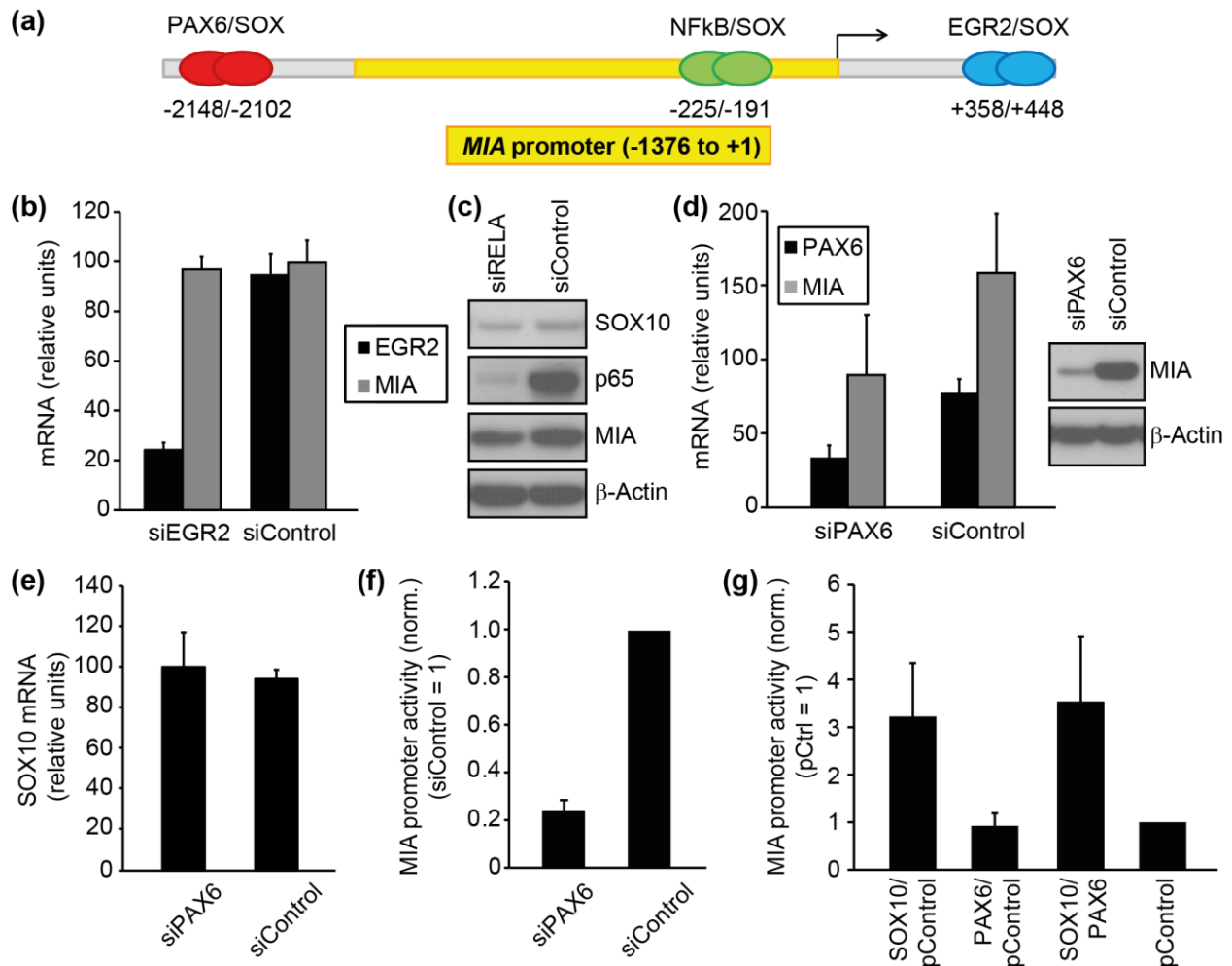


Figure 31: SOX10 transcriptional coregulator motifs upstream, within, and downstream of the *MIA* promoter region and impact of these factors on *MIA* regulation.

(a) Binding motifs of PAX6/SOX before (-2148 to -2102), NFκB/SOX within (-225 to -191), and EGR2/SOX behind (+358 to +448) the *MIA* promoter region were identified with the ModelInspector from Genomatix. **(b)** Expression of EGR2 and MIA (mean ± SD) was assessed in 1205Lu cells in three independent experiments 72 hours after transfection of an EGR2-targeting and a control siRNA. **(c)** Expression of SOX10, p65 (encoded by the gene *RELA*), and MIA was assessed by immunoblotting in 1205Lu cells 6 days after transfection of siRELA or siControl (with repeated siRNA transfection after 3 days). Detection of β-Actin served as loading control. **(d)** Messenger RNA expression (mean ± SD) of PAX6 and MIA was assessed in 1205Lu cells in three independent experiments 72 hours after transfection of siPAX6 or siControl. MIA expression on protein level was assessed in the same cells by immunoblotting. Detection of β-Actin served as loading control. **(e)** SOX10 expression was assessed in the same cells as described in (d). **(f)** Activity of the *MIA* full-length promoter was determined by luciferase reporter assay 48 hours after transfection of siPAX6 or siControl in 1205Lu cells (three independent experiments, mean ± SD). **(g)** Luciferase reporter assay of the *MIA* full-length promoter 48 hours after transfection of vectors for SOX10 (pCMV-SOX10) or PAX6 (pCMV-PAX6) ectopic overexpression or a control plasmid (pControl). Mean ± SD of three independent experiments are shown.

4.4.4 Analysis of MIA-mediated invasion after SOX10 inhibition

The role of MIA in the decrease of melanoma cell invasion after SOX10 inhibition was tested in a so-called rescue experiment. SOX10-inhibited or control 1205Lu cells were transfected with a vector for ectopic MIA overexpression (pCMX-MIA). Thereby, MIA expression levels were increased in the SOX10-inhibited cells (Figure 32 a).

As MIA is a secreted protein, MIA levels in the supernatant of SOX10-inhibited and control cells transfected with the MIA vector or a control vector were determined by immunoblotting (Figure 32 b). In contrast to cells transfected with the control plasmid and siRNA, the secretion of MIA in MIA-overexpressing cells transfected with siControl was less pronounced than expected from the intracellular expression level (Figure 32 a and b). Secretion of MIA in the SOX10-inhibited cells transfected with the MIA expression vector was at a comparable level as with the control cells transfected with the control plasmid.

Cells were applied to Matrigel invasion assays (Figure 32 c). As seen before (section 4.3.3), invasion of SOX10-inhibited 1205Lu cells was significantly reduced compared to control cells, which was not affected by co-transfection of a control vector.

However, ectopic MIA expression in the SOX10-inhibited cells significantly increased their invasion capacity compared to SOX10-inhibited cells transfected with the control vector, although it did not significantly alter the invasion of control cells.

Figure 32 d shows representative membranes with invaded and stained melanoma cells.

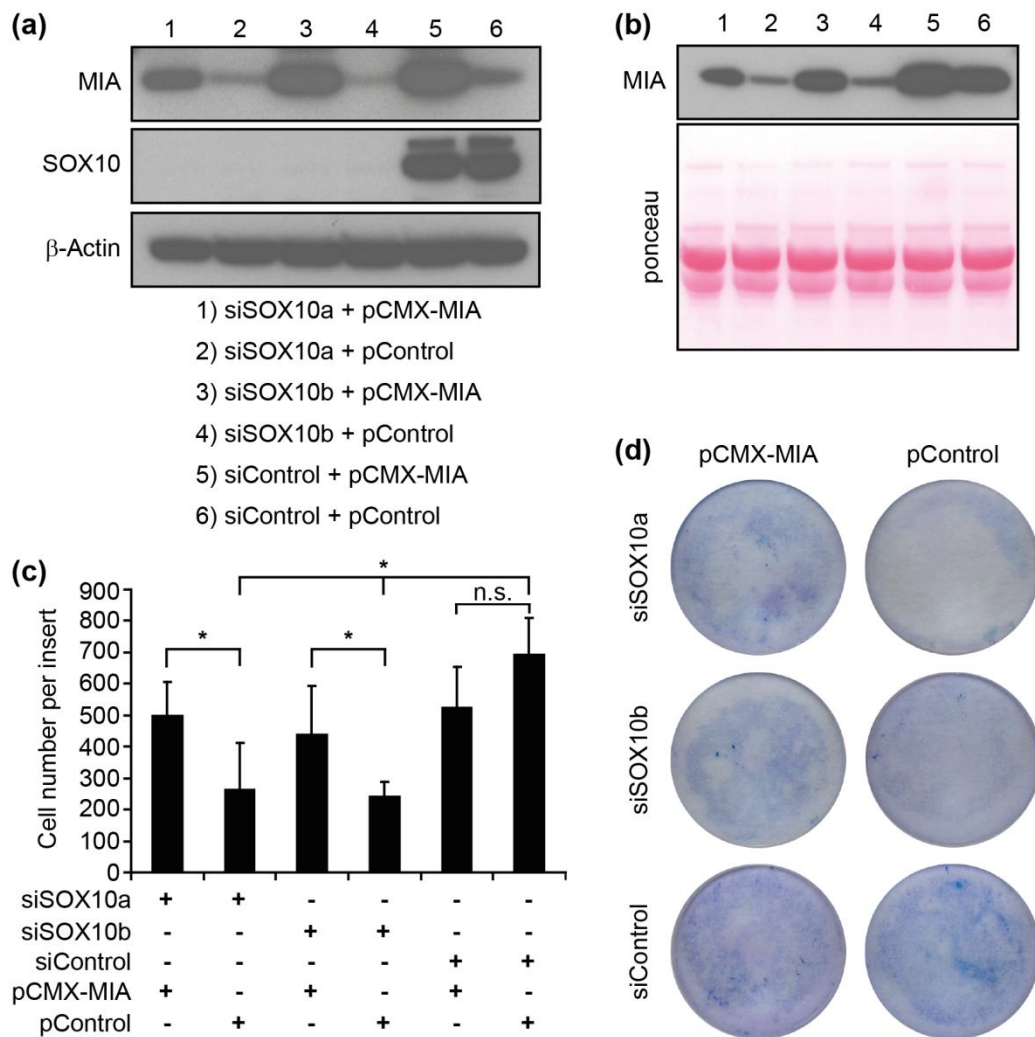


Figure 32: Ectopic MIA expression in SOX10-inhibited melanoma cells and Matrigel invasion analysis.

(a) 1205Lu cells were transfected with siSOX10a, siSOX10b, or siControl. Twenty-four hours later a vector for ectopic MIA overexpression (pCMX-MIA) or a control vector (pControl) was transfected. Immunoblot analyses of MIA, SOX10, or β -Actin (loading control) were performed 48 hours after siRNA and 24 hours after plasmid transfection. **(b)** MIA expression in supernatants of cells described in (a) was analyzed by immunoblotting. Ponceau S staining served as loading control. **(c)** 1205Lu cells treated as described before were subjected to Matrigel invasion assays. Quantification of five independent experiments is shown. SOX10 inhibition without MIA overexpression significantly decreased melanoma cell invasion (one-way ANOVA versus siControl, $*P < 0.05$). Ectopic MIA expression significantly increased the invasion capacity of SOX10-inhibited but not of control cells (t -test, $*P < 0.05$). **(d)** Representative pictures of membranes after Matrigel invasion assays are shown.

Viability of these cells was determined 4 days after siRNA and 3 days after plasmid transfection (Figure 33). Thereby, it was shown that ectopic MIA expression did not increase melanoma cell viability in SOX10-inhibited or control cells but rather led to a slight decrease at prolonged time points. Thus, the increased invasion capacity through MIA overexpression is not related to enhanced cell viability.

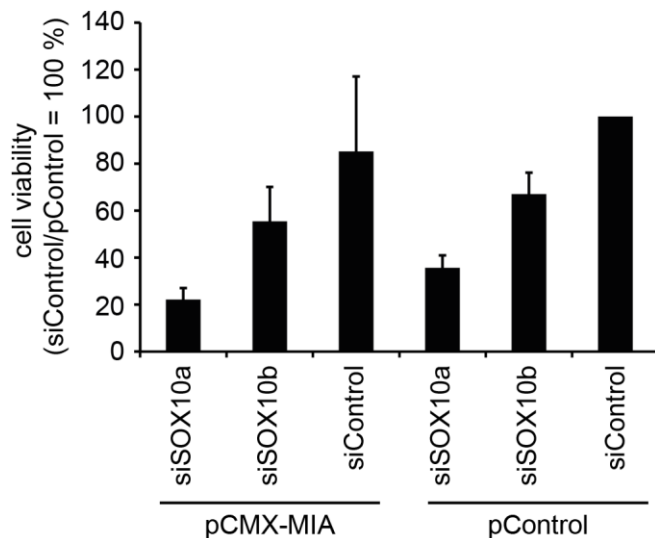


Figure 33: Analysis of cell viability after ectopic MIA expression in SOX10-inhibited melanoma cells.

Cell viability was examined 96 hours after transfection of siSOX10a, siSOX10b, or siControl and 72 hours after plasmid transfection of pCMX-MIA or pControl in 1205Lu cells. Mean \pm SD of three independent experiments are shown. MIA overexpression did not increase cell viability of SOX10-inhibited cells.

In summary, MIA seems to be critical for SOX10-mediated melanoma cell invasion. Still, other factors regulated by SOX10 might also contribute to the reduction of invasion upon SOX10 inhibition.

4.5 Analysis of known target genes of SOX10

One of the best characterized SOX10 target genes is the basic helix-loop-helix leucine zipper transcription factor MITF. MITF is a key factor for melanocyte specification as it regulates proliferation and survival of melanoblasts and activates enzymes for melanogenesis [273]. Loss of MITF is manifested in the Waardenburg syndrome type 2A [265], a dominantly inherited syndrome of hearing loss and pigmentary disturbances. Regarding melanoma, *MITF* gene amplification was found in 10-20% of cases and MITF has been shown to be a dominant oncogene by driving melanoma cell proliferation or invasion, depending on its expression levels [39], [80]. Furthermore, MITF has been described as a highly sensitive immunohistochemical marker for melanoma and as a molecular marker for tumor cells in the peripheral blood of melanoma patients [130], [136].

It has been shown that SOX10 binds to the proximal melanocyte-specific *M-MITF* promoter and an upstream enhancer [22], [152], [200], [206], [275], [285] and both factors cooperate in activating the *DCT* promoter [164], [207].

Analysis of MITF expression in melanoma cell lines WM278, WM1232, and 1205Lu demonstrated that SOX10 inhibition specifically reduced expression of the M-MITF isoform, which is present in cell line WM1232 but not in WM278 and 1205Lu (Figure 34 a upper panel). The same observation was made in the cell lines LMU-GM1 and WM9 (Figure 34 b and c). Both SOX10 and M-MITF were absent in fibroblasts and present in

melanocytes, while their expression correlated in almost all investigated melanoma cell lines (except for WM278 and 1205Lu, Figure 34 d).

Another previously suggested target gene of SOX10 is erb-b2 receptor tyrosine kinase 3 (ERBB3). The epidermal growth factor receptor ERBB3 has been shown to be required for embryonic development of NCCs and their derivatives as Schwann cells and melanocytes [33], [37]. It has also been suggested that ERBB3 contributes to the progression of benign nevi to melanoma as well as to the metastatic progression of melanoma [37]. Antibody-mediated internalization and degradation of ERBB3 inhibits melanoma cell growth and migration [11]. Therefore several functions of ERBB3 resemble SOX10 functions in embryonic development and melanoma progression. Furthermore, it was shown that SOX10 controls expression of ERBB3 in NCCs and binds to an enhancer region of the *ERBB3* gene locus [31], [36], [208].

Inhibition of SOX10 in cell lines WM278, WM1232, 1205Lu, LMU-GM1, and WM9 reduced ERBB3 expression (Figure 34 a lower panel, b, and c).

Similarly to SOX10, ERBB3 protein was absent in fibroblasts and present in melanocytes (Figure 34 e). SOX10 and ERBB3 protein levels correlated in all melanoma cell lines (Figure 34 e). Figure 34 b and c demonstrates that MIA was also downregulated in SOX10-inhibited WM9 while MIA expression was absent in LMU-GM1.

Thus, previously described target genes of SOX10, which were shown to execute similar functions in the development of melanocytes and melanoma, were also regulated by SOX10 in melanoma cell lines examined in this study and might contribute to observed phenotypes.

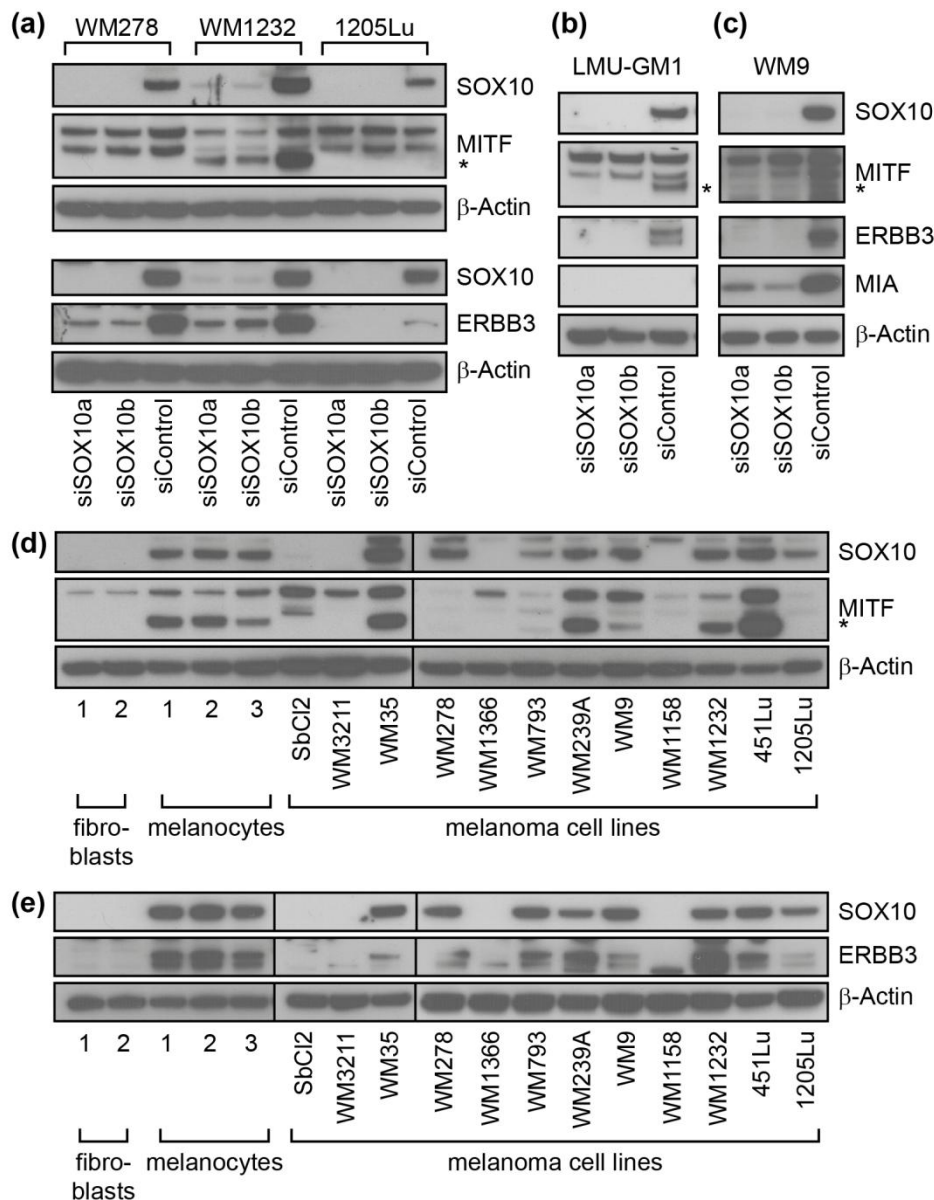


Figure 34: Expression of M-MITF and ERBB3 after SOX10 inhibition and their expression in human skin cells and melanoma cell lines.

(a) Expression of SOX10, MITF (upper panel) and ERBB3 (lower panel) was detected by immunoblotting in cell lines WM278, WM1232, and 1205Lu 72 hours after transfection of SOX10-targeting or control siRNAs. For MITF, a specific decrease in the M-isoform (asterisk) was found in SOX10-inhibited WM1232 cells. SOX10, ERBB3, MITF, and MIA expression was analyzed in cell lines LMU-GM1 (b) and WM9 (c) by immunoblotting 72 hours after transfection of siSOX10a, siSOX10b, or siControl. SOX10, MITF (d), and ERBB3 (e) protein expression was analyzed in fibroblasts (two donors), melanocytes (three donors), and 12 melanoma cell lines according to section 4.1.1. While SOX10 and M-MITF expression correlated in fibroblasts, melanocytes, and 10 of 12 melanoma cell lines (except for WM278 and 1205Lu), SOX10 and ERBB3 expression correlated in all investigated cell lines (e). Detection of β-Actin served as loading control.

4.6 Effects of SOX10 overexpression on melanoma cell invasion

Next to loss-of-function experiments via siRNA-mediated SOX10 inhibition, gain-of-function experiments were performed by SOX10 overexpression. Stable SOX10 overexpression by lentiviral transduction or selection after lenti-plasmid transfection failed (data not shown). Therefore, a transient overexpression approach with a SOX10 vector (pCMV-SOX10) with the recombinant SOX10 coding sequence under control of a *cytomegalovirus* (CMV) promoter was selected.

SOX10 overexpression was performed in SOX10 negative cell lines WM3211 and WM1366 as well as in cell line 1205Lu, which displayed a medium level of SOX10 expression compared to other melanoma cell lines (section 4.1.1).

A SOX9 vector with the recombinant SOX9 coding sequence under control of a CMV promoter (pCMV-SOX9) and a CMV promoter-containing vector without coding sequence (pControl) were included as controls.

Effects of SOX9 and SOX10 overexpression on melanoma cell invasion were examined by Matrigel invasion assays three days after plasmid transfection (Figure 35 a). SOX10 overexpression significantly increased cell invasion in all investigated cell lines. In contrast, SOX9 overexpression significantly increased invasion only in cell line 1205Lu. Overexpression of both transcription factors slightly increased cell viability only in cell line WM1366 (Figure 35 b). These data further strengthen the hypothesis that the positive influence of SOX10 on melanoma cell invasion is not related to its effect on melanoma cell viability.

Effects of SOX9 and SOX10 transient overexpression were also investigated in a three-dimensional spheroid model as described in section 4.3.3 with the cell line WM3211.

SOX10 but not SOX9 overexpression significantly increased the invasion area of WM3211 cells in this assay (Figure 35 c). Also, expression of SOX9 and SOX10 could be detected in these spheroids by immunoblotting (Figure 35 d) and thereby showing that the transient overexpression had still been lasting in the spheroids, even 6 days after transient transfection. Figure 35 e shows representative pictures of the three-dimensional spheroid assay. Thus, SOX10 rather than SOX9 promotes melanoma cell invasion.

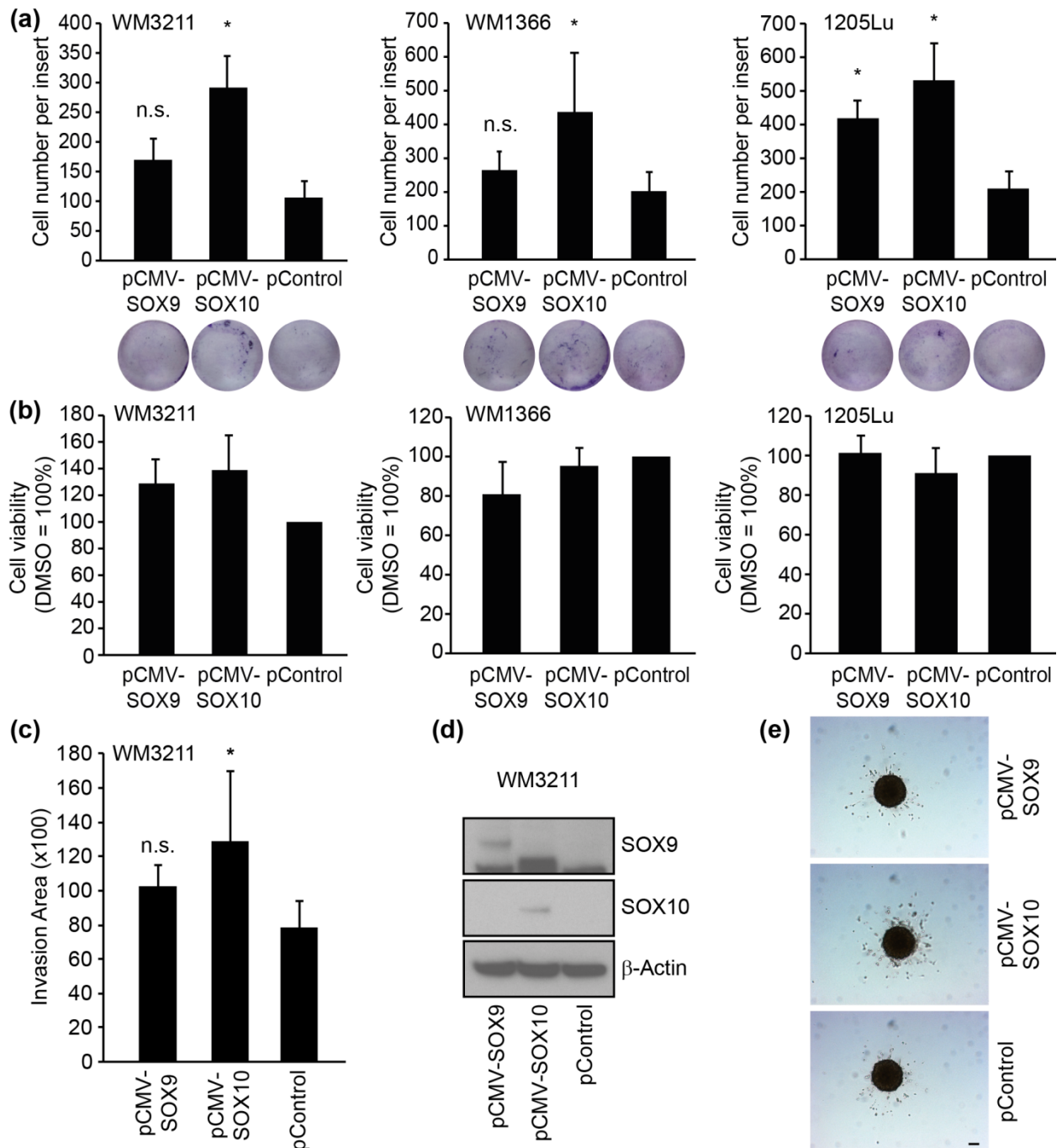


Figure 35: Two- and three-dimensional invasion assays with SOX9- and SOX10-overexpressing melanoma cells.

(a) WM3211, WM1366, and 1205Lu cells were subjected to Matrigel invasion assay 72 hours after transient transfection of vectors for SOX9 and SOX10 overexpression or a control vector (pControl). Mean \pm SD of four independent experiments are shown. An asterisk marks a significant, n.s. a non-significant increase in invasion compared to pControl (one-way ANOVA, $*P < 0.05$). Representative stained membranes after Matrigel invasion assay are shown. **(b)** Cell viability (mean \pm SD) was determined in cells mentioned in (a) in three independent experiments. **(c)** WM3211 transfected with pCMV-SOX9, pCMV-SOX10, and pControl were subjected to spheroid assays 72 hours days after transfection. Quantification of invasion areas with the Fiji ImageJ software were performed 48 hours after embedding in collagen with cultivation on agar for 24 hours in between. Mean \pm SD of four independent

experiments (with 2 to 4 technical replicates each) are shown. An asterisk marks a significant, n.s. a non-significant increase in invasion compared to pControl (one-way ANOVA, $*P < 0.05$). (d) Immunoblot with cell lysates from WM3211 spheroids 6 days after transfection demonstrates lasting expression of SOX9 and SOX10 by transient plasmid transfection. Detection of β -Actin served as loading control. (e) Representative pictures of spheroid assays are shown. Scale bar = 100 μ m.

To analyze the cellular background of this increased invasion upon SOX10 overexpression, the previously described target genes of SOX10, i.e., MIA, ERBB3, and MITF, were examined by immunoblotting (Figure 36).

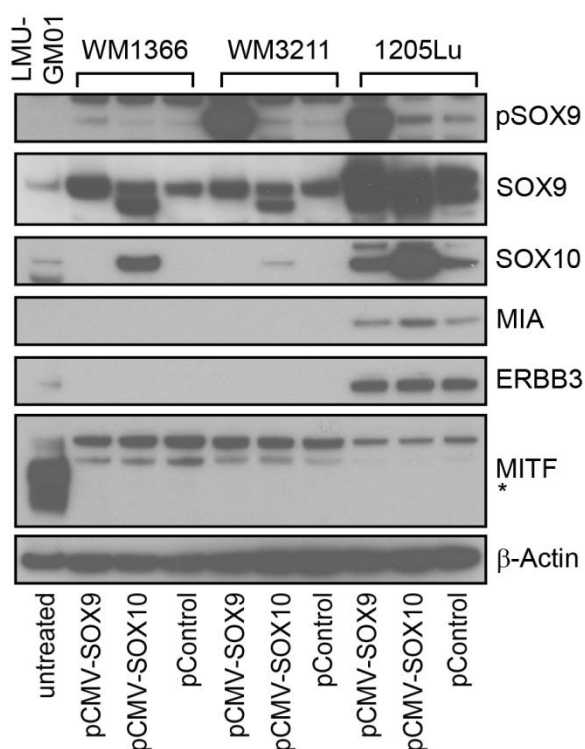


Figure 36: Investigation of MIA, ERBB3, and MITF expression after overexpression of SOX9 and SOX10.

Expression of pSOX9, SOX9, SOX10, MIA, ERBB3, and MITF was assessed by immunoblotting in WM3211, WM1366, and 1205Lu cells 72 hours after transfection of vectors for SOX9 and SOX10 overexpression or a control vector (pControl). MIA expression was increased after SOX10 overexpression in 1205Lu cells but not in the other cell lines. No increase in ERBB3 or M-MITF (asterisk) was found. LMU-GM1 served as positive control for M-MITF. Detection of β -Actin served as loading control.

MIA expression was elevated in cell line 1205Lu by SOX10 but not by SOX9 overexpression. However, neither increase nor expression of MIA was found for cell lines WM3211 and WM1366. Furthermore, no increase in ERBB3 and M-MITF levels was found in all tested cell lines.

These data indicate that SOX10 overexpression may regulate further target genes that can directly affect melanoma cell invasion.

4.7 Identification of further SOX10 target genes by RNA sequencing

RNA sequencing studies were performed in order to identify further genes regulated by SOX10 overexpression. For these studies, 1205Lu - a melanoma cell line with a median expression level of SOX10 according to section 4.1.1 - was selected. The increase of SOX10 expression after pCMV-SOX10 transfection was tested in a time course

experiment. The CMV6 vector without the SOX10 recombinant coding sequence (pCMV6) was included as control vector. SOX10 levels were highly elevated 16 hours after plasmid transfection (Figure 37 a).

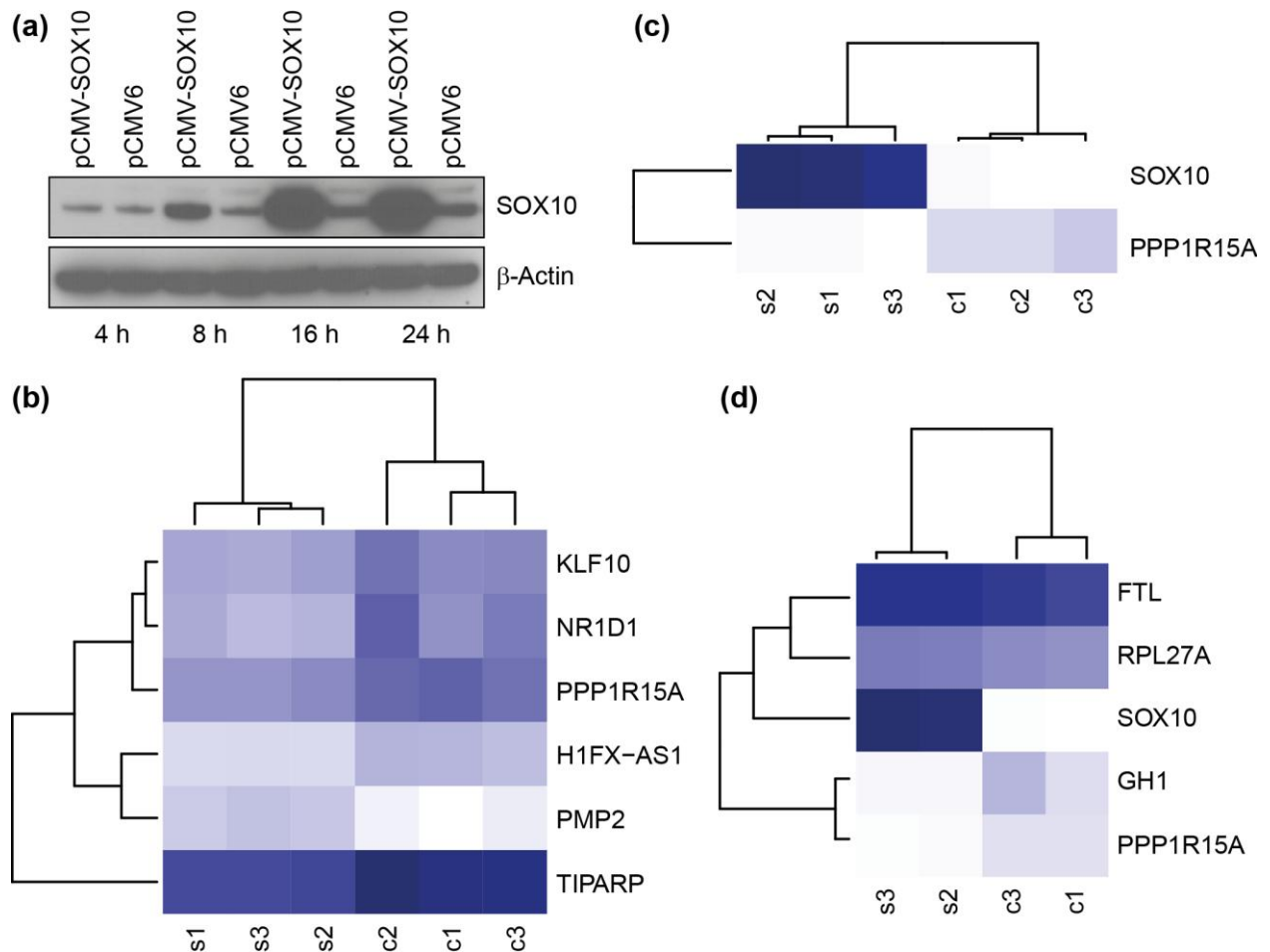


Figure 37: Significantly regulated genes after SOX10 overexpression identified by RNA sequencing.

(a) Time course analysis 4, 8, 16, and 24 hours after transfection of pCMV-SOX10 or pCMV6 control showed a strong increase of SOX10 protein expression after 16 and 24 hours. Detection of β -Actin served as loading control. (b) Three replicates of 1205Lu cells transfected with pCMV-SOX10 (s1-s3) or pCMV6 (c1-c3) for 24 hours were subjected to RNA sequencing. The heat map displays six genes that were significantly regulated by SOX10 overexpression. (c) Heat map of significantly regulated genes of cells mentioned above after DNase digestion of isolated RNA and subsequent RNA sequencing. (d) Heat map of significantly regulated genes of cells as mentioned in (c) in two (s3, s2) versus two (c3, c1) biological replicates. Dark blue indicates a high, light blue or white a low number of reads.

To ensure an effect on target gene transcription, samples for RNA sequencing were collected in QIAzol 24 hours after plasmid transfection in three biological replicates of SOX10 overexpressing and control cells. RNA sequencing was performed in collaboration with Dr. Stefan Krebs and Dr. Helmut Blum at the Gene Center of the LMU Munich with an Illumina Genome Analyzer Iix. In the first sequencing experiment, a high

rate of reads mapped to sequences of the transfected vectors and had to be excluded from the analysis. In the end, six genes were significantly regulated by SOX10 overexpression (Figure 37 b, Table 15).

Gene	Base mean	Base mean A	Base mean B	Fold change	Log2-fold change	P-value	P-value adjusted
<i>NR1D1</i>	173.925	75.597	272.252	0.278	-1.849	3.81E-06	0.016
<i>H1FX-AS1</i>	40.985	17.922	64.049	0.280	-1.837	1.26E-05	0.043
<i>KLF10</i>	168.812	106.808	230.817	0.463	-1.112	2.14E-06	0.011
<i>PPP1R15A</i>	254.715	163.241	346.189	0.472	-1.085	2.00E-08	0.0002
<i>TIPARP</i>	928.433	615.458	1241.408	0.496	-1.012	2.57E-11	5.29E-07
<i>PMP2</i>	21.9877	41.930	2.044	20.518	4.359	3.19E-08	0.0002

Table 15: Results from RNA sequencing experiment without DNase digestion.

“Base mean” equals the mean of reads, “base mean A” the reads from the cells transfected pCMV-SOX10 and “base mean B” the cells transfected with the control vector pCMV6. Log2 = binary logarithm.

Krueppel-like factor 10 (KLF10) is a zinc finger transcription factor implicated in cell differentiation and in serving as a potential marker for diseases as breast cancer, cardiac hypertrophy, and osteoporosis [260]. It is known to be involved in repressing cell proliferation and inflammation as well as inducing apoptosis. Nuclear receptor subfamily 1, group D, member 1 (NR1D1) is a ligand sensitive transcription factor that negatively regulates the expression of core clock proteins in the circadian rhythm [63]. It is also involved in the regulation of metabolism, inflammation, and cardiovascular processes. Furthermore, activation of NR1D1 has anti-proliferative effects on breast cancer cells [284]. Protein phosphatase 1 regulatory subunit 15A (PPP1R15A) recruits the serine/threonine-protein phosphatase 1 (PP1) to dephosphorylate the eukaryotic translation initiation factor 2 alpha (eIF-2 α) and thereby attenuating translational elongation [35]. It mediates growth arrest and apoptosis in response to DNA damage, negative growth signals, and protein misfolding. Staining of nevi and melanoma tissue samples showed high expression of PPP1R15A in nevi while it was decreased with melanoma thickness indicating that it might play a role in the malignant transformation of nevus to melanoma [135]. H1FX antisense RNA 1 (H1FX-AS1) is a non-coding RNA. H1FX is a member of the histone H1 family. Peripheral myelin protein 2 (PMP2) is a small basic protein that binds fatty acids and is one of the major proteins in

development and maintenance of the myelin sheath predominantly in the peripheral nervous system [96]. It can stack lipid bilayers, affect membrane dynamics, and is suggested to be important for lipid transport to and from the myelin membrane. It has not been related to melanoma or any other malignancies yet. Two, 3, 7, 8-Tetrachlorodibenzo-p-dioxin (TCDD)-inducible poly (ADP-ribose) polymerase (TIPARP) is a mono-ADP-ribosyltransferase that ribosylates core histones and functions as a repressor of aryl hydrocarbon receptor (AHR) [167]. AHR mediates toxic effects of environmental contaminants e.g. TCDD via its targets such as cytochrome p450. Single nucleotide polymorphisms in the *TIPARP* gene were found in ovarian cancer [87]. Another sequencing experiment was performed with the same isolated mRNA but with DNA digestion prior to cDNA synthesis and library generation. In this experiment, only *SOX10* and *PPP1R15A* were significantly regulated among the three replicates (Figure 37 c, Table 16).

Gene	Base mean	Base mean A	Base mean B	Fold change	Log2-fold change	P-value	P-value adjusted
<i>SOX10</i>	26584.363	52595.492	573.234	91.752	6.520	6.74E-98	1.04E-93
<i>PPP1R15A</i>	1029.113	607.423	1450.803	0.419	1.256	6.36E-09	4.88E-05

Table 16: Results from RNA sequencing experiment including DNase digestion.

Significant regulation by *SOX10* overexpression was found in five genes when two of the three biological replicates were compared. These genes were *ferritin light polypeptide 1 (FTL)*, *ribosomal protein 27 a (RPL27a)*, and *growth hormone 1 (GH1)* next to *PPP1R15A* and *SOX10* (Figure 37 d, Table 17).

Gene	Base mean	Base mean A	Base mean B	Fold change	Log2-fold change	P-value	P-value adjusted
<i>SOX10</i>	32141.329	63670.639	612.019	104.034	6.701	0	0
<i>PPP1R15A</i>	1009.057	668.175	1349.940	0.495	-1.015	2.38E-05	0.071
<i>FTL</i>	32026.134	36846.397	27205.871	1.354	0.438	4.74E-07	0.002
<i>RPL27A</i>	7646.465	8923.887	6369.043	1.401	0.487	8.40E-06	0.031
<i>GH1</i>	1508.362	747.237	2269.487	0.329	1.603	4.03E-11	3.02E-07

Table 17: Results from RNA sequencing experiment with DNase digestion comparing replicates c1 and c2 with s2 and s3.

In order to identify general and not cell line-specific target genes of SOX10, the genes mentioned above were examined for mRNA expression in cell lines WM3211, WM1366, and 1205Lu 24 hours after transfection of the SOX10 and the control vector. A heat map of the binary logarithms of the mean mRNA values is displayed in Figure 38.

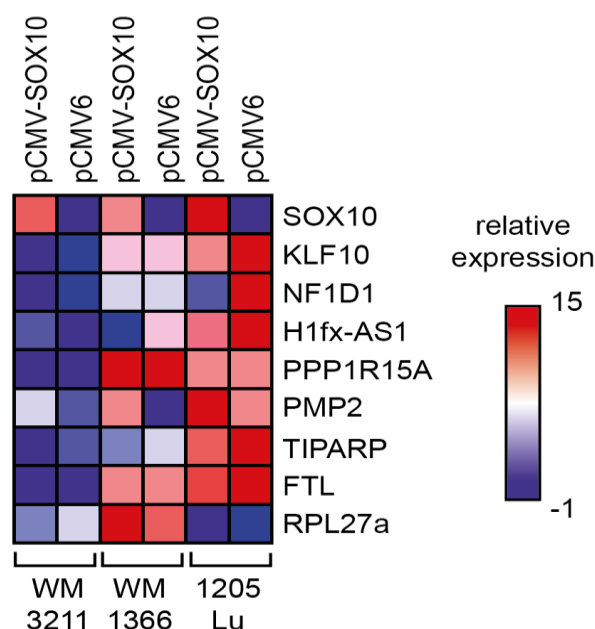


Figure 38: Expression of SOX10-regulated genes identified by RNA sequencing.

Expression of SOX10, KLF10, NR1D1, H1FX-AS1, PPP1R15A, PMP2, TIPARP, FTL, and RPL27A were analyzed in cell lines WM3211, WM1366, and 1205Lu 24 hours after transfection of pCMV-SOX10 or pCMV6 control vector. Binary logarithms of mean mRNA values from three independent experiments are displayed in a heat map generated with the HeatMapper from Broad Institute. Red indicates a relatively high, blue a relatively low expression.

GH1 mRNA was only detectable in 1205Lu (data not shown) and therefore excluded from further analyses.

mRNA	WM3211 SOX10/pCMV6	WM1366 SOX10/pCMV6	1205Lu SOX10/pCMV6
SOX10	5.78	4.79	8.48
KLF10	-0.14	-0.01	-0.80
NR1D1	-0.16	0.01	-1.64
H1fx-AS1	0.20	-0.35	-0.34
PPP1R15A	0.07	0.03	-0.08
PMP2	2.51	6.35	3.44
TIPARP	-0.20	-0.16	-0.33
FTL	-0.18	0.14	-0.22
RPL27a	-0.22	0.35	-0.12

Figure 39: Log₂-fold mRNA expression of genes identified by RNA sequencing.

Mean mRNA values of significantly regulated genes by SOX10 overexpression described in Figure 38 were analyzed by normalization of SOX10 overexpression- to pCMV6-values and converted into log₂ values. These values were related to an according color scale, in which red means high and blue means low expression. SOX10 overexpression increased SOX10 and PMP2 mRNA values in all three investigated cell lines.

Strikingly, when calculating the binary logarithm of the mRNA values normalized to the control vector (pCMV-SOX10/pCMV6) in all three analyzed cell lines, a clear

upregulation of SOX10 and of PMP2 mRNA was found (Figure 39), indicating that SOX10 transactivates PMP2.

4.8 Identification of PMP2 as a target gene of SOX10

4.8.1 Analysis of the regulation of PMP2 by SOX10

Considering the results of the RNA sequencing and the expression patterns in Figures 38 and 39, it stands to reason that PMP2 is a potential target gene of SOX10. Figure 40 displays the results of mRNA expression of SOX10 and PMP2 24 hours after transfection of the SOX10 or the control vector. SOX10 overexpression increased PMP2 mRNA expression around 10-fold in cells lines WM3211 and 1205Lu and around 100-fold in cell line WM1366.

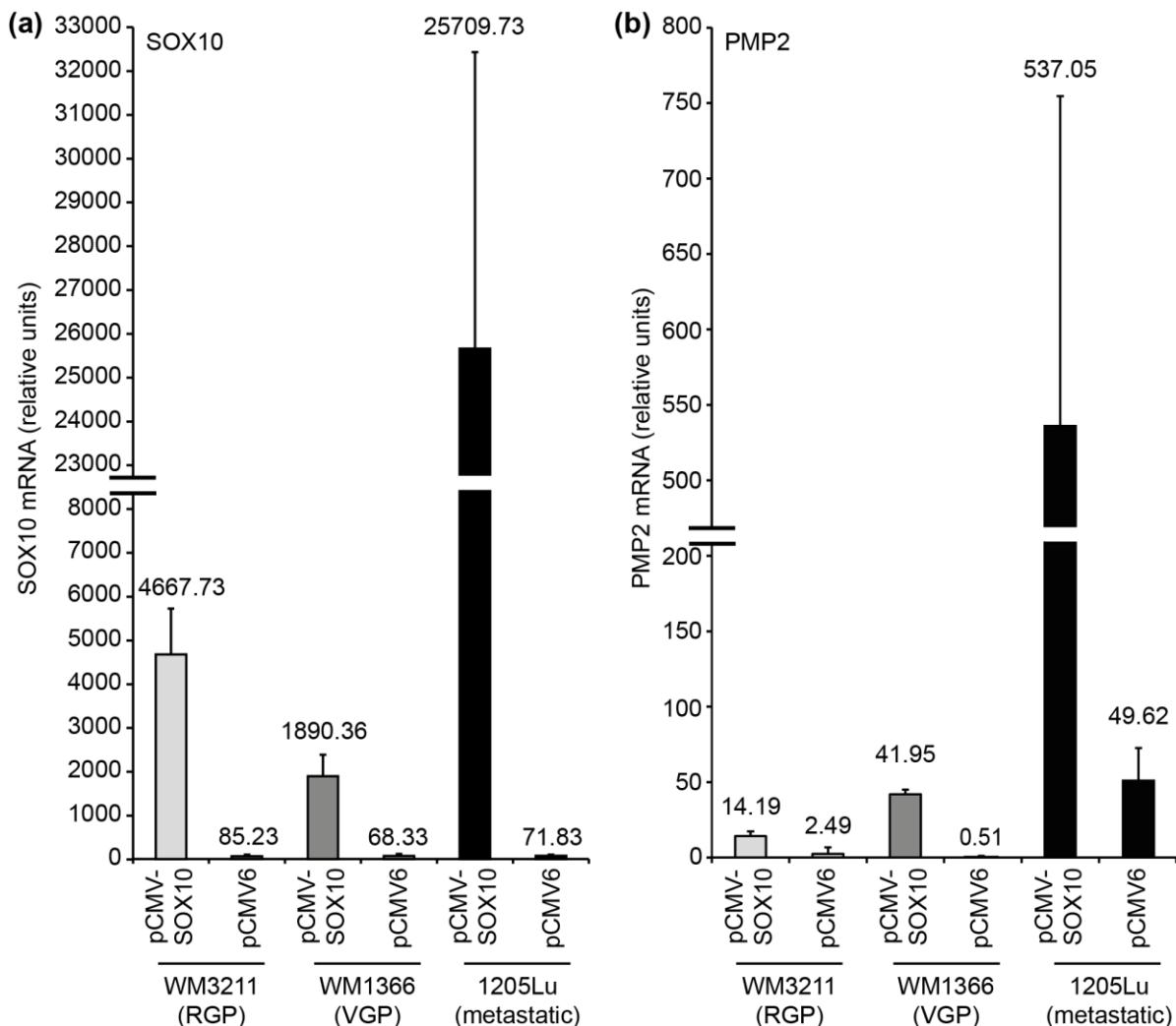


Figure 40: Analysis of PMP2 expression after SOX10 overexpression.

SOX10 (a) and PMP2 (b) mRNA expression (mean \pm SD of three independent experiments) were assessed in cell lines WM3211 (light grey bars), WM1366 (medium grey bars), and 1205Lu (black bars) 24 hours after plasmid transfection of pCMV-SOX10 or pCMV6.

Furthermore, PMP2 expression was investigated after SOX10 inhibition in cell lines WM278, WM1232, and 1205Lu. Reduction of PMP2 mRNA by SOX10 inhibition was found in all three cell lines (Figure 41 a). Apparently, WM278 cells displayed up to 150-fold increased mRNA levels in the control samples compared to cell lines WM1232 and 1205Lu. On protein level, distinct PMP2 signals were only detected in cell line WM278 (Figure 41 b). Here, SOX10 inhibition also strongly reduced PMP2 protein expression. A time course analysis demonstrated that SOX10 inhibition was capable of effectively reducing PMP2 protein expression already after 24 hours (Figure 41 c). This early regulatory event points to a direct transactivation of PMP2 by SOX10.

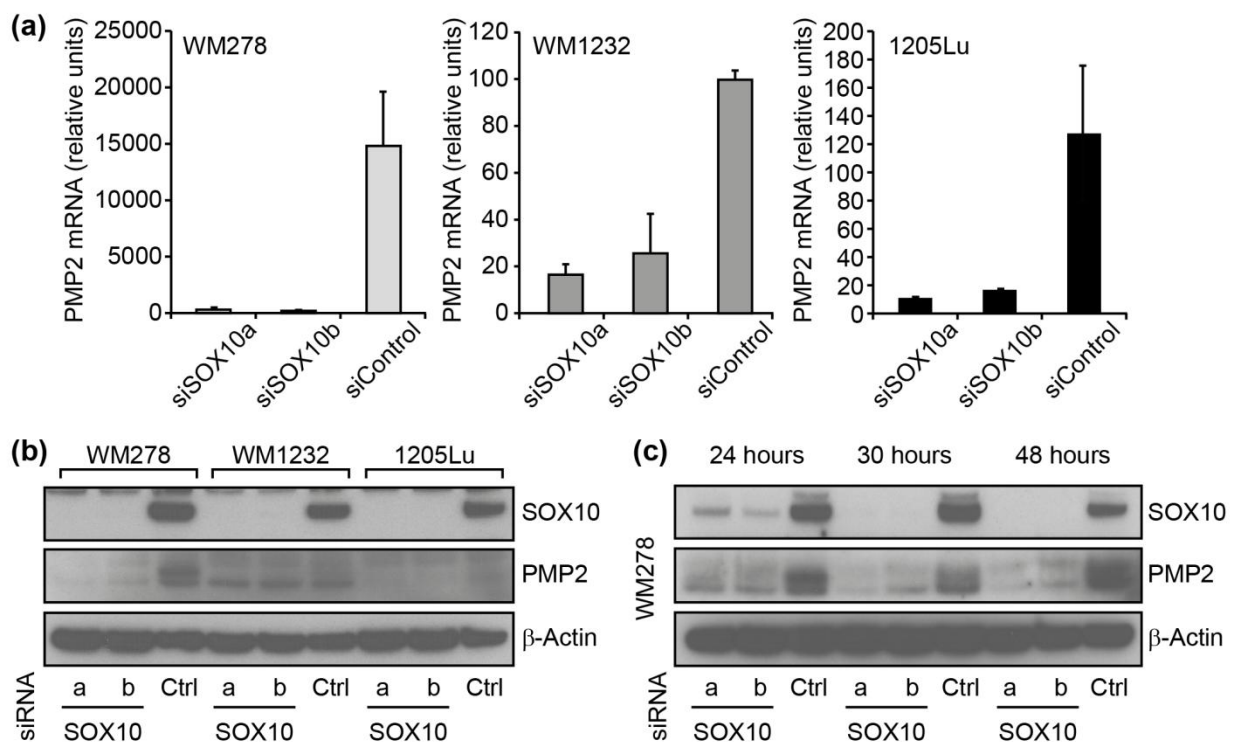


Figure 41: Analysis of PMP2 expression after SOX10 inhibition.

(a) PMP2 mRNA expression (mean \pm SD) was assessed after SOX10 inhibition in cell lines WM278 (light grey bars), WM1232 (medium grey bars), and 1205Lu (black bars) 48 hours after transfection of siSOX10a, siSOX10b, or siControl in three independent experiments. **(b)** PMP2 protein expression was assessed in the same cells described in (a) 48 hours after siRNA transfection. Detection of β -Actin served as loading control. **(c)** Time course analysis of SOX10, PMP2, and β -Actin expression by immunoblotting 24, 30, and 48 hours after transfection with SOX10-targeting or control (Ctrl) siRNAs revealed reduced PMP2 protein expression already after 24 hours.

Analysis of PMP2 protein expression after SOX10 or SOX9 overexpression is shown in Figure 42. In cell line WM278, SOX10 rather than SOX9 overexpression was sufficient to slightly increase PMP2 expression as determined by PMP2 quantification in relation to β -Actin with the FIJI ImageJ software (Figure 42 a). However, no PMP2 protein at all

was found in cell lines WM3211, WM1366, and 1205Lu (Figure 42 b) although an increase in PMP2 mRNA has been detected before (Figure 40).

To sum up these data, it was shown that SOX10 inhibition reduced PMP2 mRNA and protein expression. An increase of PMP2 by SOX10 overexpression was found on mRNA level in all investigated cell lines while increased protein expression was only observed in a PMP2-positive melanoma cell line.

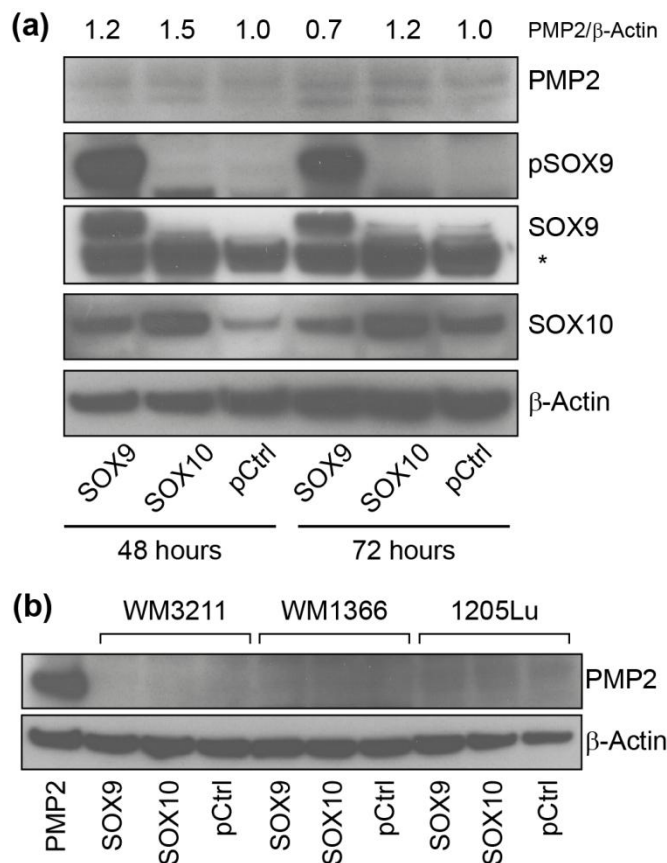


Figure 42: Investigation of PMP2 expression after SOX10 overexpression.

(a) PMP2, pSOX9, SOX9, SOX10 and β-Actin protein expression was assessed by immunoblotting in cell line WM278 48 and 72 hours after transfection of pCMV-SOX9, pCMV-SOX10 or pControl. The non-specific SOX10 signal of the SOX9 antibody is marked by an asterisk. Numbers above the blot display quantification of the PMP2 bands (upper bands) with Fiji ImageJ, normalized to β-Actin. **(b)** PMP2 protein expression was assessed by immunoblotting in cell lines WM3211, WM1366, and 1205Lu 72 hours after transfection of vectors for SOX9 and SOX10 overexpression or a control vector. Detection of β-Actin served as loading control. WM278 cells transfected with a PMP2 expression vector (pCMV-PMP2) were included as PMP2-positive control.

4.8.2 Analysis of SOX10 binding to the *PMP2* promoter

A direct transactivation of PMP2 by SOX10 was assessed by *in silico* analyses for potential SOX10 binding sites within the *PMP2* promoter as well as by ChIP (according to section 4.4.2). The first 1075 bp before the PMP2 protein start site (>gi|568815590:c81449371-81448296 Homo sapiens chromosome 8, GRCh38 Primary Assembly; NCBI database), comprising the *PMP2* promoter region, were analyzed with the MatInspector from Genomatix software and with the JASPAR database. With the MatInspector, 19 binding sites for the SOX/SRY-sex/testis determining and related HMG box factors matrix family were predicted (Table 18). G1/G2, G4/G5, G6/G7/G8, G16/G17, and G18/G19 were overlapping identified binding sites.

Binding site	Matrix	Start position	End position	Anchor position	Strand	Sequence
G1	V\$HBP1 .02	-166	-142	-154	-	actaagcAATGaatgg ctcttcaat
G2	V\$HBP1 .01	-169	-145	-157	-	aagcaatgAATGgctc ttcaatggc
G3	V\$SOX3 .01	-227	-203	-215	+	tggagaCAAaggaa gtattatgtg
G4	V\$HBP1 .01	-261	-237	-249	-	ataaaatgAATGagatt actatttg
G5	V\$HMG Y.01	-281	-257	-269	+	tcaaaaAATtttgaag attcaaat
G6	V\$HMG A.01	-367	-343	-355	-	ctgtgatcatgAATGaa tgtgtgtg
G7	V\$HBP1 .02	-371	-347	-359	-	gatcatgAATGaatgtg tgtgtgtt
G8	V\$HBP1 .01	-374	-350	-362	-	catgaatgAATGtgtgt gtgttag
G9	V\$SOX1 5.01	-425	-401	-413	-	tctgcACAAttaagaatt cttattg
G10	V\$SR.Y. 02	-478	-454	-466	-	taagtATTAtgataaca gtctcaaa
G11	V\$SOX6 .01	-598	-574	-586	-	ggcagACAagaagt cagtctattg
G12	V\$SOX6 .01	-688	-664	-676	-	gcacaCAAagatttc agctagaa
G13	V\$HBP1 .02	-756	-732	-744	+	cattttaAATGacttaa cacaat
G14	V\$HMG A.01	-760	-736	-748	+	gattcattttaAATGactt aaacac
G15	V\$HMG A.01	-814	-790	-802	+	ttgcaatataAATtagt actcttt
G16	V\$HBP1 .01	-873	-849	-861	+	tataattaAATGagatc accgtat
G17	V\$HMG A.01	-880	-856	-868	-	tgatctatttAATTatat cactaa
G18	V\$SR.Y. 02	-911	-887	-899	+	tggatATAaatagttc ctaactc
G19	V\$SR.Y. 02	-918	-894	-906	-	gaactATTattatcca tttacc

Table 18: General SOX binding sites in the *PMP2* promoter as evaluated with the MatInspector from Genomatix.

Matrices that define the binding site prediction are named. Positions of binding sites are related to the protein start ATG. Binding site prediction is related to the sense, anti-coding (+) strand or the antisense, coding (-) strand of the DNA. Capital letters in the predicted sequence mark the core binding nucleotides.

With JASPAR seven binding sites were predicted. J3, J5, and J6 were identical to the MatInspector predicted sites G3, G11, and G12 and their binding core sequence, respectively (Table 19).

Binding site	Score	Relative score	Start	End	Strand	predicted site sequence
J1	7.097	0.920	-25	-20	+	CTGTGT
J2	6.812	0.907	-137	-132	-	CAGTGT
J3	8.910	1.000	-222	-217	-	<u>CTTTGT</u>
J4	6.812	0.907	-512	-507	-	CAGTGT
J5	8.910	1.000	-584	-579	+	<u>CTTTGT</u>
J6	8.910	1.000	-674	-669	+	<u>CTTTGT</u>
J7	6.812	0.907	-835	-830	+	CAGTGT

Table 19 SOX10 binding sites in the PMP2 promoter as evaluated with the JASPAR database and model-ID MA0442.1.

Score and relative score evaluate the sequence alignment of input profile and model-ID using a modified Needleman-Wunsch algorithm. Positions of binding sites are related to the protein start ATG. Binding site prediction is related to the sense, anti-coding (+) strand or the antisense, coding (-) strand of the DNA. Bold letters mark the binding sequences, which were also predicted with the MatInspector from Genomatix. Identical core binding sites are underlined. Genomatix software. Identical core binding sites are underlined.

For CHIP analyses, primers hybridizing within the *PMP2* promoter region were designed in the Roche Assay Design Center but only two sets of primer pairs (set 1 = -608 to -532, set 2 = -1040 to -1019) were suitable for the Lightcycler Taqman Master qPCR system (Figure 43 a). Only with primer set 1 a significant enrichment of recovered DNA through SOX10 CHIP could be detected indicating that SOX10 can bind in the proximal but not further distal *PMP2* promoter region (Figure 43 b).

The three potential SOX10 binding sites that were recognized by the MatInspector and JASPAR (p1 = J3/G3, p2 = J5/G11, and p3 = J6/G12) were integrated in DIG-labeled oligonucleotides for EMSA analysis. A control DIG-labeled oligonucleotide containing a published SOX binding consensus sequence binding site [52] was included in the analysis. EMSA was performed with nuclear extracts from 1205Lu cells with ectopic SOX10 overexpression.

DIG detection on the EMSA membrane showed a strong shift signal with the control fragment that vanished through supershift with the SOX10 but not with the control antibody (Figure 43 c upper panel). Only for the p1-containing oligonucleotide, a distinct DIG-related signal could be detected, which was shifted up with the SOX10 antibody.

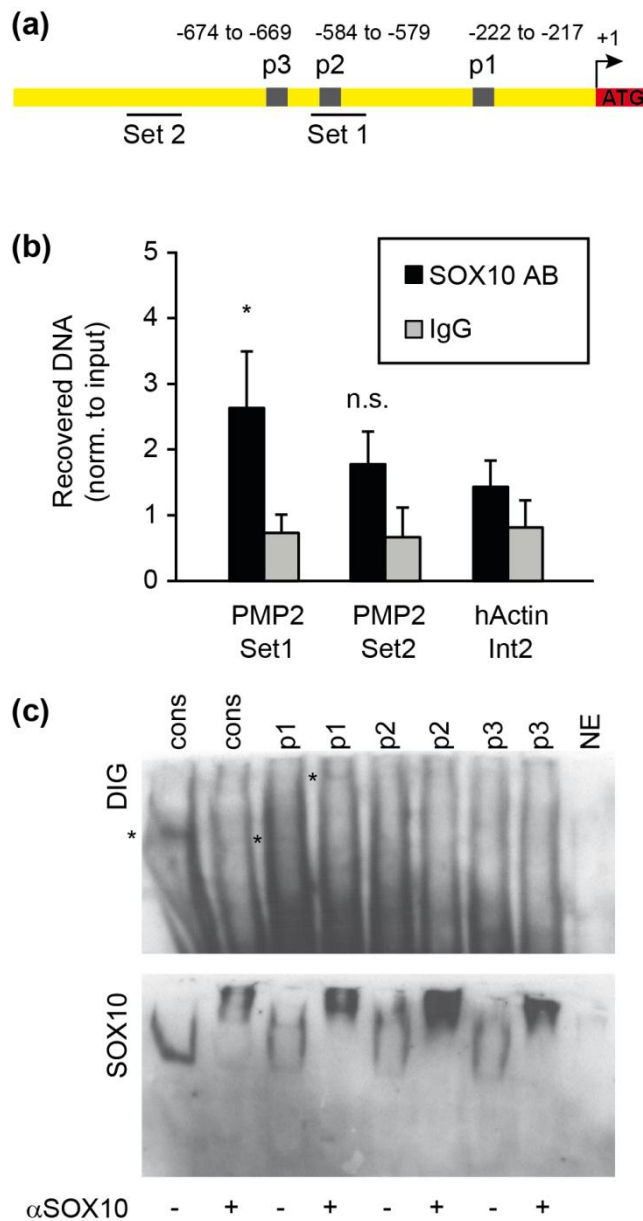


Figure 43: SOX10 binding studies in the *PMP2* promoter region.

(a) The schematic overview of the *PMP2* promoter illustrates predicted SOX10 binding sites (p1, p2, and p3) and primer pairs for ChIP assay. **(b)** Percentages of precipitated DNA in relation to the input DNA after ChIP assay with 1205Lu cells and with anti-SOX10 antibody (black bars) or IgG control (grey bars) are shown. Recovered DNA (mean ± SD) with primer pairs hybridizing in the *PMP2* promoter region or a control locus (hAct Int 2) was determined by qRT-PCR in four independent experiments. Significant increase of around two-fold was found for recovered *PMP2* promoter DNA with the SOX10-specific antibody and primer set 1 but not primer set 2 in comparison to the IgG control and the recovered DNA of hAct Int 2 (*t*-test, **P*<0.05). **(c)** EMSA with 1205Lu cells ectopically overexpressing SOX10 was performed with DIG-labeled oligonucleotides containing a consensus SOX10 binding sequence (cons) or the predicted SOX10 binding sites within the *PMP2* promoter (p1-3). DIG-detection (upper panel) revealed a strong shift of the cons oligonucleotide while a weak shift signal was found for p1, which was up-

shifted with the SOX10 antibody (signals marked by asterisks). SOX10 detection of the EMSA membrane revealed strong binding of SOX10 to the cons oligonucleotide and weak binding to p1, p2, and p3.

Detection of SOX10 on the EMSA membrane revealed a different pattern (Figure 43 c lower panel). SOX10-DNA-complexes that were specifically restricted with the SOX10 antibody were found with all DNA fragments. The signal was most prominent with the control fragment. However, signals obtained with p2 and p3 were less distinct compared to p1. Furthermore, shift patterns for p1 suggested a multiple binding of SOX10 to this oligonucleotide although no more binding sites were predicted for this sequence.

Considering the results from the ChIP and EMSA experiments, it is possible that SOX10 binds to the proximal promoter region of the *PMP2* gene.

4.8.3 Investigating EGR2 as a transcriptional coregulator of SOX10

EGR2 (also known as Krox20) has been described as a common coregulator of SOX10 in myelin gene regulation [258]. Clustering of EGR2/SOX10 binding sites in myelin gene regulatory elements appears to be common [118], [122]. EGR2 itself controls myelination in the peripheral nervous system [267] and was found to be regulated by SOX10 *in vitro* and *in vivo* in Schwann cells [211]. Furthermore, *in vivo* ChIP-sequencing and microarray analyses identified PMP2 expression to be positively regulated by both, SOX10 and EGR2, in myelinating peripheral nerves from rat pups [251].

Potential coregulation of PMP2 by SOX10 and EGR2 has been investigated (Figure 44). SOX10 inhibition was capable of reducing PMP2 but also EGR2 expression in cell line WM278 (Figure 44 b-d).

Accordingly, EGR2 inhibition reduced PMP2 expression as shown in Figure 44 c and d, but not as strong as SOX10 inhibition. However, co-inhibition of SOX10 and EGR2 significantly stronger decreased PMP2 mRNA expression than SOX10 inhibition alone, indicating cooperative regulation of PMP2 by SOX10 and EGR2 also in melanoma cells (Figure 44 c).

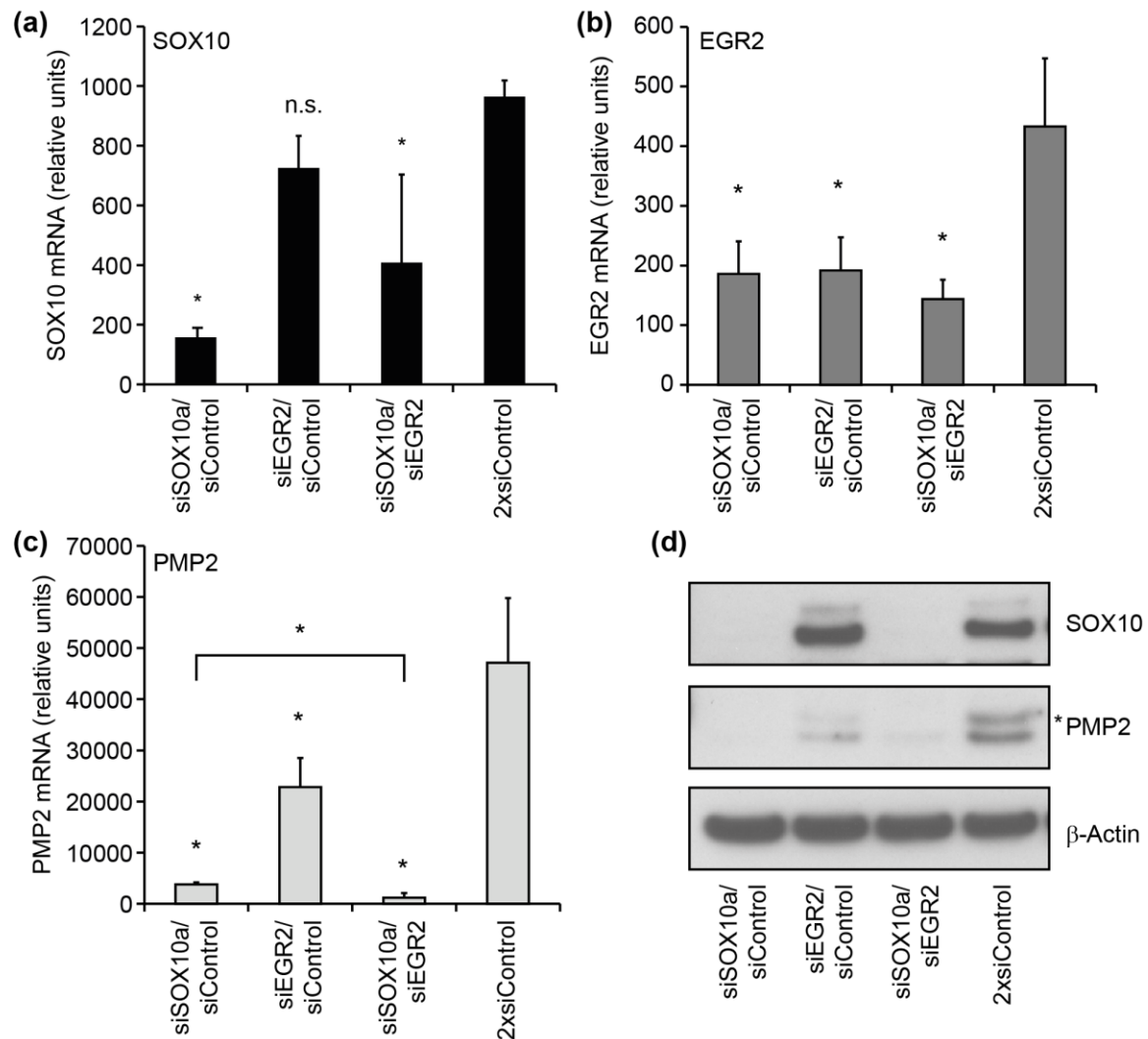


Figure 44: PMP2 expression after SOX10 and/or EGR2 inhibition.

SOX10 (a), EGR2 (b), and PMP2 (c) expression was analyzed by qRT-PCR (mean \pm SD of three independent experiments) in cell line WM278 48 hours after siRNA transfection. SOX10 was significantly downregulated by siSOX10a/siControl and siSOX10a/siEGR2 but not by siEGR2/siControl (one-way ANOVA versus 2xsiControl, $*P < 0.01$). EGR2 and PMP2 were significantly downregulated by all siRNA combinations in comparison to 2xsiControl (one-way ANOVA, $*P < 0.01$). Moreover, the combination of siEGR2 and siSOX10a led to a significantly higher downregulation of PMP2 than siSOX10a/siControl (t -test, $*P = 0.0107$). (d) Immunoblot analysis of samples mentioned above 48 hours after siRNA transfection. Detection of β -Actin served as loading control. An asterisk marks the specific PMP2 band as determined in section 4.9.2.1.

4.9 Expression and functional characterization of PMP2 in melanoma

4.9.1 PMP2 expression in human skin cells and melanoma cell lines

Expression of PMP2 mRNA was assessed in fibroblasts (2 donors), melanocytes (3 donors), and 12 melanoma cell lines as described in section 4.1.1 (Figure 45 a).

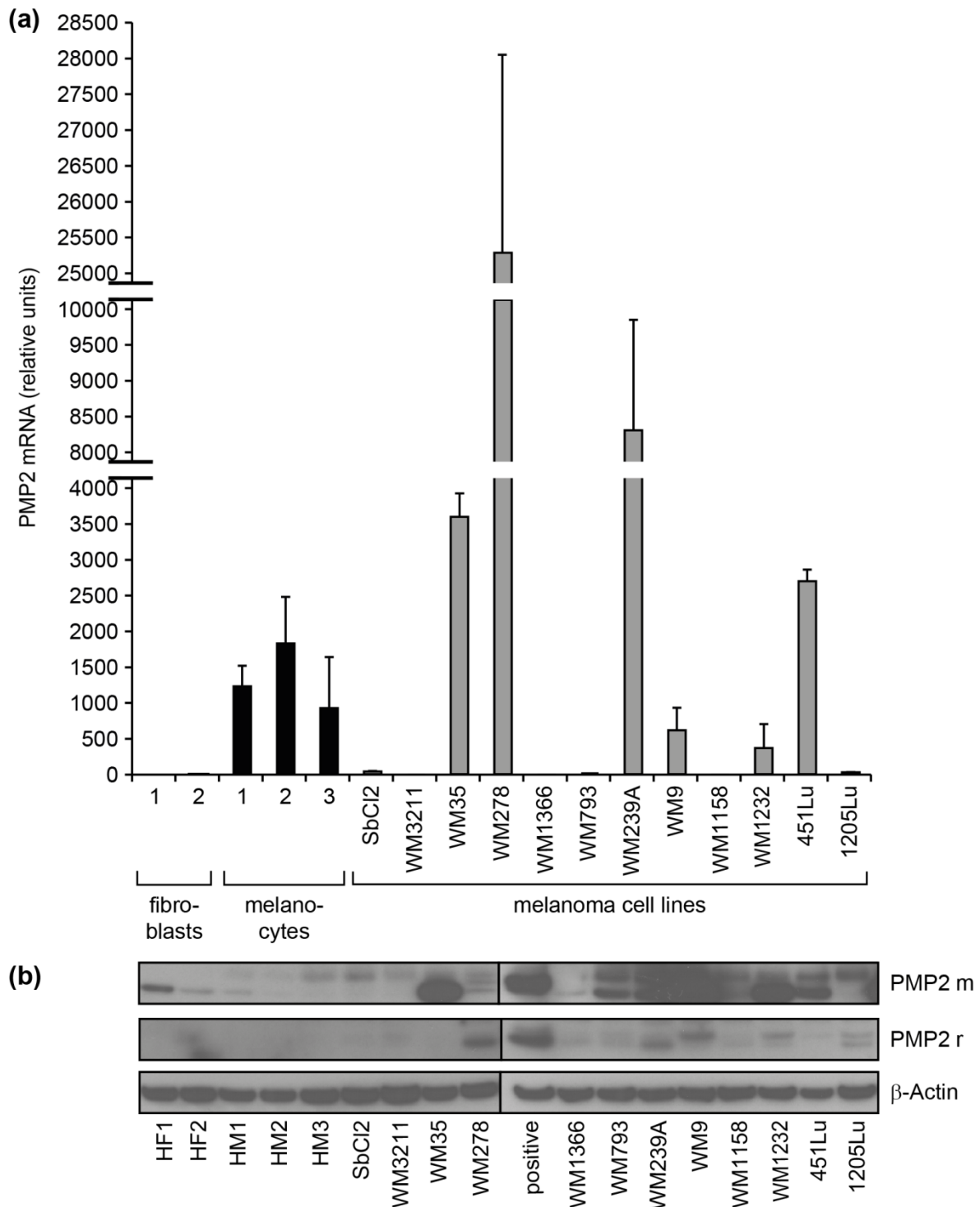


Figure 45: Expression of PMP2 in human skin cells and melanoma cell lines.

(a) PMP2 mRNA expression (mean \pm SD) was investigated in fibroblasts (2 donors), melanocytes (three donors, black bars), and 12 different melanoma cell lines (grey bars) by qRT-PCR in three independent experiments. **(b)** PMP2 protein expression was detected by immunoblotting with a PMP2 antibody from mouse (PMP2 m, used in previous immunoblots) and a PMP2 antibody derived from rabbit (PMP2 r) in cell lines described in (a). Detection of β -Actin served as loading control. PMP2 is expressed in cell lines WM278 and WM239A according to the positive control (WM278 transfected with pCMV-PMP2).

Little or no PMP2 mRNA expression was found in fibroblasts and in 6 of 12 melanoma cell lines (SbCl₂, WM3211, WM1366, WM793, WM1158, 1205Lu). Moderate PMP2 mRNA levels were found in melanocytes. Strikingly, 2 of 12 melanoma cell lines (WM278 and WM239A) showed very high expression levels. PMP2 expression was further assessed on protein level (Figure 45 b). Due to the relatively poor quality of the PMP2 antibodies tested, a positive control, i. e., WM278 cell line ectopically overexpressing PMP2, was loaded. The PMP2 antibody derived from mouse (PMP2 m) was used in the previous experiments and displayed a high background. Therefore another PMP2 antibody derived from rabbit (PMP2 r) was included for expression analyses. This antibody also displayed background bands. Nevertheless, according to the positive control, a clear signal for PMP2 protein expression was detected in cell lines WM278 and WM239A while no expression was found in fibroblasts and melanocytes. Only faint or non-specific bands were detected in the other melanoma cell lines.

Downregulation of PMP2 in SOX10-inhibited cells was also detected in cell line WM239A (Figure 46).

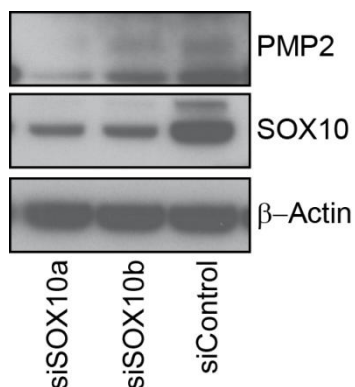


Figure 46: Analysis of PMP2 expression after SOX10 inhibition in WM239A.

PMP2, SOX10, and β -Actin (loading control) protein expression was assessed by immunoblotting 48 hours after transfection of SOX10-targeting or control siRNAs.

In the end, PMP2 seems to be only expressed in a small subset of melanoma cell lines. Nevertheless, it is interesting that a protein, which is crucial for myelination of Schwann cells, is expressed in melanoma cells at all. The expression of other known SOX10-regulated myelin proteins myelin protein zero (MPZ) [196] and proteolipid protein 1 (PLP1) [256] was investigated in a subset of fibroblasts, melanocytes, and melanoma cell lines (Figure 47 a and b, respectively). Moderate and high mRNA levels of MPZ and PLP1 were found in melanocytes, respectively. Moderate mRNA expression of PLP1 was detected in WM239A. Strikingly, both factors were found highly expressed in melanoma cell line WM278. These data indicate that SOX10-regulated myelin proteins seem to be expressed in a subset of melanoma cell lines.

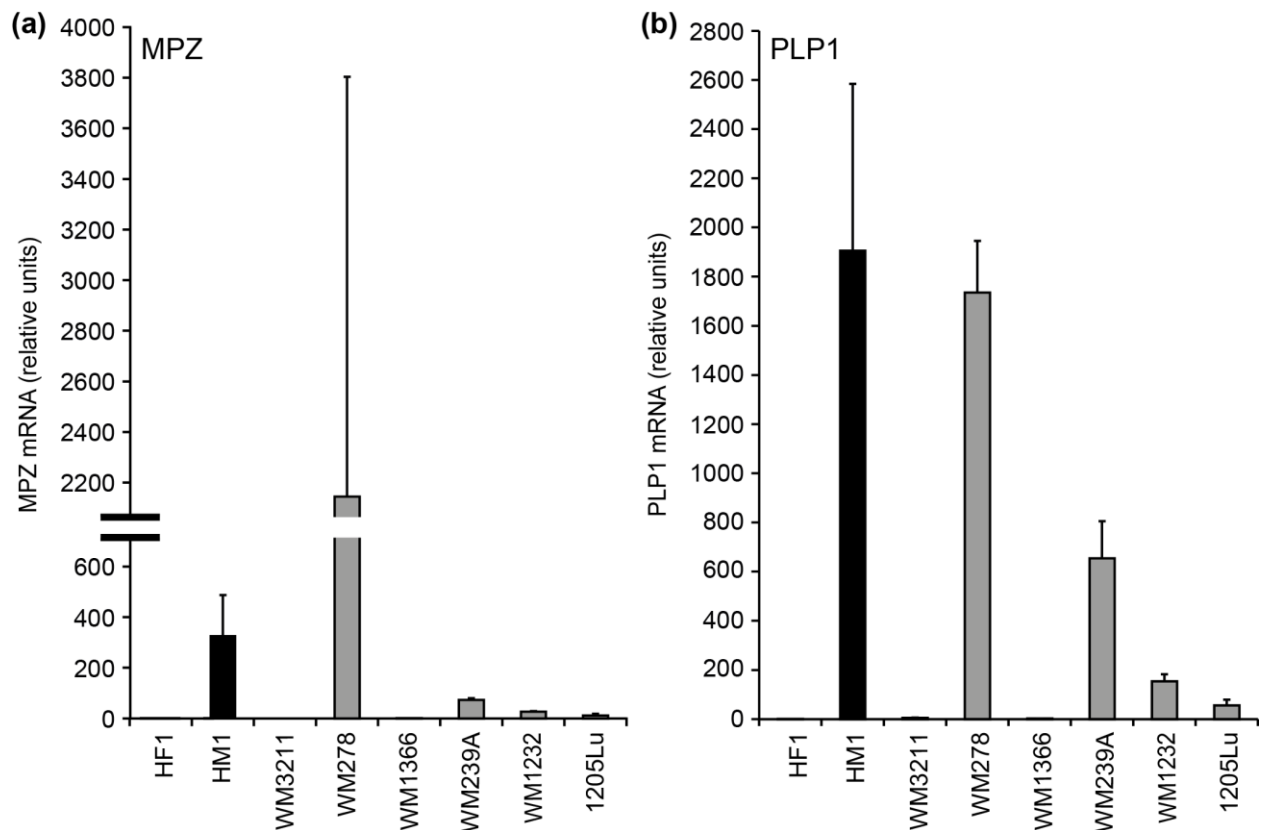


Figure 47: Expression of MPZ and PLP1 in human skin cells and melanoma cell lines.

MPZ (a) and PLP1 (b) mRNA expression was assessed by qRT-PCR (mean \pm SD of three independent experiments) in human fibroblasts (one donor), melanocytes (one donor, black bars), and in 8 melanoma cell lines (grey bars). MPZ and PLP1 are considerably higher expressed in WM278 compared to other melanoma cell lines.

4.9.2 Phenotypic effects of PMP2 inhibition and overexpression in melanoma cells

4.9.2.1 Inhibition of PMP2 via RNA interference

Loss- and gain-of-function experiments were carried out to further investigate potential functions of PMP2 in melanoma cells. PMP2 was inhibited by RNA interference with two different PMP2-targeting siRNAs (siPMP2a and b). Both siRNAs effectively inhibited PMP2 expression as shown for WM278 cells (Figure 48). Inhibition on protein level demonstrated that the specific PMP2 band detected with the PMP2 antibody (source mouse) is the upper one of the detected signals around 15 kDa, which corresponds to the theoretical molecular weight of 14.9 kDa (132 amino acids).

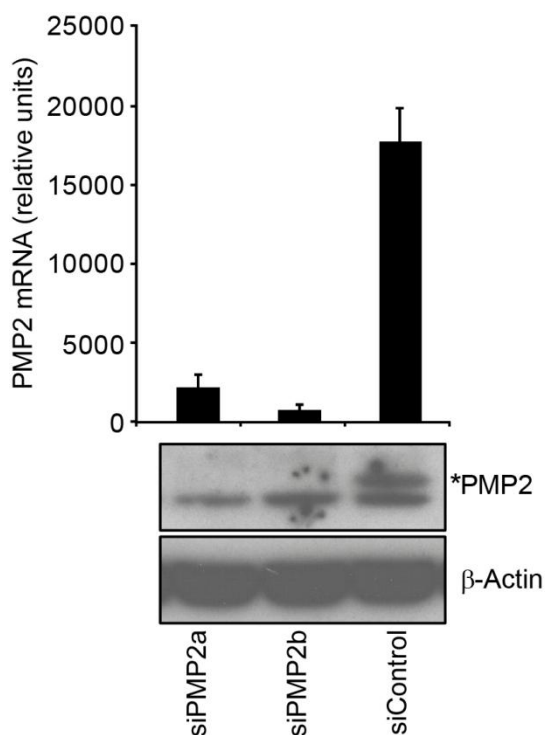


Figure 48: Inhibition of PMP2 via RNA interference. PMP2 mRNA expression (mean \pm SD of three independent experiments) was assessed 24 hours and protein expression 48 hours after transfection of PMP2-targeting siRNAs (siPMP2a and siPMP2b) and control siRNA (siControl). Detection of β -Actin served as loading control. According to these data both PMP2-targeting siRNAs effectively reduced PMP2 expression. Of the two signals around 15 kDa detected with the PMP2 antibody (source mouse), the upper one represents the specific PMP2 signal, marked by an asterisk.

4.9.2.2 Effects of PMP2 inhibition on melanoma cell proliferation

Phenotypic effects of PMP2 inhibition were analyzed in melanoma cell lines WM278, WM239A, and LMU-GM1. LMU-GM1 was established from a melanoma brain metastasis (section 4.1.2). Although PMP2 was also found expressed in the central nervous system (according to the Human Protein Atlas, section 3.1.12), it was not expressed in this metastasis originated from the brain (Figure 49), which therefore served as control cell line for further experiments.

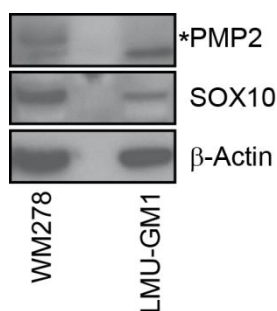


Figure 49: PMP2 is not expressed in cell line LMU-GM1.

Expression of PMP2 and SOX10 was analyzed in cell line LMU-GM1. No signal for PMP2 protein could be detected. Cell line WM278 served as positive, β -Actin as loading control. An asterisk marks the specific PMP2 signal.

Microscopically imaging revealed a change in cell number and morphology. After 96 hours, cell number of PMP2-inhibited WM278 and WM239A cells was strongly decreased compared to control cells (Figure 50). Due to a slower proliferation rate, confluence of LMU-GM1 cells was less than in cell lines WM278 and WM239A. However, the overall cell number of LMU-GM1 was not affected by PMP2 inhibition.

Furthermore, PMP2-inhibited WM278 and WM239A cells tended to display prolonged protrusions. This change in morphology was not found for PMP2-negative LMU-GM1 cells after PMP2-targeting siRNA transfection.

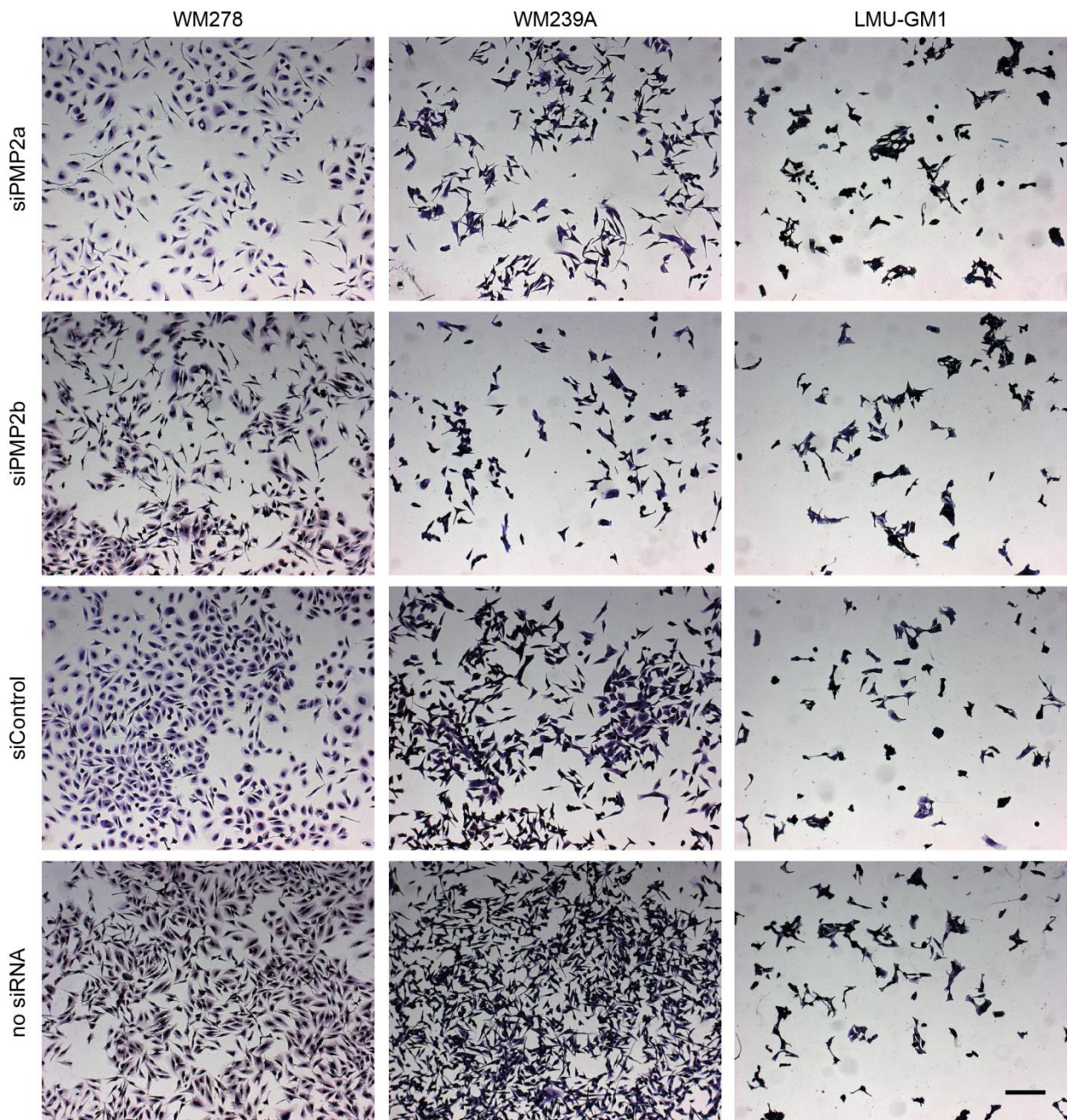


Figure 50: Analysis of cell number and morphology after PMP2 inhibition.

PMP2-positive WM278 and WM239A cells as well as PMP2-negative LMU-GM1 cells were transfected with siPMP2a, siPMP2b, siControl, or no siRNA. 96 hours later, cells were stained with the Diff-Quik staining solution and microscopical images were taken. Representative pictures of two independent experiments are shown. Scale bar = 200 μ m. PMP2 inhibition reduced the cell number and caused prolonged cell protrusions in cell lines WM278 and WM239A, but not in cell line LMU-GM1.

Analysis of cell viability 24 to 120 hours after siRNA transfection demonstrated a considerably enhanced reduction in cell viability by PMP2 inhibition in cell lines WM278 (Figure 51 a) and WM239A (Figure 51 b) in comparison to control cells. Ninety-six hours after siRNA transfection, cell viability of PMP2-inhibited WM278 cells was reduced down to 48.9% with siPMP2a and 72.5% with siPMP2b and in WM239A cells down to around 63% by both PMP2-targeting siRNAs. In contrast, cell viability of LMU-GM1 cells was hardly affected by PMP2 inhibition (Figure 51 c).

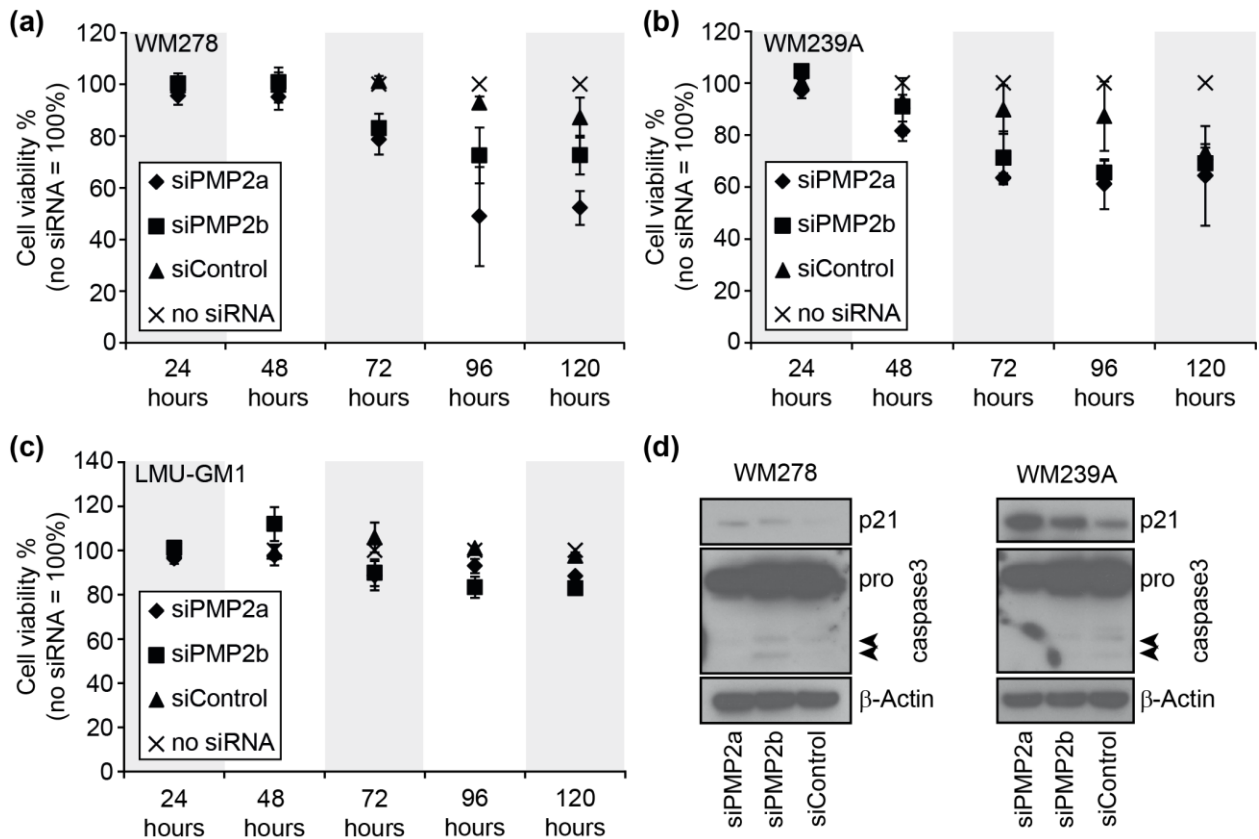


Figure 51: Analysis of cell viability, p21 expression, and caspase3 activation after PMP2 inhibition.

Small interfering RNAs siPMP2a, siPMP2b, siControl, or no siRNA were transfected in PMP2-positive WM278 (a), WM239A (b), and PMP2-negative LMU-GM1 cells (c) and cell viability was determined every 24 hours up to 120 hours after transfection. Mean \pm SD of four independent experiments are shown. (d) P21 and caspase 3 were detected by immunoblotting 120 hours after siRNA transfection. While p21 level were increased in both cell lines with both PMP2-targeting siRNAs, caspase 3 activation (arrows) was only found for siPMP2b in cell line WM278. Detection of β -Actin served as loading control.

Immunoblot analyses demonstrated an increase in p21 by siPMP2a and siPMP2b transfection compared to the control siRNA in both WM278 and WM239A, while caspase 3 was only activated by siPMP2b in cell line WM278 (Figure 51 d). A slight activation of caspase 3 was detected for siPMP2b- and siControl-transfected WM239A

cells. Thus, PMP2 inhibition seems to affect cell viability in PMP2-positive melanoma cells potentially by blocking cell cycle progression.

4.9.2.3 Analysis of PMP2-mediated invasion after SOX10 inhibition

Matrigel invasion assays with PMP2-inhibited compared to control WM278 cells showed a slight decrease in invasion that was only significant for siPMP2b (Figure 52).

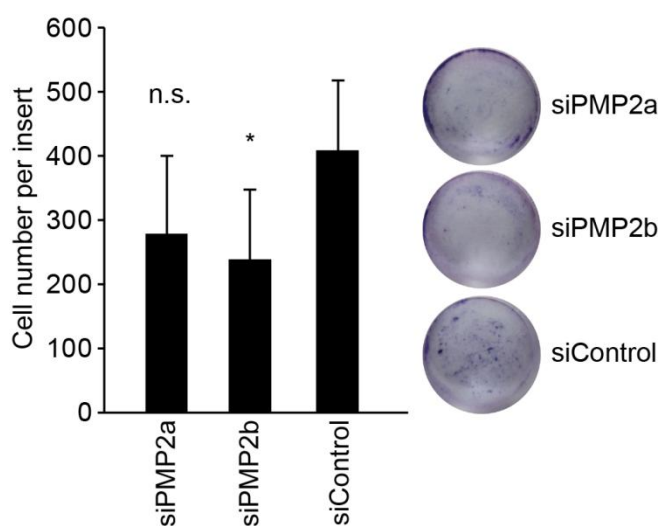


Figure 52: Matrigel invasion assay after PMP2 inhibition.

WM278 cells were subjected to Matrigel invasion assays 72 hours after transfection with siPMP2a, siPMP2b, or siControl. Quantification of invaded cells is shown as mean \pm SD of 7 independent experiments. Invasion was significantly decreased after inhibition with siPMP2b (one-way ANOVA versus siControl; $*P < 0.05$). Representative stained membranes after Matrigel invasion assay are shown.

To analyze a contribution of PMP2 in SOX10-mediated cell invasion, WM278 were stably transfected with a vector for PMP2 overexpression (pLenti-PMP2) and a control vector (pLenti-Control), both containing a puromycin resistance gene as selection marker. SOX10 was inhibited in these cells by siRNA transfection (Figure 53 a). While SOX10 inhibition reduced PMP2 expression in control cells, it did not affect PMP2 expression in the stably overexpressing cells. These cells were subjected to Matrigel invasion assays 24 hours after siRNA transfection (Figure 53 b). SOX10 inhibition significantly reduced invasion of the cells through the Matrigel layer as shown before (section 4.3.3, Figure 21) and this effect was observed in the control as well as in the PMP2-overexpressing cells.

Furthermore, the invasion capacity of PMP2-overexpressing cells was significantly increased compared to control cells. However, overexpression of PMP2 in SOX10-inhibited cells could not significantly increase the invasion compared to SOX10-inhibited control cells, although no significant change in invasion was found compared to cells transfected with the control siRNA and control vector. PMP2 overexpression had no impact on cell viability in this assay (Figure 53 c).

Thus, although PMP2 overexpression seems to enhance cell invasion, a direct effect of PMP2 on SOX10-mediated melanoma cell invasion could not be demonstrated.

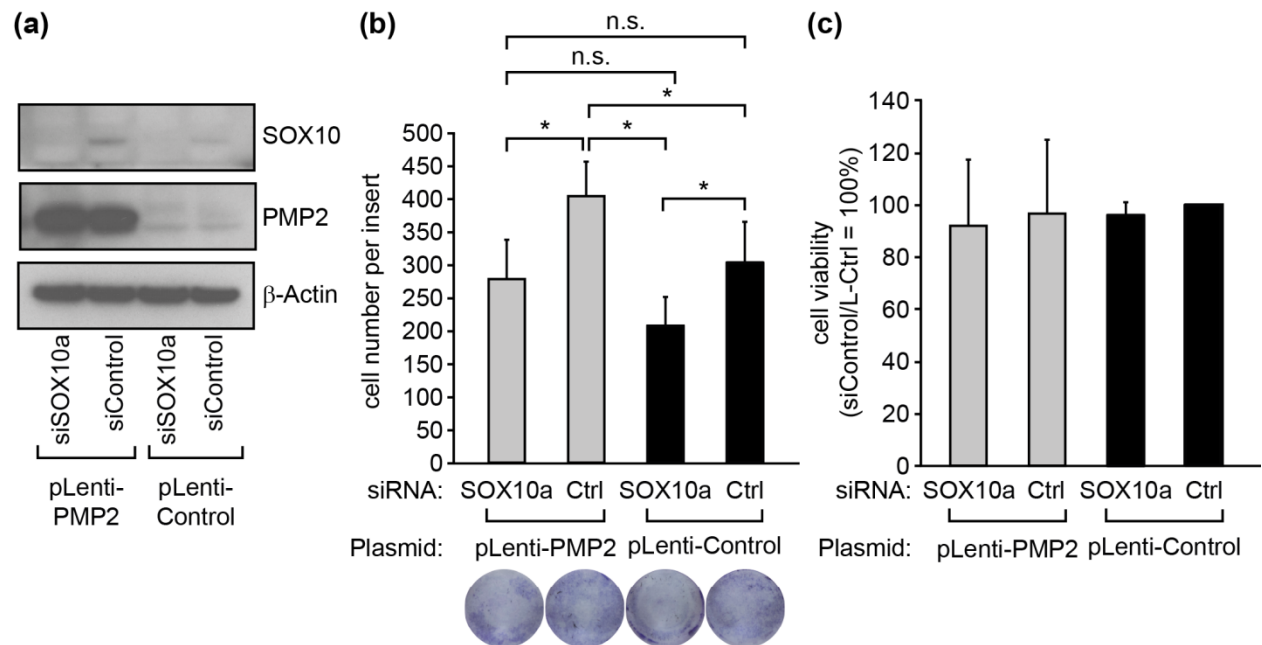


Figure 53: Invasion and cell viability of PMP2-overexpressing melanoma cells after SOX10 inhibition.

WM278 cells were transfected with vectors for stable overexpression of PMP (pLenti-PMP2) and a control vector (pLenti-control), selected with puromycin, and grown till complete confluence. **(a)** Twenty-four hours after transfection of siSOX10a or siControl (siCtrl), SOX10, PMP2, and β -Actin (loading control) were detected by immunoblotting. **(b)** Cells described in (a) were subjected to Matrigel invasion assays. Invaded cells per well are depicted as mean \pm SD of five independent experiments. SOX10 inhibition significantly decreased cell invasion in pLenti-PMP2 and pLenti-Control cells, while PMP2 overexpression significantly increased invasion compared to control cells ($*P < 0.05$, *t*-test). However, PMP2 overexpression could not significantly increase melanoma cell invasion in SOX10-inhibited cells compared to control cells transfected with siSOX10a or siControl ($P > 0.05$, *t*-test). Representative stained membranes after Matrigel invasion assay are shown below. **(c)** Cell viability of cells described in (a) is depicted.

4.9.2.4 Effects of PMP2 overexpression on melanoma cell invasion

To further investigate the influence of PMP2 on melanoma cell migration and invasion, experiments with PMP2 stable overexpression in a PMP2-negative melanoma cell line (WM3211) was carried out with vectors containing a puromycin resistance gene for selection.

In order to specify the PMP2 functions in melanoma cells, mutated variants of PMP2 were generated. A mutation of PMP2 at position 27 (L27D) prevents its binding to the cell membrane as demonstrated by Ruskamo et al. [219]. Furthermore, the three protein

residues that were shown to bind fatty acids [168] were mutated to R106E, R126E, Y128F and this mutant has been further on called Mut3.

Analysis of mRNA expression after stable transfection of pLenti-PMP2, pLenti-PMP2 L27D, and pLenti-PMP2 Mut3 in WM3211 cells demonstrated high expression levels of all PMP2 variants compared to cells stably transfected with a control plasmid (pLenti-Control) or non-transfected cells (Figure 54). However, on protein level only the PMP2 wild type- and the L27D mutant-variants could be detected. Apparently, the Mut3 mutation resulted missing PMP2 protein translation or protein degradation.

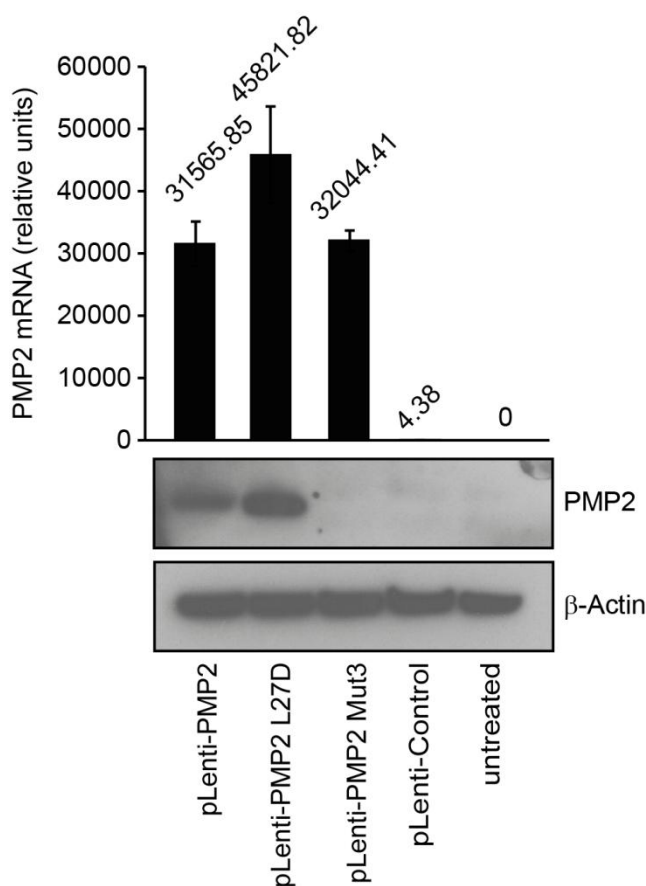


Figure 54: Stable expression of PMP2 wild type and mutants in cell line WM3211.

The PMP2-negative cell line WM3211 was transfected with vectors for stable overexpression of PMP2 (pLenti-PMP2), the L27D mutant (pLenti-PMP2 L27D), and the Mut3 mutant (pLenti-PMP2 Mut3) as well as a control vector (pLenti-Control). Cells were selected with puromycin and grown till complete confluence. PMP2 expression was assessed in these cells as well as in untreated WM3211 cells on mRNA (mean \pm SD of three independent experiments) and protein level. Expression of mRNA compared to protein shows that PMP2 or the L27D mutant of PMP2 were highly expressed while only mRNA expression could be detected for the Mut3 mutant. Numbers above the bars display mean mRNA values.

Stably overexpressing PMP2 wild type, L27D, Mut3, control and untreated WM3211 cells were subjected to spheroid assays. Quantification of the invasion areas of the different cells showed significantly increased invasion of PMP2- and PMP2 L27D mutant-overexpressing cells compared to the PMP2 Mut3 mutant-overexpressing and control cells up to 4- or 2.5-fold, respectively (Figure 55 a). Representative pictures of spheroid assays with staining of calcein AM and EthD-1 are shown in Figure 55 b. No differences in staining of living and dead cells in the different groups were found.

In conclusion, PMP2 overexpression promotes melanoma cell invasion.

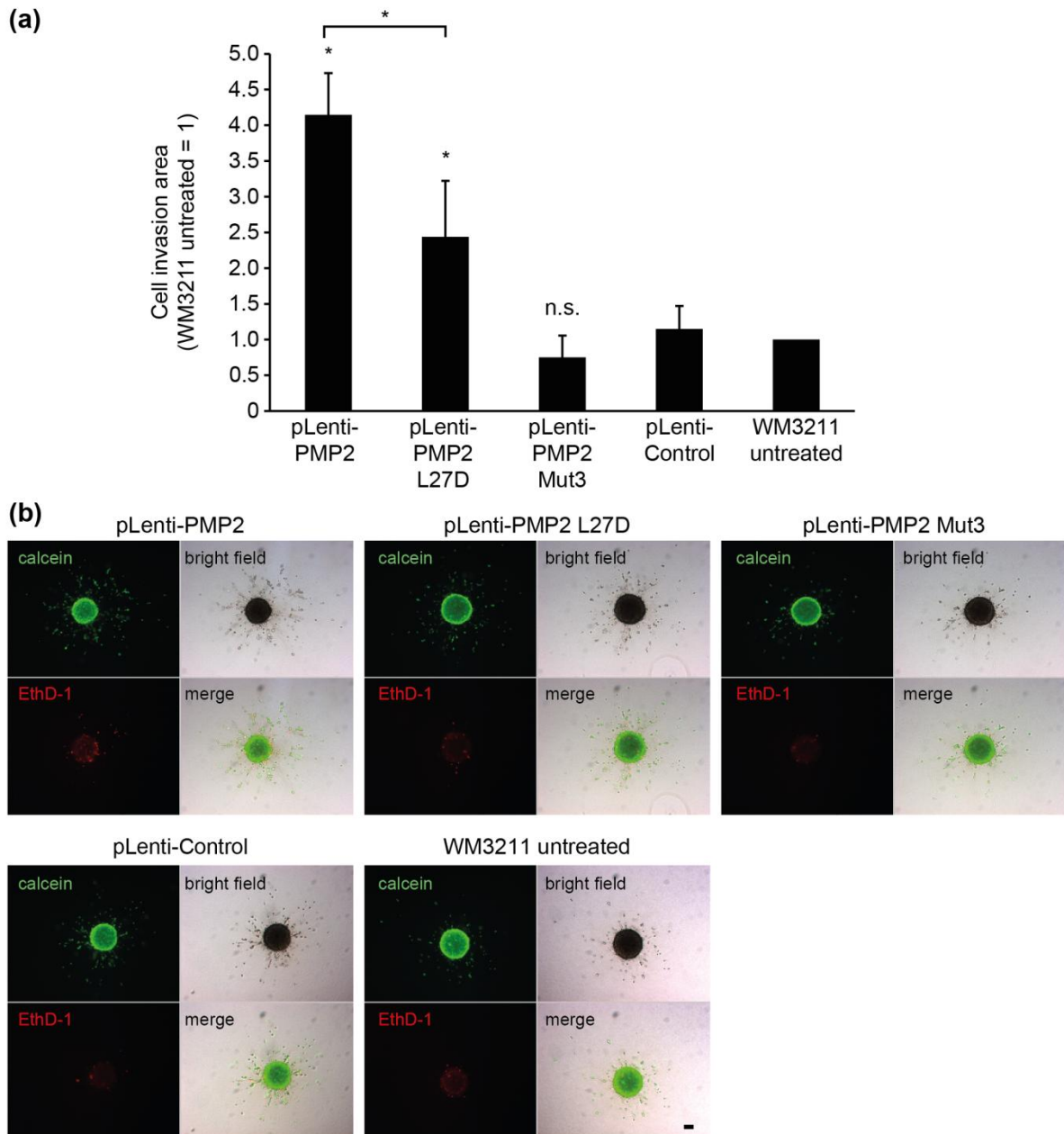


Figure 55: A three-dimensional invasion assay with PMP2 wild type- and mutant-overexpressing WM3211 melanoma cells.

WM3211 cells were stably transfected with vectors for overexpression of PMP2 (pLenti-PMP2) or the mutated forms L27D (pLenti-PMP2 L27D) and Mut3 (pLenti-PMP2 Mut3) as well a control vector (pLenti-Control). Together with untreated WM3211 cells, these cells were subjected to a three-dimensional spheroid assay. **(a)** The invasion area was determined 96 hours after cultivation on agar-coated wells and 48 hours after embedding in collagen. The invasion area of untreated WM3211 cells was set to 1. Bars show mean \pm SD of five independent experiments with 2 to 4 technical replicates each. Invasion area of PMP2 wild type- and PMP2 L27D-expressing cells was significantly increased compared to pLenti-Control transfected cells (one-way ANOVA versus siControl, $*P < 0.0001$). Invasion of PMP2 wild type-expressing cells was significantly increased compared to PMP2 L27D-expressing cells ($*P = 0.0027$; *t*-test). **(b)** Representative pictures after LIVE/DEAD staining and fluorescence microscopy are shown. Scale bar = 100 μ m.

4.10 Analysis of further SOX10 target genes

SOX10 is essential at multiple stages of Schwann cell development as for their differentiation from NCCs and for the entry into promyelinating and myelinating stages [31], [69]. The transcriptional regulation of myelination includes several genes that are not only the major myelin genes, but also genes for lipid biosynthesis and genes that control cell cycle exit [263]. It is possible that these genes also display analogous functions in other cell types. Therefore, genes that are regulated by SOX10 in Schwann cells might be also involved in melanoma cell physiology.

The regulation of the epidermal growth factor receptor ERBB3, which is essential for Schwann cell development and maintenance [33], by SOX10 in melanoma cells has already been shown in section 4.5.

EGR2 has already been described as a common coregulator and also as a target gene of SOX10 in Schwann cells [82], [122], [211], [251], [258]. Cooperative regulation of PMP2 by EGR2 and SOX10 in melanoma cells has been verified in this study (section 4.8.3). Results shown in Figure 44 indicated that SOX10 inhibition influences EGR2 expression in cell line WM278. Considerably reduced mRNA expression of EGR2 after SOX10 inhibition was found in cell lines WM278 and WM1232 (Figure 56 b) and to a lesser extend in 1205Lu (Figure 56 c).

A coordinated and balanced interaction between SOX10 and EDNRB is required for enterous nervous system and melanocyte development [253], [306]. Furthermore, it has been shown that SOX10 regulates EDNRB in human melanocytes [303]. A complex relationship between EDNRB and neurofibromin, which is mutated in neurofibromatosis type 1, has been suggested [58]. Neurofibromatosis type 1 is characterized by the development of Schwann cell-based tumors and skin hyper-pigmentation. Moreover, altered expression of EDNRB is related to brain metastases in patients and increases melanoma cell proliferation and spontaneous metastasis in the central nervous system [55]. It further seems to be specifically required for the final differentiation step of melanocytes but also for de-differentiation of mature melanocytes as well as for melanoma progression, survival and metastasis [220]. Downregulation of EDNRB was found in all three investigated melanoma cell lines after SOX10 inhibition (Figure 56 a-c, right panel). In conclusion, SOX10 regulation of genes that are critical in Schwann cell development and homeostasis as well as in other cell types of the nervous system can be found in melanoma cells and seems to be critical for melanoma cell physiology.

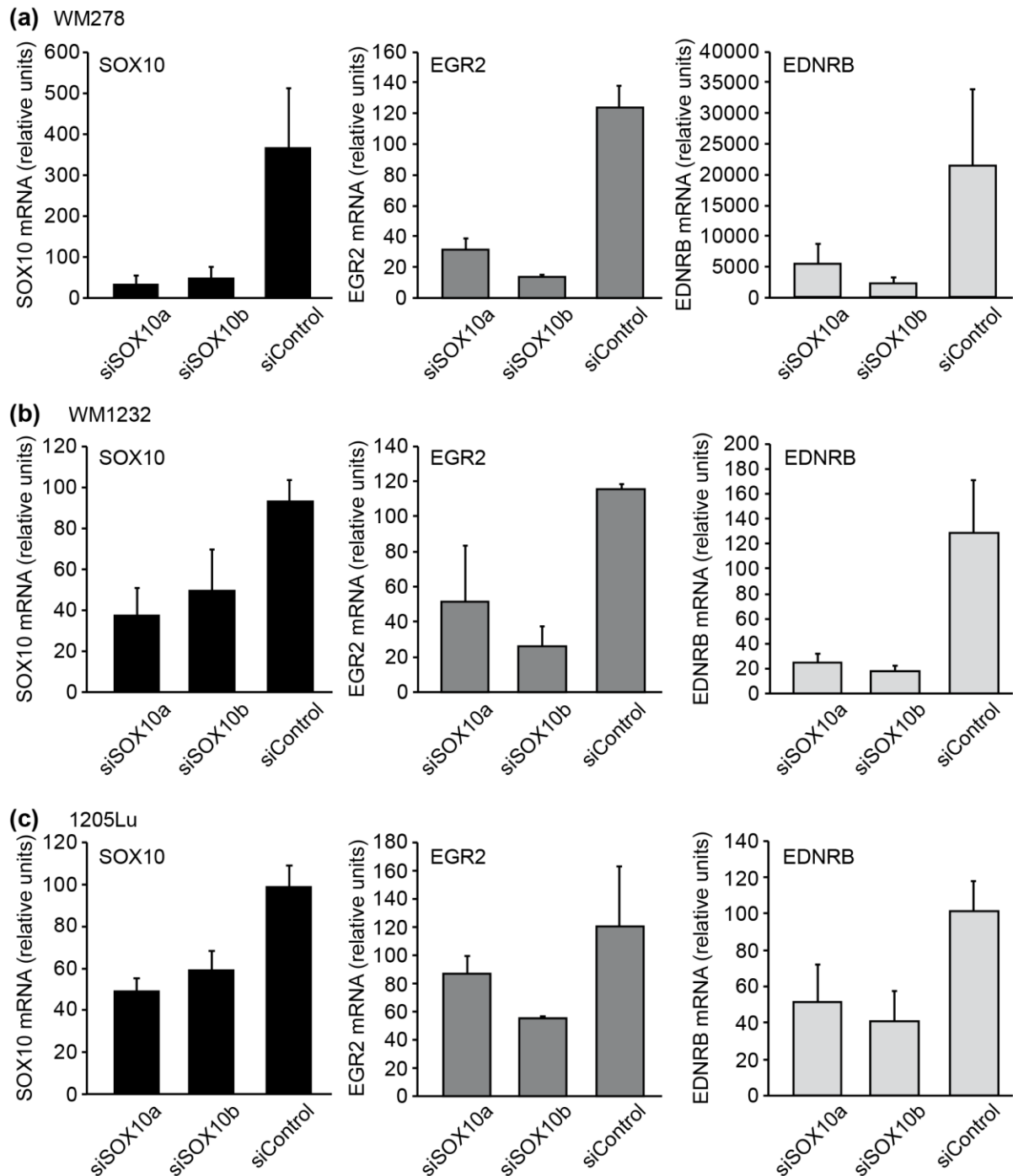


Figure 56: Expression of EGR2 and EDNRB after SOX10 inhibition in melanoma cells.

SOX10, EGR2, and EDNRB expression was assessed on mRNA level 48 hours after transfection of siSOX10a, siSOX10b, or siControl in WM278 (a), WM1232 (b), and 1205Lu (c) in three independent experiments (mean \pm SD). Downregulation of EDNRB mRNA was found in all SOX10-inhibited melanoma cells while strong downregulation of EGR2 was found in cell lines WM278 and WM1232 and to a lesser extent in cell line 1205Lu.

5 Discussion

Within recent years, the transcription factor SOX10 has been increasingly regarded to be an important player in melanoma and got into the focus of melanoma research by different groups. In this study SOX10 expression, functional, and binding studies have been performed to more deeply characterize the role of SOX10 in melanoma and led to the discovery of yet undescribed target genes.

5.1 Expression of SOX9 and SOX10 in human cell lines, tissues, and cancer

Expression of SOX10 as well as the closely related SoxE factor SOX9 were analyzed in fibroblasts, melanocytes and melanoma cells both from established and short term cultures. SOX10 expression was absent in fibroblasts while it was found expressed in melanocytes from three different donors, in 8 of 12 established melanoma cell lines, and in 2 of 7 short term-cultured melanoma cells (sections 4.1.1 and 0). SOX10 expression levels in melanocytes were considerably higher compared to melanoma cells and differed in melanoma cell lines. Moreover, SOX10 expression was more common in metastatic cell lines than in lines from primary tumors.

Notwithstanding, SOX9 expression varied throughout the different melanoma cell lines and was also detected in fibroblasts and melanocytes although in smaller amounts. In a subset of melanoma cell lines (8/12) SOX9 and SOX10 mRNA expression levels correlated inversely (section 4.1.1).

Cook et al. demonstrated that SOX10 is highly expressed in unpigmented melanocyte precursors (melanoblasts) and melanoma cells but downregulated in differentiated melanocytes *in vitro* although it seems to be transcriptionally active in all these cell types [52]. SOX10-positive IHC staining in melanocytes, benign nevi, giant congenital nevi as well as in primary and metastatic melanoma tissues was found in previous studies [4], [8], [49], [72], [176], [178], [188], [239], [243]. Broad SOX10 expression with varying protein levels in melanoma cell lines has been described before [52], [72], [173], [238].

Some studies showed that the intensity of SOX10 expression inversely correlates with the malignant potential of nevi, primary, invasive, and metastatic melanoma [4], [243]. In contrast, other groups found an increase of SOX10 expression from benign nevi to metastatic melanoma [8], [173], [238]. Moreover, strong SOX10 expression in melanoma tissues correlated with poor patient's prognosis [4], [49].

The inconsistent SOX10 expression data in melanocytes and melanoma cells may be caused by different culture conditions *in vitro* and usage of different antibodies *in situ*. Nevertheless, all data confirm that SOX10 is a marker of the melanocytic lineage and commonly expressed in melanoma.

According to the Human Protein Atlas (section 3.1.12), SOX10 protein is little expressed in the heart muscle, moderately expressed in the cerebral cortex, cerebellum, and soft tissue, while it is highly expressed in the salivary gland, hippocampus, lateral ventricle, and skin. In cancer tissues, distinct SOX10 nuclear immunoreactivity was observed in melanomas and gliomas. Elevated SOX10 expression was also found in frequently metastatic and aggressive breast cancers [62].

In general, SOX10 has been described as a sensitive and specific marker for Schwannian and melanocytic neoplasms as well as for peripheral nerve sheath tumors [176], [178], [188], [296]. Due to its widespread expression, SOX10 is not useful to differentiate between benign and malignant lesions in these tumors [178].

SOX9 has been detected in melanocytes *in vitro* and *in vivo* as well as in melanoma cell lines and melanoma tissues [8], [44], [52], [137], [194]. Shakhova et al. suggested that SOX9 acts as a repressor of SOX10 and its expression was absent in nevi and melanocytes as well as in SOX10-positive melanoma cells [238]. Cheng et al. found significantly elevated SOX9 expression levels in melanoma cell lines with an invasive phenotype and reduced levels in cell lines with a proliferative phenotype [44]. Furthermore, they described that strong SOX9 expression correlated with poor patient's prognosis *in vivo*. In contrast, Passeron et al. demonstrated that SOX9 is down-regulated in more aggressive melanomas and that SOX9 overexpression in melanoma cell lines inhibited tumorigenicity both in mice and in human *ex vivo* melanoma models [195]. Again, these differences might be caused by different model systems or antibody discrepancies. Problems with the specificity of SOX9 antibodies were described by Shakhova et al. [238] and in this study.

According to the Human Protein Atlas (section 3.1.12), nuclear SOX9 protein expression can be found in several tissues with the highest staining patterns in tissues of liver, pancreas, and the digestive tract, in prostate, seminal vesicle, uterine cervix, endometrium, fallopian tube, tonsil, thyroid gland, nasopharynx, bronchus, and skin. Cancer tissues displayed moderate to strong nuclear SOX9 staining with highest positive rates in breast, cervical, colorectal, head and neck, pancreatic, stomach cancer,

and glioma. A negative prognostic role of SOX9 was suggested in these cancer types as well as in urothelial and ovarian cancers [41], [158], [171], [182], [282], [283].

In IHC stainings, co-expression of SOX9 and SOX10 was found in nevi, primary melanomas, and metastases [8], [72]. Also some melanoma cell lines do express both SoxE transcription factors [52], [72]. In this study, co-expression of SOX9 and SOX10 was found in a subset of melanoma cell lines although the majority showed an inverse expression pattern for SOX9 and SOX10 (section 4.1.1). A mutual exclusive expression pattern for SOX9 and SOX10 in melanoma cell lines has also been shown in previous studies [44], [238] suggesting a negative cross-regulatory feedback loop between SOX9 and SOX10.

5.2 SOX9 and SOX10 inhibition in melanoma cells and mutual regulation

In this study SOX9 and SOX10 were inhibited via RNA interference. To control for possible off-target effects, two different siRNAs specifically targeting SOX9 or SOX10 were used. A control siRNA that does not interfere with the human transcriptome was included in the experiments. All SOX9- and SOX10-targeting siRNAs effectively inhibited SOX9 or SOX10, respectively (section 4.2). Furthermore, SOX10 mRNA levels were found down-regulated by SOX9 inhibition, while SOX9 mRNA levels slightly increased upon SOX10 inhibition. On protein level, both SOX9 and SOX10 were found downregulated by SOX10 or SOX9 inhibition, and vice versa. These data indicate that SOX9 might influence SOX10 on a transcriptional level and SOX10 might influence SOX9 on a post-transcriptional level.

Previous studies in chick, xenopus, and zebrafish suggested that the most important contribution of SOX9 during embryonic development is its ability to induce SOX10 expression in the neural crest in general and specifically in melanocytes and ocular glands [5], [45]–[47], [301].

However, a recent study by Shakhova et al. has shown that SOX9 and SOX10 are functional antagonistic regulators of melanoma development [238]. Next to opposing expression of these two factors, Shakhova et al. found downregulation of SOX10 by SOX9 overexpression and increase of SOX9 by SOX10 knockdown in melanoma cells. Furthermore, SOX9 overexpression led to cell cycle arrest, apoptosis, and a gene expression profile shared by melanoma cells with reduced SOX10 expression [238]. In addition, it has been shown that in SOX10-deficient mice, deletion of SOX9 rescued the hypopigmentation phenotype. On molecular level, they found SOX9 binding at the

SOX10 promoter, generating a negative feedback loop. Thus, Shakhova et al. hypothesize that SOX9 is not required for normal melanocyte stem cell function, the formation of hyperplastic lesions, and melanoma initiation but rather plays an anti-tumorigenic role in melanocytes. These data are consistent with a previous study [195]. However, SOX9 was reduced by SOX10 inhibition in the present study (section 4.2). Moreover, SOX10 was not downregulated by SOX9 overexpression and SOX10 overexpression did not affect SOX9 levels (section 4.6, Figure 36). These differences may be attributed to the heterogeneity of melanoma cell lines or different expression levels investigated in these specific settings.

In contrast to the hypothesis that SOX9 and SOX10 may function oppositionally, redundant functions in gene regulation of both factors have been described in melanoma cells and oligodendrocyte precursors [70], [72]. Furthermore, SOX9 - just as SOX10 - is able to regulate MITF, DCT, and tyrosinase expression in neonatal and adult melanocytes [194]. The analysis of several enhancers regulating SOX10 expression in neural crest derivatives indicated that spatial and temporal control of SOX10 is induced and maintained by SOX9 and SOX10 in a regulatory loop [292].

In conclusion, the impact of SOX9 on SOX10 expression in melanoma and vice versa is not clear. Previous and current data point to a mutual regulation of both transcription factors. Probably, both factors can act together or have distinct roles in gene regulation, depending on the cellular context.

In general, oncogenic functions in melanoma have been more related to SOX10 than to SOX9 as SOX10 has been suggested to be required for melanoma initiation, formation, and progression as well as for melanoma cell survival [53], [239].

5.3 Influence of SOX10 on melanoma cell survival and cell death

Results of this study demonstrate that SOX10 inhibition in different melanoma cell lines leads to G1 cell cycle arrest, considerably decreases cell viability, and induces cell death (sections 4.3.1 and 4.3.2). Enhanced activation of effector caspase 3 as well as decrease of anti-apoptotic Bcl-2 and increase of pro-apoptotic Bak and Bax in SOX10-inhibited cells indicated an onset of intrinsic apoptosis after SOX10 inhibition. Moreover, SOX10 inhibition caused DNA damage.

An essential role of SOX10 in melanoma cell proliferation and survival has been described before [53], [239]. Both studies observed a cell cycle arrest in G1 by SOX10 inhibition in different melanoma cell lines with similar kinetics compared to the present

study. Cronin et al. suggested that the G1 arrest upon SOX10 inhibition seems not to be related to p53 but rather mediated through RB-E2F transcription factor 1 signaling [53]. Like in the present study, Cronin et al. detected a decrease in phospho-RB and an increase in p21 after SOX10 inhibition, though in that study cell cycle arrest after SOX10 inhibition resulted in cell senescence but not apoptosis.

Comparable to the present study, Shakhova et al. observed apoptosis and increased caspase 3 activation upon SOX10 inhibition in melanoma cells as well as an upregulation of apoptotic and mesectodermal differentiation gene clusters [239].

Furthermore, studies that analyzed mutations in the *SOX10* gene in primary and metastatic melanoma samples found only low mutation frequencies suggesting that melanoma cells favor the retention of SOX10 wild type functions [53], [54], [110]. Sequencing of cDNA from the three cell lines (WM278, WM1232, and 1205Lu) used for SOX10 functional investigations in this study has been performed. Only one silent mutation (position 927 according to translation start site, T → C, both encoding histidine) was found in cell line 1205Lu.

All these data highlight a pivotal role of SOX10 in melanoma cell survival and proliferation. Likewise, SOX10 mutations cause apoptosis in NCCs leading to severe developmental defects as hypopigmentation, hearing deficits, aganglionosis, myelinopathies, and block generation of non-neuronal glial cells [64], [116], [125], [246]–[248]. Therefore, SOX10 seems to be a general pro-survival factor for NCC derivatives and melanoma cells.

5.4 Influence of SOX10 on melanoma cell invasion

Expression of SOX10 during embryonic development, which is initiated after emigration of NCCs from the neural tube, lasts during their migration along the dorsolateral pathway. This indicates a specific role of SOX10 in migration and invasion. Previous studies with mouse and zebrafish models indicated that SOX10 mediates enteric NCC adhesion and migration as well as the migration of oligodendrocyte and melanocyte precursors [64], [65], [70], [125], [248], [253], [286].

As the inhibition of SOX10 impaired the proper formation of melanoma spheroids (section 4.3.3, Figure 22 and chapter 7, Figure S3), the influence of SOX10 on integrin expression of various α - and β -subunits has been examined. Integrins of the α - and β -subunits form heterodimers and the different subsets are responsible for establishing cell-cell- and cell-matrix-contacts.

A synergistic interaction of SOX10 with ITGB1, which controls enteric NCC migration, has been shown before [286]. A considerable decrease of ITGA4 and ITGB3 was found in cell line WM278 after SOX10 inhibition, while ITGA3 and ITGB1 were upregulated in all three analyzed cell lines (chapter 7, Figure S2). Dysregulation of single integrin subunits in comparison between melanoma cells and melanocytes was found in different studies and, e.g., the alpha V beta 3 variant was shown to strongly support melanoma metastasis [67], [141]. Therefore, it is possible that altered integrin expression contributes to the reduced cell-cell adhesion and migratory phenotype after SOX10 inhibition.

Furthermore, SOX10 was shown to directly regulate the gap junction proteins connexin 32 [21] and connexin 47 [229] in oligodendrocytes. Therefore, it seems that SOX10 is able to regulate gap junction proteins, which might be also relevant for the melanoma spheroid formation. However, expression of connexin 32 and connexin 47 in melanoma cells has not been found in this study (data not shown).

According to LIVE/DEAD staining, the early impaired spheroid formation of SOX10-inhibited melanoma cells seems not to be caused by increased cell death (chapter 7, Figure S3).

An influence of SOX10 on melanoma cell migration has been suggested previously [4], [235]. Migration-examining experiments have been performed in transwell assays against a nutrition gradient or conditioned medium. Agnarsdóttir et al. found both an increased (WM793) and a decreased (WM115) melanoma cell migration capacity upon SOX10 inhibition via siRNA [4] while Seong et al. demonstrated a 75% decrease in migration in murine B16 melanoma cells [235]. In the present study, reduced invasion capacity upon SOX10 inhibition was found in all investigated human melanoma cell lines in a Matrigel invasion assay (section 4.3.3, Figure 21). The range was similar as described by Seong et al., with up to 75% non-invading melanoma cells [235]. The onset of impaired cell invasion occurred at an earlier time point than the onset of cell death after SOX10 inhibition *in vitro*. Moreover, blocking cell death did not affect the reduced invasion capacity upon SOX10 inhibition (chapter 7, Figure S3).

Reduced invasiveness into the surrounding host tissue was also observed in a chick embryo model in this study (section 4.3.3, Figure 23). Tumor sizes and proliferative activity did not differ between SOX10-inhibited and control melanoma nodules. This sustained survival as opposed to the *in vitro* data may be caused by the chick

microenvironment, with embryonic growth factors counteracting cell cycle arrest and apoptosis.

Moreover, Matrigel invasion and cell viability experiments with transient transfection of vectors for SOX9 and SOX10 overexpression in cell lines WM3211, WM1366 (SOX10 negative), and 1205Lu (moderate SOX10 expression) indicated that significantly increased melanoma cell invasion was specifically related to SOX10 but not SOX9 overexpression (section 4.6). These findings were also supported by a three-dimensional invasion model. Cell viability has not been considerably influenced by SOX9 or SOX10 overexpression. In the end, results mentioned above provide evidence for a pivotal role of SOX10 in melanoma cell invasion.

Hoek et al. found SOX10 to be highly expressed in proliferative and weakly in metastatic melanoma cells [112]. They described three cohorts of melanoma cell lines: cohort A characterized by highly proliferative and weakly metastatic potential, cohort B by moderate proliferative and metastatic potential, and cohort C by weakly proliferative and highly metastatic potential. SOX10 was found to be highly expressed in cohort A while it was downregulated in cohort C. The cell lines WM239A (cohort A), WM35 (cohort B), WM278, WM3211, WM1366, WM793, and 1205Lu (cohort C), respectively, have also been investigated in this study. Moderate and high SOX10 expression levels were found in WM239A and WM35, respectively (section 4.1.1). In contrast, SOX10 was highly expressed in WM278 and WM793, moderately in 1205Lu, and not at all expressed in WM3211 and WM1366. Also other studies associated SOX10 expression with a proliferative but non-invasive melanoma cell phenotype [44], [238]. Notwithstanding, the correlation of high SOX10 expression with a highly proliferative and weak metastatic potential as well as low SOX10 expression with a low proliferative and highly metastatic potential could not be reproduced in this study.

5.5 Target genes of SOX10

5.5.1 Previously identified SOX10 target genes

Several known target genes of SOX10 have been described that are related to survival and migration of NCCs and melanoma cells. Regulation of the key transcription factor for melanocyte specification MITF by SOX10 has been intensively studied before, demonstrating direct binding of SOX10 to the M-MITF promoter and an enhancer element [22], [152], [200], [206], [275], [285]. Together, SOX10 and MITF cooperate in

activating genes for melanogenesis [164], [207] and the MET promoter in melanoma [173], which drives migration, invasion, resistance to apoptosis, and tumor cell growth. The role of MITF in the melanocyte lineage extends well beyond promoting melanoblast survival. It controls expression of differentiation-associated genes required for melanosome biogenesis and intracellular transport [43], as well as metabolism [99], and also suppresses melanoma senescence [84]. Importantly, MITF plays both a positive and negative role in cell proliferation, with the pro-proliferative activity of MITF causing it to be termed a lineage-survival oncogene [80]. This paradox may be explained by the rheostat model [39]. On the one hand, low levels of functional MITF promote G1 arrest in melanocyte stem cells or invasiveness in melanoma stem-like cells. On the other hand, high MITF expression promotes proliferation, or at elevated levels, a G1 arrest associated with differentiation. Therefore, proliferation is blocked when MITF activity is too high or too low, and cell division is stimulated at a specific MITF expression level. The rheostat model for MITF functions is useful for the prediction that up- or downregulation of MITF expression could promote switching between phenotypic states that are important for melanocyte development and melanoma: invasive and stem-like, proliferative, and differentiated [111]. Similarly, it is possible that the effect of SOX10 on melanocyte survival and differentiation as well as on melanoma initiation and progression is dependent on its cellular level. In this study, levels of SOX10 expression were found to be significantly increased in melanocytes compared to melanoma cell lines (section 4.1.1, Figure 6).

The epidermal growth factor receptor ERBB3 has been shown to be required for the development of NCCs and derivatives such as Schwann cells [33]. Furthermore, it has been demonstrated that ERBB3 is also relevant for Schwann cell and melanoma proliferation and migration [11], [37], [166]. SOX10 is a key regulator in differentiation of peripheral glia cells. It regulates ERBB3 and binds to an ERBB3 enhancer element [31], [36], [208]. Both SOX10 and ERBB3 were found to be highly expressed in pilocytic astrocytomas and radiation-induced glioblastomas, suggesting that SOX10-mediated overexpression of ERBB3 may drive growth in these tumors [3], [60].

Downregulation of M-MITF and ERBB3 upon SOX10 inhibition and co-expression of SOX10 and MITF as well as SOX10 and ERBB3 were found in most investigated human melanoma cell lines and in all investigated human melanocytes in this study (section 4.5).

Therefore, several known target genes of SOX10 might be critical for SOX10 functions in melanoma survival and invasion. However, in SOX10 transiently overexpressing melanoma cell lines, no increase of M-MITF or ERBB3 expression could be detected (section 4.6, Figure 36).

5.5.2 Melanoma inhibitory activity (MIA)

SOX10 executes ERBB3- and MITF-independent functions, for instance in the melanocyte lineage and in melanoma cells [31], [53]. To examine potential target genes that might mediate the effect of SOX10 on melanoma cell invasion, genes that are migration-related and expressed in melanoma cells but not in melanocytes got into focus of this study. Literature research pointed to the secreted protein MIA, which is relevant for melanoma cell migration [205]. On a cellular level, MIA is secreted at the rear pole of migrating melanoma cells and directly interacts with cell adhesion receptors (integrins) and extracellular matrix molecules (fibronectins) promoting cell migration and invasion [10], [28], [254]. According to the Human Protein Atlas (section 3.1.12), MIA expression on protein level was found in a variety of tissues while high expression in cancers was only found in melanoma. MIA is an established melanoma marker and correlates with melanoma progression *in vivo*, although it is absent in melanocytes [26], [198]. MIA, also known as cartilage-derived retinoic acid-sensitive protein, is not only crucial for melanoma cell migration but also for chondrogenesis and it has been shown to be regulated by SOX9 in chondrocytes [299]. Data of this study revealed that SOX9 but also SOX10 inhibition can reduce MIA expression in melanoma cell lines (section 4.4.1, Figure 24). However, expression data clearly demonstrate a co-expression of SOX10 and MIA but not with SOX9 in melanoma cells on mRNA and protein level. Confirming previous publications MIA was not expressed in melanocytes from different donors in this study. Together, these data indicate a relevant function of SOX10 but not of SOX9 for MIA expression in melanoma cells.

As SOX10 but not MIA is abundantly expressed in melanocytes, binding of transcriptional repressors at the MIA promoter in melanocytes or the presence of specific coregulators of SOX10 in melanoma cells might contribute to lineage-specific MIA expression. *In silico* binding motive analyses suggested combinatory binding of SOX10 and PAX6, NFκB, or EGR2 at the *MIA* promoter or upstream and downstream regions (section 4.4.3, Figure 31). While no MIA regulation was found for the NFκB subunit p65 or EGR2, PAX6 inhibition was able to reduce MIA expression and promoter

activity. However, no increase in promoter activity was found upon PAX6 overexpression and combined overexpression of PAX6 and SOX10 could not further enhance MIA promoter activity compared to SOX10 overexpression alone, excluding PAX6 as a coactivator of SOX10 in *MIA* promoter regulation.

The transcription factors NFκB and HMG1 were described as activators of MIA in a previous study [203]. However, no correlation of the NFκB subunit p65 or HMG1 and MIA expression were found in melanoma cells (section 4.4.1, Figure 25).

The transcriptional repressor CtBP1 was suggested to be critical for MIA repression in melanocytes [204]. Indeed, significantly higher expression of CtBP1 was found in melanocytes compared to melanoma cells in this study, suggesting that absent expression of MIA in melanocytes might be mediated by enhanced expression and promoter binding of CtBP1 (section 4.4.3).

Moreover, it is possible that epigenetic changes in melanocytes and melanoma cells may have an impact on lineage-specific MIA expression. Altered SOX10 binding to melanocyte promoter regions has already been related to epigenetic differences [75]. No CpG islands were identified when analyzing the *MIA* promoter region as well as 1105 bp before the promoter start site and 530 bp after the start ATG using different algorithms (EMBOSS CpGplot and CpG Island searcher, section 3.1.12; parameters: observed GpC/expected GpC > 0.65, percentage GC > 55%, length > 200, and distance to next island > 100 bp), excluding DNA methylation but not histone acetylation/deacetylation from epigenetically *MIA* promoter regulation.

Taken together, these data suggest that absence of MIA in melanocytes, even though SOX10 is highly expressed, might be related to the presence of transcriptional repressors.

Early downregulation of MIA expression by SOX10 inhibition suggested a direct regulation of MIA by SOX10. Direct binding of SOX10 to a specific *MIA* promoter region was shown by reporter and ChIP assays (section 4.4.2). Moreover, two adjacent SOX binding sequences were identified that were crucial for *MIA* full-length promoter activity and seemed to be bound by SOX10 in a multimeric pattern. SoxE proteins are monomers in solution but they can form dimers by binding to sites on DNA in close proximity [289]. In case of SOX10, dimeric binding to such adjacent sites in the *MPZ* promoter has been shown to be important for the transcriptional function of SOX10 [228].

Interestingly, SOX9 seems to activate the same SOX consensus site in the *cartilage-derived retinoic acid-sensitive protein* promoter, which is equivalent to the SOX10 binding site in the *MIA* promoter (binding site J9) [299]. Therefore, this might represent a common binding site for SOX9 and SOX10.

When comparing results of the *MIA* promoter deletion constructs with the mutational analyses (section 4.4.2, Figure 27), it is obvious that deletion constructs shorter than 275 bp retained SOX10 responsiveness, although potential SOX binding sites within this area (sites G1/G2, J5, G3/J6) turned out to be not relevant for *MIA* promoter activity. Previous studies revealed a most active cis-regulatory element between -210 and -181 bp that activates transcription specifically in malignant but not in benign melanocytes [86]. This element contains a highly conserved region in comparison of the human and the murine promoter. Thus, it is possible that other, still unknown, transcription factors regulated by SOX10 alter *MIA* expression by binding to this area.

As a consequence, SOX10 may regulate *MIA* directly as well as indirectly by regulation of factors that bind to the proximal *MIA* promoter region.

SOX10-dependent upregulation of *MIA* was only found in the *MIA*-positive melanoma cell line 1205Lu but not in the *MIA*-negative cell lines WM3211 and WM1366 (section 4.6, Figure 36). As no increased expression of CtBP1 was found in WM3211 and WM1366 (section 4.4.3, Figure 30), it is possible that other repressors or missing coactivators can prohibit *MIA* expression in these melanoma cell lines. An elegant strategy to identify such coregulators of SOX10 in melanocytes and melanoma cells would be a co-immunoprecipitation with SOX10-specific and control antibodies followed by quantitative mass spectrometry. However, this approach has not been further pursued as the focus of this study was to discover further SOX10 target genes in melanoma.

The importance of *MIA* in mediating the pro-invasive effect of SOX10 was demonstrated in a rescue experiment (section 4.4.4). Here, *MIA* overexpression in SOX10-inhibited melanoma cells restored the invasion capacity of these cells. However, invasion was not increased by *MIA* overexpression in control cells with high endogenous *MIA* levels. It is likely that extensive amounts of *MIA* may even reverse its the pro-invasive effects, possibly by inhibiting adhesion as shown previously upon exposure to exogenous *MIA in vitro* [17] or by reducing cell viability, which is indicated in Figure 33 section 4.4.4.

Thus, the results of this study suggest that activation of *MIA* by SOX10 is a crucial event in melanoma progression. Reduced migration in B16 melanoma cells has been

attributed to known SOX10 target genes, such as MITF or MC1R [235]. Both have been shown to independently regulate melanoma cell migration but the direct correlation to SOX10 is missing and MITF has not been found upregulated in cell lines where SOX10 overexpression enhanced the invasive capacity in this study (section 4.6). Notwithstanding, as MIA overexpression in SOX10-inhibited melanoma cells did not completely restore their invasion capacity (section 4.4.4, Figure 32) the involvement of further SOX10 target genes cannot be excluded.

5.5.3 Peripheral myelin protein 2 (PMP2)

An elegant and novel tool to characterize gene expression at a specific time-point is RNA sequencing also termed whole transcriptome shotgun sequencing. It is a next generation sequencing method in which mRNA of tissues or cells in specific states is purified, reverse transcribed in cDNA, and used for library generation including specific bar labeling. With these labels several transcriptomes can be analyzed in one sequencing cycle. In this study, sequencing was performed with the Illumina Genome Analyzer IIx. Two rounds of RNA sequencing were performed, one without and one including DNA digestion after mRNA purification. The analysis was performed with SOX10 overexpressing and control 1205Lu cells in biological triplicates. The significantly regulated genes by SOX10 overexpression were KLF10, NR1D1, H1FX-AS1, PPP1R15A, PMP2, TIPARP, FTL, RPL27A, and GH1 (section 4.7). Some of these factors, i.e., KLF10, NR1D1, PPP1R15A, and TIPARP have been related to malignancies before [87], [135], [260], [284].

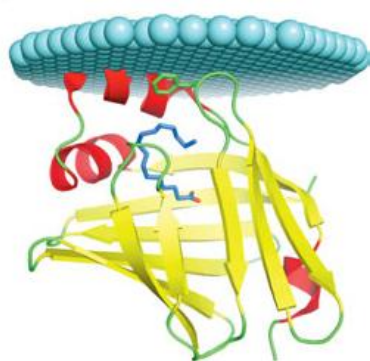


Figure 57: Structure of PMP2 predicted using the Orientation of Proteins in Membranes server according to Han et al. [96].

As generally regulated factors should be identified, the expression of these genes was analyzed in three different melanoma cell lines after SOX10 overexpression or control transfection by qRT-PCR. Comparing the log₂-fold changes, the patterns of mRNA expression were most similar comparing SOX10 and PMP2 (section 4.7, Figure 38 and Figure 39). PMP2 expression was substantially increased in SOX10-overexpressing cells.

PMP2 is a small (14.9 kDa) fatty acid binding protein (FABP) that is predominantly present in the peripheral nervous system's myelin sheath and is necessary for its composition [104], [105]. It is a candidate autoantigene in

the peripheral autoimmune neuropathy Guillain Barré syndrome [170]. Its structure forms a compact 10-stranded up-and-down β -barrel that can encapsulate a fatty acid molecule [123]. A predicted structure of PMP2 is shown in Figure 57. The helical lid segment of PMP2 is partially embedded in the membrane and another membrane-binding site was suggested to be on the opposite site of the protein.

The myelin sheath is a unique biological membrane that is essential for the development and function of the vertebrate nervous system. It contributes to a 100-fold amplification of the nerve impulse along the axon by acting as an isolator and by directing the localization of neuronal ion channels to the nodes of Ranvier. The myelination process includes a myelinating glial cell that wraps its differentiated plasma membrane dozens of times tightly around selected axons. This process requires coordinated membrane synthesis, compaction, and maintenance. Myelin-specific proteins play a central role in all these processes and are highly abundant in the myelin sheath [96]. Many of them are cell adhesion molecules of the immunoglobulin family type I transmembrane proteins, such as MPZ. These proteins can mediate extracellular interactions between the successive layers of myelin and the neuronal plasma membrane. MBP and PMP2 are the only two non-transmembrane proteins that are present in high abundance in the region of compact myelin. They are both positively charged and this biochemical property facilitates their binding to the negatively charged inner leaflet of the myelin membrane. Both are localized at the cytoplasmic position of two consecutive layers of the myelin membrane and were shown to act synergistically in the compaction and maintenance of the multilayered myelin membrane [262]. It was shown that PMP2 can stack membrane bilayers and affect lipid bilayer dynamics [132], [133], [168], [262]. In addition to its function on the integrity of the myelin multilayer, it has also been suggested to be important for lipid transport to and from the membrane.

PMP2 mRNA was also found highly expressed in the cerebral cortex according to the Human Protein Atlas (section 3.1.12). Interestingly, PMP2 and SOX10 were found upregulated in dermal Schwannomas compared to other cutaneous neoplasms of peripheral nerve sheath origin [241]. Strikingly, SOX10 is present in both myelinating glial cell populations, which are Schwann cells and oligodendrocytes, throughout development and after terminal differentiation [139]. SOX10 is required for myelination in both cell types [31], [256]. In Schwann cells, SOX10 directly activates the transcription factor EGR2 [82]. Together they activate myelin gene enhancers as MPZ, PMP-22, MBP, and myelin-associated glycoprotein (MAG) [148], [251].

In this study, PMP2 was only found specifically expressed on mRNA and protein level in two melanoma cell lines (WM278 and WM239A) out of 13 (sections 4.9.1 and 4.9.2.2). The mRNA expression of PMP2 varied highly in melanoma cells and also moderate mRNA expression was found in melanocytes.

PMP2 mRNA expression was strongly reduced upon SOX10 inhibition in all investigated melanoma cell lines but reduction on protein level was only found in cell lines WM278 and WM239A (section 4.8.1, Figure 41 and section 4.9.1, Figure 46). Although SOX10 overexpression was sufficient to increase PMP2 protein expression in WM278 cells and although its mRNA levels were considerably elevated upon SOX10 overexpression, no induced or increased PMP2 protein expression was found in cell lines WM3211, WM1366, and 1205Lu (section 4.8.1, Figure 42). This discrepancy might be explained due to a substantial role for regulatory processes occurring after mRNA transcription [278]. Several possible events can restrict PMP2 expression on protein level. In mammalian cells, mRNA is produced at a much lower rate than proteins, which means two copies of a specific mRNA per hour correlates with dozens of copies of the according protein of mRNA per hour. The stability of mRNA is less than that of proteins with 2.6-7 hours versus about 46 hours, respectively. Therefore it is possible that the PMP2 mRNA is very unstable and a very high amount of mRNA production (as it is the case for cell lines WM278 and WM239A) would be necessary for PMP2 protein expression. Strikingly, PMP2 ectopic overexpression in the PMP2-negative cell line WM3211, which generated high amounts of mRNA, led to strong PMP2 expression on protein level (section 4.9.2.4, Figure 54). Regarding the fact that PMP2 mRNA was measured in several melanoma cell lines and SOX10 regulation of PMP2 expression was also found in these cells (4.8.1), it is possible that cell lines expressing PMP2 mRNA but not PMP2 protein might miss several specific regulators for PMP2 translation or modifications that affect protein stability. Differential regulation of post-transcription (RNA processing, alternative splicing or differential splicing, regulatory elements in 5' UTR, or depletion of ternary complexes), translation, and protein degradation together with protein modifications could contribute to absent PMP2 protein. Furthermore, the presence of micro RNAs - which is certainly differing between the different cell lines - could alter protein translation.

Moreover, PMP2 expression might be regulated epigenetically. The *PMP2* promoter region as well as 1023 bp upstream of the promoter and 1049 bp downstream were analyzed by two different softwares for identification of CpG islands (EMBOSS Cpplot

and CpG Island searcher, section 3.1.12). An island was defined with the following parameters: observed GpC/expected GpC > 0.65, percentage GC > 55%, length > 200, and distance to next island > 100 bp. As no CpG islands were found DNA methylation can be excluded as a potential epigenetic regulatory mechanism for PMP2 expression. Not only PMP2 expression but also expression of other SOX10-regulated myelin proteins, i.e., MPZ and PLP1, was found in melanocytes and melanoma cell lines (section 4.9.1, Figure 47). Strikingly, MPZ and PLP1 mRNA levels were found substantially elevated in WM278 cells compared to other melanoma cells. PLP1 mRNA levels were also found elevated in WM239A cells. Thus, the restricted expression of myelin proteins in some melanoma cell lines seems to be a cell line-specific feature. The VGP cell lines WM278 derived from a nodular melanoma stage IV (<http://www.wistar.org/lab/meenhard-herlyn-dvm-dsc/page/melanoma-cell-lines-vgp>) while WM239A were established from a lymph node metastasis [293], which does not indicate that the specific expression of myelin proteins in these cell lines is related to their original tissue microenvironment. Nevertheless, the expression of myelin proteins in melanoma cells could be a forecast where the cells might preferentially metastasize according to the seed and soil hypothesis of cancer pathogenesis [68], [193]. Hereby, the term “seed” is referred to certain tumor cells that display affinity for the milieu of certain organs, denominated as “soil”.

Reed et al. [210] demonstrated that Schwann cell-resembling melanocytic nevus cells express proteins that define the earliest stages of Schwann cell development, i.e., p75, neural cell adhesion molecule (N-CAM), and growth-associated phosphoprotein-43 (GAP-43). Notwithstanding, these proteins were found limited in primary melanoma and absent in melanoma *in situ*. Another research group found histological and molecular characteristics of malignant peripheral nerve sheath tumors in amelanotic melanomas of their BRAF^{V600E}-Cdk4^{R24C} mouse model that seems to be also present in a subset of human melanomas (oral presentation of Jennifer Landsberg, [307], FV28). Therefore, expression of myelin proteins might be a specific feature in a subset of melanomas contributing to melanoma heterogeneity.

Due to an early downregulation of PMP2 protein by SOX10 inhibition in WM278 cells, a direct transactivation of PMP2 by SOX10 was suggested. *In silico* analyses identified three potential SOX10 binding sites in the *PMP2* promoter region and ChIP as well as EMSA experiments indicated binding of SOX10 to the proximal *PMP2* promoter region (section 4.8.2).

In order to investigate the role of PMP2 in melanoma cells, gain- and loss-of-function experiments were performed (section 4.9.2). PMP2 inhibition via RNA interference with two different siRNAs reduced cell number and viability in PMP2-positive but not in PMP2-negative cells (section 4.9.2.2, Figure 51). Since caspase 3 was activated by siPMP2b but not by siPMP2a, while p21 was induced by both siRNAs, it was suggested that PMP2 inhibition might be able to prevent cell cycle progression in PMP2-positive melanoma cells.

Matrigel analysis showed decreased invasion after PMP2 inhibition in WM278 cells, which was only significant in case of the caspase 3-activating siPMP2b (section 4.9.2.3, Figure 52). Since myelination of neurons by Schwann cells is a highly migratory process, the influence of PMP2 on melanoma cell migration was further investigated by PMP2 overexpression. Stable PMP2 overexpression significantly increased invasion of WM278 cells but it could not rescue the SOX10 knockdown phenotype in these cells (section 4.9.2.3, Figure 53). Cell viability was not influenced by PMP2 overexpression.

Moreover, PMP2 wild type and mutant variants were stably expressed in PMP2-negative WM3211 cells (section 4.9.2.4). The L27D mutant has been described recently by Ruskamo et al. [219] to reduce PMP2 binding to the membrane. The Mut3 mutant represents a mutated form of PMP2 where all three amino acids that allow fatty acid binding according to Majava et al. [168] were mutated. On mRNA level, expression of PMP2 wild type and mutants was highly upregulated compared to control cells while only wild type PMP2 and the L27D mutant were also found expressed on protein level. It is possible that mutations of the three amino acids in Mut3 affect protein stability and thereby cause protein degradation. Notwithstanding, WM3211 stably transfected with PMP2 wild type, both PMP2 mutant forms, and control vector were subjected to a three-dimensional spheroid assay (section 4.9.2.4). Quantification of this assay revealed that PMP2 wild type-overexpressing cells substantially increased invasiveness compared to the mutant and control cells. Overexpression of the L27D mutant also considerably increased the invasive capacity compared to the control cells but to a lesser extent than PMP2 wild type-expressing cells. Two explanations are possible for this observation: firstly, it is possible that PMP2 has another membrane binding domain that is not affected by the L27D mutation. Secondly, the membrane binding function might not be required for stimulating the invasive potential in melanoma cells.

Taken these results together, SOX10 directly transactivates PMP2 and PMP2 plays a promigratory role in melanoma cells. PMP2 overexpression increased melanoma cell

invasion but the entire functions of PMP2 in melanoma cells remain to be elucidated. Due to its roles in the myelinating process of Schwann cells it is possible that PMP2 can modify membrane dynamics during migration processes or it might be involved in lipid signaling in the migrating cell.

5.6 SOX10 regulated genes – parallels between Schwann cell, Schwannian tumor, and melanoma development

SOX10 is expressed in NCCs and a subset of NCC-derived lineages. Without SOX10, no glia development occurs throughout the peripheral nervous system [31], [139], [248]. SOX10 continues to be expressed after lineage segregation, promotes differentiation, and is still expressed in melanocytes, glial cells of the central nervous system (oligodendrocytes), and glial cells of the peripheral nervous system (Schwann cells) [126], [139]. Schwann cell precursors proliferate, migrate along the dorsolateral axis, and differentiate for myelination of the peripheral neuronal axons. SOX10 directly regulates myelin gene expression in both types of glial cells although it does not control ERBB3 expression in oligodendrocytes in contrast to Schwann cells. Thus, SOX10 functions in peripheral and central glia at different stages and through different mechanisms [256]. Another study demonstrated that siRNA-mediated downregulation of SOX10 promoted transdifferentiation of Schwannoma cells into myofibroblasts *in vitro* [218]. Thus, SOX10 is not only critical for melanocyte but also for oligodendrocyte and Schwann cell development and homeostasis.

Lee et al. [151] performed RNA interference (SOX10 siRNA and control siRNA) and subsequent DNA microarray analysis to identify SOX10 target genes in a rat Schwannoma cell line (according to GEO profile GDS3480). ERBB3 and MIA were part of the genes that were downregulated more than 4-fold upon SOX10 inhibition. Also PMP2 was strongly downregulated by SOX10 inhibition in this array. Therefore, target genes of SOX10, which were identified in this study, seem to be also regulated by SOX10 in Schwannoma cells. Schwannoma is a benign nerve sheath tumor composed of Schwann cells outside the nerve. They grow slowly and only around 1% become malignant and form tumors such as neurofibrosarcoma. An immunohistochemical study recommended SOX10 as a specific and sensitive marker not only for melanomas but also for Schwannian (peripheral nerve sheath) tumors [188]. Moreover, SOX10 seems to be a prognostic marker in neuroectodermal tumor cells (including Schwannoma and Schwann-like cells in neuroblastoma) as proposed by Gershon et al. [81]. Fujiwara S. et

al. suggested that SOX10 transactivates S100B in Schwann cells and the SOX10-S100B axis critically regulates Schwann cell proliferation and myelination [76].

As melanoma cells can be genetically and functionally connected with melanocyte precursors, it is interesting that melanocytes can directly evolve from SOX10-positive Schwann cell precursor cells during mouse embryonic development [2]. Thus, developing melanocytes and Schwann cells as well as their neoplastically transformed counterparts share several signaling molecules including SOX10.

Other target genes of SOX10 that do not only play a key role in melanocyte but also in Schwann cell development have been investigated in melanoma cells in the present study (sections 4.5 and 4.10). Fate decision of nerve-linked Schwann cell and melanocyte precursors is controlled by neuregulin signaling through their ERBB3 receptor [2]. It was shown that ERBB3 is required for Schwann cell precursor proliferation and migration along peripheral axons as well as for myelination in zebrafish and mouse models [166], [268]. Complete knockout of ERBB3 results in embryonic lethality with a complete loss of Schwann cell precursors and effects similar to various peripheral neuropathy symptoms [215]. SOX10 has been shown to regulate ERBB3 in NCCs and Schwann cells, where functional ERBB3 is required for differentiation, growth, and survival [212], [223]. Furthermore, neoplastic Schwann cells almost uniformly express ERBB3 and ERBB2 (with which it forms heterodimers upon activation) and they were suggested to promote Schwannoma pathogenesis [259]. Thus, ERBB3 is not only essential for Schwann cell differentiation and maintenance but also plays a role in neoplastic transformation similar to its function in melanomagenesis. Similarly, the endothelin receptor EDNRB is required for melanocyte and enterous nerve system development but also related to Schwann cell tumor formation and melanoma progression [55]. SOX10 interacts with EDNRB in the enteric nervous system as well as in melanocyte development and it was shown that SOX10 regulates EDNRB in melanocytes and enteric neuron precursors [253], [303], [306]. EDNRB is furthermore related to melanoma progression and also to the development of Schwann cell-derived tumors.

The transcription factor EGR2 is critical for the differentiation of immature into myelinating Schwann cells [267]. EGR2 is a common coactivator of SOX10 in the regulation of myelin gene transcription and was shown to be regulated by SOX10 in Schwann cells [82], [122], [211], [258]. In this study, coregulation of PMP2 by SOX10 and EGR2 was found in the PMP2-positive melanoma cell line WM278 (section 4.8.3).

Moreover, downregulation of expression was found for ERBB3, EDNRB, and EGR2 upon SOX10 inhibition in different melanoma cell lines (sections 4.5 and 4.10).

Regarding these data, it is hypothesized that SOX10 regulates common target genes and could thereby possess analogous functions in melanocytes and Schwann cell precursors but also in their neoplastic counterparts.

5.7 Conclusion and outlook

This study provides evidences for a hitherto undescribed regulatory role of SOX10 during melanoma cell invasion and further highlights its role as a pro-survival factor in melanoma. However, the role of SOX10 in melanoma is most likely multifaceted. SOX10 is associated with stem cell development and maintenance. During neural crest development, SOX10 plays a role as stem cell factor maintaining multipotency and preventing premature neurogenesis [128]. SOX10 is not only relevant for the differentiation of melanocytes and glial cells, it is also crucial for survival and proliferation of multipotent neural crest stem cells [31]. Furthermore, SOX10 was found to be relevant for melanocyte stem cell maintenance in the adult organism [103]. A recent study revealed important roles of SOX10 promoting stem and EMT-like properties in mammary stem cells [62]. Several publications highlight common molecular and cellular mechanisms affecting self-renewal, phenotypic, and functional similarities between neural crest stem cells and melanoma cells that can be linked to SOX10 [237]. Co-expression of SOX10 and the neural crest stem cell marker p75 correlates with a high metastatic potential and worse patient's prognosis [49]. Together with SOX9, SOX10 regulates the putative stem cell marker nestin [72]. Tumor formation of subcutaneously injected SOX10-inhibited melanoma cells in non-obese diabetic-severe combined immunodeficient and nude mice was impaired completely [239]. Cronin et al. [53] suggested that reduced tumor formation in mice that harbor SOX10 heterozygosity is independent of the function of SOX10 as MITF activator. In summary, SOX10 is able to regulate stem cell functions, which seem to be specifically required for initiating and propagating melanoma. As suggested in the present and previous studies, SOX10 regulates targets genes whose functions have been related to Schwann cell differentiation. Therefore, SOX10 might be also relevant for the initiation and progression of glial cell tumors.

In this study novel direct targets genes of SOX10 have been identified, i.e., the secreted factor MIA, which directly affects melanoma cell migration, and the cellular membrane-

attached lipid binding protein PMP2, which entire functions in melanoma still need to be elucidated. SOX10 in general and both target genes specifically promote melanoma cell invasion (Figure 58). Strikingly, this is an important feature, as tumor metastases are the cause of 90% of human cancer deaths [250].

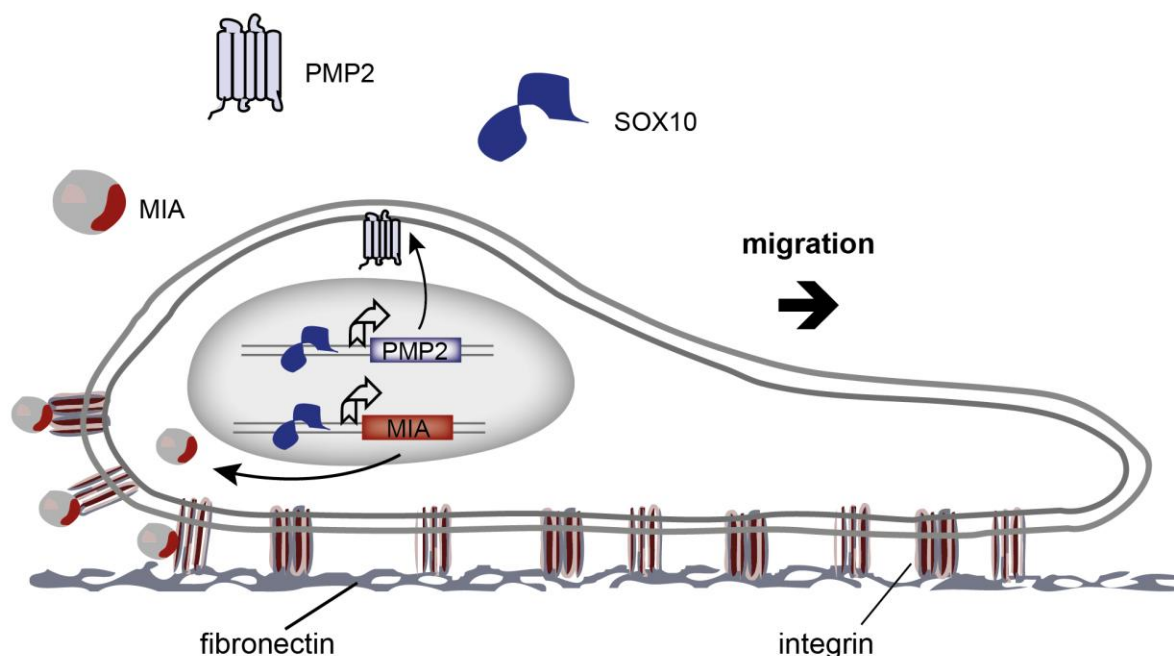


Figure 58 SOX10 regulates migration-associated genes in melanoma cells.

In this study the direct regulation of MIA and PMP2 by SOX10 has been demonstrated. Both proteins can influence melanoma cell invasion and might therefore promote melanoma metastasis.

This study highlights that transcription factors, which are essential for proliferation and migration of developing melanocytes, may contribute to melanoma progression. Curing therapies for patients with metastatic melanoma are still missing. Thus, manipulating the SOX10 signaling pathway could have a great therapeutical value [159]. To inhibit SOX10 *in vivo* in patients, SOX10-targeting siRNAs attached to nanoparticles could be injected. However, this method has not found its way to clinics yet. Another option is to search for small molecule inhibitors impairing SOX10 binding to DNA. As the DNA binding motif of SOX10, the HMG box, is found in all other SOX and HMG factors, this approach would have most likely toxic effects. Another problem is the general expression of SOX10 in a variety of tissues and intervention of SOX10 wild type functions is related to many severe organic defects. Therefore, targeting SOX10-regulated genes that directly execute specific functions in melanoma would improve tumor-specific therapy. Affecting PMP2 functions might be beneficial in a subset of

melanomas but might be most likely a problem due to its essential contribution to myelination.

MIA inhibition is a novel objective in melanoma therapy [230]. Schmidt et al. [231] showed that dimerization of MIA is required for its functional activity. The dodecapeptide AR71 prevented MIA dimerization and reduced melanoma cell migration and formation of metastasis *in vitro* and *in vivo* [231]. In conclusion, the analysis of melanoma-specific target genes of SOX10 is important for generating novel therapies to prevent melanoma cell migration and invasion.

It further remains to be elucidated, how SOX10 promotes melanoma progression on the one hand and regulates differentiation and pigmentation in melanoblasts on the other hand. Besides, it would be interesting to determine the molecular mechanisms driving SOX10 to regulate the same target genes as PMP2, EDNRB, ERBB3, and EGR2 in melanoma and in Schwann or Schwannoma cells. Lineage-specific functions of these proteins might be related to altered protein levels, specific post-translational modification, the absence or presence of coregulators, or other contextual features.

In conclusion, this study describes a crucial function of SOX10 in melanoma cell survival and invasion and led to the identification of novel target genes that mediate the functions of SOX10 in melanoma.

6 References

- [1] J. Ackermann, M. Frutschi, K. Kaloulis, T. McKee, A. Trumpp, and F. Beermann, "Metastasizing melanoma formation caused by expression of activated N-RasQ61K on an INK4a-deficient background," *Cancer Res.*, vol. 65, no. 10, pp. 4005–4011, May 2005.
- [2] I. Adameyko, F. Lallemand, J. B. Aquino, J. A. Pereira, P. Topilko, T. Müller, N. Fritz, A. Beljajeva, M. Mochii, I. Liste, D. Usoskin, U. Suter, C. Birchmeier, and P. Ernfors, "Schwann Cell Precursors from Nerve Innervation Are a Cellular Origin of Melanocytes in Skin," *Cell*, vol. 139, no. 2, pp. 366–379, Oct. 2009.
- [3] S. O. Addo-Yobo, J. Straessle, A. Anwar, A. M. Donson, B. K. Kleinschmidt-Demasters, and N. K. Foreman, "Paired overexpression of ErbB3 and Sox10 in pilocytic astrocytoma," *J. Neuropathol. Exp. Neurol.*, vol. 65, no. 8, pp. 769–775, Aug. 2006.
- [4] M. Agnarsdóttir, L. Sooman, A. Bolander, S. Strömberg, E. Rexhepaj, M. Bergqvist, F. Ponten, W. Gallagher, J. Lennartsson, S. Ekman, M. Uhlen, and H. Hedstrand, "SOX10 expression in superficial spreading and nodular malignant melanomas," *Melanoma Res.*, vol. 20, no. 6, pp. 468–478, Dec. 2010.
- [5] Y. Aoki, N. Saint-Germain, M. Gyda, E. Magner-Fink, Y.-H. Lee, C. Credidio, and J.-P. Saint-Jeannet, "Sox10 regulates the development of neural crest-derived melanocytes in *Xenopus*," *Dev. Biol.*, vol. 259, no. 1, pp. 19–33, Jul. 2003.
- [6] D. J. Arndt-Jovin and T. M. Jovin, "Fluorescence labeling and microscopy of DNA," *Methods Cell Biol.*, vol. 30, pp. 417–448, 1989.
- [7] P. A. Ascierto, D. Schadendorf, C. Berking, S. S. Agarwala, C. M. van Herpen, P. Queirolo, C. U. Blank, A. Hauschild, J. T. Beck, A. St-Pierre, F. Niazi, S. Wandel, M. Peters, A. Zobel, and R. Dummer, "MEK162 for patients with advanced melanoma harbouring NRAS or Val600 BRAF mutations: a non-randomised, open-label phase 2 study," *Lancet Oncol.*, vol. 14, no. 3, pp. 249–256, Mar. 2013.
- [8] R. M. Bakos, T. Maier, R. Besch, D. S. Mestel, T. Ruzicka, R. A. Sturm, and C. Berking, "Nestin and SOX9 and SOX10 transcription factors are coexpressed in melanoma," *Exp. Dermatol.*, vol. 19, no. 8, pp. e89–94, Aug. 2010.
- [9] C. M. Balch, J. E. Gershenwald, S. -j. Soong, J. F. Thompson, M. B. Atkins, D. R. Byrd, A. C. Buzaid, A. J. Cochran, D. G. Coit, S. Ding, A. M. Eggermont, K. T. Flaherty, P. A. Gimotty, J. M. Kirkwood, K. M. McMasters, M. C. Mihm, D. L. Morton, M. I. Ross, A. J. Sober, and V. K. Sondak, "Final Version of 2009 AJCC Melanoma Staging and Classification," *J. Clin. Oncol.*, vol. 27, no. 36, pp. 6199–6206, Dec. 2009.
- [10] R. Bauer, M. Humphries, R. Fässler, A. Winklmeier, S. E. Craig, and A.-K. Bosserhoff, "Regulation of integrin activity by MIA," *J. Biol. Chem.*, vol. 281, no. 17, pp. 11669–11677, Apr. 2006.
- [11] F. Belleudi, E. Marra, F. Mazzetta, L. Fattore, M. R. Giovagnoli, R. Mancini, L. Aurisicchio, M. R. Torrisi, and G. Ciliberto, "Monoclonal antibody-induced ErbB3 receptor internalization and degradation inhibits growth and migration of human melanoma cells," *Cell Cycle Georget. Tex.*, vol. 11, no. 7, pp. 1455–1467, Apr. 2012.
- [12] C. Berking, "[The role of ultraviolet irradiation in malignant melanoma]," *Hautarzt Z. Für Dermatol. Venerol. Verwandte Geb.*, vol. 56, no. 7, pp. 687–696; quiz 697, Jul. 2005.
- [13] C. Berking, R. Takemoto, K. Satyamoorthy, T. Shirakawa, M. Eskandarpour, J. Hansson, P. A. VanBelle, D. E. Elder, and M. Herlyn, "Induction of melanoma phenotypes in human skin by growth factors and ultraviolet B," *Cancer Res.*, vol. 64, no. 3, pp. 807–811, Feb. 2004.
- [14] C. Berking and M. Herlyn, "Human skin reconstruct models: a new application for studies of melanocyte and melanoma biology," *Histol. Histopathol.*, vol. 16, no. 2, pp. 669–674, Apr. 2001.
- [15] C. Berking, R. Takemoto, K. Satyamoorthy, R. Elenitsas, and M. Herlyn, "Basic fibroblast growth factor and ultraviolet B transform melanocytes in human skin," *Am. J. Pathol.*, vol. 158, no. 3, pp. 943–953, Mar. 2001.
- [16] D. T. Bishop, F. Demenais, A. M. Goldstein, W. Bergman, J. N. Bishop, B. Bressac-de Paillerets, A. Chompret, P. Ghiorzo, N. Gruis, J. Hansson, M. Harland, N. Hayward, E. A.

- Holland, G. J. Mann, M. Mantelli, D. Nancarrow, A. Platz, M. A. Tucker, and Melanoma Genetics Consortium, "Geographical variation in the penetrance of CDKN2A mutations for melanoma," *J. Natl. Cancer Inst.*, vol. 94, no. 12, pp. 894–903, Jun. 2002.
- [17] A. Blesch, A. K. Bosserhoff, R. Apfel, C. Behl, B. Hessdoerfer, A. Schmitt, P. Jachimczak, F. Lottspeich, R. Buettner, and U. Bogdahn, "Cloning of a novel malignant melanoma-derived growth-regulatory protein, MIA," *Cancer Res.*, vol. 54, no. 21, pp. 5695–5701, Nov. 1994.
- [18] U. Bogdahn, R. Apfel, M. Hahn, M. Gerlach, C. Behl, J. Hoppe, and R. Martin, "Autocrine tumor cell growth-inhibiting activities from human malignant melanoma," *Cancer Res.*, vol. 49, no. 19, pp. 5358–5363, Oct. 1989.
- [19] A. D. Boiko, O. V. Razorenova, M. van de Rijn, S. M. Swetter, D. L. Johnson, D. P. Ly, P. D. Butler, G. P. Yang, B. Joshua, M. J. Kaplan, M. T. Longaker, and I. L. Weissman, "Human melanoma-initiating cells express neural crest nerve growth factor receptor CD271," *Nature*, vol. 466, no. 7302, pp. 133–137, Jul. 2010.
- [20] N. Bondurand, F. Dastot-Le Moal, L. Stanchina, N. Collot, V. Baral, S. Marlin, T. Attie-Bitach, I. Giurgea, L. Skopinski, W. Reardon, A. Toutain, P. Sarda, A. Echaieb, M. Lackmy-Port-Lis, R. Touraine, J. Amiel, M. Goossens, and V. Pingault, "Deletions at the SOX10 gene locus cause Waardenburg syndrome types 2 and 4," *Am. J. Hum. Genet.*, vol. 81, no. 6, pp. 1169–1185, Dec. 2007.
- [21] N. Bondurand, M. Girard, V. Pingault, N. Lemort, O. Dubourg, and M. Goossens, "Human Connexin 32, a gap junction protein altered in the X-linked form of Charcot-Marie-Tooth disease, is directly regulated by the transcription factor SOX10," *Hum. Mol. Genet.*, vol. 10, no. 24, pp. 2783–2795, Nov. 2001.
- [22] N. Bondurand, V. Pingault, D. E. Goerich, N. Lemort, E. Sock, C. Le Caignec, M. Wegner, and M. Goossens, "Interaction among SOX10, PAX3 and MITF, three genes altered in Waardenburg syndrome," *Hum. Mol. Genet.*, vol. 9, no. 13, pp. 1907–1917, Aug. 2000.
- [23] J. B. Boonyaratanakornkit, L. Yue, L. R. Strachan, K. J. Scalapino, P. E. LeBoit, Y. Lu, S. P. Leong, J. E. Smith, and R. Ghadially, "Selection of tumorigenic melanoma cells using ALDH," *J. Invest. Dermatol.*, vol. 130, no. 12, pp. 2799–2808, Dec. 2010.
- [24] A. K. Bosserhoff, B. Echtenacher, R. Hein, and R. Buettner, "Functional role of melanoma inhibitory activity in regulating invasion and metastasis of malignant melanoma cells in vivo," *Melanoma Res.*, vol. 11, no. 4, pp. 417–421, Aug. 2001.
- [25] A. K. Bosserhoff, R. Hein, U. Bogdahn, and R. Buettner, "Structure and promoter analysis of the gene encoding the human melanoma-inhibiting protein MIA," *J. Biol. Chem.*, vol. 271, no. 1, pp. 490–495, Jan. 1996.
- [26] A. K. Bosserhoff, M. Kaufmann, B. Kaluza, I. Bartke, H. Zirngibl, R. Hein, W. Stolz, and R. Buettner, "Melanoma-inhibiting activity, a novel serum marker for progression of malignant melanoma," *Cancer Res.*, vol. 57, no. 15, pp. 3149–3153, Aug. 1997.
- [27] A. K. Bosserhoff, M. Lederer, M. Kaufmann, R. Hein, W. Stolz, R. Apfel, U. Bogdahn, and R. Buettner, "MIA, a novel serum marker for progression of malignant melanoma," *Anticancer Res.*, vol. 19, no. 4A, pp. 2691–2693, Aug. 1999.
- [28] A.-K. Bosserhoff, R. Stoll, J. P. Sleeman, F. Bataille, R. Buettner, and T. A. Holak, "Active detachment involves inhibition of cell-matrix contacts of malignant melanoma cells by secretion of melanoma inhibitory activity," *Lab. Invest. J. Tech. Methods Pathol.*, vol. 83, no. 11, pp. 1583–1594, Nov. 2003.
- [29] J. Bowles, G. Schepers, and P. Koopman, "Phylogeny of the SOX family of developmental transcription factors based on sequence and structural indicators," *Dev. Biol.*, vol. 227, no. 2, pp. 239–255, Nov. 2000.
- [30] M. M. Bradford, "A rapid and sensitive method for the quantitation of microgram quantities of protein utilizing the principle of protein-dye binding," *Anal. Biochem.*, vol. 72, pp. 248–254, May 1976.
- [31] S. Britsch, D. E. Goerich, D. Riethmacher, R. I. Peirano, M. Rossner, K. A. Nave, C. Birchmeier, and M. Wegner, "The transcription factor Sox10 is a key regulator of peripheral glial development," *Genes Dev.*, vol. 15, no. 1, pp. 66–78, Jan. 2001.

- [32] S. Britsch, D. E. Goerich, D. Riethmacher, R. I. Peirano, M. Rossner, K. A. Nave, C. Birchmeier, and M. Wegner, "The transcription factor Sox10 is a key regulator of peripheral glial development," *Genes Dev.*, vol. 15, no. 1, pp. 66–78, Jan. 2001.
- [33] S. Britsch, L. Li, S. Kirchhoff, F. Theuring, V. Brinkmann, C. Birchmeier, and D. Riethmacher, "The ErbB2 and ErbB3 receptors and their ligand, neuregulin-1, are essential for development of the sympathetic nervous system," *Genes Dev.*, vol. 12, no. 12, pp. 1825–1836, Jun. 1998.
- [34] M. Bronner-Fraser and S. E. Fraser, "Cell lineage analysis reveals multipotency of some avian neural crest cells," *Nature*, vol. 335, no. 6186, pp. 161–164, Sep. 1988.
- [35] M. H. Brush, D. C. Weiser, and S. Shenolikar, "Growth arrest and DNA damage-inducible protein GADD34 targets protein phosphatase 1 alpha to the endoplasmic reticulum and promotes dephosphorylation of the alpha subunit of eukaryotic translation initiation factor 2," *Mol. Cell. Biol.*, vol. 23, no. 4, pp. 1292–1303, Feb. 2003.
- [36] K. Buac, D. E. Watkins-Chow, S. K. Loftus, D. M. Larson, A. Incao, G. Gibney, and W. J. Pavan, "A Sox10 expression screen identifies an amino acid essential for Erbb3 function," *PLoS Genet.*, vol. 4, no. 9, p. e1000177, 2008.
- [37] K. Buac, M. Xu, J. Cronin, A. T. Weeraratna, S. M. Hewitt, and W. J. Pavan, "NRG1 / ERBB3 signaling in melanocyte development and melanoma: inhibition of differentiation and promotion of proliferation," *Pigment Cell Melanoma Res.*, vol. 22, no. 6, pp. 773–784, Dec. 2009.
- [38] C. Busch, J. Krochmann, and U. Drews, "The chick embryo as an experimental system for melanoma cell invasion," *PLoS One*, vol. 8, no. 1, p. e53970, 2013.
- [39] S. Carreira, J. Goodall, L. Denat, M. Rodriguez, P. Nuciforo, K. S. Hoek, A. Testori, L. Larue, and C. R. Goding, "Mitf regulation of Dia1 controls melanoma proliferation and invasiveness," *Genes Dev.*, vol. 20, no. 24, pp. 3426–3439, Dec. 2006.
- [40] M.-C. Chaboissier, A. Kobayashi, V. I. P. Vidal, S. Lützkendorf, H. J. G. van de Kant, M. Wegner, D. G. de Rooij, R. R. Behringer, and A. Schedl, "Functional analysis of Sox8 and Sox9 during sex determination in the mouse," *Dev. Camb. Engl.*, vol. 131, no. 9, pp. 1891–1901, May 2004.
- [41] G. Chakravarty, K. Moroz, N. M. Makridakis, S. A. Lloyd, S. E. Galvez, P. R. Canavello, M. R. Lacey, K. Agrawal, and D. Mondal, "Prognostic significance of cytoplasmic SOX9 in invasive ductal carcinoma and metastatic breast cancer," *Exp. Biol. Med.*, vol. 236, no. 2, pp. 145–155, Feb. 2011.
- [42] P. B. Chapman, A. Hauschild, C. Robert, J. B. Haanen, P. Ascierto, J. Larkin, R. Dummer, C. Garbe, A. Testori, M. Maio, D. Hogg, P. Lorigan, C. Lebbe, T. Jouary, D. Schadendorf, A. Ribas, S. J. O'Day, J. A. Sosman, J. M. Kirkwood, A. M. M. Eggermont, B. Dreno, K. Nolop, J. Li, B. Nelson, J. Hou, R. J. Lee, K. T. Flaherty, and G. A. McArthur, "Improved Survival with Vemurafenib in Melanoma with BRAF V600E Mutation," *N. Engl. J. Med.*, vol. 364, no. 26, pp. 2507–2516, Jun. 2011.
- [43] Y. Cheli, M. Ohanna, R. Ballotti, and C. Bertolotto, "Fifteen-year quest for microphthalmia-associated transcription factor target genes," *Pigment Cell Melanoma Res.*, vol. 23, no. 1, pp. 27–40, Feb. 2010.
- [44] P. F. Cheng, O. Shakhova, D. S. Widmer, O. M. Eichhoff, D. Zingg, S. C. Frommel, B. Belloni, M. I. Raaijmakers, S. M. Goldinger, R. Santoro, S. Hemmi, L. Sommer, R. Dummer, and M. P. Levesque, "Methylation-dependent SOX9 expression mediates invasion in human melanoma cells and is a negative prognostic factor in advanced melanoma," *Genome Biol.*, vol. 16, p. 42, 2015.
- [45] Z. Chen, J. Huang, Y. Liu, L. K. Dattilo, S.-H. Huh, D. Ornitz, and D. C. Beebe, "FGF signaling activates a Sox9-Sox10 pathway for the formation and branching morphogenesis of mouse ocular glands," *Dev. Camb. Engl.*, vol. 141, no. 13, pp. 2691–2701, Jul. 2014.
- [46] M. Cheung and J. Briscoe, "Neural crest development is regulated by the transcription factor Sox9," *Dev. Camb. Engl.*, vol. 130, no. 23, pp. 5681–5693, Dec. 2003.
- [47] M. Cheung, M.-C. Chaboissier, A. Mynett, E. Hirst, A. Schedl, and J. Briscoe, "The Transcriptional Control of Trunk Neural Crest Induction, Survival, and Delamination," *Dev. Cell*, vol. 8, no. 2, pp. 179–192, Feb. 2005.

- [48] Y. Chudnovsky, A. E. Adams, P. B. Robbins, Q. Lin, and P. A. Khavari, "Use of human tissue to assess the oncogenic activity of melanoma-associated mutations," *Nat. Genet.*, vol. 37, no. 7, pp. 745–749, Jul. 2005.
- [49] G. Civenni, A. Walter, N. Kobert, D. Mihic-Probst, M. Zipser, B. Belloni, B. Seifert, H. Moch, R. Dummer, M. van den Broek, and L. Sommer, "Human CD271-positive melanoma stem cells associated with metastasis establish tumor heterogeneity and long-term growth," *Cancer Res.*, vol. 71, no. 8, pp. 3098–3109, Apr. 2011.
- [50] W. H. Clark, D. E. Elder, D. Guerry, M. N. Epstein, M. H. Greene, and M. Van Horn, "A study of tumor progression: the precursor lesions of superficial spreading and nodular melanoma," *Hum. Pathol.*, vol. 15, no. 12, pp. 1147–1165, Dec. 1984.
- [51] W. H. Clark, L. From, E. A. Bernardino, and M. C. Mihm, "The histogenesis and biologic behavior of primary human malignant melanomas of the skin," *Cancer Res.*, vol. 29, no. 3, pp. 705–727, Mar. 1969.
- [52] A. L. Cook, A. G. Smith, D. J. Smit, J. H. Leonard, and R. A. Sturm, "Co-expression of SOX9 and SOX10 during melanocytic differentiation in vitro," *Exp. Cell Res.*, vol. 308, no. 1, pp. 222–235, Aug. 2005.
- [53] J. C. Cronin, D. E. Watkins-Chow, A. Incao, J. H. Hasskamp, N. Schönewolf, L. G. Aoude, N. K. Hayward, B. C. Bastian, R. Dummer, S. K. Loftus, and W. J. Pavan, "SOX10 ablation arrests cell cycle, induces senescence, and suppresses melanomagenesis," *Cancer Res.*, vol. 73, no. 18, pp. 5709–5718, Sep. 2013.
- [54] J. C. Cronin, J. Wunderlich, S. K. Loftus, T. D. Prickett, X. Wei, K. Ridd, S. Vemula, A. S. Burrell, N. S. Agrawal, J. C. Lin, C. E. Banister, P. Buckhaults, S. A. Rosenberg, B. C. Bastian, W. J. Pavan, and Y. Samuels, "Frequent mutations in the MITF pathway in melanoma," *Pigment Cell Melanoma Res.*, vol. 22, no. 4, pp. 435–444, Aug. 2009.
- [55] W. Cruz-Muñoz, M. L. Jaramillo, S. Man, P. Xu, M. Banville, C. Collins, A. Nantel, G. Francia, S. S. Morgan, L. D. Cranmer, M. D. O'Connor-McCourt, and R. S. Kerbel, "Roles for endothelin receptor B and BCL2A1 in spontaneous CNS metastasis of melanoma," *Cancer Res.*, vol. 72, no. 19, pp. 4909–4919, Oct. 2012.
- [56] J. A. Curtin, K. Busam, D. Pinkel, and B. C. Bastian, "Somatic activation of KIT in distinct subtypes of melanoma," *J. Clin. Oncol. Off. J. Am. Soc. Clin. Oncol.*, vol. 24, no. 26, pp. 4340–4346, Sep. 2006.
- [57] H. Davies, G. R. Bignell, C. Cox, P. Stephens, S. Edkins, S. Clegg, J. Teague, H. Woffendin, M. J. Garnett, W. Bottomley, N. Davis, E. Dicks, R. Ewing, Y. Floyd, K. Gray, S. Hall, R. Hawes, J. Hughes, V. Kosmidou, A. Menzies, C. Mould, A. Parker, C. Stevens, S. Watt, S. Hooper, R. Wilson, H. Jayatilake, B. A. Gusterson, C. Cooper, J. Shipley, D. Hargrave, K. Pritchard-Jones, N. Maitland, G. Chenevix-Trench, G. J. Riggins, D. D. Bigner, G. Palmieri, A. Cossu, A. Flanagan, A. Nicholson, J. W. C. Ho, S. Y. Leung, S. T. Yuen, B. L. Weber, H. F. Seigler, T. L. Darrow, H. Paterson, R. Marais, C. J. Marshall, R. Wooster, M. R. Stratton, and P. A. Futreal, "Mutations of the BRAF gene in human cancer," *Nature*, vol. 417, no. 6892, pp. 949–954, Jun. 2002.
- [58] M. Deo, J. L.-Y. Huang, and C. D. Van Raamsdonk, "Genetic interactions between neurofibromin and endothelin receptor B in mice," *PLoS One*, vol. 8, no. 3, p. e59931, 2013.
- [59] P. De Santa Barbara, N. Bonneaud, B. Boizet, M. Desclozeaux, B. Moniot, P. Sudbeck, G. Scherer, F. Poulat, and P. Berta, "Direct interaction of SRY-related protein SOX9 and steroidogenic factor 1 regulates transcription of the human anti-Müllerian hormone gene," *Mol. Cell. Biol.*, vol. 18, no. 11, pp. 6653–6665, Nov. 1998.
- [60] A. M. Donson, N. S. Erwin, B. K. Kleinschmidt-DeMasters, J. R. Madden, S. O. Addo-Yobo, and N. K. Foreman, "Unique molecular characteristics of radiation-induced glioblastoma," *J. Neuropathol. Exp. Neurol.*, vol. 66, no. 8, pp. 740–749, Aug. 2007.
- [61] J. Downward, "Targeting RAS signalling pathways in cancer therapy," *Nat. Rev. Cancer*, vol. 3, no. 1, pp. 11–22, Jan. 2003.
- [62] C. Dravis, B. T. Spike, J. C. Harrell, C. Johns, C. L. Trejo, E. M. Southard-Smith, C. M. Perou, and G. M. Wahl, "Sox10 Regulates Stem/Progenitor and Mesenchymal Cell States in Mammary Epithelial Cells," *Cell Rep.*, vol. 12, no. 12, pp. 2035–2048, Sep. 2015.

- [63] H. Duez and B. Staels, "Rev-erb- α : an integrator of circadian rhythms and metabolism," *J. Appl. Physiol.*, vol. 107, no. 6, pp. 1972–1980, Dec. 2009.
- [64] K. A. Dutton, A. Pauliny, S. S. Lopes, S. Elworthy, T. J. Carney, J. Rauch, R. Geisler, P. Haffter, and R. N. Kelsh, "Zebrafish colourless encodes sox10 and specifies non-ectomesenchymal neural crest fates," *Dev. Camb. Engl.*, vol. 128, no. 21, pp. 4113–4125, Nov. 2001.
- [65] S. Elworthy, "Transcriptional regulation of mitfa accounts for the sox10 requirement in zebrafish melanophore development," *Development*, vol. 130, no. 12, pp. 2809–2818, Jun. 2003.
- [66] Y. Endo, N. Osumi, and Y. Wakamatsu, "Bimodal functions of Notch-mediated signaling are involved in neural crest formation during avian ectoderm development," *Dev. Camb. Engl.*, vol. 129, no. 4, pp. 863–873, Feb. 2002.
- [67] B. Felding-Habermann, E. Fransvea, T. E. O'Toole, L. Manzuk, B. Faha, and M. Hensler, "Involvement of tumor cell integrin α v β 3 in hematogenous metastasis of human melanoma cells," *Clin. Exp. Metastasis*, vol. 19, no. 5, pp. 427–436, 2002.
- [68] I. J. Fidler, "Timeline: The pathogenesis of cancer metastasis: the 'seed and soil' hypothesis revisited," *Nat. Rev. Cancer*, vol. 3, no. 6, pp. 453–458, Jun. 2003.
- [69] M. Finzsch, S. Schreiner, T. Kichko, P. Reeh, E. R. Tamm, M. R. Bösl, D. Meijer, and M. Wegner, "Sox10 is required for Schwann cell identity and progression beyond the immature Schwann cell stage," *J. Cell Biol.*, vol. 189, no. 4, pp. 701–712, May 2010.
- [70] M. Finzsch, C. C. Stolt, P. Lommes, and M. Wegner, "Sox9 and Sox10 influence survival and migration of oligodendrocyte precursors in the spinal cord by regulating PDGF receptor expression," *Development*, vol. 135, no. 4, pp. 637–646, Feb. 2008.
- [71] A. Fire, S. Xu, M. K. Montgomery, S. A. Kostas, S. E. Driver, and C. C. Mello, "Potent and specific genetic interference by double-stranded RNA in *Caenorhabditis elegans*," *Nature*, vol. 391, no. 6669, pp. 806–811, Feb. 1998.
- [72] A. Flammiger, R. Besch, A. L. Cook, T. Maier, R. A. Sturm, and C. Berking, "SOX9 and SOX10 but not BRN2 are required for nestin expression in human melanoma cells," *J. Invest. Dermatol.*, vol. 129, no. 4, pp. 945–953, Apr. 2009.
- [73] N. Y. Frank, A. Margaryan, Y. Huang, T. Schatton, A. M. Waaga-Gasser, M. Gasser, M. H. Sayegh, W. Sadee, and M. H. Frank, "ABC5-mediated doxorubicin transport and chemoresistance in human malignant melanoma," *Cancer Res.*, vol. 65, no. 10, pp. 4320–4333, May 2005.
- [74] R. J. Friedman, D. S. Rigel, and A. W. Kopf, "Early Detection of Malignant Melanoma: The Role of Physician Examination and Self-Examination of the Skin," *CA. Cancer J. Clin.*, vol. 35, no. 3, pp. 130–151, May 1985.
- [75] T. D. Fufa, M. L. Harris, D. E. Watkins-Chow, D. Levy, D. U. Gorkin, D. E. Gildea, L. Song, A. Safi, G. E. Crawford, E. V. Sviderskaya, D. C. Bennett, A. S. McCallion, S. K. Loftus, and W. J. Pavan, "Genomic analysis reveals distinct mechanisms and functional classes of SOX10-regulated genes in melanocytes," *Hum. Mol. Genet.*, vol. 24, no. 19, pp. 5433–5450, Oct. 2015.
- [76] S. Fujiwara, S. Hoshikawa, T. Ueno, M. Hirata, T. Saito, T. Ikeda, H. Kawaguchi, K. Nakamura, S. Tanaka, and T. Ogata, "SOX10 Transactivates S100B to Suppress Schwann Cell Proliferation and to Promote Myelination," *PLoS ONE*, vol. 9, no. 12, p. e115400, Dec. 2014.
- [77] K. Furuyama, Y. Kawaguchi, H. Akiyama, M. Horiguchi, S. Kodama, T. Kuhara, S. Hosokawa, A. Elbahrawy, T. Soeda, M. Koizumi, T. Masui, M. Kawaguchi, K. Takaori, R. Doi, E. Nishi, R. Kakinoki, J. M. Deng, R. R. Behringer, T. Nakamura, and S. Uemoto, "Continuous cell supply from a Sox9-expressing progenitor zone in adult liver, exocrine pancreas and intestine," *Nat. Genet.*, vol. 43, no. 1, pp. 34–41, Jan. 2011.
- [78] S. Gandini, F. Sera, M. S. Cattaruzza, P. Pasquini, R. Zanetti, C. Masini, P. Boyle, and C. F. Melchi, "Meta-analysis of risk factors for cutaneous melanoma: III. Family history, actinic damage and phenotypic factors," *Eur. J. Cancer Oxf. Engl. 1990*, vol. 41, no. 14, pp. 2040–2059, Sep. 2005.
- [79] M. I. García-Castro, C. Marcelle, and M. Bronner-Fraser, "Ectodermal Wnt function as a neural crest inducer," *Science*, vol. 297, no. 5582, pp. 848–851, Aug. 2002.

- [80] L. A. Garraway, H. R. Widlund, M. A. Rubin, G. Getz, A. J. Berger, S. Ramaswamy, R. Beroukhi, D. A. Milner, S. R. Granter, J. Du, C. Lee, S. N. Wagner, C. Li, T. R. Golub, D. L. Rimm, M. L. Meyerson, D. E. Fisher, and W. R. Sellers, "Integrative genomic analyses identify MITF as a lineage survival oncogene amplified in malignant melanoma," *Nature*, vol. 436, no. 7047, pp. 117–122, Jul. 2005.
- [81] T. R. Gershon, O. Oppenheimer, S. S. Chin, and W. L. Gerald, "Temporally Regulated Neural Crest Transcription Factors Distinguish Neuroectodermal Tumors of Varying Malignancy and Differentiation," *Neoplasia*, vol. 7, no. 6, pp. 575–584, Jun. 2005.
- [82] J. Ghislain and P. Charnay, "Control of myelination in Schwann cells: a Krox20 cis-regulatory element integrates Oct6, Brn2 and Sox10 activities," *EMBO Rep.*, vol. 7, no. 1, pp. 52–58, Jan. 2006.
- [83] C. Giacinti and A. Giordano, "RB and cell cycle progression," *Oncogene*, vol. 25, no. 38, pp. 5220–5227, Aug. 2006.
- [84] S. Giuliano, Y. Cheli, M. Ohanna, C. Bonet, L. Beuret, K. Bille, A. Loubat, V. Hofman, P. Hofman, G. Ponzio, P. Bahadoran, R. Ballotti, and C. Bertolotto, "Microphthalmia-Associated Transcription Factor Controls the DNA Damage Response and a Lineage-Specific Senescence Program in Melanomas," *Cancer Res.*, vol. 70, no. 9, pp. 3813–3822, May 2010.
- [85] V. K. Goel, A. J. F. Lazar, C. L. Warneke, M. S. Redston, and F. G. Haluska, "Examination of mutations in BRAF, NRAS, and PTEN in primary cutaneous melanoma," *J. Invest. Dermatol.*, vol. 126, no. 1, pp. 154–160, Jan. 2006.
- [86] M. Golob, R. Buettner, and A. K. Bosserhoff, "Characterization of a transcription factor binding site, specifically activating MIA transcription in melanoma," *J. Invest. Dermatol.*, vol. 115, no. 1, pp. 42–47, Jul. 2000.
- [87] E. L. Goode, G. Chenevix-Trench, H. Song, S. J. Ramus, M. Notaridou, K. Lawrenson, M. Widschwendter, R. A. Vierkant, M. C. Larson, S. K. Kjaer, M. J. Birrer, A. Berchuck, J. Schildkraut, I. Tomlinson, L. A. Kiemeny, L. S. Cook, J. Gronwald, M. Garcia-Closas, M. E. Gore, I. Campbell, A. S. Whittemore, R. Sutphen, C. Phelan, H. Anton-Culver, C. L. Pearce, D. Lambrechts, M. A. Rossing, J. Chang-Claude, K. B. Moysich, M. T. Goodman, T. Dörk, H. Nevanlinna, R. B. Ness, T. Rafnar, C. Hogdall, E. Hogdall, B. L. Fridley, J. M. Cunningham, W. Sieh, V. McGuire, A. K. Godwin, D. W. Cramer, D. Hernandez, D. Levine, K. Lu, E. S. Iversen, R. T. Palmieri, R. Houlston, A. M. van Altena, K. K. H. Aben, L. F. A. G. Massuger, A. Brooks-Wilson, L. E. Kelemen, N. D. Le, A. Jakubowska, J. Lubinski, K. Medrek, A. Stafford, D. F. Easton, J. Tyrer, K. L. Bolton, P. Harrington, D. Eccles, A. Chen, A. N. Molina, B. N. Davila, H. Arango, Y.-Y. Tsai, Z. Chen, H. A. Risch, J. McLaughlin, S. A. Narod, A. Ziogas, W. Brewster, A. Gentry-Maharaj, U. Menon, A. H. Wu, D. O. Stram, M. C. Pike, Wellcome Trust Case-Control Consortium, J. Beesley, P. M. Webb, Australian Cancer Study (Ovarian Cancer), Australian Ovarian Cancer Study Group, Ovarian Cancer Association Consortium (OCAC), X. Chen, A. B. Ekici, F. C. Thiel, M. W. Beckmann, H. Yang, N. Wentzensen, J. Lissowska, P. A. Fasching, E. Despiere, F. Amant, I. Vergote, J. Doherty, R. Hein, S. Wang-Gohrke, G. Lurie, M. E. Carney, P. J. Thompson, I. Runnebaum, P. Hillemanns, M. Dürst, N. Antonenkova, N. Bogdanova, A. Leminen, R. Butzow, T. Heikkinen, K. Stefansson, P. Sulem, S. Besenbacher, T. A. Sellers, S. A. Gayther, P. D. P. Pharoah, and Ovarian Cancer Association Consortium (OCAC), "A genome-wide association study identifies susceptibility loci for ovarian cancer at 2q31 and 8q24," *Nat. Genet.*, vol. 42, no. 10, pp. 874–879, Oct. 2010.
- [88] M. D. Goulding, G. Chalepakis, U. Deutsch, J. R. Erselius, and P. Gruss, "Pax-3, a novel murine DNA binding protein expressed during early neurogenesis," *EMBO J.*, vol. 10, no. 5, pp. 1135–1147, May 1991.
- [89] A. M. Gown, A. M. Vogel, D. Hoak, F. Gough, and M. A. McNutt, "Monoclonal antibodies specific for melanocytic tumors distinguish subpopulations of melanocytes," *Am. J. Pathol.*, vol. 123, no. 2, pp. 195–203, May 1986.
- [90] A. Graf, S. Krebs, M. Heininen-Brown, V. Zakhartchenko, H. Blum, and E. Wolf, "Genome activation in bovine embryos: review of the literature and new insights from RNA sequencing experiments," *Anim. Reprod. Sci.*, vol. 149, no. 1–2, pp. 46–58, Sep. 2014.

- [91] P. B. Gupta, C. Kuperwasser, J.-P. Brunet, S. Ramaswamy, W.-L. Kuo, J. W. Gray, S. P. Naber, and R. A. Weinberg, "The melanocyte differentiation program predisposes to metastasis after neoplastic transformation," *Nat. Genet.*, vol. 37, no. 10, pp. 1047–1054, Oct. 2005.
- [92] C. E. Haldin and C. LaBonne, "SoxE factors as multifunctional neural crest regulatory factors," *Int. J. Biochem. Cell Biol.*, vol. 42, no. 3, pp. 441–444, Mar. 2010.
- [93] E. K. Hale, J. Stein, L. Ben-Porat, K. S. Panageas, M. S. Eichenbaum, A. A. Marghoob, I. Osman, A. W. Kopf, and D. Polsky, "Association of melanoma and neurocutaneous melanocytosis with large congenital melanocytic naevi--results from the NYU-LCMN registry," *Br. J. Dermatol.*, vol. 152, no. 3, pp. 512–517, Mar. 2005.
- [94] V. Hamburger and H. L. Hamilton, "A series of normal stages in the development of the chick embryo. 1951," *Dev. Dyn. Off. Publ. Am. Assoc. Anat.*, vol. 195, no. 4, pp. 231–272, Dec. 1992.
- [95] D. Hanahan and R. A. Weinberg, "The hallmarks of cancer," *Cell*, vol. 100, no. 1, pp. 57–70, Jan. 2000.
- [96] H. Han, M. Myllykoski, S. Ruskamo, C. Wang, and P. Kursula, "Myelin-specific proteins: A structurally diverse group of membrane-interacting molecules," *BioFactors*, vol. 39, no. 3, pp. 233–241, May 2013.
- [97] G. J. Hannon, "RNA interference," *Nature*, vol. 418, no. 6894, pp. 244–251, Jul. 2002.
- [98] C. Haqq, M. Nosrati, D. Sudilovsky, J. Crothers, D. Khodabakhsh, B. L. Pulliam, S. Federman, J. R. Miller, R. E. Allen, M. I. Singer, S. P. L. Leong, B.-M. Ljung, R. W. Sagebiel, and M. Kashani-Sabet, "The gene expression signatures of melanoma progression," *Proc. Natl. Acad. Sci. U. S. A.*, vol. 102, no. 17, pp. 6092–6097, Apr. 2005.
- [99] R. Haq, J. Shoag, P. Andreu-Perez, S. Yokoyama, H. Edelman, G. C. Rowe, D. T. Frederick, A. D. Hurley, A. Nellore, A. L. Kung, J. A. Wargo, J. S. Song, D. E. Fisher, Z. Arany, and H. R. Widlund, "Oncogenic BRAF regulates oxidative metabolism via PGC1 α and MITF," *Cancer Cell*, vol. 23, no. 3, pp. 302–315, Mar. 2013.
- [100] J. W. Harper, G. R. Adami, N. Wei, K. Keyomarsi, and S. J. Elledge, "The p21 Cdk-interacting protein Cip1 is a potent inhibitor of G1 cyclin-dependent kinases," *Cell*, vol. 75, no. 4, pp. 805–816, Nov. 1993.
- [101] M. L. Harris, L. L. Baxter, S. K. Loftus, and W. J. Pavan, "Sox proteins in melanocyte development and melanoma," *Pigment Cell Melanoma Res.*, vol. 23, no. 4, pp. 496–513, Aug. 2010.
- [102] M. L. Harris, K. Buac, O. Shakhova, R. M. Hakami, M. Wegner, L. Sommer, and W. J. Pavan, "A Dual Role for SOX10 in the Maintenance of the Postnatal Melanocyte Lineage and the Differentiation of Melanocyte Stem Cell Progenitors," *PLoS Genet.*, vol. 9, no. 7, p. e1003644, Jul. 2013.
- [103] M. L. Harris, D. J. Levy, D. E. Watkins-Chow, and W. J. Pavan, "Ectopic differentiation of melanocyte stem cells is influenced by genetic background," *Pigment Cell Melanoma Res.*, vol. 28, no. 2, pp. 223–228, Mar. 2015.
- [104] K. Hayasaka, M. Himoro, G. Takada, E. Takahashi, S. Minoshima, and N. Shimizu, "Structure and localization of the gene encoding human peripheral myelin protein 2 (PMP2)," *Genomics*, vol. 18, no. 2, pp. 244–248, Nov. 1993.
- [105] K. Hayasaka, K. Nanao, M. Tahara, W. Sato, G. Takada, M. Miura, and K. Uyemura, "Isolation and sequence determination of cDNA encoding P2 protein of human peripheral myelin," *Biochem. Biophys. Res. Commun.*, vol. 181, no. 1, pp. 204–207, Nov. 1991.
- [106] M. V. Heppt, J. K. Tietze, S. A. Graf, and C. Berking, "Combination therapy of melanoma using kinase inhibitors," *Curr. Opin. Oncol.*, vol. 27, no. 2, pp. 134–140, Mar. 2015.
- [107] B. Herbarth, V. Pingault, N. Bondurand, K. Kuhlbrodt, I. Hermans-Borgmeyer, A. Puliti, N. Lemort, M. Goossens, and M. Wegner, "Mutation of the Sry-related Sox10 gene in Dominant megacolon, a mouse model for human Hirschsprung disease," *Proc. Natl. Acad. Sci. U. S. A.*, vol. 95, no. 9, pp. 5161–5165, Apr. 1998.
- [108] M. Herlyn, J. Thurin, G. Balaban, J. L. Bannicelli, D. Herlyn, D. E. Elder, E. Bondi, D. Guerry, P. Nowell, and W. H. Clark, "Characteristics of cultured human melanocytes isolated from different stages of tumor progression," *Cancer Res.*, vol. 45, no. 11 Pt 2, pp. 5670–5676, Nov. 1985.

- [109] F. S. Hodi, S. J. O'Day, D. F. McDermott, R. W. Weber, J. A. Sosman, J. B. Haanen, R. Gonzalez, C. Robert, D. Schadendorf, J. C. Hassel, W. Akerley, A. J. M. van den Eertwegh, J. Lutzky, P. Lorigan, J. M. Vaubel, G. P. Linette, D. Hogg, C. H. Ottensmeier, C. Lebbé, C. Peschel, I. Quirt, J. I. Clark, J. D. Wolchok, J. S. Weber, J. Tian, M. J. Yellin, G. M. Nichol, A. Hoos, and W. J. Urba, "Improved survival with ipilimumab in patients with metastatic melanoma," *N. Engl. J. Med.*, vol. 363, no. 8, pp. 711–723, Aug. 2010.
- [110] E. Hodis, I. R. Watson, G. V. Kryukov, S. T. Arold, M. Imielinski, J.-P. Theurillat, E. Nickerson, D. Auclair, L. Li, C. Place, D. DiCara, A. H. Ramos, M. S. Lawrence, K. Cibulskis, A. Sivachenko, D. Voet, G. Saksena, N. Stransky, R. C. Onofrio, W. Winckler, K. Ardlie, N. Wagle, J. Wargo, K. Chong, D. L. Morton, K. Stemke-Hale, G. Chen, M. Noble, M. Meyerson, J. E. Ladbury, M. A. Davies, J. E. Gershenwald, S. N. Wagner, D. S. B. Hoon, D. Schadendorf, E. S. Lander, S. B. Gabriel, G. Getz, L. A. Garraway, and L. Chin, "A Landscape of Driver Mutations in Melanoma," *Cell*, vol. 150, no. 2, pp. 251–263, Jul. 2012.
- [111] K. S. Hoek and C. R. Goding, "Cancer stem cells versus phenotype-switching in melanoma," *Pigment Cell Melanoma Res.*, vol. 23, no. 6, pp. 746–759, Dec. 2010.
- [112] K. S. Hoek, N. C. Schlegel, P. Brafford, A. Sucker, S. Ugurel, R. Kumar, B. L. Weber, K. L. Nathanson, D. J. Phillips, M. Herlyn, D. Schadendorf, and R. Dummer, "Metastatic potential of melanomas defined by specific gene expression profiles with no BRAF signature," *Pigment Cell Res.*, vol. 19, no. 4, pp. 290–302, Aug. 2006.
- [113] M. Y. Hsu, M. J. Wheelock, K. R. Johnson, and M. Herlyn, "Shifts in cadherin profiles between human normal melanocytes and melanomas," *J. Investig. Dermatol. Symp. Proc. Soc. Investig. Dermatol. Inc Eur. Soc. Dermatol. Res.*, vol. 1, no. 2, pp. 188–194, Apr. 1996.
- [114] B. A. Inman, X. Frigola, H. Dong, and E. D. Kwon, "Costimulation, coinhibition and cancer," *Curr. Cancer Drug Targets*, vol. 7, no. 1, pp. 15–30, Feb. 2007.
- [115] K. Inoue, M. Khajavi, T. Ohyama, S. Hirabayashi, J. Wilson, J. D. Reggin, P. Mancias, I. J. Butler, M. F. Wilkinson, M. Wegner, and J. R. Lupski, "Molecular mechanism for distinct neurological phenotypes conveyed by allelic truncating mutations," *Nat. Genet.*, vol. 36, no. 4, pp. 361–369, Apr. 2004.
- [116] K. Inoue, Y. Tanabe, and J. R. Lupski, "Myelin deficiencies in both the central and the peripheral nervous systems associated with a SOX10 mutation," *Ann. Neurol.*, vol. 46, no. 3, pp. 313–318, Sep. 1999.
- [117] S. Jamal and R. J. Schneider, "UV-induction of keratinocyte endothelin-1 downregulates E-cadherin in melanocytes and melanoma cells," *J. Clin. Invest.*, vol. 110, no. 4, pp. 443–452, Aug. 2002.
- [118] S.-W. Jang, R. Srinivasan, E. A. Jones, G. Sun, S. Keles, C. Krueger, L.-W. Chang, R. Nagarajan, and J. Svaren, "Locus-wide identification of Egr2/Krox20 regulatory targets in myelin genes," *J. Neurochem.*, vol. 115, no. 6, pp. 1409–1420, Dec. 2010.
- [119] Z. Jiao, R. Mollaaghababa, W. J. Pavan, A. Antonellis, E. D. Green, and T. J. Hornyak, "Direct interaction of Sox10 with the promoter of murine Dopachrome Tautomerase (Dct) and synergistic activation of Dct expression with Mitf," *Pigment Cell Res. Spons. Eur. Soc. Pigment Cell Res. Int. Pigment Cell Soc.*, vol. 17, no. 4, pp. 352–362, Aug. 2004.
- [120] K. Jimbow, W. C. Quevedo Jr, T. B. Fitzpatrick, and G. Szabo, "SOME ASPECTS OF MELANIN BIOLOGY: 1950–1975," *J. Invest. Dermatol.*, no. 67, pp. 72–89, 1976.
- [121] A. Jo, S. Denduluri, B. Zhang, Z. Wang, L. Yin, Z. Yan, R. Kang, L. L. Shi, J. Mok, M. J. Lee, and R. C. Haydon, "The versatile functions of Sox9 in development, stem cells, and human diseases," *Genes Dis.*, vol. 1, no. 2, pp. 149–161, Dec. 2014.
- [122] E. A. Jones, S.-W. Jang, G. M. Mager, L.-W. Chang, R. Srinivasan, N. G. Gokey, R. M. Ward, R. Nagarajan, and J. Svaren, "Interactions of Sox10 and Egr2 in myelin gene regulation," *Neuron Glia Biol.*, vol. 3, no. 4, pp. 377–387, Nov. 2007.
- [123] T. A. Jones, T. Bergfors, J. Sedzik, and T. Unge, "The three-dimensional structure of P2 myelin protein," *EMBO J.*, vol. 7, no. 6, pp. 1597–1604, Jun. 1988.
- [124] Y. Kamachi, M. Uchikawa, A. Tanouchi, R. Sekido, and H. Kondoh, "Pax6 and SOX2 form a co-DNA-binding partner complex that regulates initiation of lens development," *Genes Dev.*, vol. 15, no. 10, pp. 1272–1286, May 2001.

- [125] R. P. Kapur, "Early death of neural crest cells is responsible for total enteric aganglionosis in Sox10(Dom)/Sox10(Dom) mouse embryos," *Pediatr. Dev. Pathol. Off. J. Soc. Pediatr. Pathol. Paediatr. Pathol. Soc.*, vol. 2, no. 6, pp. 559–569, Dec. 1999.
- [126] R. N. Kelsh, "Sorting out Sox10 functions in neural crest development," *BioEssays News Rev. Mol. Cell. Dev. Biol.*, vol. 28, no. 8, pp. 788–798, Aug. 2006.
- [127] J. F. Kerr, A. H. Wyllie, and A. R. Currie, "Apoptosis: a basic biological phenomenon with wide-ranging implications in tissue kinetics," *Br. J. Cancer*, vol. 26, no. 4, pp. 239–257, Aug. 1972.
- [128] J. Kim, L. Lo, E. Dormand, and D. J. Anderson, "SOX10 maintains multipotency and inhibits neuronal differentiation of neural crest stem cells," *Neuron*, vol. 38, no. 1, pp. 17–31, Apr. 2003.
- [129] R. King, K. N. Weilbaecher, G. McGill, E. Cooley, M. Mihm, and D. E. Fisher, "Microphthalmia transcription factor. A sensitive and specific melanocyte marker for MelanomaDiagnosis," *Am. J. Pathol.*, vol. 155, no. 3, pp. 731–738, Sep. 1999.
- [130] R. King, K. N. Weilbaecher, G. McGill, E. Cooley, M. Mihm, and D. E. Fisher, "Microphthalmia transcription factor. A sensitive and specific melanocyte marker for MelanomaDiagnosis," *Am. J. Pathol.*, vol. 155, no. 3, pp. 731–738, Sep. 1999.
- [131] A. K. Knecht and M. Bronner-Fraser, "Induction of the neural crest: a multigene process," *Nat. Rev. Genet.*, vol. 3, no. 6, pp. 453–461, Jun. 2002.
- [132] W. Knoll, J. Peters, P. Kursula, Y. Gerelli, J. Ollivier, B. Demé, M. Telling, E. Kemner, and F. Natali, "Structural and dynamical properties of reconstituted myelin sheaths in the presence of myelin proteins MBP and P2 studied by neutron scattering," *Soft Matter*, vol. 10, no. 3, pp. 519–529, Jan. 2014.
- [133] W. Knoll, J. Peters, P. Kursula, Y. Gerelli, and F. Natali, "Influence of myelin proteins on the structure and dynamics of a model membrane with emphasis on the low temperature regime," *J. Chem. Phys.*, vol. 141, no. 20, p. 205101, Nov. 2014.
- [134] H. Kondoh, M. Uchikawa, and Y. Kamachi, "Interplay of Pax6 and SOX2 in lens development as a paradigm of genetic switch mechanisms for cell differentiation," *Int. J. Dev. Biol.*, vol. 48, no. 8–9, pp. 819–827, 2004.
- [135] M. Korabiowska, H. Betke, S. Kellner, J. Stachura, and A. Schauer, "Differential expression of growth arrest, DNA damage genes and tumour suppressor gene p53 in naevi and malignant melanomas," *Anticancer Res.*, vol. 17, no. 5A, pp. 3697–3700, Oct. 1997.
- [136] K. Koyanagi, S. J. O'Day, R. Gonzalez, K. Lewis, W. A. Robinson, T. T. Amatruda, C. Kuo, H.-J. Wang, R. Milford, D. L. Morton, and D. S. B. Hoon, "Microphthalmia transcription factor as a molecular marker for circulating tumor cell detection in blood of melanoma patients," *Clin. Cancer Res. Off. J. Am. Assoc. Cancer Res.*, vol. 12, no. 4, pp. 1137–1143, Feb. 2006.
- [137] D. Krahl and K. Sellheyer, "Sox9, more than a marker of the outer root sheath: spatiotemporal expression pattern during human cutaneous embryogenesis," *J. Cutan. Pathol.*, vol. 37, no. 3, pp. 350–356, Mar. 2010.
- [138] S. Krispin, E. Nitzan, Y. Kassem, and C. Kalcheim, "Evidence for a dynamic spatiotemporal fate map and early fate restrictions of premigratory avian neural crest," *Dev. Camb. Engl.*, vol. 137, no. 4, pp. 585–595, Feb. 2010.
- [139] K. Kuhlbrodt, B. Herbarth, E. Sock, I. Hermans-Borgmeyer, and M. Wegner, "Sox10, a novel transcriptional modulator in glial cells," *J. Neurosci. Off. J. Soc. Neurosci.*, vol. 18, no. 1, pp. 237–250, Jan. 1998.
- [140] L. A. Kunz-Schughart, "The Use of 3-D Cultures for High-Throughput Screening: The Multicellular Spheroid Model," *J. Biomol. Screen.*, vol. 9, no. 4, pp. 273–285, Jun. 2004.
- [141] S. Kuphal, R. Bauer, and A.-K. Bosserhoff, "Integrin signaling in malignant melanoma," *Cancer Metastasis Rev.*, vol. 24, no. 2, pp. 195–222, Jun. 2005.
- [142] C. LaBonne and M. Bronner-Fraser, "Neural crest induction in *Xenopus*: evidence for a two-signal model," *Dev. Camb. Engl.*, vol. 125, no. 13, pp. 2403–2414, Jul. 1998.
- [143] R. Lahav, G. Heffner, and P. H. Patterson, "An endothelin receptor B antagonist inhibits growth and induces cell death in human melanoma cells in vitro and in vivo," *Proc. Natl. Acad. Sci. U. S. A.*, vol. 96, no. 20, pp. 11496–11500, Sep. 1999.

- [144] D. P. Lane, "Cancer. p53, guardian of the genome," *Nature*, vol. 358, no. 6381, pp. 15–16, Jul. 1992.
- [145] D. Lang, F. Chen, R. Milewski, J. Li, M. M. Lu, and J. A. Epstein, "Pax3 is required for enteric ganglia formation and functions with Sox10 to modulate expression of c-ret," *J. Clin. Invest.*, vol. 106, no. 8, pp. 963–971, Oct. 2000.
- [146] D. Lang and J. A. Epstein, "Sox10 and Pax3 physically interact to mediate activation of a conserved c-RET enhancer," *Hum. Mol. Genet.*, vol. 12, no. 8, pp. 937–945, Apr. 2003.
- [147] J. Larkin, P. A. Ascierto, B. Dréno, V. Atkinson, G. Liskay, M. Maio, M. Mandalà, L. Demidov, D. Stroyakovskiy, L. Thomas, L. de la Cruz-Merino, C. Dutriaux, C. Garbe, M. A. Sovak, I. Chang, N. Choong, S. P. Hack, G. A. McArthur, and A. Ribas, "Combined vemurafenib and cobimetinib in BRAF-mutated melanoma," *N. Engl. J. Med.*, vol. 371, no. 20, pp. 1867–1876, Nov. 2014.
- [148] S. E. LeBlanc, S.-W. Jang, R. M. Ward, L. Wrabetz, and J. Svaren, "Direct regulation of myelin protein zero expression by the Egr2 transactivator," *J. Biol. Chem.*, vol. 281, no. 9, pp. 5453–5460, Mar. 2006.
- [149] S. E. LeBlanc, R. M. Ward, and J. Svaren, "Neuropathy-associated Egr2 mutants disrupt cooperative activation of myelin protein zero by Egr2 and Sox10," *Mol. Cell. Biol.*, vol. 27, no. 9, pp. 3521–3529, May 2007.
- [150] J.-H. Lee, J.-W. Choi, and Y.-S. Kim, "Frequencies of BRAF and NRAS mutations are different in histological types and sites of origin of cutaneous melanoma: a meta-analysis: BRAF and NRAS mutations in melanoma," *Br. J. Dermatol.*, vol. 164, no. 4, pp. 776–784, Apr. 2011.
- [151] K. Lee, S. Nam, E. Cho, I. Seong, J.-K. Limb, S. Lee, and J. Kim, "Identification of direct regulatory targets of the transcription factor Sox10 based on function and conservation," *BMC Genomics*, vol. 9, no. 1, p. 408, 2008.
- [152] M. Lee, J. Goodall, C. Verastegui, R. Ballotti, and C. R. Goding, "Direct regulation of the Microphthalmia promoter by Sox10 links Waardenburg-Shah syndrome (WS4)-associated hypopigmentation and deafness to WS2," *J. Biol. Chem.*, vol. 275, no. 48, pp. 37978–37983, Dec. 2000.
- [153] V. Lefebvre, W. Huang, V. R. Harley, P. N. Goodfellow, and B. de Crombrughe, "SOX9 is a potent activator of the chondrocyte-specific enhancer of the pro alpha1(II) collagen gene," *Mol. Cell. Biol.*, vol. 17, no. 4, pp. 2336–2346, Apr. 1997.
- [154] C. Levy, M. Khaled, and D. E. Fisher, "MITF: master regulator of melanocyte development and melanoma oncogene," *Trends Mol. Med.*, vol. 12, no. 9, pp. 406–414, Sep. 2006.
- [155] H. Lewis, W. Kaszubska, J. F. DeLamarter, and J. Whelan, "Cooperativity between two NF-kappa B complexes, mediated by high-mobility-group protein I(Y), is essential for cytokine-induced expression of the E-selectin promoter," *Mol. Cell. Biol.*, vol. 14, no. 9, pp. 5701–5709, Sep. 1994.
- [156] G. Li, H. Schaidler, K. Satyamoorthy, Y. Hanakawa, K. Hashimoto, and M. Herlyn, "Downregulation of E-cadherin and Desmoglein 1 by autocrine hepatocyte growth factor during melanoma development," *Oncogene*, vol. 20, no. 56, pp. 8125–8135, Dec. 2001.
- [157] H. Li, H. Zhu, C. J. Xu, and J. Yuan, "Cleavage of BID by caspase 8 mediates the mitochondrial damage in the Fas pathway of apoptosis," *Cell*, vol. 94, no. 4, pp. 491–501, Aug. 1998.
- [158] S. Ling, X. Chang, L. Schultz, T. K. Lee, A. Chaux, L. Marchionni, G. J. Netto, D. Sidransky, and D. M. Berman, "An EGFR-ERK-SOX9 Signaling Cascade Links Urothelial Development and Regeneration to Cancer," *Cancer Res.*, vol. 71, no. 11, pp. 3812–3821, Jun. 2011.
- [159] J. Liu, M. Fukunaga-Kalabis, L. Li, and M. Herlyn, "Developmental pathways activated in melanocytes and melanoma," *Arch. Biochem. Biophys.*, vol. 563, pp. 13–21, Dec. 2014.
- [160] G. V. Long, C. Fung, A. M. Menzies, G. M. Pupo, M. S. Carlino, J. Hyman, H. Shahheydari, V. Tembe, J. F. Thompson, R. P. Saw, J. Howle, N. K. Hayward, P. Johansson, R. A. Scolyer, R. F. Kefford, and H. Rizos, "Increased MAPK reactivation in early resistance to dabrafenib/trametinib combination therapy of BRAF-mutant metastatic melanoma," *Nat. Commun.*, vol. 5, p. 5694, Dec. 2014.

- [161] G. V. Long, D. Stroyakovskiy, H. Gogas, E. Levchenko, F. de Braud, J. Larkin, C. Garbe, T. Jouary, A. Hauschild, J. J. Grob, V. C. Sileni, C. Lebbe, M. Mandalà, M. Millward, A. Arance, I. Bondarenko, J. B. A. G. Haanen, J. Hansson, J. Utikal, V. Ferraresi, N. Kovalenko, P. Mohr, V. Probachai, D. Schadendorf, P. Nathan, C. Robert, A. Ribas, D. J. DeMarini, J. G. Irani, M. Casey, D. Ouellet, A.-M. Martin, N. Le, K. Patel, and K. Flaherty, "Combined BRAF and MEK Inhibition versus BRAF Inhibition Alone in Melanoma," *N. Engl. J. Med.*, p. 140930054051009, Sep. 2014.
- [162] G. V. Long, A. M. Menzies, A. M. Nagrial, L. E. Haydu, A. L. Hamilton, G. J. Mann, T. M. Hughes, J. F. Thompson, R. A. Scolyer, and R. F. Kefford, "Prognostic and Clinicopathologic Associations of Oncogenic BRAF in Metastatic Melanoma," *J. Clin. Oncol.*, vol. 29, no. 10, pp. 1239–1246, Apr. 2011.
- [163] C. M. Lovly, K. B. Dahlman, L. E. Fohn, Z. Su, D. Dias-Santagata, D. J. Hicks, D. Hucks, E. Berry, C. Terry, M. Duke, Y. Su, T. Sobolik-Delmaire, A. Richmond, M. C. Kelley, C. L. Vnencak-Jones, A. J. Iafrate, J. Sosman, and W. Pao, "Routine Multiplex Mutational Profiling of Melanomas Enables Enrollment in Genotype-Driven Therapeutic Trials," *PLoS ONE*, vol. 7, no. 4, p. e35309, Apr. 2012.
- [164] A. Ludwig, S. Rehberg, and M. Wegner, "Melanocyte-specific expression of dopachrome tautomerase is dependent on synergistic gene activation by the Sox10 and Mitf transcription factors," *FEBS Lett.*, vol. 556, no. 1–3, pp. 236–244, Jan. 2004.
- [165] X. Luo, I. Budihardjo, H. Zou, C. Slaughter, and X. Wang, "Bid, a Bcl2 interacting protein, mediates cytochrome c release from mitochondria in response to activation of cell surface death receptors," *Cell*, vol. 94, no. 4, pp. 481–490, Aug. 1998.
- [166] D. A. Lyons, H.-M. Pogoda, M. G. Voas, I. G. Woods, B. Diamond, R. Nix, N. Arana, J. Jacobs, and W. S. Talbot, "erbb3 and erbb2 Are Essential for Schwann Cell Migration and Myelination in Zebrafish," *Curr. Biol.*, vol. 15, no. 6, pp. 513–524, Mar. 2005.
- [167] L. MacPherson, L. Tamblyn, S. Rajendra, F. Bralha, J. P. McPherson, and J. Matthews, "2,3,7,8-Tetrachlorodibenzo-p-dioxin poly(ADP-ribose) polymerase (TiPARP, ARTD14) is a mono-ADP-ribosyltransferase and repressor of aryl hydrocarbon receptor transactivation," *Nucleic Acids Res.*, vol. 41, no. 3, pp. 1604–1621, Feb. 2013.
- [168] V. Majava, E. Polverini, A. Mazzini, R. Nanekar, W. Knoll, J. Peters, F. Natali, P. Baumgärtel, I. Kursula, and P. Kursula, "Structural and Functional Characterization of Human Peripheral Nervous System Myelin Protein P2," *PLoS ONE*, vol. 5, no. 4, p. e10300, Apr. 2010.
- [169] M. Maka, C. C. Stolt, and M. Wegner, "Identification of Sox8 as a modifier gene in a mouse model of Hirschsprung disease reveals underlying molecular defect," *Dev. Biol.*, vol. 277, no. 1, pp. 155–169, Jan. 2005.
- [170] A. Makowska, J. Pritchard, L. Sanvito, N. Gregson, M. Peakman, A. Hayday, and R. Hughes, "Immune responses to myelin proteins in Guillain-Barré syndrome," *J. Neurol. Neurosurg. Psychiatry*, vol. 79, no. 6, pp. 664–671, Jun. 2008.
- [171] S. Malki, F. Bibeau, C. Notarnicola, S. Roques, P. Berta, F. Poulat, and B. Boizet-Bonhoure, "Expression and biological role of the prostaglandin D synthase/SOX9 pathway in human ovarian cancer cells," *Cancer Lett.*, vol. 255, no. 2, pp. 182–193, Oct. 2007.
- [172] S. Malki, S. Nef, C. Notarnicola, L. Thevenet, S. Gasca, C. Méjean, P. Berta, F. Poulat, and B. Boizet-Bonhoure, "Prostaglandin D2 induces nuclear import of the sex-determining factor SOX9 via its cAMP-PKA phosphorylation," *EMBO J.*, vol. 24, no. 10, pp. 1798–1809, May 2005.
- [173] J. B. Mascarenhas, E. L. Littlejohn, R. J. Wolsky, K. P. Young, M. Nelson, R. Salgia, and D. Lang, "PAX3 and SOX10 activate MET receptor expression in melanoma," *Pigment Cell Melanoma Res.*, vol. 23, no. 2, pp. 225–237, Apr. 2010.
- [174] G. A. McArthur, P. B. Chapman, C. Robert, J. Larkin, J. B. Haanen, R. Dummer, A. Ribas, D. Hogg, O. Hamid, P. A. Ascierto, C. Garbe, A. Testori, M. Maio, P. Lorigan, C. Lebbé, T. Jouary, D. Schadendorf, S. J. O'Day, J. M. Kirkwood, A. M. Eggermont, B. Dréno, J. A. Sosman, K. T. Flaherty, M. Yin, I. Caro, S. Cheng, K. Trunzer, and A. Hauschild, "Safety and efficacy of vemurafenib in BRAF(V600E) and BRAF(V600K)

- mutation-positive melanoma (BRIM-3): extended follow-up of a phase 3, randomised, open-label study," *Lancet Oncol.*, vol. 15, no. 3, pp. 323–332, Mar. 2014.
- [175] J. M. McGregor, M. Newell, J. Ross, N. Kirkham, D. H. McGibbon, and C. Darley, "Cutaneous malignant melanoma and human immunodeficiency virus (HIV) infection: a report of three cases," *Br. J. Dermatol.*, vol. 126, no. 5, pp. 516–519, May 1992.
- [176] M. Miettinen, P. A. McCue, M. Sarlomo-Rikala, W. Biernat, P. Czapiewski, J. Kopczynski, L. D. Thompson, J. Lasota, Z. Wang, and J. F. Fetsch, "Sox10—a marker for not only schwannian and melanocytic neoplasms but also myoepithelial cell tumors of soft tissue: a systematic analysis of 5134 tumors," *Am. J. Surg. Pathol.*, vol. 39, no. 6, pp. 826–835, Jun. 2015.
- [177] A. J. Miller and H. Tsao, "New insights into pigmentary pathways and skin cancer," *Br. J. Dermatol.*, vol. 162, no. 1, pp. 22–28, Jan. 2010.
- [178] A. Mohamed, R. S. Gonzalez, D. Lawson, J. Wang, and C. Cohen, "SOX10 expression in malignant melanoma, carcinoma, and normal tissues," *Appl. Immunohistochem. Mol. Morphol. AIMM Off. Publ. Soc. Appl. Immunohistochem.*, vol. 21, no. 6, pp. 506–510, Dec. 2013.
- [179] R. Mollaaghababa and W. J. Pavan, "The importance of having your SOX on: role of SOX10 in the development of neural crest-derived melanocytes and glia," *Oncogene*, vol. 22, no. 20, pp. 3024–3034, May 2003.
- [180] F. Murisier, S. Guichard, and F. Beermann, "The tyrosinase enhancer is activated by Sox10 and Mitf in mouse melanocytes," *Pigment Cell Res. Spons. Eur. Soc. Pigment Cell Res. Int. Pigment Cell Soc.*, vol. 20, no. 3, pp. 173–184, Jun. 2007.
- [181] V. Muthusamy, C. Hobbs, C. Nogueira, C. Cordon-Cardo, P. H. McKee, L. Chin, and M. W. Bosenberg, "Amplification of CDK4 and MDM2 in malignant melanoma," *Genes. Chromosomes Cancer*, vol. 45, no. 5, pp. 447–454, May 2006.
- [182] D. M. Muzny, M. N. Bainbridge, K. Chang, H. H. Dinh, J. A. Drummond, G. Fowler, C. L. Kovar, L. R. Lewis, M. B. Morgan, I. F. Newsham, J. G. Reid, J. Santibanez, E. Shinbrot, L. R. Trevino, Y.-Q. Wu, M. Wang, P. Gunaratne, L. A. Donehower, C. J. Creighton, D. A. Wheeler, R. A. Gibbs, M. S. Lawrence, D. Voet, R. Jing, K. Cibulskis, A. Sivachenko, P. Stojanov, A. McKenna, E. S. Lander, S. Gabriel, G. Getz, L. Ding, R. S. Fulton, D. C. Koboldt, T. Wylie, J. Walker, D. J. Dooling, L. Fulton, K. D. Delehaunty, C. C. Fronick, R. Demeter, E. R. Mardis, R. K. Wilson, A. Chu, H.-J. E. Chun, A. J. Mungall, E. Pleasance, A. Gordon Robertson, D. Stoll, M. Balasundaram, I. Birol, Y. S. N. Butterfield, E. Chuah, R. J. N. Coope, N. Dhalla, R. Guin, C. Hirst, M. Hirst, R. A. Holt, D. Lee, H. I. Li, M. Mayo, R. A. Moore, J. E. Schein, J. R. Slobodan, A. Tam, N. Thiessen, R. Varhol, T. Zeng, Y. Zhao, S. J. M. Jones, M. A. Marra, A. J. Bass, A. H. Ramos, G. Saksena, A. D. Cherniack, S. E. Schumacher, B. Tabak, S. L. Carter, N. H. Pho, H. Nguyen, R. C. Onofrio, A. Crenshaw, K. Ardlie, R. Beroukhir, W. Winckler, G. Getz, M. Meyerson, A. Protopopov, J. Zhang, A. Hadjipanayis, E. Lee, R. Xi, L. Yang, X. Ren, H. Zhang, N. Sathiamoorthy, S. Shukla, P.-C. Chen, P. Haseley, Y. Xiao, S. Lee, J. Seidman, L. Chin, P. J. Park, R. Kucherlapati, J. Todd Auman, K. A. Hoadley, Y. Du, M. D. Wilkerson, Y. Shi, C. Liquori, S. Meng, L. Li, Y. J. Turman, M. D. Topal, D. Tan, S. Waring, E. Buda, J. Walsh, C. D. Jones, P. A. Mieczkowski, D. Singh, J. Wu, A. Gulabani, P. Dolina, T. Bodenheimer, A. P. Hoyle, J. V. Simons, M. Soloway, L. E. Mose, S. R. Jefferys, S. Balu, B. D. O'Connor, J. F. Prins, D. Y. Chiang, D. Neil Hayes, C. M. Perou, T. Hinoue, D. J. Weisenberger, D. T. Maglinte, F. Pan, B. P. Berman, D. J. Van Den Berg, H. Shen, T. Triche Jr, S. B. Baylin, P. W. Laird, G. Getz, M. Noble, D. Voet, G. Saksena, N. Gehlenborg, D. DiCara, J. Zhang, H. Zhang, C.-J. Wu, S. Yingchun Liu, S. Shukla, M. S. Lawrence, L. Zhou, A. Sivachenko, P. Lin, P. Stojanov, R. Jing, R. W. Park, M.-D. Nazaire, J. Robinson, H. Thorvaldsdottir, J. Mesirov, P. J. Park, L. Chin, V. Thorsson, S. M. Reynolds, B. Bernard, R. Kreisberg, J. Lin, L. Iype, R. Bressler, T. Erkkilä, M. Gundapuneni, Y. Liu, A. Norberg, T. Robinson, D. Yang, W. Zhang, I. Shmulevich, J. J. de Ronde, N. Schultz, E. Cerami, G. Ciriello, A. P. Goldberg, B. Gross, A. Jacobsen, J. Gao, B. Kaczkowski, R. Sinha, B. Arman Aksoy, Y. Antipin, B. Reva, R. Shen, B. S. Taylor, T. A. Chan, M. Ladanyi, C. Sander, R. Akbani, N. Zhang, B. M. Broom, T. Casasent, A. Unruh, C. Wakefield, S. R. Hamilton, R. Craig Cason, K. A. Baggerly, J. N.

- Weinstein, D. Haussler, C. C. Benz, J. M. Stuart, S. C. Benz, J. Zachary Sanborn, C. J. Vaske, J. Zhu, C. Szeto, G. K. Scott, C. Yau, S. Ng, T. Goldstein, K. Ellrott, E. Collisson, A. E. Cozen, D. Zerbino, C. Wilks, B. Craft, P. Spellman, R. Penny, T. Shelton, M. Hatfield, S. Morris, P. Yena, C. Shelton, M. Sherman, J. Paulauskis, J. M. Gastier-Foster, J. Bowen, N. C. Ramirez, A. Black, R. Pyatt, L. Wise, P. White, M. Bertagnolli, J. Brown, T. A. Chan, G. C. Chu, C. Czerwinski, F. Denstman, R. Dhir, A. Dörner, C. S. Fuchs, J. G. Guillem, M. Iacocca, H. Juhl, A. Kaufman, B. Kohl III, X. Van Le, M. C. Mariano, E. N. Medina, M. Meyers, G. M. Nash, P. B. Paty, N. Petrelli, B. Rabeno, W. G. Richards, D. Solit, P. Swanson, L. Temple, J. E. Tepper, R. Thorp, E. Vakiani, M. R. Weiser, J. E. Willis, G. Witkin, Z. Zeng, M. J. Zinner, C. Zornig, M. A. Jensen, R. Sfeir, A. B. Kahn, A. L. Chu, P. Kothiyal, Z. Wang, E. E. Snyder, J. Pontius, T. D. Pihl, B. Ayala, M. Backus, J. Walton, J. Whitmore, J. Baboud, D. L. Berton, M. C. Nicholls, D. Srinivasan, R. Raman, S. Girshik, P. A. Kigonya, S. Alonso, R. N. Sanbhadti, S. P. Barletta, J. M. Greene, D. A. Pot, K. R. Mills Shaw, L. A. L. Dillon, K. Buetow, T. Davidsen, J. A. Demchok, G. Eley, M. Ferguson, P. Fielding, C. Schaefer, M. Sheth, L. Yang, M. S. Guyer, B. A. Ozenberger, J. D. Palchik, J. Peterson, H. J. Sofia, and E. Thomson., "Comprehensive molecular characterization of human colon and rectal cancer," *Nature*, vol. 487, no. 7407, pp. 330–337, Jul. 2012.
- [183] P. G. Natali, M. R. Nicotra, A. B. Winkler, R. Cavaliere, A. Bigotti, and A. Ullrich, "Progression of human cutaneous melanoma is associated with loss of expression of c-kit proto-oncogene receptor," *Int. J. Cancer J. Int. Cancer*, vol. 52, no. 2, pp. 197–201, Sep. 1992.
- [184] R. Nazarian, H. Shi, Q. Wang, X. Kong, R. C. Koya, H. Lee, Z. Chen, M.-K. Lee, N. Attar, H. Sazegar, T. Chodon, S. F. Nelson, G. McArthur, J. A. Sosman, A. Ribas, and R. S. Lo, "Melanomas acquire resistance to B-RAF(V600E) inhibition by RTK or N-RAS upregulation," *Nature*, vol. 468, no. 7326, pp. 973–977, Dec. 2010.
- [185] E. A. Nigg, "Cyclin-dependent protein kinases: key regulators of the eukaryotic cell cycle," *BioEssays News Rev. Mol. Cell. Dev. Biol.*, vol. 17, no. 6, pp. 471–480, Jun. 1995.
- [186] E. K. Nishimura, S. R. Granter, and D. E. Fisher, "Mechanisms of hair graying: incomplete melanocyte stem cell maintenance in the niche," *Science*, vol. 307, no. 5710, pp. 720–724, Feb. 2005.
- [187] E. K. Nishimura, S. A. Jordan, H. Oshima, H. Yoshida, M. Osawa, M. Moriyama, I. J. Jackson, Y. Barrandon, Y. Miyachi, and S.-I. Nishikawa, "Dominant role of the niche in melanocyte stem-cell fate determination," *Nature*, vol. 416, no. 6883, pp. 854–860, Apr. 2002.
- [188] D. Nonaka, L. Chiriboga, and B. P. Rubin, "Sox10: a pan-schwannian and melanocytic marker," *Am. J. Surg. Pathol.*, vol. 32, no. 9, pp. 1291–1298, Sep. 2008.
- [189] M. D. Onken, L. A. Worley, M. D. Long, S. Duan, M. L. Council, A. M. Bowcock, and J. W. Harbour, "Oncogenic mutations in GNAQ occur early in uveal melanoma," *Invest. Ophthalmol. Vis. Sci.*, vol. 49, no. 12, pp. 5230–5234, Dec. 2008.
- [190] K. Opdecamp, A. Nakayama, M. T. Nguyen, C. A. Hodgkinson, W. J. Pavan, and H. Arnheiter, "Melanocyte development in vivo and in neural crest cell cultures: crucial dependence on the Mitf basic-helix-loop-helix-zipper transcription factor," *Dev. Camb. Engl.*, vol. 124, no. 12, pp. 2377–2386, Jun. 1997.
- [191] L. Ouyang, Z. Shi, S. Zhao, F.-T. Wang, T.-T. Zhou, B. Liu, and J.-K. Bao, "Programmed cell death pathways in cancer: a review of apoptosis, autophagy and programmed necrosis," *Cell Prolif.*, vol. 45, no. 6, pp. 487–498, Dec. 2012.
- [192] R. A. Padua, N. Barrass, and G. A. Currie, "A novel transforming gene in a human malignant melanoma cell line," *Nature*, vol. 311, no. 5987, pp. 671–673, Oct. 1984.
- [193] S. Paget, "The distribution of secondary growths in cancer of the breast. 1889," *Cancer Metastasis Rev.*, vol. 8, no. 2, pp. 98–101, Aug. 1989.
- [194] T. Passeron, J. C. Valencia, C. Bertolotto, T. Hoashi, E. Le Pape, K. Takahashi, R. Ballotti, and V. J. Hearing, "SOX9 is a key player in ultraviolet B-induced melanocyte differentiation and pigmentation," *Proc. Natl. Acad. Sci. U. S. A.*, vol. 104, no. 35, pp. 13984–13989, Aug. 2007.

- [195] T. Passeron, J. C. Valencia, T. Namiki, W. D. Vieira, H. Passeron, Y. Miyamura, and V. J. Hearing, "Upregulation of SOX9 inhibits the growth of human and mouse melanomas and restores their sensitivity to retinoic acid," *J. Clin. Invest.*, vol. 119, no. 4, pp. 954–963, Apr. 2009.
- [196] R. I. Peirano, D. E. Goerich, D. Riethmacher, and M. Wegner, "Protein zero gene expression is regulated by the glial transcription factor Sox10," *Mol. Cell. Biol.*, vol. 20, no. 9, pp. 3198–3209, May 2000.
- [197] R. I. Peirano and M. Wegner, "The glial transcription factor Sox10 binds to DNA both as monomer and dimer with different functional consequences," *Nucleic Acids Res.*, vol. 28, no. 16, pp. 3047–3055, Aug. 2000.
- [198] R. P. Perez, P. Zhang, A. K. Bosserhoff, R. Buettner, and M. Abu-Hadid, "Expression of melanoma inhibitory activity in melanoma and nonmelanoma tissue specimens," *Hum. Pathol.*, vol. 31, no. 11, pp. 1381–1388, Nov. 2000.
- [199] D. Pfeifer, F. Poulat, E. Holinski-Feder, F. Kooy, and G. Scherer, "The SOX8 gene is located within 700 kb of the tip of chromosome 16p and is deleted in a patient with ATR-16 syndrome," *Genomics*, vol. 63, no. 1, pp. 108–116, Jan. 2000.
- [200] V. Pingault, N. Bondurand, K. Kuhlbrodt, D. E. Goerich, M. O. Préhu, A. Puliti, B. Herbarth, I. Hermans-Borgmeyer, E. Legius, G. Matthijs, J. Amiel, S. Lyonnet, I. Ceccherini, G. Romeo, J. C. Smith, A. P. Read, M. Wegner, and M. Goossens, "SOX10 mutations in patients with Waardenburg-Hirschsprung disease," *Nat. Genet.*, vol. 18, no. 2, pp. 171–173, Feb. 1998.
- [201] P. M. Pollock, U. L. Harper, K. S. Hansen, L. M. Yudt, M. Stark, C. M. Robbins, T. Y. Moses, G. Hostetter, U. Wagner, J. Kakareka, G. Salem, T. Pohida, P. Heenan, P. Duray, O. Kallioniemi, N. K. Hayward, J. M. Trent, and P. S. Meltzer, "High frequency of BRAF mutations in nevi," *Nat. Genet.*, vol. 33, no. 1, pp. 19–20, Jan. 2003.
- [202] I. Poser, D. Domínguez, A. G. de Herreros, A. Varnai, R. Buettner, and A. K. Bosserhoff, "Loss of E-cadherin expression in melanoma cells involves up-regulation of the transcriptional repressor Snail," *J. Biol. Chem.*, vol. 276, no. 27, pp. 24661–24666, Jul. 2001.
- [203] I. Poser, M. Golob, R. Buettner, and A. K. Bosserhoff, "Upregulation of HMG1 leads to melanoma inhibitory activity expression in malignant melanoma cells and contributes to their malignancy phenotype," *Mol. Cell. Biol.*, vol. 23, no. 8, pp. 2991–2998, Apr. 2003.
- [204] I. Poser, M. Golob, M. Weidner, R. Buettner, and A. K. Bosserhoff, "Down-regulation of COOH-terminal binding protein expression in malignant melanomas leads to induction of MIA expression," *Cancer Res.*, vol. 62, no. 20, pp. 5962–5966, Oct. 2002.
- [205] I. Poser, J. Tatzel, S. Kuphal, and A. K. Bosserhoff, "Functional role of MIA in melanocytes and early development of melanoma," *Oncogene*, vol. 23, no. 36, pp. 6115–6124, Aug. 2004.
- [206] S. B. Potterf, M. Furumura, K. J. Dunn, H. Arnheiter, and W. J. Pavan, "Transcription factor hierarchy in Waardenburg syndrome: regulation of MITF expression by SOX10 and PAX3," *Hum. Genet.*, vol. 107, no. 1, pp. 1–6, Jul. 2000.
- [207] S. B. Potterf, R. Mollaaghababa, L. Hou, E. M. Southard-Smith, T. J. Hornyak, H. Arnheiter, and W. J. Pavan, "Analysis of SOX10 function in neural crest-derived melanocyte development: SOX10-dependent transcriptional control of dopachrome tautomerase," *Dev. Biol.*, vol. 237, no. 2, pp. 245–257, Sep. 2001.
- [208] M. K. Prasad, X. Reed, D. U. Gorkin, J. C. Cronin, A. R. McAdow, K. Chain, C. J. Hodonsky, E. A. Jones, J. Svaren, A. Antonellis, S. L. Johnson, S. K. Loftus, W. J. Pavan, and A. S. McCallion, "SOX10 directly modulates ERBB3 transcription via an intronic neural crest enhancer," *BMC Dev. Biol.*, vol. 11, p. 40, 2011.
- [209] V. W. Rebecca, G. M. Alicea, K. H. T. Paraiso, H. Lawrence, G. T. Gibney, and K. S. M. Smalley, "Vertical inhibition of the MAPK pathway enhances therapeutic responses in NRAS-mutant melanoma," *Pigment Cell Melanoma Res.*, vol. 27, no. 6, pp. 1154–1158, Nov. 2014.
- [210] J. A. Reed, B. Finnerty, and A. P. Albino, "Divergent Cellular Differentiation Pathways during the Invasive Stage of Cutaneous Malignant Melanoma Progression," *Am. J. Pathol.*, vol. 155, no. 2, pp. 549–555, Aug. 1999.

- [211] S. Reiprich, J. Kriesch, S. Schreiner, and M. Wegner, "Activation of Krox20 gene expression by Sox10 in myelinating Schwann cells," *J. Neurochem.*, vol. 112, no. 3, pp. 744–754, Feb. 2010.
- [212] S. Reiprich, C. C. Stolt, S. Schreiner, R. Parlato, and M. Wegner, "SoxE proteins are differentially required in mouse adrenal gland development," *Mol. Biol. Cell*, vol. 19, no. 4, pp. 1575–1586, Apr. 2008.
- [213] T. Reya, S. J. Morrison, M. F. Clarke, and I. L. Weissman, "Stem cells, cancer, and cancer stem cells," *Nature*, vol. 414, no. 6859, pp. 105–111, Nov. 2001.
- [214] A. Reynolds, D. Leake, Q. Boese, S. Scaringe, W. S. Marshall, and A. Khvorova, "Rational siRNA design for RNA interference," *Nat. Biotechnol.*, vol. 22, no. 3, pp. 326–330, Mar. 2004.
- [215] D. Riethmacher, E. Sonnenberg-Riethmacher, V. Brinkmann, T. Yamaai, G. R. Lewin, and C. Birchmeier, "Severe neuropathies in mice with targeted mutations in the ErbB3 receptor," *Nature*, vol. 389, no. 6652, pp. 725–730, Oct. 1997.
- [216] H. Rizos, A. M. Menzies, G. M. Pupo, M. S. Carlino, C. Fung, J. Hyman, L. E. Haydu, B. Mijatov, T. M. Becker, S. C. Boyd, J. Howle, R. Saw, J. F. Thompson, R. F. Kefford, R. A. Scolyer, and G. V. Long, "BRAF Inhibitor Resistance Mechanisms in Metastatic Melanoma: Spectrum and Clinical Impact," *Clin. Cancer Res.*, vol. 20, no. 7, pp. 1965–1977, Apr. 2014.
- [217] C. Robert, L. Thomas, I. Bondarenko, S. O'Day, J. Weber, C. Garbe, C. Lebbe, J.-F. Baurain, A. Testori, J.-J. Grob, N. Davidson, J. Richards, M. Maio, A. Hauschild, W. H. Miller, P. Gascon, M. Lotem, K. Harmankaya, R. Ibrahim, S. Francis, T.-T. Chen, R. Humphrey, A. Hoos, and J. D. Wolchok, "Ipilimumab plus dacarbazine for previously untreated metastatic melanoma," *N. Engl. J. Med.*, vol. 364, no. 26, pp. 2517–2526, Jun. 2011.
- [218] J. Roh, E. Cho, I. Seong, J. Limb, S. Lee, S. Han, and J. Kim, "Down-regulation of Sox10 with specific small interfering RNA promotes transdifferentiation of Schwannoma cells into myofibroblasts," *Differ. Res. Biol. Divers.*, vol. 74, no. 9–10, pp. 542–551, Dec. 2006.
- [219] S. Ruskamo, R. P. Yadav, S. Sharma, M. Lehtimäki, S. Laulumaa, S. Aggarwal, M. Simons, J. Bürck, A. S. Ulrich, A. H. Juffer, I. Kursula, and P. Kursula, "Atomic resolution view into the structure–function relationships of the human myelin peripheral membrane protein P2," *Acta Crystallogr. D Biol. Crystallogr.*, vol. 70, no. 1, pp. 165–176, Jan. 2014.
- [220] A. Saldana-Caboverde and L. Kos, "Roles of endothelin signaling in melanocyte development and melanoma," *Pigment Cell Melanoma Res.*, vol. 23, no. 2, pp. 160–170, Apr. 2010.
- [221] M. Sánchez-Martín, A. Rodríguez-García, J. Pérez-Losada, A. Sagrera, A. P. Read, and I. Sánchez-García, "SLUG (SNAI2) deletions in patients with Waardenburg disease," *Hum. Mol. Genet.*, vol. 11, no. 25, pp. 3231–3236, Dec. 2002.
- [222] A. Sarkar and K. Hochedlinger, "The sox family of transcription factors: versatile regulators of stem and progenitor cell fate," *Cell Stem Cell*, vol. 12, no. 1, pp. 15–30, Jan. 2013.
- [223] T. Sauka-Spengler and M. Bronner-Fraser, "A gene regulatory network orchestrates neural crest formation," *Nat. Rev. Mol. Cell Biol.*, vol. 9, no. 7, pp. 557–568, Jul. 2008.
- [224] T. Sauka-Spengler, D. Meulemans, M. Jones, and M. Bronner-Fraser, "Ancient evolutionary origin of the neural crest gene regulatory network," *Dev. Cell*, vol. 13, no. 3, pp. 405–420, Sep. 2007.
- [225] T. Schatton, G. F. Murphy, N. Y. Frank, K. Yamaura, A. M. Waaga-Gasser, M. Gasser, Q. Zhan, S. Jordan, L. M. Duncan, C. Weishaupt, R. C. Fuhlbrigge, T. S. Kupper, M. H. Sayegh, and M. H. Frank, "Identification of cells initiating human melanomas," *Nature*, vol. 451, no. 7176, pp. 345–349, Jan. 2008.
- [226] G. E. Schepers, M. Bullejos, B. M. Hosking, and P. Koopman, "Cloning and characterisation of the Sry-related transcription factor gene Sox8," *Nucleic Acids Res.*, vol. 28, no. 6, pp. 1473–1480, Mar. 2000.
- [227] G. E. Schepers, R. D. Teasdale, and P. Koopman, "Twenty pairs of sox: extent, homology, and nomenclature of the mouse and human sox transcription factor gene families," *Dev. Cell*, vol. 3, no. 2, pp. 167–170, Aug. 2002.

- [228] B. Schlierf, A. Ludwig, K. Klenovsek, and M. Wegner, "Cooperative binding of Sox10 to DNA: requirements and consequences," *Nucleic Acids Res.*, vol. 30, no. 24, pp. 5509–5516, Dec. 2002.
- [229] B. Schlierf, T. Werner, G. Glaser, and M. Wegner, "Expression of connexin47 in oligodendrocytes is regulated by the Sox10 transcription factor," *J. Mol. Biol.*, vol. 361, no. 1, pp. 11–21, Aug. 2006.
- [230] J. Schmidt, A. Riechers, and A.-K. Bosserhoff, "MIA--a new target protein for malignant melanoma therapy," *Histol. Histopathol.*, vol. 28, no. 4, pp. 421–426, Apr. 2013.
- [231] J. Schmidt, A. Riechers, R. Stoll, T. Amann, F. Fink, T. Spruss, W. Gronwald, B. König, C. Hellerbrand, and A. K. Bosserhoff, "Targeting Melanoma Metastasis and Immunosuppression with a New Mode of Melanoma Inhibitory Activity (MIA) Protein Inhibition," *PLoS ONE*, vol. 7, no. 5, p. e37941, May 2012.
- [232] N. L. Schoenewolf, C. Bull, B. Belloni, D. Holzmann, S. Tonolla, R. Lang, D. Mihic-Probst, C. Andres, and R. Dummer, "Sinonasal, genital and acrolentiginous melanomas show distinct characteristics of KIT expression and mutations," *Eur. J. Cancer Oxf. Engl. 1990*, vol. 48, no. 12, pp. 1842–1852, Aug. 2012.
- [233] M. A. Selleck, T. Y. Scherson, and M. Bronner-Fraser, "Origins of neural crest cell diversity," *Dev. Biol.*, vol. 159, no. 1, pp. 1–11, Sep. 1993.
- [234] D. Senft, C. Berking, S. A. Graf, C. Kammerbauer, T. Ruzicka, and R. Besch, "Selective Induction of Cell Death in Melanoma Cell Lines through Targeting of Mcl-1 and A1," *PLoS ONE*, vol. 7, no. 1, p. e30821, Jan. 2012.
- [235] I. Seong, H. J. Min, J.-H. Lee, C.-Y. Yeo, D. M. Kang, E.-S. Oh, E. S. Hwang, and J. Kim, "Sox10 controls migration of B16F10 melanoma cells through multiple regulatory target genes," *PLoS One*, vol. 7, no. 2, p. e31477, 2012.
- [236] A. H. Shain, I. Yeh, I. Kovalyshyn, A. Sriharan, E. Talevich, A. Gagnon, R. Dummer, J. North, L. Pincus, B. Ruben, W. Rickaby, C. D'Arrigo, A. Robson, and B. C. Bastian, "The Genetic Evolution of Melanoma from Precursor Lesions," *N. Engl. J. Med.*, vol. 373, no. 20, pp. 1926–1936, Nov. 2015.
- [237] O. Shakhova, "Neural crest stem cells in melanoma development," *Curr. Opin. Oncol.*, vol. 26, no. 2, pp. 215–221, Mar. 2014.
- [238] O. Shakhova, P. Cheng, P. J. Mishra, D. Zingg, S. M. Schaefer, J. Debbache, J. Häusel, C. Matter, T. Guo, S. Davis, P. Meltzer, D. Mihic-Probst, H. Moch, M. Wegner, G. Merlino, M. P. Levesque, R. Dummer, R. Santoro, P. Cinelli, and L. Sommer, "Antagonistic cross-regulation between Sox9 and Sox10 controls an anti-tumorigenic program in melanoma," *PLoS Genet.*, vol. 11, no. 1, p. e1004877, Jan. 2015.
- [239] O. Shakhova, D. Zingg, S. M. Schaefer, L. Hari, G. Civenni, J. Blunschli, S. Claudinot, M. Okoniewski, F. Beermann, D. Mihic-Probst, H. Moch, M. Wegner, R. Dummer, Y. Barrandon, P. Cinelli, and L. Sommer, "Sox10 promotes the formation and maintenance of giant congenital naevi and melanoma," *Nat. Cell Biol.*, vol. 14, no. 8, pp. 882–890, Aug. 2012.
- [240] Y. Shao and A. E. Aplin, "BH3-only protein silencing contributes to acquired resistance to PLX4720 in human melanoma," *Cell Death Differ.*, vol. 19, no. 12, pp. 2029–2039, Dec. 2012.
- [241] S. Sheth, X. Li, S. Binder, and S. M. Dry, "Differential gene expression profiles of neurothekeomas and nerve sheath myxomas by microarray analysis," *Mod. Pathol.*, vol. 24, no. 3, pp. 343–354, Mar. 2011.
- [242] H. Shi, A. Hong, X. Kong, R. C. Koya, C. Song, G. Moriceau, W. Hugo, C. C. Yu, C. Ng, T. Chodon, R. A. Scolyer, R. F. Kefford, A. Ribas, G. V. Long, and R. S. Lo, "A novel AKT1 mutant amplifies an adaptive melanoma response to BRAF inhibition," *Cancer Discov.*, vol. 4, no. 1, pp. 69–79, Jan. 2014.
- [243] J. Shin, J. G. Vincent, J. D. Cuda, H. Xu, S. Kang, J. Kim, and J. M. Taube, "Sox10 is expressed in primary melanocytic neoplasms of various histologies but not in fibrohistiocytic proliferations and histiocytoses," *J. Am. Acad. Dermatol.*, vol. 67, no. 4, pp. 717–726, Oct. 2012.

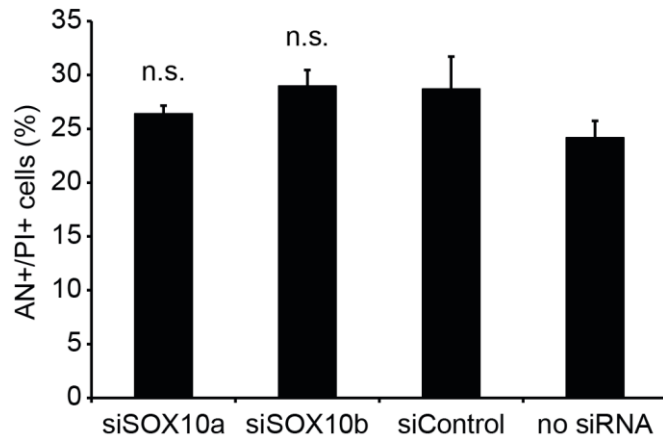
- [244] A. Slominski and R. Paus, "Melanogenesis is coupled to murine anagen: toward new concepts for the role of melanocytes and the regulation of melanogenesis in hair growth," *J. Invest. Dermatol.*, vol. 101, no. 1 Suppl, p. 90S–97S, Jul. 1993.
- [245] E. Sock, K. Schmidt, I. Hermanns-Borgmeyer, M. R. Bösl, and M. Wegner, "Idiopathic weight reduction in mice deficient in the high-mobility-group transcription factor Sox8," *Mol. Cell. Biol.*, vol. 21, no. 20, pp. 6951–6959, Oct. 2001.
- [246] E. Sonnenberg-Riethmacher, M. Mieke, C. C. Stolt, D. E. Goerich, M. Wegner, and D. Riethmacher, "Development and degeneration of dorsal root ganglia in the absence of the HMG-domain transcription factor Sox10," *Mech. Dev.*, vol. 109, no. 2, pp. 253–265, Dec. 2001.
- [247] E. M. Southard-Smith, M. Angrist, J. S. Ellison, R. Agarwala, A. D. Baxevasis, A. Chakravarti, and W. J. Pavan, "The Sox10(Dom) mouse: modeling the genetic variation of Waardenburg-Shah (WS4) syndrome," *Genome Res.*, vol. 9, no. 3, pp. 215–225, Mar. 1999.
- [248] E. M. Southard-Smith, L. Kos, and W. J. Pavan, "Sox10 mutation disrupts neural crest development in Dom Hirschsprung mouse model," *Nat. Genet.*, vol. 18, no. 1, pp. 60–64, Jan. 1998.
- [249] R. F. Spokony, Y. Aoki, N. Saint-Germain, E. Magner-Fink, and J.-P. Saint-Jeannet, "The transcription factor Sox9 is required for cranial neural crest development in *Xenopus*," *Dev. Camb. Engl.*, vol. 129, no. 2, pp. 421–432, Jan. 2002.
- [250] M. B. Sporn, "The war on cancer," *Lancet Lond. Engl.*, vol. 347, no. 9012, pp. 1377–1381, May 1996.
- [251] R. Srinivasan, G. Sun, S. Keles, E. A. Jones, S.-W. Jang, C. Krueger, J. J. Moran, and J. Svaren, "Genome-wide analysis of EGR2/SOX10 binding in myelinating peripheral nerve," *Nucleic Acids Res.*, vol. 40, no. 14, pp. 6449–6460, Aug. 2012.
- [252] J. Stahlecker, A. Gauger, A. Bosserhoff, R. Büttner, J. Ring, and R. Hein, "MIA as a reliable tumor marker in the serum of patients with malignant melanoma," *Anticancer Res.*, vol. 20, no. 6D, pp. 5041–5044, Dec. 2000.
- [253] L. Stanchina, V. Baral, F. Robert, V. Pingault, N. Lemort, V. Pachnis, M. Goossens, and N. Bondurand, "Interactions between Sox10, Edn3 and EdnrB during enteric nervous system and melanocyte development," *Dev. Biol.*, vol. 295, no. 1, pp. 232–249, Jul. 2006.
- [254] R. Stoll, "The extracellular human melanoma inhibitory activity (MIA) protein adopts an SH3 domain-like fold," *EMBO J.*, vol. 20, no. 3, pp. 340–349, Feb. 2001.
- [255] C. C. Stolt, P. Lommes, R. P. Friedrich, and M. Wegner, "Transcription factors Sox8 and Sox10 perform non-equivalent roles during oligodendrocyte development despite functional redundancy," *Dev. Camb. Engl.*, vol. 131, no. 10, pp. 2349–2358, May 2004.
- [256] C. C. Stolt, S. Rehberg, M. Ader, P. Lommes, D. Riethmacher, M. Schachner, U. Bartsch, and M. Wegner, "Terminal differentiation of myelin-forming oligodendrocytes depends on the transcription factor Sox10," *Genes Dev.*, vol. 16, no. 2, pp. 165–170, Jan. 2002.
- [257] C. C. Stolt and M. Wegner, "SoxE function in vertebrate nervous system development," *Int. J. Biochem. Cell Biol.*, vol. 42, no. 3, pp. 437–440, Mar. 2010.
- [258] C. C. Stolt and M. Wegner, "Schwann cells and their transcriptional network: Evolution of key regulators of peripheral myelination," *Brain Res.*, Sep. 2015.
- [259] M. S. Stonecypher, A. R. Chaudhury, S. J. Byer, and S. L. Carroll, "Neuregulin growth factors and their ErbB receptors form a potential signaling network for schwannoma tumorigenesis," *J. Neuropathol. Exp. Neurol.*, vol. 65, no. 2, pp. 162–175, Feb. 2006.
- [260] M. Subramaniam, J. R. Hawse, N. M. Rajamannan, J. N. Ingle, and T. C. Spelsberg, "Functional role of KLF10 in multiple disease processes," *BioFactors*, p. NA–NA, 2010.
- [261] C. Sun, L. Wang, S. Huang, G. J. J. E. Heynen, A. Prahallad, C. Robert, J. Haanen, C. Blank, J. Wesseling, S. M. Willems, D. Zecchin, S. Hobor, P. K. Bajpe, C. Liefink, C. Mateus, S. Vagner, W. Grenrum, I. Hofland, A. Schlicker, L. F. A. Wessels, R. L. Beijersbergen, A. Bardelli, F. Di Nicolantonio, A. M. M. Eggermont, and R. Bernards, "Reversible and adaptive resistance to BRAF(V600E) inhibition in melanoma," *Nature*, vol. 508, no. 7494, pp. 118–122, Apr. 2014.

- [262] S. Suresh, C. Wang, R. Nanekar, P. Kursula, and J. M. Edwardson, "Myelin basic protein and myelin protein 2 act synergistically to cause stacking of lipid bilayers," *Biochemistry (Mosc.)*, vol. 49, no. 16, pp. 3456–3463, Apr. 2010.
- [263] J. Svaren and D. Meijer, "The molecular machinery of myelin gene transcription in Schwann cells," *Glia*, vol. 56, no. 14, pp. 1541–1551, Nov. 2008.
- [264] A. Tang, M. S. Eller, M. Hara, M. Yaar, S. Hirohashi, and B. A. Gilchrist, "E-cadherin is the major mediator of human melanocyte adhesion to keratinocytes in vitro," *J. Cell Sci.*, vol. 107 (Pt 4), pp. 983–992, Apr. 1994.
- [265] M. Tassabehji, V. E. Newton, and A. P. Read, "Waardenburg syndrome type 2 caused by mutations in the human microphthalmia (MITF) gene," *Nat. Genet.*, vol. 8, no. 3, pp. 251–255, Nov. 1994.
- [266] D. Thanos and T. Maniatis, "The high mobility group protein HMG I(Y) is required for NF-kappa B-dependent virus induction of the human IFN-beta gene," *Cell*, vol. 71, no. 5, pp. 777–789, Nov. 1992.
- [267] P. Topilko, S. Schneider-Maunoury, G. Levi, A. Baron-Van Evercooren, A. B. Chennoufi, T. Seitanidou, C. Babinet, and P. Charnay, "Krox-20 controls myelination in the peripheral nervous system," *Nature*, vol. 371, no. 6500, pp. 796–799, Oct. 1994.
- [268] T. Torii, Y. Miyamoto, S. Takada, H. Tsumura, M. Arai, K. Nakamura, K. Ohbuchi, M. Yamamoto, A. Tanoue, and J. Yamauchi, "In vivo knockdown of ErbB3 in mice inhibits Schwann cell precursor migration," *Biochem. Biophys. Res. Commun.*, vol. 452, no. 3, pp. 782–788, Sep. 2014.
- [269] L. A. Torre, F. Bray, R. L. Siegel, J. Ferlay, J. Lortet-Tieulent, and A. Jemal, "Global cancer statistics, 2012: Global Cancer Statistics, 2012," *CA. Cancer J. Clin.*, vol. 65, no. 2, pp. 87–108, Mar. 2015.
- [270] H. Tsao, V. Goel, H. Wu, G. Yang, and F. G. Haluska, "Genetic interaction between NRAS and BRAF mutations and PTEN/MMAC1 inactivation in melanoma," *J. Invest. Dermatol.*, vol. 122, no. 2, pp. 337–341, Feb. 2004.
- [271] K. Ui-Tei, Y. Naito, F. Takahashi, T. Haraguchi, H. Ohki-Hamazaki, A. Juni, R. Ueda, and K. Saigo, "Guidelines for the selection of highly effective siRNA sequences for mammalian and chick RNA interference," *Nucleic Acids Res.*, vol. 32, no. 3, pp. 936–948, 2004.
- [272] E. M. Van Allen, N. Wagle, A. Sucker, D. J. Treacy, C. M. Johannessen, E. M. Goetz, C. S. Place, A. Taylor-Weiner, S. Whittaker, G. V. Kryukov, E. Hodis, M. Rosenberg, A. McKenna, K. Cibulskis, D. Farlow, L. Zimmer, U. Hillen, R. Gutzmer, S. M. Goldinger, S. Ugurel, H. J. Gogas, F. Egberts, C. Berking, U. Trefzer, C. Loquai, B. Weide, J. C. Hassel, S. B. Gabriel, S. L. Carter, G. Getz, L. A. Garraway, D. Schadendorf, and Dermatologic Cooperative Oncology Group of Germany (DeCOG), "The genetic landscape of clinical resistance to RAF inhibition in metastatic melanoma," *Cancer Discov.*, vol. 4, no. 1, pp. 94–109, Jan. 2014.
- [273] K. W. Vance and C. R. Goding, "The transcription network regulating melanocyte development and melanoma," *Pigment Cell Res. Spons. Eur. Soc. Pigment Cell Res. Int. Pigment Cell Soc.*, vol. 17, no. 4, pp. 318–325, Aug. 2004.
- [274] C. D. Van Raamsdonk, K. G. Griewank, M. B. Crosby, M. C. Garrido, S. Vemula, T. Wiesner, A. C. Obenaus, W. Wackernagel, G. Green, N. Bouvier, M. M. Sozen, G. Baimukanova, R. Roy, A. Heguy, I. Dolgalev, R. Khanin, K. Busam, M. R. Speicher, J. O'Brien, and B. C. Bastian, "Mutations in GNA11 in uveal melanoma," *N. Engl. J. Med.*, vol. 363, no. 23, pp. 2191–2199, Dec. 2010.
- [275] C. Verastegui, K. Bille, J. P. Ortonne, and R. Ballotti, "Regulation of the microphthalmia-associated transcription factor gene by the Waardenburg syndrome type 4 gene, SOX10," *J. Biol. Chem.*, vol. 275, no. 40, pp. 30757–30760, Oct. 2000.
- [276] B. Verhoven, R. A. Schlegel, and P. Williamson, "Mechanisms of phosphatidylserine exposure, a phagocyte recognition signal, on apoptotic T lymphocytes," *J. Exp. Med.*, vol. 182, no. 5, pp. 1597–1601, Nov. 1995.
- [277] J. Villanueva, A. Vultur, J. T. Lee, R. Somasundaram, M. Fukunaga-Kalabis, A. K. Cipolla, B. Wubbenhorst, X. Xu, P. A. Gimotty, D. Kee, A. E. Santiago-Walker, R. Letrero, K. D'Andrea, A. Pushparajan, J. E. Hayden, K. D. Brown, S. Laquerre, G. A. McArthur, J.

- A. Sosman, K. L. Nathanson, and M. Herlyn, "Acquired Resistance to BRAF Inhibitors Mediated by a RAF Kinase Switch in Melanoma Can Be Overcome by Cotargeting MEK and IGF-1R/PI3K," *Cancer Cell*, vol. 18, no. 6, pp. 683–695, Dec. 2010.
- [278] C. Vogel and E. M. Marcotte, "Insights into the regulation of protein abundance from proteomic and transcriptomic analyses," *Nat. Rev. Genet.*, Mar. 2012.
- [279] T. Wagner, J. Wirth, J. Meyer, B. Zabel, M. Held, J. Zimmer, J. Pasantes, F. D. Bricarelli, J. Keutel, E. Hustert, U. Wolf, N. Tommerup, W. Schempp, and G. Scherer, "Autosomal sex reversal and campomelic dysplasia are caused by mutations in and around the SRY-related gene SOX9," *Cell*, vol. 79, no. 6, pp. 1111–1120, Dec. 1994.
- [280] Y. Wakamatsu, M. Mochii, K. S. Vogel, and J. A. Weston, "Avian neural crest-derived neurogenic precursors undergo apoptosis on the lateral migration pathway," *Dev. Camb. Engl.*, vol. 125, no. 21, pp. 4205–4213, Nov. 1998.
- [281] T. Waldman, K. W. Kinzler, and B. Vogelstein, "p21 is necessary for the p53-mediated G1 arrest in human cancer cells," *Cancer Res.*, vol. 55, no. 22, pp. 5187–5190, Nov. 1995.
- [282] H. Wang, I. Leav, S. Ibaragi, M. Wegner, G. -f. Hu, M. L. Lu, S. P. Balk, and X. Yuan, "SOX9 Is Expressed in Human Fetal Prostate Epithelium and Enhances Prostate Cancer Invasion," *Cancer Res.*, vol. 68, no. 6, pp. 1625–1630, Mar. 2008.
- [283] H. Wang, N. C. McKnight, T. Zhang, M. L. Lu, S. P. Balk, and X. Yuan, "SOX9 Is Expressed in Normal Prostate Basal Cells and Regulates Androgen Receptor Expression in Prostate Cancer Cells," *Cancer Res.*, vol. 67, no. 2, pp. 528–536, Jan. 2007.
- [284] Y. Wang, D. Kojetin, and T. P. Burris, "Anti-proliferative actions of a synthetic REV-ERBa/β agonist in breast cancer cells," *Biochem. Pharmacol.*, vol. 96, no. 4, pp. 315–322, Aug. 2015.
- [285] K.-I. Watanabe, K. Takeda, K.-I. Yasumoto, T. Udono, H. Saito, K. Ikeda, T. Takasaka, K. Takahashi, T. Kobayashi, M. Tachibana, and S. Shibahara, "Identification of a distal enhancer for the melanocyte-specific promoter of the MITF gene," *Pigment Cell Res. Spons. Eur. Soc. Pigment Cell Res. Int. Pigment Cell Soc.*, vol. 15, no. 3, pp. 201–211, Jun. 2002.
- [286] Y. Watanabe, F. Broders-Bondon, V. Baral, P. Paul-Gilloteaux, V. Pingault, S. Dufour, and N. Bondurand, "Sox10 and Itgb1 interaction in enteric neural crest cell migration," *Dev. Biol.*, vol. 379, no. 1, pp. 92–106, Jul. 2013.
- [287] S. C. Weatherhead and C. M. Lawrence, "Melanoma screening clinics: are we detecting more melanomas or reassuring the worried well?," *Br. J. Dermatol.*, vol. 154, no. 3, pp. 539–541, Mar. 2006.
- [288] M. Wegner, "From head to toes: the multiple facets of Sox proteins," *Nucleic Acids Res.*, vol. 27, no. 6, pp. 1409–1420, Mar. 1999.
- [289] M. Wegner, "All purpose Sox: The many roles of Sox proteins in gene expression," *Int. J. Biochem. Cell Biol.*, vol. 42, no. 3, pp. 381–390, Mar. 2010.
- [290] B. Wehrle-Haller, "The role of Kit-ligand in melanocyte development and epidermal homeostasis," *Pigment Cell Res. Spons. Eur. Soc. Pigment Cell Res. Int. Pigment Cell Soc.*, vol. 16, no. 3, pp. 287–296, Jun. 2003.
- [291] M. C. Wei, W. X. Zong, E. H. Cheng, T. Lindsten, V. Panoutsakopoulou, A. J. Ross, K. A. Roth, G. R. MacGregor, C. B. Thompson, and S. J. Korsmeyer, "Proapoptotic BAX and BAK: a requisite gateway to mitochondrial dysfunction and death," *Science*, vol. 292, no. 5517, pp. 727–730, Apr. 2001.
- [292] T. Werner, A. Hammer, M. Wahlbuhl, M. R. Bösl, and M. Wegner, "Multiple conserved regulatory elements with overlapping functions determine Sox10 expression in mouse embryogenesis," *Nucleic Acids Res.*, vol. 35, no. 19, pp. 6526–6538, 2007.
- [293] B. Westermarck, A. Johnsson, Y. Paulsson, C. Betsholtz, C. H. Heldin, M. Herlyn, U. Rodeck, and H. Koprowski, "Human melanoma cell lines of primary and metastatic origin express the genes encoding the chains of platelet-derived growth factor (PDGF) and produce a PDGF-like growth factor," *Proc. Natl. Acad. Sci. U. S. A.*, vol. 83, no. 19, pp. 7197–7200, Oct. 1986.
- [294] R. M. White and L. I. Zon, "Melanocytes in Development, Regeneration, and Cancer," *Cell Stem Cell*, vol. 3, no. 3, pp. 242–252, Sep. 2008.

- [295] M. Z. Whitley, D. Thanos, M. A. Read, T. Maniatis, and T. Collins, "A striking similarity in the organization of the E-selectin and beta interferon gene promoters," *Mol. Cell. Biol.*, vol. 14, no. 10, pp. 6464–6475, Oct. 1994.
- [296] B. C. Willis, G. Johnson, J. Wang, and C. Cohen, "SOX10: a useful marker for identifying metastatic melanoma in sentinel lymph nodes," *Appl. Immunohistochem. Mol. Morphol. AIMM Off. Publ. Soc. Appl. Immunohistochem.*, vol. 23, no. 2, pp. 109–112, Feb. 2015.
- [297] S. Wissmüller, T. Kosian, M. Wolf, M. Finzsch, and M. Wegner, "The high-mobility-group domain of Sox proteins interacts with DNA-binding domains of many transcription factors," *Nucleic Acids Res.*, vol. 34, no. 6, pp. 1735–1744, 2006.
- [298] J. D. Wolchok, H. Kluger, M. K. Callahan, M. A. Postow, N. A. Rizvi, A. M. Lesokhin, N. H. Segal, C. E. Ariyan, R.-A. Gordon, K. Reed, M. M. Burke, A. Caldwell, S. A. Kronenberg, B. U. Agunwamba, X. Zhang, I. Lowy, H. D. Inzunza, W. Feely, C. E. Horak, Q. Hong, A. J. Korman, J. M. Wigginton, A. Gupta, and M. Sznol, "Nivolumab plus ipilimumab in advanced melanoma," *N. Engl. J. Med.*, vol. 369, no. 2, pp. 122–133, Jul. 2013.
- [299] W. F. Xie, X. Zhang, S. Sakano, V. Lefebvre, and L. J. Sandell, "Trans-activation of the mouse cartilage-derived retinoic acid-sensitive protein gene by Sox9," *J. Bone Miner. Res. Off. J. Am. Soc. Bone Miner. Res.*, vol. 14, no. 5, pp. 757–763, May 1999.
- [300] V. Yadav, X. Zhang, J. Liu, S. Estrem, S. Li, X.-Q. Gong, S. Buchanan, J. R. Henry, J. J. Starling, and S.-B. Peng, "Reactivation of Mitogen-activated Protein Kinase (MAPK) Pathway by FGF Receptor 3 (FGFR3)/Ras Mediates Resistance to Vemurafenib in Human B-RAF V600E Mutant Melanoma," *J. Biol. Chem.*, vol. 287, no. 33, pp. 28087–28098, Aug. 2012.
- [301] Y.-L. Yan, "A pair of Sox: distinct and overlapping functions of zebrafish sox9 co-orthologs in craniofacial and pectoral fin development," *Development*, vol. 132, no. 5, pp. 1069–1083, Feb. 2005.
- [302] J. Yie, S. Liang, M. Merika, and D. Thanos, "Intra- and intermolecular cooperative binding of high-mobility-group protein I(Y) to the beta-interferon promoter," *Mol. Cell. Biol.*, vol. 17, no. 7, pp. 3649–3662, Jul. 1997.
- [303] S. Yokoyama, K. Takeda, and S. Shibahara, "SOX10, in combination with Sp1, regulates the endothelin receptor type B gene in human melanocyte lineage cells," *FEBS J.*, vol. 273, no. 8, pp. 1805–1820, Apr. 2006.
- [304] R. J. Youle and A. Strasser, "The BCL-2 protein family: opposing activities that mediate cell death," *Nat. Rev. Mol. Cell Biol.*, vol. 9, no. 1, pp. 47–59, Jan. 2008.
- [305] J. Yuan, R. Adamski, and J. Chen, "Focus on histone variant H2AX: to be or not to be," *FEBS Lett.*, vol. 584, no. 17, pp. 3717–3724, Sep. 2010.
- [306] L. Zhu, H.-O. Lee, C. S. Jordan, V. A. Cantrell, E. M. Southard-Smith, and M. K. Shin, "Spatiotemporal regulation of endothelin receptor-B by SOX10 in neural crest-derived enteric neuron precursors," *Nat. Genet.*, vol. 36, no. 7, pp. 732–737, Jul. 2004.
- [307] "Freie Vorträge," *JDDG J. Dtsch. Dermatol. Ges.*, vol. 13, pp. 1–19, Aug. 2015.

7 Supplementary figures



SOX10 inhibition (one-way ANOVA versus siControl).

Figure S1: SOX10 inhibition in the SOX10-negative cell line WM3211.

Cell death was analyzed by staining with AN-Fluos and PI followed by flow cytometry in SOX10-negative WM3211 cells 96 hours after transfection of siSOX10a, siSOX10b, siControl, or no siRNA. AN- and PI-positive cells were examined in three independent experiments (mean \pm SD). No significant increase in AN- and PI-positive cell fractions could be detected after

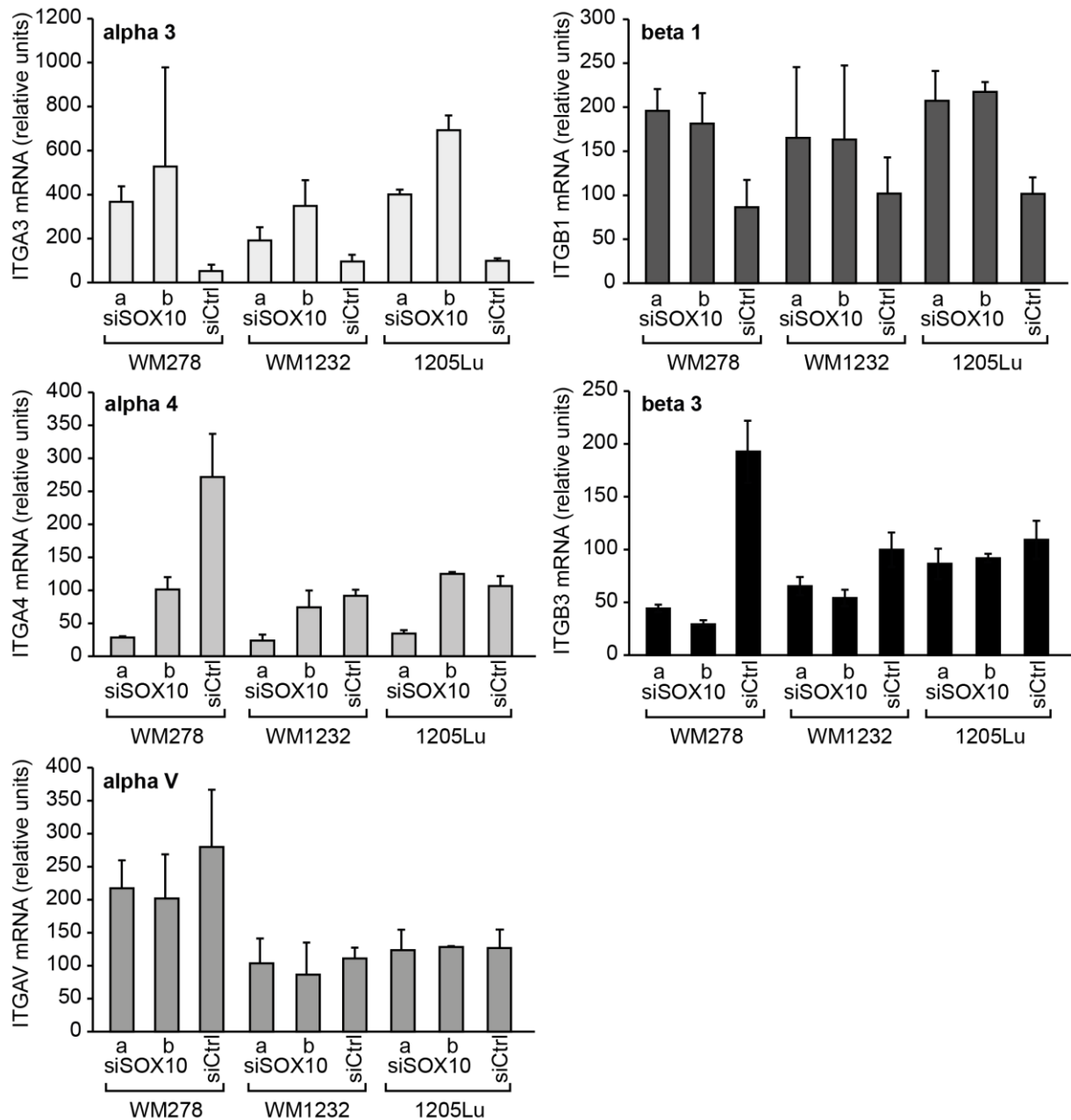


Figure S2: Expression of integrin α -subunits 3, 4, and V as well as integrin β -subunits 1 and 3 after SOX10 inhibition.

Expression of the integrin α -subunits 3 (ITGA3), 4 (ITGA4), and V (ITGAV) and the integrin β -subunits 1 (ITGB1) and 3 (ITGB3) was analyzed by qRT-PCR in cell lines WM278, WM1232, and 1205Lu (mean \pm SD of three independent experiments) 48 hours after transfection of siSOX10a, siSOX10b, or siControl (siCtrl). ITGA3 and ITGB1 were upregulated in all three cell lines after SOX10 inhibition. ITGA4 was downregulated with both SOX10-targeting siRNAs in WM278 and with siSOX10a in WM1232 and 1205Lu. ITGB3 was downregulated in SOX10-inhibited WM278 and WM1232. No change was found for ITGAV after SOX10 inhibition.

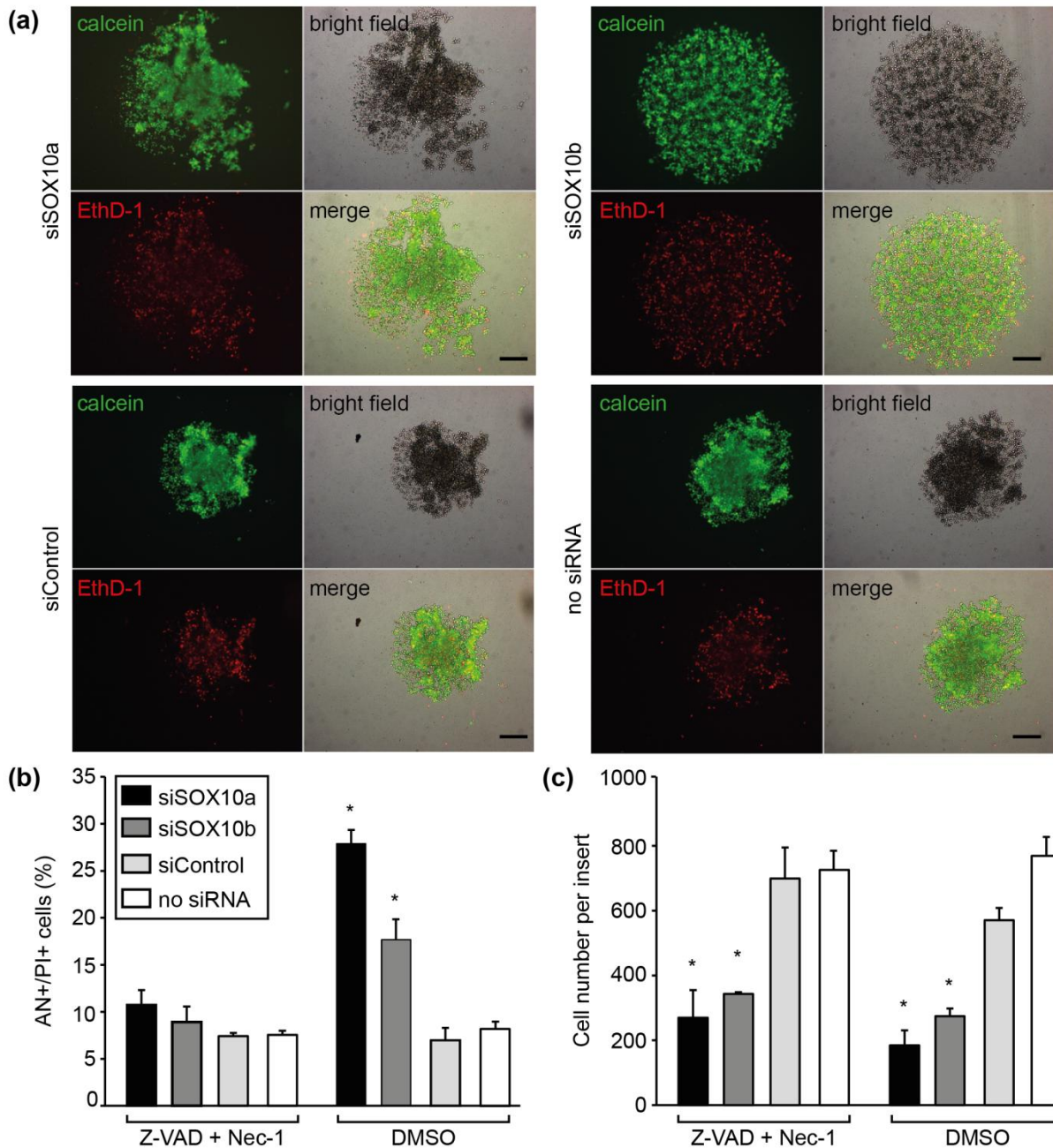


Figure S3: LIVE/DEAD staining of spheroids after SOX10 inhibition and Matrigel invasion assay after blocking cell death with Z-VAD and Nec-1.

(a) Representative pictures of spheroid formation 54 hours after transfection of siSOX10a, siSOX10b, siControl, or no siRNA, staining with calcein AM and EthD-1, and fluorescence microscopy are shown. Scale bar = 50 μ m. **(b)** 1205Lu cells were treated with Z-VAD and Nec-1 or DMSO and transfected with siSOX10a, siSOX10b, siControl, or no siRNA one hour later. Cell death by staining with Annexin V-Fluos and PI and subsequent flow cytometry was investigated after 96 hours. Onset of cell death upon SOX10 inhibition and with DMSO but not with Z-VAD and Nec-1 treatment was observed (mean \pm SD of three independent experiments; $*P < 0.0001$, one-way ANOVA versus siControl). **(c)** Cells were treated and transfected as described in (b). Matrigel invasion assays were carried out after 24 hours. SOX10 inhibition significantly reduced cell invasion as determined in three independent experiments ($*P < 0.0001$, one-way ANOVA versus siControl).

8 Abbreviations

°C	degree Celsius
ABAM	antibiotics and antimycotics
ABCB5	adenosine triphosphate binding cassette sub-family B member 5
ADP	adenosine diphosphate
AHR	aryl hydrocarbon receptor
AIDS	acquired immune deficiency syndrome
AIM1	absent in melanoma 1
ALM	acral lentiginous melanoma
AN	Annexin V
AP-2	activator protein 2
APAF-1	apoptotic protease activating factor 1
APAAP	alkaline phosphatase-anti-alkaline-phosphatase
APC	antigen presenting cell
bp	base pairs
BCA	bicinchoninic acid
Bcl-2	B-cell lymphoma 2
BH	Bcl-2 homology
BMP	bone morphogenetic protein
BRAF	V-Raf murine sarcoma viral oncogene homolog B
BSA	bovine serum albumin
cAMP	cyclic adenosine monophosphate
CDKs	cyclin-dependent kinases
cDNA	copy deoxyribonucleic acid
CMV	Cytomegalovirus
c-Myc	myelocytomatosis viral oncogene homolog c
ChIP	chromatin immunoprecipitation
CREB	cAMP response element-binding protein
CSH	cold spring harbor
CtBP1	COOH-terminal binding protein 1
CTLA-4	cytotoxic T-lymphocyte-associated protein 4
dT	deoxythymidine
DCT	dopachrome tautomerase
DIG	digoxigenin
DISC	death-inducing signaling complex
DLX	distal-less homeobox
DMEM	Dulbecco's modified Eagle Medium

DMSO	dimethyl sulfoxide
DNA	deoxyribonucleic acid
dNTP	deoxyribonucleotide triphosphate
ds	double-stranded
DTT	dithiothreitol
ECM	extracellular matrix
EDNRB	endothelin receptor type B
EDTA	ethylenediaminetetraacetic acid
e.g.	exempli gratia (Latin), for example
EGR2	early growth response 2
EHS	Engelbreth-Holm-Swarm
eIF-2 α	eukaryotic translation initiation factor 2 alpha
EMA	European medicines agency
EMEM	Eagle's Minimum Essential Medium
EMT	epithelial-to-mesenchymal transition
ERBB3	erb-b2 receptor tyrosine kinase 3
ERK	extracellular signal-related kinase
EthD-1	ethidium homodimer-1
FABP	fatty acid binding protein
FACS	fluorescence-associated cell sorting
FADD	Fas-associated protein with death domain
FBS	fetal bovine serum
FDA	Food and drug administration
FGF	fibroblast growth factor
FGFR	fibroblast growth factor receptor
FOXD3	forkhead box D3
FTL	ferritin light polypeptide 1
G1-phase	gap-phase 1
G2-phase	gap-phase 2
GAP-43	growth-associated phosphoprotein-43
GF	growth factor
GH1	growth hormone 1
GNA11	guanine nucleotide binding protein 11
GNAQ	guanine nucleotide binding protein Q
GTP	guanosine triphosphate
H1FX-AS1	H1FX antisense RNA 1
hAct Int2	human actin intron 2

HBSS	Hank's balanced salt solution
HEPES	4- (2-hydroxyethyl)-1-piperazinethanesulfonic acid
HMB45	human melanoma black 45
HMG	high-mobility group
HMGS-2	human melanocyte growth supplement-2
HPRT	hypoxanthin-guanine phosphoribosyltransferase
HRP	horse radish peroxydase
IARC	International Agency for Research on Cancer
Id	inhibitor of DNA-binding protein
i.e.	id est (Latin), that is
IFN	interferon
IGF1R	insulin-like growth factor 1 receptor
IHC	immunohistochemistry
IL-2	interleukin-2
ITGA	integrin alpha
ITGB	integrin beta
IUPAC	International Union of pure and Applied Chemistry
kb	kilo base pairs
kDa	kilo Dalton
KLF10	Krueppel-like factor 10
LB	Luria-Bertani broth
Lef1	lymphoid enhancer-binding factor-1
M	molar = mol/l
M-phase	mitosis
MAG	myelin-associated glycoprotein
MAPK	mitogen-activated protein kinase
MBP	myelin basic protein
MC1R	melanocortin 1 receptor
McSCs	melanocyte stem cells
MEK	mitogen-activated protein kinase kinase
MeI-CAM	melanoma cell adhesion molecule
MIA	melanoma inhibitory activity
MIB1	mindbomb E3 ubiquitin protein ligase 1
MITF	microphthalmia-associated transcription factor
MLANA	melanoma antigen
MPZ	myelin protein zero
mRNA	messenger RNA

MSX	msh homeobox
NADPH	nicotinamide adenine dinucleotide phosphate
N-CAM	neural cell adhesion molecule
NCBI	National Center for Biotechnology Information
NCC	neural crest cell
NF1	neurofibromin 1
NFκB	nuclear factor kappa B
NR1D1	Nuclear receptor subfamily 1, group D, member 1
n.s.	not significant
p.a.	per analysi
PARP1	poly (ADP-ribose) polymerase-1
PAX	paired box protein
PBS	phosphate-buffered saline
PCD	programmed cell death
PCR	polymerase chain reaction
PCWH	Peripheral demyelinating neuropathy, central dysmyelination, Waardenburg syndrome, and Hirschsprung disease
PD-1	programmed cell death 1 receptor
PD-L1	programmed cell death ligand 1
PDGFR	platelet-derived growth factor receptor
PI	propidium iodide
piRNA	PIWI interacting RNA
PIWI	P-element induced wimpy testis
PI3K	phosphoinositide 3-kinase
PIK3CA	phosphatidylinositol-4,5-bisphosphate 3-kinase catalytic subunit alpha
PIPES	piperazine-N,N'bis(2-ethanesulfonic acid)
PKA	protein kinase A
PLP1	proteolipid protein 1
PMP2	peripheral myelin protein 2
PPP1R15A	Protein phosphatase 1 regulatory subunit 15A
pRB	phosphorylated retinoblastoma protein
PS	phosphatidyl serine
PTEN	phosphatase and tensin homolog
PVDF	polyvinylidene fluoride
qRT-PCR	quantitative real-time PCR
rel. u.	relative units
RGP	radial growth phase

RISC	RNA-induced silencing complex
RIP	receptor interacting protein
RNA	ribonucleic acid
RNAi	RNA interference
RPL27a	ribosomal protein 27 a
rpm	revolutions per minute
RTK	receptor tyrosine kinase
RT-PCR	reverse transcriptase PCR
S-phase	synthesis phase
SD	standard deviation
SDS	sodium dodecyl sulfate
siRNA	small interfering RNA
shRNA	small hairpin RNA
SOX	(sex determining region-Y)-box
SRY	sex determining region-Y
TBX2	T-box 2
TCDD	2, 3, 7, 8-Tetrachlorodibenzo-p-dioxin
TCTAP2 α	transcription factor Ap-2 alpha
TERT	telomerase reverse transcriptase
TF	transcription factor
TIPARP	TCDD-inducible poly (ADP-ribose) polymerase
TNF	tumor necrosis factor
TP53	tumor protein 53
TRAIL	TNF-related apoptosis-inducing ligand
Tris	Tris(hydroxymethyl)aminomethane
TYRP1	Tyrosinase-related protein 1
UV	ultraviolet
VGP	vertical growth phase
Wnt	wingless
w/v	weight per volume
ZIC1	zink finger protein 1

9 Acknowledgements

First of all, I want to thank my supervisor Prof. Dr. Carola Berking for giving me the opportunity to work in her laboratory on this interesting topic. Thank you for your advices and your confidence in my skills. The tasks you gave me let me learn a lot and helped to develop myself.

I am most grateful to Prof. Dr. Karl-Peter Hopfner, who represents my thesis at the Department of Chemistry and Pharmacy at the LMU. Accordingly, I would like to thank PD Dr. Silke Kuphal, PD Dr. Dr. Christian Grimm, Prof. Dr. Klaus Förstemann, and Prof. Dr. Mario Halic for reviewing my work and participating in the defence of my thesis.

Thanks also to PD Dr. Robert Besch for his ideas and his guidance during the first years of my work in the laboratory.

I would like to thank Prof. Dr. Anja Bosserhoff, who initiated the German Melanoma Research Network, creating an interesting and informative scientific platform that gave a basis for fruitful discussions and collaborations during the last 4 years. Furthermore, Prof. Bosserhoff was a great support for my project. Many thanks to my other collaborators: Dr. Christian Busch, Dr. Tobias Sinnberg, Dr. Heike Niessner, PD Dr. Silke Kuphal, Dr. Melanie Kappelmann, and Corinna Kosnopfel. Corinna, Heike and Melanie, it has always been a pleasure to visit you and to meet you at conferences.

I am deeply grateful to have spent the last years in the lab in a friendly atmosphere together with my great colleagues. My special thanks go to Claudia Kammerbauer, our “angel of the lab”, not only helping me in case of lab affairs, but also to have always an open ear for everything. Thanks to Dr. Daniela Senft for introducing me into the lab’s daily routine. Thank you so much, Dr. Markus Heppt and Dr. Akiko Arakawa for interesting discussions and for your amicable support. Claudia, Eva, and Annamarie, it has been a great and joyful experience to work with so much “women power”.

Besides the lab, I want to thank my family and friends, especially Sonja and Sarah, to spend so much happy times together and to wake me up when I was sunken in (scientific) thoughts.

Last but not least, I want to thank the people to whom this work is dedicated to. Thank you, Mum and Dad, for your endless love and support. Without you, I would have never ever come this far. Mum, without your encouraging words, I would have been often lost. Simon, words cannot express my feelings for you. Thank you for everything you are and everything you have done for me.

10 Curriculum vitae

Personal data

Name: Saskia Anna Graf
 Academic degree: Dipl.-Biochem. (Univ.)
 Address: Rapotostr. 8, D-80687 Munich
 Date of birth: 10th August 1985
 Place of birth: Neumarkt in der Oberpfalz
 Email: saskia.graf@med.uni-muenchen.de



Education and Academic Career

Since 07/2011 Doctoral thesis
 Ludwig Maximilian University of Munich
 Department of Dermatology (Prof. Dr. Carola Berking)

10/2010 – 06/2011 Scientific assistant
 University of Regensburg
 Department of Biochemistry III (Prof. Dr. Herbert
 Tschochner)

10/2005 – 09/2010 Studies of Biochemistry (Diploma), overall grade 1.1
 University of Regensburg
 Diploma thesis at the Department of Biochemistry III (Prof.
 Dr. Herbert Tschochner) with the title “Experiments to
 reconstitute the RNA polymerase I transcription machinery of
 saccharomyces cerevisiae”

03 – 06/2009 Foreign internship
 University of New South Wales, Sydney, Australia
 School of Biotechnology and Biomolecular Sciences (Prof.
 Ian Dawes)

09/1996 – 06/2005 Final secondary-school examination, overall grade 1.6
 Willibald-Gluck-Gymnasium in Neumarkt i. d. Opf.

Publications

Graf SA, Krebs S, Hornig E, Heppt MV, Kammerbauer C, Hamel A, Besch R, Blum H,
 Berking C. The myelin protein PMP2 is regulated by SOX10 and drives

- melanoma cell invasion. (2015). Manuscript in preparation for the *Journal of Investigative Dermatology*.
- Heppt MV, Graf SA, Berking C. Aktuelle Therapieoptionen beim fortgeschrittenen Melanom. Tumorzentrum München Jahrbuch 2016. *Agileum Verlag & Gesundheitsakademie GmbH*, ISBN 978-3-939415-25-1 (2016)
- Heppt MV, Tietze JK, Graf SA, Berking C. Combination therapy of melanoma using kinase inhibitors. *Current Opinion in Oncology* 27: 134-40 (2015) Review Impact Factor 4.466
- Graf SA, Busch C, Bosserhoff AK, Besch R, Berking C. SOX10 promotes melanoma cell invasion by regulating melanoma inhibitory activity. *Journal of Investigative Dermatology* 134: 2212-20 (2014) Impact Factor 7.216
- Hohenauer T, Berking C, Schmidt A, Haferkamp S, Senft D, Kammerbauer C, Fraschka S, Graf SA, Irmeler M, Beckers J, Flaig M, Aigner A, Höbel S, Hoffmann F, Hermeking H, Rothenfusser S, Endres S, Ruzicka T, Besch R. The neural crest transcription factor Brn3a is expressed in melanoma and required for cell cycle progression and survival. *EMBO Molecular Medicine* 5: 919-34 (2013) Impact Factor 8.245
- Senft D, Berking C, Graf SA, Kammerbauer C, Ruzicka T, Besch R. Selective induction of cell death in melanoma cell lines through targeting of Mcl-1 and A1. *Plos One* 7: e30821 (2012) Impact Factor 3.73

Abstracts

- Graf SA, Busch C, Bosserhoff AK, Krebs S, Blum H, Besch R, Berking C. Neue Zielgene von SOX10 im Melanom. New target genes of SOX10 in melanoma. *Pigment Cell and Melanoma Research*. Volume 27, Issue 6, 1194 (2014)
- Graf SA, Busch C, Bosserhoff AK, Irmeler M, Besch R, Berking C. The role of SOX10 in melanoma cell invasion. *Experimental Dermatology*. Issue 23, e42 (2014)
- Graf SA, Busch C, Bosserhoff AK, Irmeler M, Besch R, Berking C. SOX10 promotes melanoma cell invasion by regulating melanoma inhibitory activity (MIA). *Pigment Cell and Melanoma Research*. Volume 26, Issue 6, 955 (2013)
- Graf SA, Busch C, Bosserhoff AK, Irmeler M, Besch R, Berking C. SOX10 promotes melanoma cell invasion by regulating melanoma inhibitory activity (MIA). 6th *Mildred Scheel Cancer Conference*, Königswinter, Poster 25 (2013)
- Graf SA, Bosserhoff AK, Irmeler M, Ruzicka T, Besch R, Berking C. The neural transcription factor SOX10 promotes melanoma cell invasion and regulates

migration-associated genes. *Pigment Cell and Melanoma Research*. Volume 25, Issue 6, 860 (2012)

Graf SA, Besch R, Berking C. Characterizing the role of SOX9 and SOX10 in melanoma. *Experimental Dermatology*. Issue 21, e42 (2012)

Oral presentations

Graf SA, Krebs S, Blum H, Besch R, Berking C. PMP2, a major myelin protein in Schwann cells, is regulated by SOX10 and drives melanoma cell invasion. *Journal der Deutschen Dermatologischen Gesellschaft*. Volume 13, Issue Supplement S2, page 9, FV22 (2015)

Graf SA, Busch C, Bosserhoff AK, Krebs S, Blum H, Besch R, Berking C. Neue Zielgene von SOX10 im Melanom. *Journal der Deutschen Dermatologischen Gesellschaft* Volume 12, Issue Supplement s3, page 39 (2014)

Graf SA. SOX10 promotes melanoma cell invasion by regulating melanoma inhibitory activity (MIA). *5th Novartis Research Oncology Day*, Nürnberg. (2013)

Graf SA, Busch C, Bosserhoff AK, Irmeler M, Besch R, Berking C. The neural transcription factor SOX10 promotes melanoma cell invasion and regulates migration-associated genes. *Experimental Dermatology*. Issue 22, e41 (2013)

Granted funds

Helmut Legerlotz-Foundation, Title "Targeted combination therapy of inhibitor-resistant melanoma cells", October 2014, 12,000 €

Follow up grant from the *Legerlotz-Foundation*, November 2015, 12,000 €

Hiege Foundation against skin cancer, Title "Targeted combination therapy of inhibitor-resistant melanoma cells", September 2015, 23,000 €

Weigand Foundation, Title "Targeted combination therapy of inhibitor-resistant melanoma cells", October 2015, 6,683.56 €

Awards and travel grants

Poster awards at the 41st Congress of the *Arbeitsgemeinschaft Dermatologische Forschung* (ADF) 2014 in Cologne and at the 6th Mildred Scheel Cancer Conference 2013 in Königswinter, Germany.

Travel award of the *Society for Melanoma Research* at the 11th Congress 2014 in Zurich, Switzerland.

Travel grants from the *Deutscher Akademischer Austauschdienst (DAAD)* to attend the congresses of the *Society for Melanoma Research* 2012 in Hollywood, USA, and 2013 in Philadelphia, USA.

Peer reviews and memberships

Reviewer for the journals *Melanoma Research*, *Experimental Dermatology*, *PLoS One*, *Pigment Cell and Melanoma Research*, *Journal of Investigative Dermatology*, *Clinical Cancer Research*, *General Research Fund (GRF)*, and *Swiss Cancer League*.

Member of the *Melanoma Research Network* (2011-2014), the *Arbeitsgemeinschaft Dermatologische Forschung* (since 2012), the *Society for Melanoma Research* (since 2012), the *Verband Biologie, Biowissenschaften und Biomedizin VBIO e.V.* (since 2014), and the *Deutsche Krebsgesellschaft* (since 2014).

Associated member of the LMU graduate school *GraKo 1202* (2011-2014) and *i-Target* from the *Elitenetzwerk Bayern* (2014-2015).

Extracurricular activities

Participation at the 2nd *ADF Winter School* (31st January – 2nd February 2013) at the *Zugspitze* and at the 2nd *Student Retreat* of the *Arbeitsgemeinschaft Dermatologische Onkologie* (9th – 10th September 2014) in Frankfurt, Germany.

Co-organization of the international symposium „*Immunofest Munich 2014*“ of the *GraKo 1202* (25th – 26th September 2014) and the 3rd *Student Retreat* of the *Arbeitsgemeinschaft Dermatologische Onkologie* (8th – 9th September 2015) in Munich, Germany.

Munich, 1st March 2016

Saskia Graf